

The function of the WHIRLY1 protein in photosynthetic light acclimation of barley

Dissertation

zur Erlangung des Doktorgrades der Mathematisch-Naturwissenschaftlichen
Fakultät der Christian-Albrechts-Universität zu Kiel

vorgelegt von
Monireh Saeid Nia
aus Tehran

Kiel, 2023

Supervisor: Prof. Dr. Wolfgang Bilger
Co-supervisor: Prof. Dr. Karin Krupinska

Date of the oral examination: 28.08.2023

To my mother, to my father,
To my love and our son

Contents

Chapter I: Introduction	1
1.1. Light absorption by pigments in the photosynthetic apparatus	1
<i>Chlorophyll fluorescence</i>	4
1.2. Light acclimation	5
<i>Chloroplast to nucleus retrograde signaling</i>	7
1.3. The DNA-binding protein WHIRLY1 is dually localized in the chloroplast and nucleus of the same cell	8
<i>The plastid-located WHIRLY1 protein is an architectural nucleoid-association protein</i>	9
<i>The nucleus located WHIRLY1 protein regulates nuclear genes transcription</i>	10
<i>The role of WHIRLY1 protein in retrograde signaling</i>	11
1.4. Objectives of this study	13
Chapter II: WHIRLY1 protein and plastid DNA stability against UV-B radiation	15
Abstract	16
Introduction	16
Material and methods	18
Plant material and growth conditions	18
UV screening pigments	18
Isolation of intact chloroplasts	19
Isolation of nuclei	19
UV-B exposure	19
DNA isolation and detection of cyclobutane pyrimidine dimers	20
Staining of nucleoids	21
Statistical analysis	21
Results and discussion	21
Morphology of nucleoids in chloroplasts	21
UV-B screening in leaves	22
DNA lesions in plastid, nuclear and total DNA	22
Author contributions	26
Acknowledgments	26
Data availability statement	26
References	26
Chapter III: WHIRLY1 protein and high light acclimation	29
Chapter IV: WHIRLY1-deficient barley plants and light stress	45

Abstract	46
Introduction.....	47
Material and Methods.....	49
Plant material and growth conditions.....	49
Chlorophyll fluorescence measurements.....	49
Transmission electron microscopy (TEM) for the analysis of plastoglobules (PGs).....	50
High-performance liquid chromatography (HPLC) analysis of pigments	51
HPLC analysis of tocopherols	51
Analysis of leaf flavonoid content and composition by HPLC	52
Identification of flavonoids by mass spectrometry	52
Localization of leaf flavonoids	53
Gene expression analysis by quantitative RT-PCR	54
Determination of the glutathione content and its redox state.....	55
Statistical analysis.....	55
Results	56
Photosynthetic electron transport rate (ETR).....	56
The maximal quantum yield of photosystem II.....	57
The fate of excitation energy in PS II.....	58
Ultrastructural analyses revealed an accumulation of plastoglobules in high-light grown W1 leaves.....	59
Pigments of the photosynthetic apparatus.....	61
Expression of genes required for zeaxanthin formation and its epoxidation	63
Tocopherol content of leaves.....	64
HPLC analysis of flavonoid content	65
Flavonoid composition of leaves	66
Localization of saponarin and lutoanarin.....	67
The ratio of reduced (GSH) to oxidized (GSSG) glutathione.....	69
Discussion	69
Author Contribution Statement	77
Acknowledgments	77
Data availability	78
References.....	78
Supplementary data.....	91
Chapter V: The balance between growth and resistance in WHIRLY1-overexpressing barley plants	95
Summary	96

Introduction.....	97
Results	99
Overexpression of HvWHIRLY1 altered the abundance of HvWHIRLY1 in chloroplasts and the nucleus	99
Growth of barley oeW1 plants	101
Characterization of the photosynthetic apparatus	102
Chloroplast ultrastructure and nucleoid morphology.....	106
Hormone levels and defense-related gene expression.....	108
Response of oeW1 plants to high light.....	113
Response of oeW1 plants to powdery mildew	115
Discussion	116
Impact of WHIRLY1 overexpression on growth and photosynthesis.....	117
Overexpression of WHIRLY1 caused changes in the equilibrium of hormones	118
The role of chloroplast-nucleus located WHIRLY1 in the growth-defense tradeoff.....	121
Experimental procedures	123
Plant material and growth conditions.....	123
Quantum yields of the photosystems and electron transport rate	124
Determination of pigments by high-performance liquid chromatography	124
Immunoblot analyses	124
Determination of hormones.....	125
RNA isolation and real-time PCR analysis.....	125
Transmission electron microscopy.....	126
Staining and localization of nucleoids	126
Infection with powdery mildew	126
Author Contribution Statement	127
Acknowledgments.....	127
References.....	127
Chapter VI: Discussion.....	133
<i>WHIRLY1 protein, the main architectural protein of nucleoids, compacts the nucleoids</i>	<i>133</i>
<i>Light acclimation is impaired in WHIRLY1-deficient barley plants (W1) at the levels of photosynthesis and leaf morphology</i>	<i>134</i>
<i>Despite missing light acclimation and appropriate nucleoid compactness, W1 plants survived excessive excitation energy</i>	<i>135</i>
<i>Barley plants overexpressing WHIRLY1 protein (oeW1) with similar nucleoid compactness as the wild type are impaired in photosynthesis.....</i>	<i>137</i>
Chapter VII: Summary	141
References.....	145

Acknowledgments 156
Erklärung..... 157

Chapter I: Introduction

1.1. Light absorption by pigments in the photosynthetic apparatus

Light energy from the sun is the main source of energy on the earth captured in higher plants by different pigments like chlorophyll, carotenoids, and flavonoids. Light absorption by a pigment happens rapidly in a femtosecond. The light energy absorbed by this pigment will cause the electron to jump to a higher-energy orbital. The latter is called the excited state, which has a very short lifetime. The excited pigment must get back to its ground state by losing energy. Therefore, either the excess energy or the excited electron can be transferred to an adjacent molecule. This transfer can be done very efficiently if pigment molecules are in the proper distance to each other.

In the photosynthetic apparatus, two photosystems (PS), PS I and PS II are large pigment-protein complexes linked together by the cytochrome complex b_6/f . These complexes are operating in series and make the photosynthetic electron transport chain (e.g. Duysens, 1951; 1989; Foyer and Harbinson, 1994). PS I and PS II contain a collection of chlorophyll and

carotenoid molecules, as the core antenna, associated with different proteins. As an extended antenna and in addition to the core antenna, there are two light-harvesting complexes (LHC) in close contact with PS I and PS II. Since the pigments in the antenna are in close association, the excitation energy can pass from one to another through resonance or radiationless energy transfer and eventually reach the chlorophyll in the reaction center (Gaffron and Wohl, 1936; Knox, 1996; Andrews et al., 2015). In the reaction center, the trapped excitation energy initiates an electron transfer chain converting the light energy to chemical energy (e.g. Rosenqvist and van Kooten, 2003). This energy is eventually used to fix atmospheric CO₂ onto Ribulose-1,5-bisphosphate (RuBP) to produce 3-phosphoglycerate (3-PGA), which is reduced to triose phosphates (TPs) and later converted to sugar or starch as end products of photosynthesis. Moreover, during photosynthesis molecular oxygen is also released into the atmosphere.

The fate of absorbed light energy in PS II

As noted earlier, the excited pigment is unstable and must get back to its ground state by losing the excitation energy. But converting this energy to chemical energy by photosynthesis is not the only possible pathway which absorbed light can pass through. Absorbed light energy in PS II can go into three complementary pathways. As mentioned above, a portion of absorbed energy can be used in photochemistry, the remaining energy may be either thermally dissipated through regulated non-photochemical quenching (NPQ) or lost via fluorescence or non-regulated heat dissipation (Hendrickson et al., 2004; Klughammer and Schreiber, 2008).

The portion of energy going through each pathway depends on the light conditions that the plants were exposed to (Figure 1). These three complementary pathways are in competition. This means if one pathway gets a higher portion of the energy, the other ones will get less, e.g. under low light conditions, higher portion of energy goes through the photochemistry. However, under high light conditions, when the electron flow in CO₂ assimilation, photorespiration and the water-water cycle (Asada, 2000; Ort and Backer, 2002; Curien et al., 2016) cannot take over the high energy flow, the photochemical quantum yield is downregulated (Asada, 2006) and the regulated non-photochemical quenching receives the larger portion (Hendrickson et al., 2004) (Figure 1).

Light absorption exceeding the plants' photosynthetic capacities for electron transport and CO₂ assimilation is called excess excitation energy (EEE) which has to be dissipated through the other pathways of regulated and non-regulated energy dissipation to avoid or reduce EEE. Exposure to excessive light can cause electron or energy transfer to oxygen producing different powerful oxidants such as singlet oxygen and superoxide or hydrogen peroxide, known as reactive oxygen species (ROS) (Asada, 2006). If ROS formation cannot be avoided or already formed ROS cannot be gotten under control, this excess energy may eventually cause photoinhibition of PS II or photooxidation of membrane lipids.

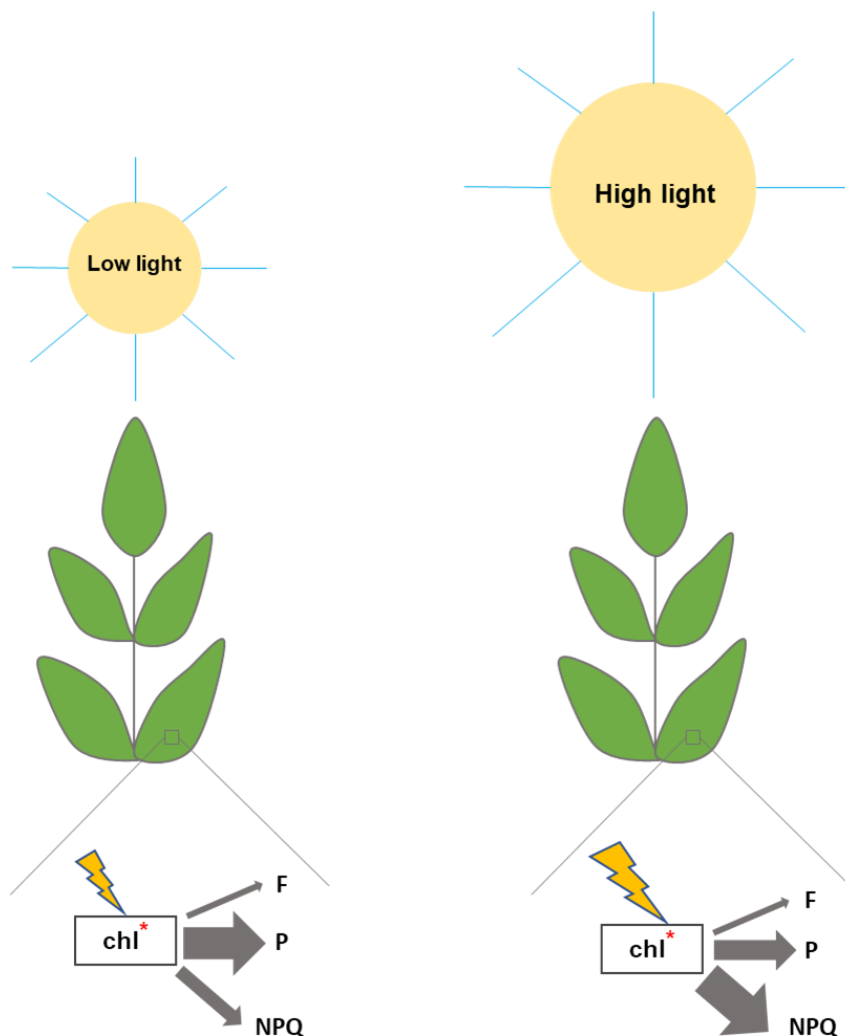


Figure 1. Schematic model for the fate of absorbed light energy in PS II under low and high light. F stands for chlorophyll fluorescence, P stands for photochemistry and NPQ stands for non-photochemical quenching.

Chlorophyll fluorescence

Besides driving photosynthesis and heat dissipation, excited chlorophylls within pigment-protein complexes and in the light-harvesting complexes can reach the ground state by re-emitting the excess energy as light, which is called chlorophyll fluorescence. Moreover, since the three pathways for the fate of absorbed light energy are complementary, the yield of chlorophyll fluorescence emission provides comprehensive information about the quantum yields of photochemistry and heat dissipation of energy, too.

The portion of chlorophyll fluorescence in the fate of absorbed light energy is small. However, since it has a different spectrum with a longer wavelength peak than the absorbed light (Maxwell and Johnson, 2000), exposing the leaf to a known wavelength and measuring the amount of re-emitted light at the longer wavelength can quantify the amount of chlorophyll fluorescence. At room temperature and wavelengths below 700 nm, PS I contribution to fluorescence is negligible, hence, the variation in chlorophyll fluorescence signals under these conditions is assumed to arise only from PS II (Butler, 1978; Baker, 2008; Murchie and Lawson, 2013). Chlorophyll fluorescence measurement, using the Pulse Amplitude Modulated fluorescence method (Schreiber, 1986; Schreiber and Bilger, 1987), is a simple non-invasive technique that is widely used to gain detailed information about the PS II efficiency and whether plants are under stress or not (Butler, 1978; Björkman and Demmig, 1987).

To gain information about photochemical and regulated non-photochemical quenching by heat dissipation (NPQ), these two processes must be distinguished from each other. One possible method is to switch off one of these contributors (Maxwell and Johnson, 2000). Photochemistry can be nearly zero when all PS II reaction centers are light saturated and closed (Bradbury and Baker, 1981; Quick et al., 1984; Rosenqvist and van Kooten, 2003). Then the extent of NPQ from chlorophyll fluorescence can be determined. In non-stressed plants which were kept in darkness, the NPQ is minimized (Maxwell and Johnson, 2000). By exposing a pre-darkened leaf to a high-intensity flash of saturating light for a short time, the maximum chlorophyll fluorescence (F_M) in the absence of photochemistry can be achieved. In this condition, NPQ is assumed to be zero. Comparing F_M with the steady-state fluorescence before the saturating light (F_0), is an estimation of the maximum quantum yield of PS II (Butler, 1978; Baker, 2008) (Table 1).

In the presence of light driving photosynthesis (actinic light), maximal chlorophyll fluorescence (F_M') can also be achieved by saturating pulses providing information about PS II photochemical quantum yield $\Phi(\text{PSII})$ and heat dissipation under actinic light (Genty et al., 1989) (Table 1). Similar to $\Phi(\text{PSII})$, one can formulate quantum yield of regulated non-photochemical quenching, $\Phi(\text{NPQ})$. This parameter depends on different environmental factors as well as internal ones and can be calculated from F_M' values relative to the maximum chlorophyll fluorescence from the pre-darkened leaf (F_M) (Maxwell and Johnson, 2000) (Table 1).

In principle, all quantum yields of a process must add up to 1. A quantum yield complementing the sum of $\Phi(\text{PSII})$ and $\Phi(\text{NPQ})$ to 1, is called $\Phi(\text{NO})$ (Genty et al., 1996; Klughammer and Schreiber, 2008). It includes non-regulated non-photochemical quenching observed at dark adapted state and chlorophyll fluorescence (Genty et al., 1996; Klughammer and Schreiber, 2008)

Pre-darkened leaf		
$\Phi(\text{PS II})$	Efficiency of PS II photochemistry	$\Phi_{\text{PSII}} = (F_M - F_0)/F_M$ $\Phi_{\text{PSII}} = F_V/F_M$
Leaf under actinic light		
$\Phi(\text{PS II})$	Efficiency of PS II photochemistry	$\Phi_{\text{PSII}} = (F_M' - F)/F_M'$
$\Phi(\text{NPQ})$	Efficiency of regulated non-photochemical quenching	$\Phi_{\text{NPQ}} = F/F_M' - F/F_M$
$\Phi(\text{NO})$	Efficiency of non-regulated non-photochemical quenching	$\Phi_{\text{NO}} = F/F_M$

Table 1. Some fluorescence parameters for the pre-darkened leaf or leaf under photosynthetic (actinic) light (Genty et al., 1996; Maxwell and Johnson, 2000; Klughammer and Schreiber, 2008)

1.2. Light acclimation

Acclimation in general involves all the processes that change in plants to cope with the fluctuations in environmental conditions. Appropriate acclimation happens first by sensing the variations in the environment and subsequently by the appropriate molecular programs as a response to these variations. In other words, acclimation is a consequence of adjustments at

transcriptional, translational, and post-translational levels (Kloppstech, 1997) leading to changes at various levels, such as photosynthesis as well as anatomical and morphological levels, too (Givnish, 1988).

Chloroplasts are endosymbiotic organelles with prokaryotic ancestors. During evolution, a larger part of their prokaryotic genomes was eventually lost or transferred to the nucleus. Consequently, the majority of 3000 to 4000 different plastid proteins (Fey et al., 2005) are nuclear-encoded and imported into the chloroplasts after being synthesized at 80S ribosomes in the cytoplasm. However, the plastid genome of higher plants still encodes a minute part of their proteome, about 50 proteins (Green, 2011). An adjustment in the composition of the photosynthetic apparatus in response to e.g. variable light intensities requires both changes in the nucleus as well as plastid-encoded proteins.

Hence, as plants have two more genomes from their mitochondria and chloroplasts besides their nuclear genome, environmental changes sensed by them must first be communicated to the nucleus. The latter is mediated through organelles to nucleus retrograde signaling orchestrating the gene expression in both organelles and nucleus in response to the environmental stimuli.

The most variable environmental factor, light, as the only energy source for photosynthesis varies over different orders of magnitude in the short and long term. Therefore, acclimation ensures efficient electron transport under different conditions to provide energy (Fey et al., 2005) and adjusts the rate of ATP and NADPH production to the rate of their utilization in the Calvin cycle (Foyer et al., 2012).

Light acclimation of plants may take place at various levels, such as at the canopy, plant, leaf, and also at anatomy, morphology, and biochemistry levels (Givnish, 1988). It has been well established that plants growing under different intensities of light are displaying distinct photosynthetic activity and efficiency (Boardman, 1977).

High light acclimated plants usually have a higher rate for the photosynthetic light response (Givnish, 1988), electron transport (Boardman et al., 1975; Boardman, 1977) and maximum photosynthetic CO₂ assimilation or so-called photosynthetic capacity (Lichtenthaler et al., 2007). In other words, due to the acclimation of their photosynthesis to higher irradiance

and, in comparison to low light-grown plants, the portion of energy that goes through photochemistry pathways is larger than the other two pathways, regulated and non-regulated non-photochemical quenching, in these plants. They also show an increase in RubisCO content and in the other components of the Calvin cycle (Dietz, 2015). They have thicker leaves with higher leaf mass per area (Givnish, 1988; Lichtenthaler et al., 2007), higher total chlorophyll (chlorophyll $a+b$) and carotenoid content per leaf area (Lichtenthaler et al., 2007).

Chloroplast to nucleus retrograde signaling

Besides its function in the conversion of light energy to chemical energy, the chloroplast is a redox sensor of environmental conditions such as light quality and quantity, temperature, and nutrient availability which can affect the photosynthetic electron transport efficiency and energy production. The sensing of environmental changes plays an important role in triggering acclimatory responses toward fluctuating environmental conditions by coordinating nuclear and chloroplast gene expression through retrograde signaling.

The redox state of components of the electron transport chain, especially the plastoquinone (PQ) pool and cytochrome b_6/f complex, are important factors in acclimatory adjustments of the photosynthetic machinery in both short and long terms. For example, the cytochrome b_6/f complex-associated protein kinase STN7 is suggested to sense the redox state of PQ and regulate the distribution of LHCs between PS I and PS II. This kinase is also involved in long-term responses mediating nuclear and chloroplast gene regulation (Foyer et al., 2014).

Environment-induced perturbations in photosynthesis may result in the generation of hydrogen peroxide (H_2O_2) and superoxide ($\cdot O_2^-$) at PS I and singlet oxygen (1O_2) at PS II, known as reactive oxygen species (ROS). ROS molecules are considered as signal transducers or triggers of some signaling pathways, transducing information from chloroplast to the nucleus through retrograde signaling. Because H_2O_2 itself can leave the chloroplast and can translocate to the nucleus (Exposito-Rodriguez et al., 2017), it is suggested to act as a direct retrograde signal. $\cdot O_2^-$ and 1O_2 are considered to be required for the signal transduction pathways due to their short half-lives (Chan et al., 2016).

Intriguingly, while high levels of $^1\text{O}_2$ are formed in plants under excessive light causing photoinhibition of PS II, H_2O_2 and $^{\bullet}\text{O}_2^-$ can constantly be produced at the PS I site and prior to photoinhibition. These ROS are shown to cause different changes in nuclear gene expression. For instance, in the study by Laloi et al. (2006) by transferring *flu* mutant of *Arabidopsis thaliana* from darkness to light, both $^1\text{O}_2$ and H_2O_2 were produced in these mutants leading to distinct changes in the expression of the nuclear genes. Moreover, it was shown that plastid-generated H_2O_2 affects nuclear gene transcription in a distinct way from H_2O_2 generated from any other compartments (Sewelam et al., 2014). Therefore, ROS-mediated retrograde signaling transfers clear detailed messages to the nucleus on which compartments or photosystems are under stress or have perturbed function.

Besides ROS, other products of chloroplasts can be involved in retrograde signaling. For instance, under severe high light stress, an enhanced amount of $^1\text{O}_2$ showed to cause the production of volatile β -carotene-derived oxidation products which can affect nuclear gene expression in a similar way to $^1\text{O}_2$ (Chan et al., 2016).

Moreover and in addition to many other possible ways, proteins that are dually located in the plastid and nucleus of the same cell are suggested by many studies to be involved in chloroplasts and nuclear genomes communication (Bobik and Burch-Smith, 2015). Among them, the DNA-binding WHIRLY1 protein is a promising candidate.

1.3. The DNA-binding protein WHIRLY1 is dually localized in the chloroplast and nucleus of the same cell

The WHIRLY1 protein is a nuclear-encoded plastid protein that belongs to the small family of WHIRLY ssDNA/RNA binding proteins found in angiosperms. They share a characteristic secondary structure and a conserved DNA binding domain. The WHIRLY1 protein is found in both chloroplast and nucleus of the same cell (Grabowski et al., 2008) and is associated with DNA and/or RNA in both organelles (Prikryl et al., 2008; Melonek et al., 2010).

Crystal structure analysis of WHIRLY1 and 2 (Desveaux et al., 2002; Cappadocia et al., 2008) showed that WHIRLY proteins, together with melted double-strand DNA, form tetrameric

complexes. In this complex, each monomer binds to a symmetrical inverted repeat sequence of one DNA strand causing the quaternary structure of tetramers. This structure exhibits a whirling appearance which is the reason for the name of this protein (Desveaux et al., 2002).

A study in barley by Grabowski et al. (2008) using immunogold analysis together with a specific antibody against WHIRLY1 clearly showed that the WHIRLY1 protein is dually located in the chloroplast and nucleus of the same cell with the same molecular weight. The latter means that nuclear-located WHIRLY1 must have been processed first inside chloroplasts and then translocated to the nucleus (Isemer et al., 2012).

Initially, Desveaux et al. (2000) identified the WHIRLY1 protein as a subunit of a factor binding to the PR-10a gene promoter in potato and therefore this protein was initially named PR-10a binding factor 2 (PBF-2) (Desveaux et al., 2002). Most plant species like *Hordeum vulgare* have two members of this family but some other species like *Arabidopsis thaliana* have three WHIRLY proteins. The WHIRLY1 and 3 proteins were predicted to be targeted to chloroplasts, whereas WHIRLY2 is targeted to the mitochondria (Desveaux et al., 2005; Krause et al., 2005).

There is an amino acid motif consisting of six amino acids, Lys-Gly-Lys-Ala-Ala-Leu, KGKAAL, on both β -strands of protomer which is critical for WHIRLY1 and DNA interaction (Desveaux et al., 2002; Krause et al., 2009) and is highly-conserved by all WHIRLIES in all plants (Desveaux et al., 2005). The second lysine of this motif was shown to be important for the hexamerization of WHIRLY1 tetramers to 24-mers which creates hollow sphere structures with 12 nm diameter (Cappadocia et al., 2012).

The plastid-located WHIRLY1 protein is an architectural nucleoid-association protein

The WHIRLY1 protein is an abundant protein of chloroplast nucleoids, detected also in the proteome of transcriptionally active chromosomes (TAC), and therefore named also pTAC1 (Melonek et al., 2010; Majeran et al., 2012). In *A. thaliana* both WHIRLY1 and WHIRLY3 have been found in the TAC (Pfalz et al., 2006). The TAC was shown to have a large overlap with nucleoids (Melonek et al., 2016) and in fact, co-localization of WHIRLY1 in nucleoids was shown to be in accordance with the detection of this protein in the TAC (Melonek et al., 2010).

The WHIRLY1 protein as a major nucleoid-associated protein (Pfalz et al., 2006, Melonek et al., 2010; Majeran et al., 2012) was shown to be required for the compact structure of nucleoids (Krupinska et al., 2014) mediated by a proline-rich motif, i.e. Pro-Arg-Ala-Pro-Pro, PRAPP, which specifically exists in Poaceae family members (Krupinska et al., 2014; Oetke et al., 2022).

Due to the uniform and sequence-unspecific distribution of WHIRLY1 over the plastid genome, the involvement of the WHIRLY1 protein in the regulation of plastid gene transcription is rather unlikely (Melonek et al., 2010). Moreover, and due to the detection of the WHIRLY1 protein in the nucleoids (TAC), it was suggested that plastid-located WHIRLY1 is more likely to be involved in RNA rather than DNA metabolism (Prikryl et al., 2008; Melonek et al., 2010).

The nucleus located WHIRLY1 protein regulates nuclear genes transcription

As mentioned before, the WHIRLY1 protein has been initially found to bind to the promoters of stress responses and senescence genes in the nucleus when it regulates the expression of target genes. For example, it is a repressor of senescence-associated genes, S40, and WRKY53 genes, in barley and Arabidopsis, respectively (Miao et al., 2013; Krupinska et al., 2014), or functions in an opposite way as an activator of certain pathogen-response genes (Desveaux et al., 2000, Krupinska et al., 2014).

Unlike transcription factors that bind to the dsDNA, the WHIRLY1 protein is known to be an ssDNA binding protein that binds to the melted regions of the promoters and is suggested to regulate the accessibility of transcription factors, such as WRKY, to the promoters, and in this way affecting specific nuclear gene transcription (Krupinska et al., 2022). It has been proposed that the WHIRLY1 protein in both chloroplast and nucleus might be involved in chromatin remodeling (Krupinska et al., 2022).

Dually located proteins, like WHIRLY proteins, may be initially located in the mitochondria and plastids, but under certain circumstances, they may translocate to the nucleus as signal transducers (Krause and Krupinska, 2009; Foyer et al., 2014). Therefore, they are promising candidates to be involved in the organelles to nucleus retrograde signaling.

The role of WHIRLY1 protein in retrograde signaling

In chloroplasts, the WHIRLY1 protein is the major organizer of nucleoids that are attached to the thylakoid membrane (Foyer et al., 2014) (Figure 2). This is an interesting position for a protein with a putative role in retrograde signaling and for the coordination of photosynthetic electron transport function with nuclear gene expression. It is tempting to suggest that the WHIRLY1 protein is involved in the perception of the redox state of the electron transport chain due to its location (Foyer et al., 2014). This is in accordance with the fact that the WHIRLY3 protein, corresponding to the WHIRLY1 protein in barley (Krupinska et al., 2022), is known to be a redox-affected protein in the chloroplast (Ströher and Dietz, 2008; Foyer et al., 2014).

WHIRLY1 and WHIRLY3 proteins both share a conserved cysteine residue in a conserved position which is probably involved in disulfide bridge formation between two WHIRLY proteins (Foyer et al., 2014). Cysteine residue reduction or even phosphorylation by the same kinases that are activated when the PQ pool is reduced could also be involved in the destabilization of the protein oligomer structure (Foyer et al., 2014). Stress-induced redox changes occurring in the photosynthetic apparatus have been hypothesized to induce WHIRLY1 translocation from chloroplasts to the nucleus (Foyer et al., 2014). High rates of reduction of components in the electron transport chain such as the PQ pool and the cytochrome b_6/f complex, may destabilize the oligomer (24-mer) structure of WHIRLY1, and consequently, monomers may translocate to the nucleus as signal transducers by an unknown mechanism (Figure 2).

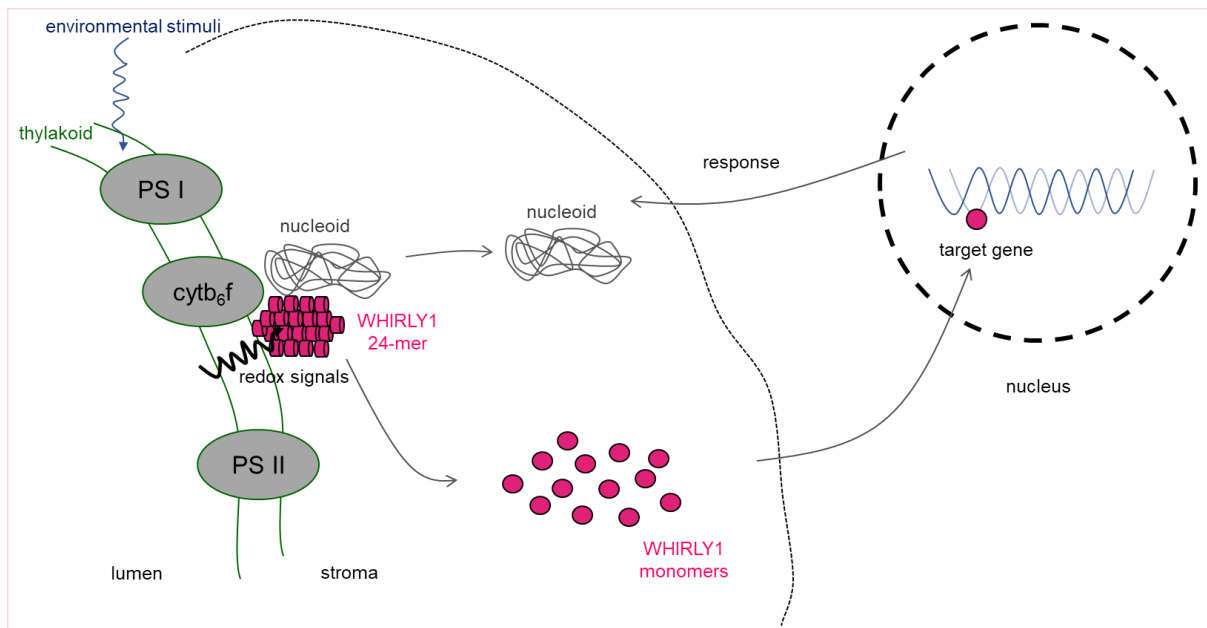


Figure 2. Schematic model explaining that environmental stimuli-induced redox signals from the photosynthetic apparatus may be perceived by the 24-mer WHIRLY1 protein and consequently destabilize the oligomer structure to its monomers. These monomers were suggested to translocate to the nucleus as signal transducers (Foyer et al., 2014). This figure is adapted from Foyer et al. (2014).

Investigations with plants having altered amounts of the WHIRLY1 protein are in accordance with the proposed role of this protein in communication between chloroplast and nucleus. For example, it was shown in tomato that overexpression of WHIRLY1 protein enhanced CO₂ assimilation rate and RubisCO content under chilling conditions in comparison to WT plants. In contrast, plants with an RNAi-mediated knockdown of SIWHIRLY1 protein had lower RubisCO content with decreased photosynthesis in comparison to WT (Zhuang et al., 2020). SIWHIRLY1 was also demonstrated to increase tomato tolerance to chilling stress by regulating starch degradation and also protecting PS II (Zhuang et al., 2019). However, there is a lack of evidence for the involvement of the WHIRLY1 protein in acclimatory processes through retrograde signaling in monocots.

RNAi-mediated WHIRLY1 knockdown barley plants (W1) were shown to have a stay-green phenotype under high light (Kucharewicz et al., 2017), although they accumulated a high amount of senescence promoting hormones such as salicylic acid (SA) and abscisic acid (ABA) (Pérez-Llorca and Munné-Bosch, 2021). This result suggests that the WHIRLY1 protein must have a function downstream of SA and ABA signaling (Foyer et al., 2014). On the other hand, these hormones are known to be important for the high-light acclimation of plants (Dietz, 2015). Therefore, W1 plants with a higher amount of SA and deficiency in WHIRLY1 protein

are an excellent model to investigate the possible role of the WHIRLY1 protein in high light acclimation of barley plants through retrograde signaling.

1.4. Objectives of this study

In this thesis, the major objective was to investigate the involvement of WHIRLY1 in high light acclimation through either retrograde signaling or its impact on the nucleoid compactness in more detail by comparing barley wild-type plants with an RNA-mediated knockdown of the *HvWHIRLY1* gene (W1) and also later with the line overexpressing *HvWHIRLY1* gene, oeW1 plants.

Due to its effect on nucleoid compaction, the potential impact of the chloroplast-nucleus located WHIRLY1 protein on the protection of DNA from UV-B radiation in both nucleus and chloroplast was investigated and presented in **Chapter II** in a manuscript which has been submitted to *Physiologia Plantarum*.

To check WHIRLY1 contribution in the light acclimation of barley plants through retrograde signaling, different photosynthetic parameters such as CO₂ assimilation rate, maximum photosynthesis (P_{max}), RubisCO content, and its *in vivo* activity were analyzed in both WHIRLY1 deficient and wild-type leaves growing under low and high irradiance and at different developmental stages. Additionally, light acclimation was also investigated at the level of leaf morphology, too. Since the W1 plants showed delayed chloroplast development (Kucharewicz et al., 2017; Krupinska et al., 2019), light acclimation was studied at different developmental stages. The corresponding results are presented in **Chapter III** as a published paper in the journal of *Planta* (Saeid Nia et al., 2022; <https://doi.org/10.1007/s00425-022-03854-x>) with the right for secondary publication, in this thesis, from the publisher.

Barley plants deficient in WHIRLY1 protein have been shown to be impaired in acclimation to high light (Saeid Nia et al., 2022) and might thereby be prone to photoinhibition. However, W1 plants did not show any decline in their maximum quantum yield of PS II when grown under high light (Kucharewicz et al., 2017). In this thesis, further investigations were done to elucidate how WHIRLY1 deficient barley plants can survive the high irradiance while avoiding photoinhibition despite their lower photosynthetic capacity (Saeid Nia et al., 2022). The

manuscript with corresponding results, presented in **Chapter IV**, which has been submitted to *Planta*.

Recently, a WHIRLY1 overexpressing line (oeW1) has been provided and it became possible to investigate the effect of the higher amount of this protein on some parameters regarding photosynthetic light acclimation and stress responses. The results of this study are presented in **Chapter V** in a form of a manuscript that is published in *Biorxiv*.

Chapter II: WHIRLY1 protein and plastid DNA stability against UV-B radiation

WHIRLY1-mediated compaction of nucleoids reduces the formation of cyclobutane pyrimidine dimers during exposure of chloroplasts to UV-B radiation

Monireh Saeid Nia¹, Christine Desel¹, Frauke Pescheck¹, Karin Krupinska¹, Wolfgang Bilger¹

¹Institute of Botany, Christian-Albrechts-University of Kiel, Olshausenstraße 40, 24098 Kiel, Germany

Abstract

The single-stranded DNA/RNA binding protein WHIRLY1 is a major chloroplast nucleoid-associated protein which was shown to be required for the compactness of nucleoids. Most nucleoids in chloroplasts of barley plants with a knockdown of *WHIRLY1* are less compact compared to wild-type plants. To investigate whether WHIRLY1 may increase the stability of plastid DNA by its function in plastid DNA packaging, primary foliage leaves, chloroplasts, and nuclei from wild type and WHIRLY1 knockdown plants were exposed to UV-B radiation. Thereafter, total genomic and plastid DNA were isolated, respectively, and analyzed for the occurrence of cyclobutane pyrimidine dimers (CPDs), which is a parameter for genome stability. The results of this study revealed that in chloroplasts the WHIRLY1-dependent compaction of nucleoids prevented the formation of CPDs, whereas WHIRLY1 abundance had no impact on the formation of CPDs in the nucleus.

Keywords: CPDs, DNA stability, nucleoids compactness, UV-BR, WHIRLY1

Introduction

Plants are obligatorily dependent on sunlight for their survival and can't avoid being exposed simultaneously to potentially harmful UV-B radiation (UV-BR). High irradiance in combination with UV-BR shares the production of ROS with other environmental stress situations. ROS may have many detrimental effects on plants (oxidation of DNA, proteins, lipids) and thereby reduce growth (Takahashi et al., 2002; Frohnmeyer and Staiger, 2003). In addition to these indirect effects, UV-BR has a direct photophysical damaging impact on genome integrity leading to the inhibition of cell division and even cell death (Jansen et al., 1998).

UV-B radiation gives rise to different types of DNA damage, which can be mutagenic and eventually lethal by impeding replication and transcription (Strid et al., 1994; Takahashi et al., 2011). The most common damage of DNA induced by UV-BR is the formation of cyclobutane pyrimidine dimers (CPDs). CPDs account for approximately 75% of DNA lesions, and further pyrimidine adducts account for the remainder of the DNA lesions. CPDs are induced by UV-BR between adjacent pyrimidines on the same DNA strand through dimerization (Mitchell &

Narin, 1989; Takahashi et al., 2011). In plant cells, DNA is distributed among nuclei, mitochondria, and plastids. UV-BR-induced CPD formation can occur in organelle DNA as well as in nuclear DNA.

Plastids are descendants of cyanobacteria and contain multiple copies of a remnant prokaryotic genome. The multiple copies of the genome together with RNA and proteins are organized in structures that resemble bacterial nucleoids. These structures are remarkably variable in number, shape, and distribution within different types of plastids (Powikrowska et al., 2014). In proplastids, nucleoids are attached to the envelope membrane. During chloroplast development, nucleoids change their position and become attached to thylakoid membranes where unpacked DNA could be damaged by ROS formed as a byproduct of photosynthetic electron transport (Prowikowska et al., 2014). Chloroplast nucleoids, however, contain numerous DNA-binding proteins mediating the shaping and organization of the nucleoid (Melonek et al., 2016, Krupinska et al. 2022). These so-called nucleoid-associated proteins (NAPs) have replaced the histone-like proteins of bacteria such as the heat unstable (HU) and histone-like nucleoid-structuring proteins (H-NS) (Kobayashi et al., 2016), which in bacteria determine the shape and topology of nucleoids in response to internal and external factors (Hołówka & Zakrzewska-Czerwińska, 2020). These histone-like proteins are abundant proteins binding unspecifically to DNA. They help the cell to quickly react to changing conditions by coating and condensing the nucleoid thereby protecting the DNA from damage and creating physical protection for the DNA (Hołówka & Zakrzewska-Czerwińska, 2020). In a *Deinococcus radiodurans* mutant lacking one of these NAPs the survival rate during UV exposure was eightfold reduced (Wang et al., 2012).

While in tobacco the sulfite reductase has acquired a specific DNA binding motif conferring nucleoid compaction (Cannon et al., 1999), at least in barley and likely other monocot species WHIRLY1 is the major protein determining nucleoid architecture. WHIRLY1 belongs to the small family of WHIRLY ssDNA-binding proteins being specific for angiosperms (Krupinska et al., 2022). Using an antibody against maize WHIRLY1 the protein was found to unspecifically bind to ptDNA by nucleic acid co-immunoprecipitation and, hence, was compared to the bacterial HU (Krupinska et al., 2022). In barley, WHIRLY1 had been shown to be responsible for the compaction of chloroplast nucleoids. Staining of DNA in leaf cells of barley plants with an RNAi-mediated knockdown of the *WHIRLY1* gene revealed that the nucleoid population is

much more heterogeneous and that most nucleoids are significantly less compact than those of wild-type plants (Krupinska et al., 2014). Accordingly, it was shown that WHIRLY1 is required for the compact structure of nucleoids mediated by a proline-rich motif, i.e. Pro-Arg-Ala-Pro-Pro, PRAPP, which specifically exists in Poaceae family members (Krupinska et al., 2014; Oetke et al., 2022). Besides its role in architecture of chloroplast nucleoids, WHIRLY1 has also been shown to act as transcription factor in the nucleus (Krupinska et al., 2022).

In line with the function of WHIRLY1 in compacting chloroplast nucleoids, WHIRLY1 deficiency in barley *WHIRLY1* knockdown plants (W1) resulted in nucleoids with heterogeneous sizes which were mostly loosely packed (Krupinska et al., 2014). The target theory says that the probability that a given target is hit by radiation is proportional to the volume of the target (Ballarini, 2010). Hence, it was hypothesized that higher compaction of ptDNA in nucleoids mediated by WHIRLY1 lowers the susceptibility of ptDNA towards UVBR-induced photodamage. In this study, the potential impact of the chloroplast-nucleus located WHIRLY1 protein on the resistance of DNA towards UV-B radiation in chloroplasts and nuclei prepared from WHIRLY1 deficient barley plants and wild-type plants was investigated.

Material and methods

Plant material and growth conditions

In this study, *Hordeum vulgare* L., cv. “Golden Promise” as wild-type (WT) and the RNAi-mediated *WHIRLY1* knockdown line of barley having a minute amount of WHIRLY1 (RNAi-W1-7 = W1) (Krupinska et al., 2014) were used. Growth conditions were as described before by Saeid Nia et al. (2022). Plants were grown side by side and under irradiances of about 250-350 $\mu\text{mol photon m}^{-2} \text{s}^{-1}$ measured by a quantum sensor (Li-185 A, Li-Cor Biosciences, Lincoln, NE, USA) in the leaf plane.

UV screening pigments

In vivo UV screening of the adaxial side of primary foliage leaves exposed to UV-B was determined with a Xenon-PAM fluorometer (Walz, Effeltrich, Germany) before UV-B exposure. The technical information about the setup of optical filters, light source, sample holder, and fluorescence detector has been described by Burchard et al. (2000) and Pescheck

et al. (2010). Detached primary leaves were kept in petri dishes and on wet filter paper for this measurement.

Isolation of intact chloroplasts

About 250 primary leaves from each genotype were harvested very early in the morning and before the onset of illumination to minimize the formation of starch granules. Isolation of intact chloroplasts was done in dim light and in a cold room at 4°C with the method described by Gruijsem et al. (1986).

Intact chloroplasts from each genotype were counted three times using a hemocytometer (Thoma, Germany) under a brightfield microscope (Microscope: Axiophot, Plan-Apochromat, 20x/0.45, Zeiss, Jena, Germany; camera: Olympus DP7, Olympus, Japan; image recorded by CELL[^]F software version 5.1, Olympus). Before UV-B exposure, the isolated chloroplasts were diluted in GM buffer until a final density of about 12×10^5 chloroplasts per μl .

Isolation of nuclei

About 250 primary foliage leaves of each genotype were harvested at the same time of the day as described for chloroplasts. Leaves were kept on ice and the nuclei isolation was done at dim light in a cold room (4°C) according to Pilartz and Jeske (2003).

For quantification of isolated intact nuclei, 2 μl of nuclei suspension from each genotype was mixed with 2 μl DAPI solution ($1 \mu\text{g ml}^{-1}$) on the hemocytometer, and intact nuclei were counted under a fluorescence microscope (Microscope: Axiophot, Plan-Apochromat, 20x/0.45, Zeiss; camera: Olympus DP7, Olympus, Japan; image recorded by CELL[^]F software version 5.1, Olympus; Filter: Filter set 02 with excitation: G 365, beamsplitter: FT 395 and emission: LP 420, Zeiss). This procedure was repeated three times. For exposing intact nuclei to UV-B, the isolated nuclei were kept in 1x GB buffer (as described by Pilartz & Jeske, 2003) at a final density of about 13×10^3 nuclei per μl .

UV-B exposure

For the induction of DNA damage, chloroplasts or nuclei were pipetted in multiwell plates (Cell culture plate, 24-well, Sarstedt, Germany) while detached primary leaves were placed on wet

filter paper in petri dishes. Exposure to UV-B radiation was done for one hour. To minimize the repair of DNA damage by the photolyase enzyme via UV-A and blue light-dependent photoreactivation, UV-B lamps with a fairly low contribution of UV-A and blue light were used. UV-B radiation was provided by fluorescent tubes (TL40/12RS, Philips, Amsterdam, Netherlands) which were installed in a growth cabinet (GroBanks, CLF plant climatics, Emersacker, Germany). Desired irradiances were obtained by a variable distance towards the fluorescent tubes, whose output was tuneable. A portable UV-B sensor (Veit et al., 1996) was used to measure UV-B irradiance. This sensor was calibrated against a DM150 double monochromator spectroradiometer (Bentham Instruments, Ltd, Reading, UK). Incident UV-B irradiances were 13, 6, and 13 W m⁻² for leaves, chloroplasts, and nuclei respectively. Each exposure experiment was conducted three times.

In the case of chloroplasts or nuclei, each marked well in the multiwell plates was filled by 1 ml of either isolated chloroplasts or nuclei suspension in a random arrangement. Multiwell plates were kept on ice during the UV-B exposure. Plates were turned clockwise and the solution in the wells also was very gently mixed every quarter of an hour.

During UV-B exposure, plates and petri dishes were covered with WG 295 glass filters (Schott, Mainz, Germany) whereas controls were covered with UV-excluding plexiglass filters (GS 321, Röhm, Darmstadt, Germany, T_{50%} at 390 nm). After UV-B exposure of primary leaves, segments approximately 1 cm in length were excised at a position of 1.5 cm below the tip of primary leaves and leaf segments were immediately frozen in liquid nitrogen. In case of chloroplasts or nuclei, the suspensions from at least 6 wells of each genotype were pooled in one tube, respectively, and were centrifuged at 2000 x g for 2-3 minutes to sediment the chloroplasts or nuclei, respectively. Afterwards, the supernatants were discarded and pellets were immediately frozen in liquid nitrogen. Frozen samples were kept at -80 °C until DNA isolation.

DNA isolation and detection of cyclobutane pyrimidine dimers

DNA extraction from frozen leaf segments, chloroplasts, and nuclei was done as described by Pescheck et al. (2014). In the case of DNA isolation from chloroplasts and nuclei, 500 µl of extraction buffer was added directly to the frozen pellet. The detection of cyclobutane pyrimidine dimers (CPDs) was done as described by Pescheck et al. (2014). UV-B-induced DNA

damage was shown in the graphs as the numbers of detected CPD by immunoblotting per megabase pair of DNA (CPDs Mb⁻¹).

Staining of nucleoids

Leaf cross-sections were produced from the primary foliage leaf of 10 d old plants by a hand microtome at a 2-2.5 cm distance from the tip. Sections were immediately fixed by 4% (w/v) paraformaldehyde in phosphate-buffered saline pH 7.4 (PBS) overnight at 4°C. After washing with buffer, the sections were stained with SYBR®Green (1:5000, S7563 Invitrogen™) for 45 min at room temperature. After washing with 1x PBS, the sections were transferred onto a slide, capped with PBS/glycerol (v/v: 1:1).

Imaging was done at Leica SP5 confocal microscope system with an HCX PL APO CS 63.0 x 1.2 W objective. Excitation was done by an argon laser line at 488 nm (6% power). Emission was detected between 510-570 nm (HV 768V) and 690-760 nm (HV 510V). Z stacks with six layers were taken in a window of 61.57 x 61.57 µm and a depth of 5 µm (1024 x 1024, 8-Bit). A minimum of four stacks out of different regions of the specimen were taken from each sample.

Statistical analysis

UV-B transmittance and UV-B induced DNA lesions in total, nuclear and plastid DNA isolated from leaf segments, nuclei, and chloroplasts, respectively, were compared in wildtype and transgenic plants by the *t*-test. In case of failure in the normality test or equal variance test, the Mann-Whitney Rank Sum test was used by Sigmaplot 13 (Systat Software GmbH, Erkrath, Germany).

Results and discussion

Morphology of nucleoids in chloroplasts

Using laser scanning microscopy, the compaction of nucleoids in the leaves was investigated (Fig. 1A). The observed fluorescence signals from chloroplast nucleoids and nuclei were similar to those reported previously (Krupinska et al., 2014). Microscopic analysis of nucleoid morphology (Fig. 1A) revealed that the major portion of the nucleoid population in the chloroplasts of transgenic barley plants with an RNAi-mediated knockdown of WHIRLY1 (W1)

was obviously less compact than that of wild-type plants (WT). The residual amount of WHIRLY1 in these plants, amounting to about 1% of the wild type level, likely was responsible for packaging of few nucleoids resulting in a rather heterogeneous nucleoid morphology (Krupinska et al. 2014). The repeated staining of nucleoids confirmed that this trait is preserved in plants of the barley W1 line used in this study.

UV-B screening in leaves

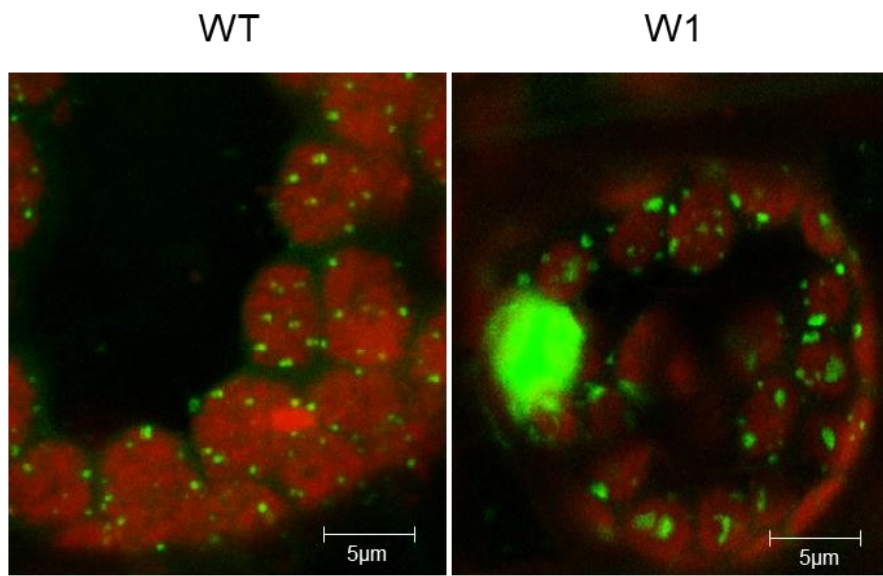
In order to investigate whether UV-screening of the leaves used for isolation of chloroplasts and nuclei differed between W1 and WT plants, the epidermal UV-B transmittance was investigated. Although the thickness of leaves differed between WHIRLY1 deficient and wild-type leaves (Saeid Nia et al., 2022), no significant difference in epidermal UV screening was detected (Fig. 1B). Similarly, and in accordance with this result, it was shown by Saeid Nia et al. (see Chapter IV) that WT and W1 plants did not differ in their content of flavonoids being one of the main groups of screening pigments (Agati et al., 2009). Altogether, these results suggest that the same amount of UV-B could penetrate through the epidermis and reach the mesophyll cells in the WT and W1 plants.

DNA lesions in plastid, nuclear and total DNA

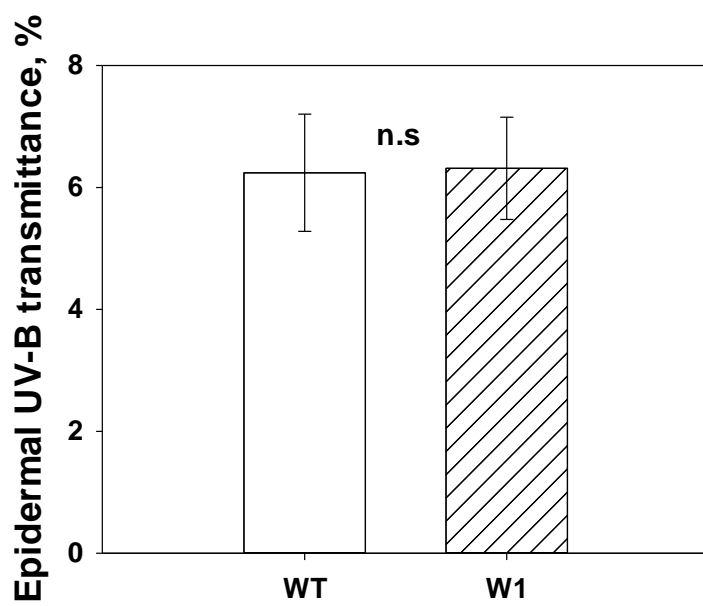
After UV-B exposure, no significant differences between genotypes in CPDs were detected in DNA isolated from UV-B-exposed primary leaves (Fig. 1C). Exposed to a similar amount of UV-B, nuclei were shown to be 60 times more sensitive than the leaves, but also here, no significant differences between WT and W1 mutant were detected. However, in chloroplasts, W1 mutants displayed a three times higher CPD formation than the WT (Fig. 1C). Nucleoid compaction by WHIRLY1 in WT plants decreased the volume exposed to UV-B radiation. In contrast, WHIRLY1 deficiency caused loosely packed nucleoids with a higher volume in the chloroplasts which consequently have a higher chance to get hit by UV-B (Ballarini, 2010). Moreover, since in this study the experimental setup that kept isolated chloroplasts and nuclei on ice during UV-B exposure, strongly minimized the contribution of any enzymatic repair processes to the impact of UV-B on DNA, our results suggest that WHIRLY1 in barley chloroplasts protects ptDNA against UV-B-induced formation of CPDs most probably by its structural impact on the compactness of nucleoids. This reminds to the situation in the

radiation-resistant bacterium *Deinococcus radiodurans*, where a mutant lacking a histone-like protein binding to DNA was much more sensitive to UV exposure than the wild type (Wang et al., 2012).

(A)



(B)



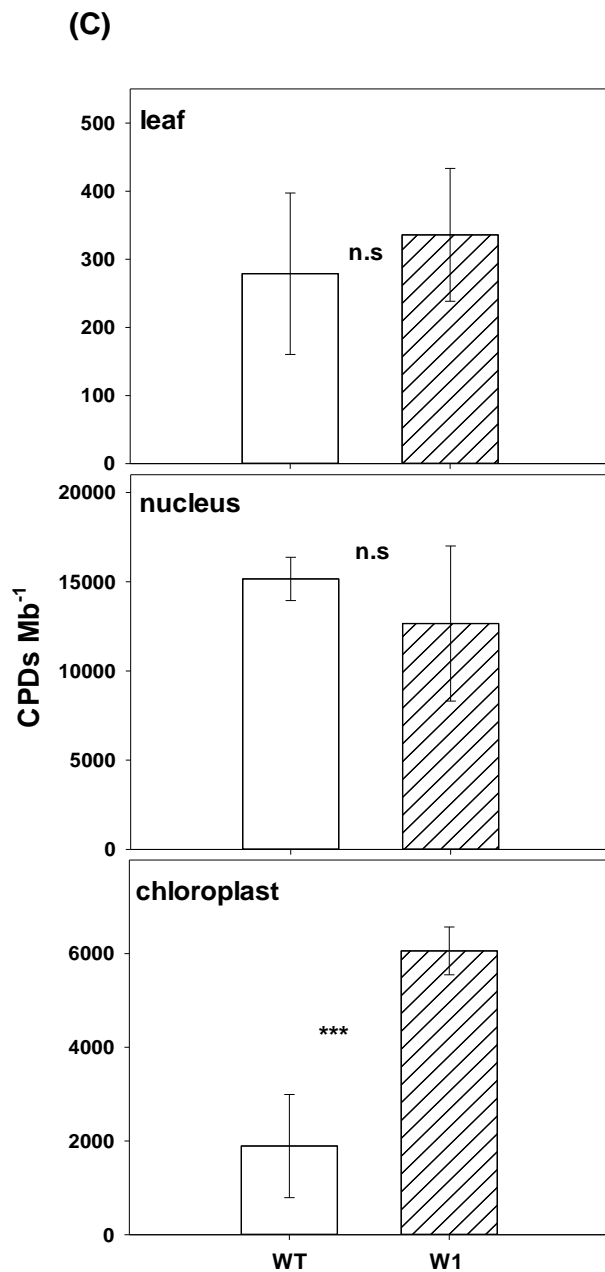


Fig. 1 (A) Staining of chloroplast nucleoids in leaf sections from WT and W1 plants by SYBR Green. The bar represents 5 μm . (B) Epidermal UV-B transmittance in percent measured in WT and W1 plants. Columns are means \pm standard deviation of $n=20-21$ leaves from three independent experiments, each comprising 6-7 leaves. (C) Total DNA lesion, detected as CPDs Mb^{-1} , induced by UV-B exposure of primary leaves, nuclei, and chloroplasts. Columns are means \pm standard deviation of 12-13 leaves, 14 nuclei samples (each sample is a pool of at least 6 samples), and 6 chloroplast samples (each sample is a pool of at least 6 samples) from three independent UV-B exposure experiments, each comprising 4-5 leaves, 4-5 nuclei samples, and 2 chloroplast samples, respectively. Statistical significance was tested for epidermal transmittance and CPDs in chloroplasts using a t -test. For CPDs detected in leaves and nuclei, a Mann-Whitney rank sum test was used. n.s, not significant; *** $p < 0.001$.

In comparison to chloroplasts, CPD formation in nuclei was not significantly different in nuclei prepared from the WHIRLY1 deficient plants than in WT. The function of WHIRLY1 in the nucleus is different than in chloroplasts. The packaging of DNA in the nucleus is mediated by histones and the chromatin compaction is regulated by posttranslational modifications of histones. WHIRLY1 is known as the repressor or activator of nuclear genes and has been found to bind to promoters of stress responses and senescence-associated genes (Krupinska et al., 2022). WHIRLIES might contribute to the regulated accessibility of promoters for transcription factors (Krupinska et al., 2022), but they obviously don't play a role as chromatin architects in the nucleus. Accordingly, and by considering the physical protecting role of WHIRLY1 via its architectural role, presence or absence of WHIRLY1 protein in the nuclei (in WT and W1 plants, respectively) most probably might not have any effect on UV-BR-induced CPD formation in nuclear DNA.

The absolute CPD formation was in intact leaves much lower than in the isolated organelles. This difference reflects the presence of UV screening compounds and the complex optical properties within leaves. Furthermore, the leaf damage mirrors the proportions between nuclear and organellar DNA, which are about 50% for each. This diluted presumably the difference between WT and W1 that would follow from the chloroplast data.

Comparison between UV-B induced CPD formation in nuclear and plastid DNA showed that although nuclear DNA was irradiated with two times of the dose received by the plastid DNA, it showed a roughly 10 times higher damage. An explanation of the reduced damage in chloroplasts could be the absorption of UV-B radiation by chlorophyll. The absorption spectra of chlorophyll *a* and *b* reach well into the UV-B spectral region (Bilger et al., 2001) and it has even been speculated that chlorophyll might initially in the evolution have served as UV-protectant before it was recruited by photosynthesis as a light-harvesting pigment (Mulkidjanian & Junge, 1997). Therefore, the chlorophyll in the chloroplast suspension may have competed effectively with the plastid DNA for absorption of UV-B radiation.

It is well-known that chloroplast nucleoids are dynamic structures changing in shape and organization during development and likely also in response to environmental change. In this study it has been shown for the first time that the high compactness of nucleoids can effectively prevent the formation of CPDs, the most important lesions induced by UV-BR. The

importance of nucleoid restructuring during plant responses to environmental change deserves more attention in research.

Author contributions

MSN, WB, and KK conceived and designed the research. Material preparation and conduction of experiments (except detection of nucleoids and quantification of fluorescence signal areas which was done by CD) were performed by MSN with assistance of FP. Graphs and statistical analysis were performed by MSN. The first draft of the manuscript was written by MSN. All authors commented and revised the first version of the manuscript. All authors read and approved the final manuscript.

Acknowledgments

We greatly thank Luca Boschian (Institute of Botany, CAU Kiel, Germany) for his support during isolation of chloroplasts and nuclei. The technical assistance of Ulrike Voigt (Institute of Botany, CAU Kiel, Germany) who prepared seeds is acknowledged. Louis Scholz (Institute of Botany, CAU Kiel, Germany) is acknowledged for his help in measuring leaf epidermal transmittance.

Data availability statement

The data that support the findings of this study are available in the Supplementary Information of this article. The raw datasets in this study are available from the first author or corresponding author on reasonable request.

References

- Agati, G., Stefano, G., Biricolti, S. & Tattini, M. (2009) Mesophyll distribution of “antioxidant” flavonoid glycosides in *Ligustrum vulgare* leaves under contrasting sunlight irradiance. *Annals of Botany*, 104 (5), 853–861
- Ballarini, F. (2010) From DNA radiation damage to cell death: theoretical approaches. *Journal of Nucleic Acids*. 2010:350608
- Bilger, W., Johnsen, T. & Schreiber, U. (2001) UV-excited chlorophyll fluorescence as a tool for the assessment of UV-protection by the epidermis of plants. *Journal of Experimental Botany*, 52 (363), 2007–2014

- Burchard, P., Bilger, W. & Weissenböck, G. (2000) Contribution of hydroxycinnamates and flavonoids to epidermal shielding of UV-A and UV-B radiation in developing rye primary leaves as assessed by ultraviolet-induced chlorophyll fluorescence measurements. *Plant Cell & Environment*, 23 (12), 1373–80
- Cannon, G.C., Ward, L.N., Case, C.I. & Heinhorst, S. (1999) The 68 kDa DNA compacting nucleoid protein from soybean chloroplasts inhibits DNA synthesis in vitro. *Plant Molecular Biology*, 39 (4), 835-845
- Frohnmeier, H. & Staiger, D. (2003) Ultraviolet-B radiation-mediated responses in plants. balancing damage and protection. *Plant Physiology* 133 (4), 1420–1428
- Gruissem, W., Greenberg, B.M., Zurawski, G. & Hallick, R.B. (1986) Chloroplast gene expression and promoter identification in chloroplast extracts, in: *Methods in Enzymology, Plant Molecular Biology*. Academic Press, pp. 253–270
- Hołówka, J. & Zakrzewska-Czerwińska, J. (2020) Nucleoid associated proteins: the small organizers that help to cope with stress. *Frontiers in Microbiology*, 11:590.
- Jansen, M.A.K., Gaba, V. & Greenberg, B.M. (1998) Higher plants and UV-B radiation: balancing damage, repair and acclimation. *Trends in Plant Sciences* 3, 131-135
- Kobayashi, Y., Takusagawa, M., Harada, N., Fukao, Y., Yamaoka, S., Kohchi, T., Hori, K., Ohta, H., Shikanai, T. & Nishimura, Y. (2016) Eukaryotic components remodelled chloroplast nucleoid organization during the green plant evolution. *Genome Biology and Evolution*, 8 (1), 1-16
- Krupinska, K., Desel, C., Frank, S. & Hensel, G. (2022) WHIRLIES are multifunctional DNA binding proteins with impact on plant development and stress resistance. *Frontiers in Plant Sciences*, 13:880423
- Krupinska, K., Oetke, S., Desel, C., Mulisch, M., Schäfer, A., Hollmann, J., Kumlehn, J. & Hensel, G. (2014) WHIRLY1 is a major organizer of chloroplast nucleoids. *Frontiers in Plant Science*, 5:432
- Melonek, J., Oetke, S. & Krupinska, K. (2016) Multifunctionality of plastid nucleoids as revealed by proteome analyses. *Biochimica et Biophysica Acta-Proteins and Proteomics*, 1864 (8), 1016-1038
- Mitchell, D.L. & Nairn, R.A. (1989) The biology of the (6-4) photoproduct. *Photochem and Photobiology*, 49 (6), 805–819

- Mulkidjanian, A.Y. & Junge, W. (1997) On the origin of photosynthesis as inferred from sequence analysis. *Photosynthesis Research*, 51, 27–42
- Oetke, S., Scheidig, A. & Krupinska, K. (2022) WHIRLY1 of barley and maize share a PRAPP motif conferring nucleoid compaction. *Plant Cell Physiology*, 63 (2), 234–247
- Pescheck, F., Bischof, K. & Bilger, W. (2010) Screening of ultraviolet-A and ultraviolet-B radiation in marine green macroalgae (chlorophyta). *Journal of Phycology*, 46 (3), 444–455
- Pescheck, F., Lohbeck, K.T., Roleda, M.Y. & Bilger, W. (2014) UVB-induced DNA and photosystem II damage in two intertidal green macroalgae: Distinct survival strategies in UV-screening and non-screening Chlorophyta. *Journal of Photochemistry and Photobiology, B: Biology* 132, 85–93
- Pilartz, M. & Jeske, H. (2003) Mapping of Abutilon Mosaic Geminivirus Minichromosomes. *Journal of Virology*, 77, 10808–10818
- Powikrowska, M., Oetke, S., Jensen, P.E. & Krupinska, K. (2014) Dynamic composition, shaping and organization of plastid nucleoids. *Frontiers in Plant Science*, 5:424
- Saeid Nia, M., Repnik, U., Krupinska, K., Bilger, W. (2022) The plastid-nucleus localized DNA-binding protein WHIRLY1 is required for acclimation of barley leaves to high light. *Planta* 255,84.
- Strid, Å., Chow, W.S. & Anderson, J.M. (1994) UV-B damage and protection at the molecular level in plants. *Photosynthesis Research*, 39 (3), 475–489
- Takahashi, M., Teranishi, M., Ishida, H., Kawasaki, J., Takeuchi, A., Yamaya, T., Watanabe, M., Makino, A. & Hidema, J. (2011) Cyclobutane pyrimidine dimer (CPD) photolyase repairs ultraviolet-B-induced CPDs in rice chloroplast and mitochondrial DNA. *The Plant Journal*, 66 (3), 433–442
- Takahashi, S., Nakajima, N., Saji, H. & Kondo, N. (2002) Diurnal change of cucumber CPD photolyase gene (*CsPHR*) expression and its physiological role in growth under UV-B irradiation. *Plant and Cell Physiology*, 43 (3), 342–349
- Veit, M., Bilger, W., Mühlbauer, T., Brummet, W. & Winter, K. (1996) Diurnal Changes in Flavonoids. *Journal of Plant Physiology* 148, 478–482
- Wang, H., Wang, F., Hua, X.T., Ma, T.T., Chen, J.H., Xu, X., Wang, L.Y., Tian, B. & Hua, Y.J. (2012) Genetic and biochemical characteristics of the histone-like protein DR0199 in *Deinococcus radiodurans*. *Microbiology*, 158 (4), 936–943

Chapter III: WHIRLY1 protein and high light acclimation



The plastid-nucleus localized DNA-binding protein WHIRLY1 is required for acclimation of barley leaves to high light

Monireh Saeid Nia¹ · Urska Repnik² · Karin Krupinska¹ · Wolfgang Bilger¹

Received: 23 December 2021 / Accepted: 11 February 2022 / Published online: 13 March 2022
 © The Author(s) 2022

Abstract

Main conclusion In accordance with a key role of WHIRLY1 in light-acclimation mechanisms, typical features of acclimation to high light, including photosynthesis and leaf morphology, are compromised in WHIRLY1 deficient plants.

Abstract Acclimation to the environment requires efficient communication between chloroplasts and the nucleus. Previous studies indicated that the plastid-nucleus located WHIRLY1 protein is required for the communication between plastids and the nucleus in situations of high light exposure. To investigate the consequences of WHIRLY1 deficiency on the light acclimation of photosynthesis and leaf anatomy, transgenic barley plants with an RNAi-mediated knockdown of *HvWHIRLY1* were compared to wild-type plants when growing at low and high irradiance. While wild-type plants showed the typical light acclimation responses, i.e. higher photosynthetic capacity and thicker leaves, the WHIRLY1 deficient plants were not able to respond to differences in irradiance. The results revealed a systemic role of WHIRLY1 in light acclimation by coordinating responses at the level of the chloroplast and the level of leaf morphology.

Keywords WHIRLY1 · High light acclimation · Photosynthetic capacity · Carboxylation efficiency · RubisCO abundance · Leaf thickness · Leaf mass per area (LMA)

Introduction

Due to their sessile way of life, plants continuously encounter dynamic environmental conditions and their survival depends on appropriate responses to these variations (Nelson and Ben-Shem 2004; Dietzel and Pfannschmidt 2008). Chloroplasts are important sensors of environmental changes (Kleine et al. 2021) such as high light (Munné-Bosch 2019). Compounds produced by chloroplasts act as retrograde signals regulating nuclear gene expression to allow for acclimation to the environment (Chan et al. 2016; Pfannschmidt

et al. 2020). Plants may encounter stress-induced damage, if the acclimation is not achieved (Dietz 2015).

Acclimation to the environment involves mechanisms ensuring efficient photosynthesis by adjustments in the composition of the photosynthetic apparatus consisting of plastid and nucleus-encoded proteins (Björkman 1981; Race et al. 1999; Allen et al. 2011) as well as by changes in the morphology of leaves (Givnish 1988; Terashima et al. 2006; Poorter et al. 2009; 2019) such as increased leaf thickness and leaf mass per area (LMA).

Plants acclimated to high irradiance have a higher photosynthetic capacity, defined as leaf area-based light and CO₂ saturated rate of CO₂-fixation, than low light acclimated plants (Boardman et al. 1975; Lichtenthaler et al. 2007; Athanasiou et al. 2010). Acclimation involves changes in the abundance or organization of protein complexes in thylakoid membranes (Zivcak et al. 2014), a higher rate of electron transport (Leong and Anderson 1984a; Evans, 1987), higher levels of photosystem II (PSII), cytochrome b/f complex (Leong and Anderson 1984a, b), together with higher photophosphorylation

Communicated by Anastasios Melis.

✉ Karin Krupinska
 kkrupinska@bot.uni-kiel.de

¹ Institute of Botany, Christian-Albrechts-University, Kiel, Germany

² Central Microscopy, Department of Biology, Christian-Albrechts-University, Kiel, Germany

rate (Murchie and Horton 1997) as well as a greater concentration of different components of the Calvin–Benson cycle, especially ribulose-1,5-bisphosphate carboxylase/oxygenase (RubisCO) (Leong and Anderson 1984a, b; Foyer et al. 2012; Vialet-Chabrand et al. 2017; Poorter et al. 2019).

The acclimation of photosynthesis in response to changes in the environment is based on massive changes in gene expression. The majority of about 3000 different plastid proteins is nuclear-encoded. Their transcription during high light is controlled by various signal compounds produced by chloroplasts such as ROS, cyclocitral, methylerythriol cyclodiphosphate (MEcPP), and phosphoadenosine 5'-phosphate (PAP) (Pfannschmidt et al. 2020). In recent years, it became obvious that also dually located plastid-nucleus proteins such as the DNA binding protein WHIRLY1 are involved in the communication between chloroplasts and the nuclear genomes (Bobik and Burch-Smith 2015; Krupinska et al. 2020). In transplastomic tobacco plants, WHIRLY1 was shown to translocate from chloroplasts to the nucleus (Isemer et al. 2012). It has been hypothesized that the translocation of WHIRLY1 from chloroplasts to the nucleus is induced upon stress-associated redox changes in the photosynthetic apparatus (Foyer et al. 2014). To investigate its role in plastid-nucleus communication, barley plants with a very strongly reduced level of WHIRLY1 were prepared by RNAi-mediated knockdown of *HvWHIRLY1* (Krupinska et al. 2014). Leaves of one of these lines, i.e. RNAi-WHIRLY1-7, contain only about 1–5% of the WHIRLY1 amount of wild-type leaves (Krupinska et al. 2014). These plants showed retardation of all phases of leaf development including senescence. While high irradiance was able to promote senescence of wild-type leaves, it barely affected the senescence of the WHIRLY1 deficient plants (Kucharczewicz et al. 2017). When the WHIRLY1 deficient plants were grown in continuous light of different irradiances, their leaves showed severe symptoms of oxidative stress (Swida-Barteczka et al. 2018) such as bleaching, reduction of PSII efficiency, and the accumulation of ROS. The severity of these symptoms, that are typical for oxidative stress resulting from excess excitation energy in chloroplasts, correlated with the amount of residual WHIRLY1. The phenotype of the WHIRLY1 deficient leaves suggested that they are impaired in acclimation to light.

This study aimed to investigate the involvement of WHIRLY1 in retrograde signaling during high light acclimation of the photosynthetic apparatus in more detail. For this purpose, photosynthetic parameters such as CO₂ assimilation rate, RubisCO content, and its *in vivo* activity were characterized in both WHIRLY1 deficient and wild-type leaves at different irradiances and different developmental stages. In addition, acclimation was investigated at the level of leaf morphology. The results revealed that acclimation of

the photosynthetic apparatus as well as of leaf morphology require a high abundance of the WHIRLY1 protein.

Materials and methods

Plant material and growth conditions

Grains of *Hordeum vulgare* L., cv. “Golden Promise” wild-type (WT) and the WHIRLY1 deficient plants prepared by RNAi-mediated knockdown of *HvWHIRLY1* (W1) (Krupinska et al. 2014) were sown in soil (Einheitserde ED73, Einheitswerk Werner Tantau, Uetersen, Germany). Pots were kept in darkness at 6 °C for three days to synchronize germination and were then transferred to climate chambers (Johnson Control, Mannheim, Germany) equipped with ceramic metal halide lamps (CMT360LS WBH EYE Iwasaki Electric Co., Japan). Plants were grown in a light/dark regime of 16/8 h, and a temperature of 21 °C and ca. 60% air humidity. Photosynthetic photon flux densities incident on the leaf surface were either 350–500 $\mu\text{mol m}^{-2} \text{s}^{-1}$ (high light, HL) or 40–70 $\mu\text{mol m}^{-2} \text{s}^{-1}$ (low light, LL), which corresponded to horizontal irradiances of 1000 or 150 $\mu\text{mol m}^{-2} \text{s}^{-1}$. Irradiances incident on the adaxial and abaxial sides of the leaves were measured using a quantum sensor (Li-185 A, Li-Cor Biosciences, Lincoln, NE, USA). This was done for every individual primary leaf. The area between 1.5 and 3 cm below the tip of the primary leaves was used for all measurements. Ten-day-old primary leaves were used for most measurements if not otherwise mentioned.

Gas exchange measurements

Light dependences of the CO₂ assimilation rate (*A*) at the constant CO₂ concentration of 1500 ppm and *A/C_i* curves at a PPFD of either 1000 $\mu\text{mol m}^{-2} \text{s}^{-1}$ or 1500 $\mu\text{mol m}^{-2} \text{s}^{-1}$ (selected based on preliminary measurements of photosynthetic light dependencies with the aim to assure light saturation but to avoid photoinhibitory damage) were measured by a portable Gas Exchange Fluorescence System GFS-3000 (Heinz Walz GmbH, Effeltrich, Germany). The instrument was set up at 750 $\mu\text{mol min}^{-1}$ flow rate, a cuvette temperature of 21 °C, and 60% relative humidity. Attached primary leaves of both genotypes grown either in HL or LL were measured at different developmental stages from day 10 until day 19. A stable photosynthesis rate was induced at 380 ppm CO₂ and a PPFD of 100 $\mu\text{mol m}^{-2} \text{s}^{-1}$ for about 10 min, followed by a stepwise increase in irradiance until light saturation of photosynthesis was reached. Afterwards, CO₂ was reduced from 380 to 50 ppm in five steps. The *in vivo* activity of RubisCO can be indicated by the carboxylation efficiency (CE) of RubisCO, and calculated as the initial slope of the *A/C_i* curve determined at an internal CO₂

concentration (C_i) below 200 ppm (von Caemmerer and Farquhar 1981; Cheng and Fuchigami 2000). CO_2 concentration was set back to 380 ppm and increased stepwise to a maximum of 2000 ppm to measure the photosynthetic capacity (P_{max}) which is defined here as the light and CO_2 saturated rate of CO_2 -fixation per leaf area (Oguchi et al. 2003; Athanasiou et al. 2010; Townsend et al. 2018) and was measured at light saturation in the presence of 2000 ppm CO_2 .

The leaf segment area included in the cuvette was determined from a photograph using ImageJ software (US National Institutes of Health, Bethesda, Maryland, USA) to correct the photosynthetic rate according to the equations provided in the manual (Walz GmbH). Errors that might be caused by CO_2 absorption in the cuvette at very low CO_2 concentrations were corrected by measuring the same parameters, as done for leaves, in the absence of a leaf according to Long and Bernacchi (2003).

Leaf segments used for gas exchange measurements were frozen in liquid nitrogen and kept in a freezer at $-80\text{ }^\circ\text{C}$ to be later analysed for their RubisCO content (see the section on determination of RbcL abundances by SDS-PAGE).

Non-invasive measurements of chlorophyll contents

Chlorophyll contents were measured non-invasively by a Dualex Scientific instrument (Force A, Paris, France). Measurements at three points between 1.5 and 3 cm below the tip in each leaf were averaged. Readings of the Dualex instrument were calibrated by extraction of leaf segments and determination of chlorophyll contents by HPLC (see below). The calibration function determined by linear regression was $\text{Chl} [\text{nmol cm}^{-2}] = 1.0381 \times \text{Dualex reading} + 8.7495$.

HPLC analysis of chlorophyll contents

Exactly 1 cm long leaf segments from the area between 1.5 and 3 cm below the tip were cut in the climate chamber under growth irradiance. After a quick determination of the segments' widths, they were immediately frozen in liquid nitrogen and stored at $-80\text{ }^\circ\text{C}$. To extract pigments, frozen segments were ground with 0.9 ml 80% (v/v) acetone (prepared with an aqueous solution of 30 mM Tris-buffered at pH 7.8) and 5–6 glass beads in a Geno Grinder (Type 2000; SPEX CertiPrep, Munich, Germany). After centrifugation for six minutes at 12,000 rpm at $4\text{ }^\circ\text{C}$ (Kendro Biofuge fresco, Osterode, Germany), the pellets were extracted two more times with 0.3 ml of pure acetone. Finally, 0.05 ml of the combined supernatants were used for pigment analysis using an Agilent 1100 HPLC system (Waldbronn, Germany). As described by Nichelmann et al. (2016), pigment separation was done using a Hypersil ODS-column (4.6×250 mm, 5 μm particle size, Thermo Fisher Scientific Inc., Waltham, U.S.A.) using a mobile phase consisting of a gradient from

25% solvent A (10 mM Tris buffer (Roth) at pH 7.8) to 100% solvent B (100% acetone (Roth)). Chl *a* and *b* were identified through their retention time and absorption spectra monitored by a photodiode array detector (Agilent). Chlorophyll *a* and *b* were externally calibrated using the equations of Porra et al. (1989). For further details, see Nichelmann et al. (2016).

Determination of the amount of the large subunit of RubisCO (RbcL) by SDS-PAGE

Proteins were extracted from a pool of 3–6 leaf segments. SDS-PAGE was performed with samples adjusted to five different protein concentrations (20, 15, 8, 4, and 2 μg per lane) using 16% (w/v) polyacrylamide gels (Laemmli 1970). Gels were stained in colloidal Coomassie (Dyballa and Metzger 2009). To estimate the amount of RubisCO, gel photographs were analyzed by ImageJ software. Signal intensities of different bands were plotted against protein concentrations loaded on the gels. For the initial linear relationship between both parameters, a linear regression was calculated and its slope considered as the relative amount of RubisCO per protein. This was then related to leaf area by multiplication with the amount of total proteins per leaf area (relative content of RubisCO cm^{-2}). All the values were normalized to the relative amount of RubisCO in low light-grown WT plants at day 10 (as 100%) in each independent experiment and accordingly, the final values are presented as % relative RubisCO cm^{-2} .

Leaf morphology

Leaf cross section

Resin embedding for morphological and ultrastructural analyses

A mid part of a primary foliage leaf was cut into several 2–3 mm broad transverse stripes and fixed with 1% glutaraldehyde in 200 mM HEPES, pH 7.4, initially under moderate vacuum pressure. For resin embedding, stripes were cut further into 2–3 mm broad longitudinal segments. These were post-fixed with 1% osmium tetroxide (Roth, Karlsruhe, Germany) in 1.5% aqueous potassium ferricyanide (Merck, Darmstadt, Germany) for 1 h on ice, followed by incubation with 2% aqueous uranyl acetate (Science Services, München, Germany) for 1.5 h at room temperature, protected from light. Tissue was dehydrated using a graded ethanol series (50–70–80–90–96–100%), each step for 15–30 min, followed by acetone (100%), 2×30 min, and then gradually infiltrated with epoxy resin diluted with acetone (25–50–75–100%), each step for minimum 12 h. Finally, tissue was flat embedded in silicone molds and resin was heat polymerised at $70\text{ }^\circ\text{C}$ for 24 h. Sections were cut

using a Leica UC7 ultramicrotome and Diatome diamond knives.

Semithin, 500-nm epon sections were transferred on water drops onto Superfrost Plus glass slides (Gerhard Menzel GmbH, Braunschweig, Germany), which were placed on a heated plate (90 °C) to allow water to evaporate and sections to adhere. Adhered sections were stained with Richardson's solution (alkaline solution of azure II and methylene blue (Sigma-Aldrich)) for about 60 s at 90 °C and then washed with water. Stained sections were mounted with a Leica CV mount reagent, and imaged in a Zeiss Primostar upright microscope equipped with an AxioCam 105 color camera and the ZEN 3.2 software (Zeiss, Oberkochen, Germany), using 10× and 40× Plan-Achromat objectives.

Leaf thickness

Leaf thickness was determined in manual cross-sections by bright field microscopy (Microscope: AxioPhot, Plan-Apochromat, 10×/0.45, Zeiss; camera: Olympus DP7, Olympus, Japan; image recorded by cell[^]F software version 5.1, Olympus) for two sections per sample and the average of these two measurements was used.

Leaf mass per area (LMA)

The LMA was calculated as the ratio between leaf dry mass and area. Leaf segments taken at 1.5–3 cm below the tip were scanned and the area determined using the Sigma Scan Pro 5 software (Systat Software, San José, CA). Afterwards, the leaf segments were dried in a laboratory oven at 60 °C for 24 h before dry weight was determined on a lab scale (AW-224, Sartorius, Germany).

Transmission electron microscopy (TEM) for analysis of cytoplasm/cell volume

Ultra-thin, 80-nm epon sections were transferred onto formvar coated slot grids, and contrasted with saturated aqueous uranyl acetate for 10 min, followed by 0.2% lead citrate for 3 min. Sections were inspected in a Tecnai G2 Spirit BioTWIN transmission electron microscope (FEI, now Thermo Fisher Scientific), operated at 80 kV, and equipped with a LaB6 filament, an Eagle 4 k×4 k CCD camera and a TIA software (both FEI, now Thermo Fisher Scientific).

The volume fraction of cytoplasm in mesophyll cells was determined by a stereological analysis of electron micrographs. Images were collected at 890× magnification by systematic uniform random (SUR) sampling. In the Fiji software (Schindelin et al. 2012), 15 and 30 μm² square test grids were used for point counting to estimate the area of the cytoplasm and of cell profiles, respectively. For each leaf, between 15 and 23 electron micrographs were analysed. The

cytoplasm to cell volume fraction was calculated as a ratio between the total count of points over the cytoplasm and the total count of points over the reference area of cells. For each sample group, at least three leaves were analysed to obtain three estimates.

Statistical analysis

For the statistical analysis, Sigmaplot 13 (Systat Software GmbH, Ekrath, Germany) or GraphPad PRISM (Prism 9 for Windows, version 9.2.0 (332), GraphPad software, San Diego, California USA) was used. One-way, two-way (with the factors of genotype and light conditions), or three-way ANOVA (with the factors of genotype, light conditions, and age) were used to analyze the data and the Holm–Sidak method was used for post hoc analysis. All the graphs were prepared using Sigmaplot 13 software.

Results

Photosynthetic gas exchange

Light dependency of CO₂ assimilation

The CO₂ assimilation rate (*A*) at saturating light (in the presence of 380 ppm CO₂) in barley wild-type (WT) plants showed significantly (analyzed for the *A* values at maximum irradiance by two-way ANOVA, Tab. S1, *P* < 0.001) higher values for plants grown in high light in comparison to low light at day 10 (Fig. 1a).

While photosynthesis of 10-day-old wild-type plants showed significant responses to growth irradiance, WHIRLY1-deficient transgenic plants (W1) did not show acclimation and had even significantly (*P* = 0.008) lower rates of CO₂ assimilation when grown under HL than LL (Fig. 1b). Both, in HL and LL, the CO₂ assimilation rates of the WHIRLY1 deficient plants were significantly (*P* < 0.001) lower than those of the wild type (Fig. 1b).

A/C_i curve

To further analyze photosynthesis, CO₂ assimilation rate was measured at saturating irradiance employing different CO₂ concentrations. The increased assimilation rate in wild-type plants grown under high light in comparison to those from low light was especially obvious in the presence of a high CO₂ concentration (Fig. 2a). In the WHIRLY1 deficient plants, no acclimation of CO₂ assimilation rate was detectable (Fig. 2b). High light-grown W1 plants showed even lower *A* than LL-grown plants, indicating potential photoinhibitory damage.

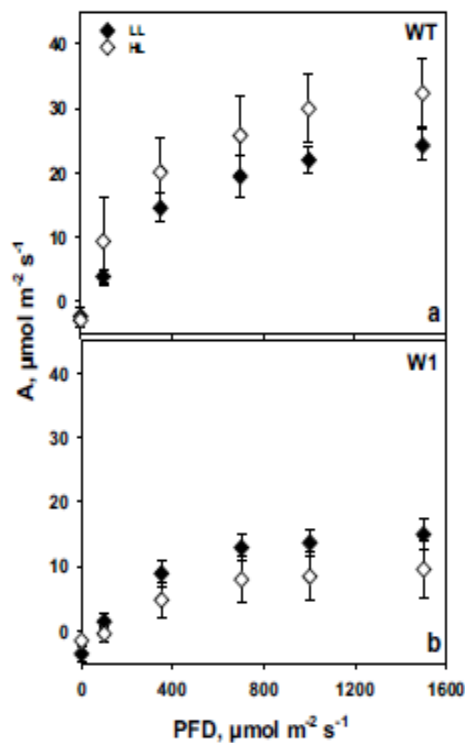


Fig. 1 CO₂ assimilation rate as a function of incident irradiance (PFD) measured in the presence of 380 ppm CO₂ in LL (filled symbols) and HL (open symbols) grown plants for both WT (a) and W1 (b) at day 10 after sowing. Depicted values are means \pm standard deviation of $n=9-15$ leaves in total from three independent experiments each comprising 3–5 leaves

Besides the large difference in CO₂ saturated assimilation rate, also the initial slope of the A/C_i curves, representing carboxylation efficiency (CE), showed a positive light acclimation in WT leaves and was clearly lower in W1 plants.

Non-invasive analysis of chlorophyll contents

WHIRLY1 deficient plants showed a delayed chloroplast development which was apparent in their chlorophyll contents, which were determined non-invasively (Fig. 3b). In total, 10-day-old WT plants did not show significant differences (Three-way ANOVA, Tab. S2, $P=0.289$) in their leaf chlorophyll content when plants grown under LL and HL were compared (Fig. 3a). However, in contrast to the rather stable chlorophyll content of wild-type plants grown in low light over time (no statistical difference), chlorophyll contents of high light-grown wild-type plants decreased strongly from day 15 to day 19 ($P<0.0001$).

In the W1 plants, chlorophyll content increased significantly ($P<0.0001$, for both LL and HL plants) from day 10 to day 15 (Fig. 3b) which is in accordance with the reported delayed chloroplast development (Krupinska et al. 2019).

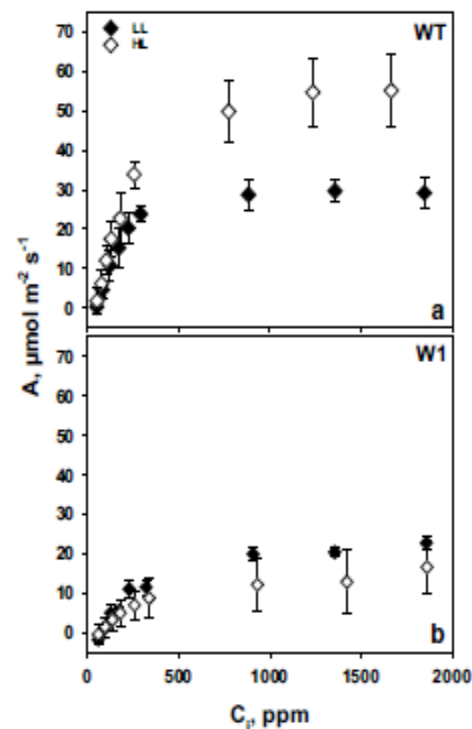


Fig. 2 CO₂ assimilation rate as a function of internal CO₂ concentration (C_i) measured in LL (filled symbols) and HL (open symbols) grown plants for both WT (a) and W1 (b) at day 10 with 1000–1500 $\mu\text{mol m}^{-2} \text{s}^{-1}$ light as the saturating light. Depicted values are means \pm standard deviation of $n=9-15$ leaves in total from three independent experiments each comprising 3–5 leaves

Three-way ANOVA analysis (Tab. S2) showed significant differences between WT and W1 plants grown under either low or high light at days 10 and 15 ($P<0.0001$).

Because of the potential developmental influence on photosynthesis, all CO₂ assimilation rates at different irradiances and CO₂ concentrations were also calculated per chlorophyll content of 10-day-old primary leaves of WT and W1 plants (Supplementary data Fig. S1 and Fig. S2, respectively) and showed similar tendencies as the results calculated per leaf area (Figs. 1 and 2).

Photosynthetic capacity

To further investigate whether the delay in chloroplast development was responsible for the observed differences in photosynthesis, the photosynthetic capacity (P_{max}) and carboxylation efficiency (CE) were also measured in 15- and 19-day-old WT and transgenic plants grown under low and high irradiances.

Wild-type plants grown under high light showed significantly (three-way ANOVA, Tab. S3, $P<0.0001$) higher

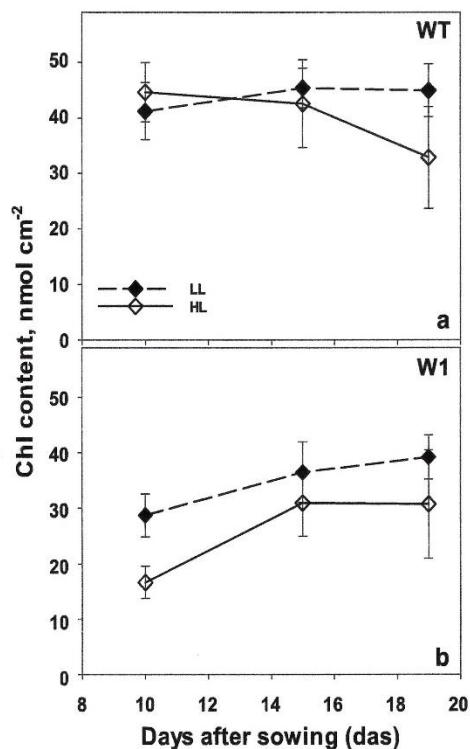


Fig. 3 Chlorophyll content as a function of days after sowing in WT (a) and W1 (b) plants grown under low (LL, filled symbols) and high light (HL, open symbols). Depicted values are means \pm standard deviation of $n=23$ –37 leaves in total from three independent experiments each comprising 7–13 leaves

maximum photosynthesis as compared to the low light-grown WT (Fig. 4a). Despite of the significant difference ($P=0.001$) between HL and LL grown WT plants at day 15, the P_{\max} values decreased in older HL-grown WT leaves and showed similar values (no significant difference, $P=0.999$) as LL-grown WT plants at day 19.

In 10-day-old transgenic plants, P_{\max} values did not differ significantly ($P=0.909$) between plants grown under low and high light. P_{\max} had an increasing tendency at days 15 and 19 showing virtually the same values in both groups (Fig. 4b). In addition, there were no significant differences between WT and W1 plants, neither in LL nor in HL ($P>0.9999$ in both cases) on day 19. However, at days 10 and 15, high light-grown W1 plants showed significantly lower photosynthetic capacity compared to that of WT ($P<0.0001$ and $P=0.0115$, respectively). The results show that even after full leaf development, the photosynthetic capacity of WHIRLY1 deficient HL plants never exceeded that of LL-grown WT plants. The larger difference in photosynthetic capacity at early stages of development is likely caused by the delayed chloroplast development which is also obvious by lower F_v/F_m values (Krupinska et al. 2019).

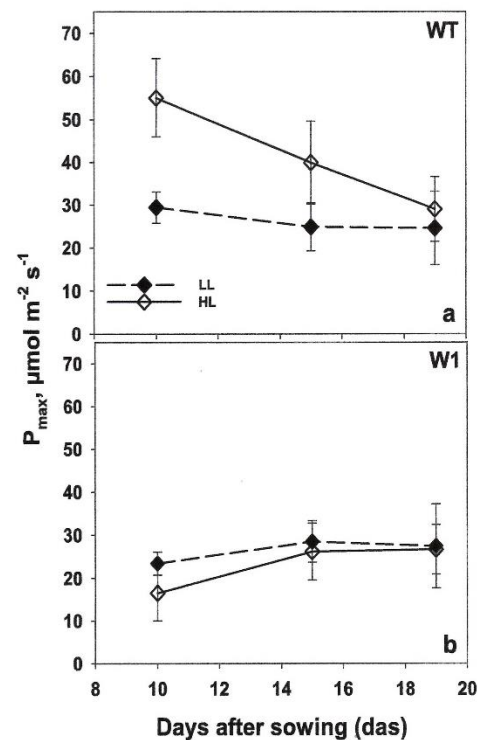


Fig. 4 Maximum photosynthesis of primary foliage leaves of LL (filled symbols) and HL (open symbols) grown plants for both WT (a) and W1 (b) plants as a function of days after sowing in saturating light and at 2000 ppm CO_2 . Depicted values are means \pm standard deviation of $n=9$ –15 leaves in total from three independent experiments each comprising 3–5 leaves

The differences in the responses of photosynthetic capacity of WT and W1 plants to higher irradiance can be clearly seen in the starch granule formation in their chloroplasts (Fig. S3). Only WT plants from HL conditions showed appreciable starch granules.

RubisCO limited photosynthesis

A similar developmentally affected time course was observed when carboxylation efficiency (CE) was calculated (Fig. 5). CE in high light-grown WT plants was significantly (three-way ANOVA, $P<0.0001$) higher than in low light-grown WT plants (Fig. 5a). But afterward, CE values declined to values similar to those of low light-grown ones at day 19 (no significant differences, $P=0.983$ for 15 days and $P=0.504$ for 19 days).

In WHIRLY1 deficient plants, CE in 10-day-old plants from the high light group was significantly (three-way ANOVA, Tab. S4, $P=0.0027$) lower than that of low light-grown plants (Fig. 5b). While CE stayed almost constant from day 10 to 19 in low light plants ($P>0.9999$), these values increased significantly in high light plants from day

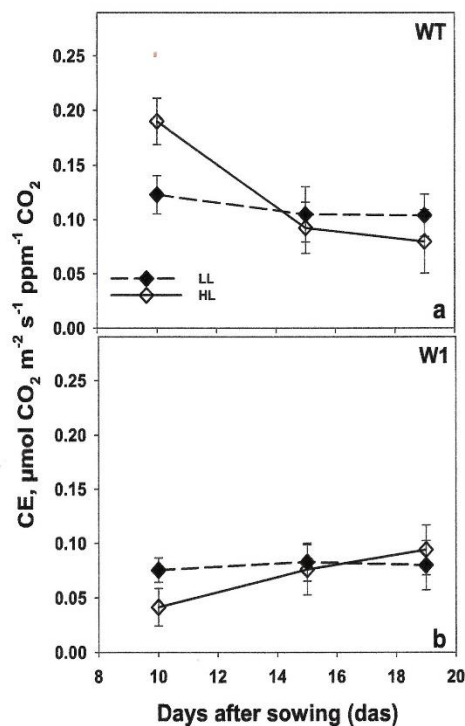


Fig. 5 Carboxylation efficiencies (initial slope of A/C_i curve, CE) as a function of days after sowing in LL (filled symbols) and HL (open symbols) grown plants for both WT (a) and W1 (b). Depicted values are means \pm standard deviation of $n=9-15$ leaves in total from three independent experiments each comprising 3–5 leaves

10 to day 19 ($P < 0.0001$) to become similar to those in LL plants ($P = 0.983$) (Fig. 5b).

In comparison to the wild type, the WHIRLY1 deficient plants at day 10 showed significantly lower CE values grown under either HL or LL ($P < 0.0001$). No significant differences were detected in CE values of WT and W1 plants at day 19 ($P = 0.440$ for LL and $P = 0.985$ for HL plants). While CE values decreased during the development of wild-type leaves, they slowly increased in the WHIRLY1 deficient plants at HL, but not at LL, and never reached the CE values of WT at day 10.

RubisCO abundance

To investigate whether the low RubisCO activity of the WHIRLY1 deficient leaves indicated by CE could be a result of a lower amount of RubisCO, RubisCO abundance was analyzed by SDS-PAGE (Fig. 6a). 10-day-old WT plants grown under high light had higher relative RbcL content in comparison to low light grown ones (Fig. 6b). However, in WT plants, the abundance of large subunits of RubisCO in HL-plants decreased strongly from day 10 to day 19,

whereas it remained rather stable in low light-grown WT plants during this time course (Fig. 6b).

RubisCO contents in LL-grown W1 plants showed similar levels as in LL-grown WT plants at 10 days. Nevertheless, RubisCO abundance in HL-grown transgenic plants remained slightly lower than in LL-grown ones despite an increase from day 10 to day 19 (Fig. 6c) which ultimately reached to similar values as in 10-day-old WT plants. While RbcL abundance decreased during development in the WT, it stayed almost stable in WHIRLY1 deficient leaves being in accordance with the observation that senescence processes negligibly respond to HL in the WHIRLY1 deficient plants (Kucharewicz et al. 2017).

RubisCO abundance and carboxylation efficiency

To investigate if carboxylation efficiency was dependent on the RubisCO amount, CE calculated for day 10, 15, and 19 was plotted against the relative RbcL content per leaf area, derived from SDS-PAGE, in the corresponding leaf segments (Fig. 7).

Overall, there was a correlation between RubisCO protein contents and CE in the high light-grown plants. In contrast, the RubisCO amount had no effect on carboxylation efficiency in LL plants. The slopes of the regression lines for the LL-grown plants did not differ significantly from zero (dotted regression lines shown in Fig. 7). However, data points from LL-grown WT leaves were shifted to higher CE values as compared to those of W1 plants. The same was observed for HL-grown plants.

Apparently, CE is not only dependent on the RubisCO abundance, but also on other factors, presumably the activation state of the enzyme.

Leaf cross-sections and leaf mass per area (LMA)

Part of high light acclimation of area-based photosynthesis is normally due to increases in leaf thickness (Givnish 1988; Murchie et al. 2005). In bifacial leaves, especially the palisade parenchyma increases (Lichtenthaler et al. 1981). Therefore, leaf anatomy was also investigated to further analyze the reasons for the lack of HL acclimation in W1 plants.

Leaf thickness and mass per area were determined for 15- and 19-day-old plants (Fig. 8). As expected, leaf thickness did not further change after day 10. While W1 leaves from both LL and HL had a thickness not different from that of LL grown WT leaves (Fig. 8c, d) (three-way ANOVA, Tab. S5, $P > 0.9999$ in case of all 3 days), HL-grown WT leaves were about 20% thicker than LL grown leaves ($P = 0.0002$, $P = 0.0005$ and, $P < 0.0001$ for days 10, 15 and, 19, respectively) (Fig. 8c). This was not caused by an increased

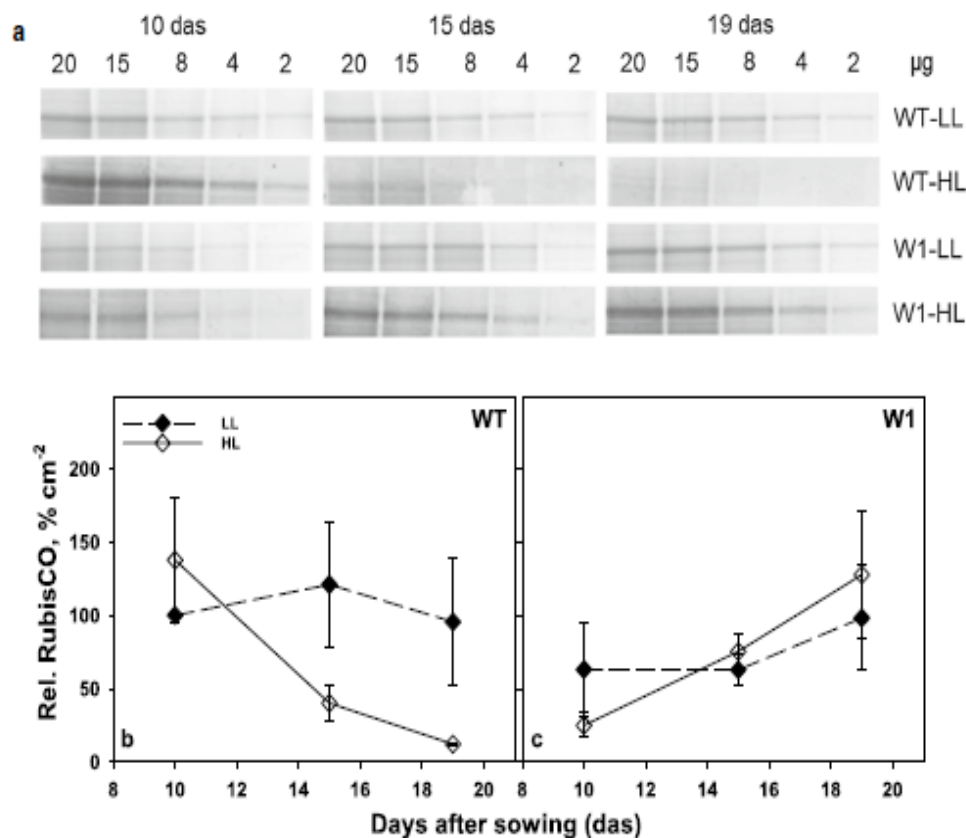


Fig. 6 a Representative SDS-PAGE from one of three independent experiments showing RbcL bands at different total protein concentrations loaded on the gels. **(b and c)** Relative RbcL content per total protein per leaf area derived from SDS-PAGE as a function of days

after sowing in WT **(b)** and W1 **(c)** grown under low and high light. Values are expressed in % of the values obtained for LL grown WT leaves at day 10. Depicted values are means \pm standard deviation of three independent experiments

number of cells but by an increased volume especially of the layers close to the adaxial and abaxial epidermis (Fig. 8a, b).

Wild type plants grown in high light showed significantly higher LMA than in low light (three-way ANOVA, Tab. S6, $P < 0.0001$ for all three days) (Fig. 8e). Moreover, leaves of wild-type plants had a stable leaf mass per area from day 10 to day 19 (Fig. 8e). However, WHIRLY1-deficient transgenic plants showed the same leaf mass per area at days 10 and 15 in both light conditions ($P = 0.9923$ and $P = 0.0954$, respectively, Fig. 8f) with an increasing tendency leading to a significant difference between LL and HL-grown transgenic plants ($P = 0.007$) on day 19.

Relative cytoplasmic volume

In order to elucidate the reasons for the higher leaf mass per area value in WT plants grown at HL, morphological and ultrastructural analyses of leaf mesophyll were performed. No differences in the number of cell layers were observed between the samples when semi-thin resin sections were imaged in a light microscope. Stereological analysis, based

on electron micrographs of thin sections (Fig. 9a) however, revealed that the cytoplasm to cell volume ratio was higher in WT plants grown for 10 days under high light compared to low light (two-way ANOVA, Tab. S7, $P < 0.001$) (Fig. 9b). This difference between LL and HL conditions was not observed in the case of the WHIRLY1 deficient plants ($P = 0.673$). Ultrastructural analysis therefore suggests that the relative cytoplasmic volume increased in response to higher irradiance in WT plants, but not in transgenic plants (Fig. 9b).

Discussion

Since decades, it has been discussed that the photosynthetic apparatus is an environmental sensor involved in acclimation to changes in irradiance (Anderson et al. 1995; Brütigam et al. 2009; Dietz 2015) resulting in changes in nuclear gene expression (Pogson et al. 2008; Pfannschmidt et al. 2020). Due to its dual localization in chloroplasts and nucleus, WHIRLY1 is an excellent candidate for communication

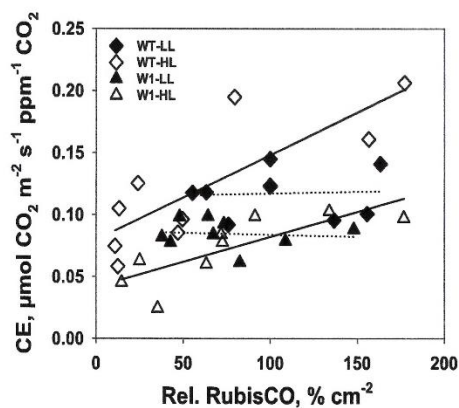


Fig. 7 Relationship between carboxylation efficiency (CE) and relative RbcL content per leaf area derived from SDS-PAGE in WT (diamonds) and W1 plants (triangles) growing under low (filled symbols) and high light (open symbols), at different developmental stages. The lines were calculated by regression analysis, where the regressions for the WT and W1 plants growing in low light were not significant, as indicated by the dotted representation

between chloroplasts and nucleus. The results of previous investigations with WHIRLY1 deficient plants (Kucharewicz et al. 2017; Swida-Barteczka et al. 2018) indicated that WHIRLY1 augments the responsiveness of barley to light. It remained an open question whether WHIRLY1 boosts light responses by a specific impact on photosynthesis or whether it has a more general function in plant responses to light. To investigate whether WHIRLY1 affects light acclimation at different levels, besides parameters of photosynthesis also leaf morphology parameters related to high light acclimation have been compared between barley WHIRLY1 deficient plants and wild-type plants in a high light situation requiring acclimation to avoid oxidative stress.

WHIRLY1 is important for acclimation of photosynthesis to high light

It has been reported before that in WHIRLY1 deficient plants, chloroplast development is delayed (Kucharewicz et al. 2017; Krupinska et al. 2019). According to the leaf chlorophyll contents observed in this study, maturity of W1 leaves was reached after 15 days instead of 10 days as observed in WT plants. Hence, photosynthesis should be compared between the 15-day-old W1 leaves and the 10-day-old wild-type leaves.

Acclimation of plants to high light involves an increase in photosynthesis as measurable as the light saturated CO_2 fixation rate and carboxylation efficiency (Björkman 1981; Leong and Anderson 1984a, b). Whereas wild-type barley plants showed the expected increase in light saturated rate of photosynthesis, WHIRLY1 deficient plants had no higher photosynthesis in high light compared to low light (Fig. 1).

Rather, the CO_2 assimilation rate was initially lower at high light compared to low light, potentially due to oxidative stress, which had been shown for these plants when they were grown in continuous light of high irradiance (Swida-Barteczka et al. 2018). An important mechanism for adjustment of the capacity of photosynthetic dark reactions to the high rate of delivery of NADPH_2 and ATP in high light would be an increase in RubisCO concentration and activity (Björkman 1981; Evans 1988). This had been shown for a number of different species using in vitro measurements of RubisCO activity. Indeed, in wild-type leaves at day 10, the relative amount of the large subunit of RubisCO (RbcL) at high light was higher than at low light as shown by SDS-PAGE analyses (Fig. 6). With increasing age, P_{max} , CE and RbcL content declined strongly in WT leaves at HL, presumably because of high light-promoted premature senescence, which was apparent by the decline of chlorophyll content after day 15 (Fig. 3). A decrease of the RubisCO content accompanied by a decline in photosynthesis after the leaves have reached full expansion has been reported for many grasses (Mae et al. 1983; Makino et al. 1984; Suzuki et al. 2010). Also in rice, an age-related decline of photosynthetic capacity (P_{max}) together with a decrease of RubisCO content was reported to be accelerated under high light (Makino et al. 1985; Hidema et al. 1991, 1992; Murchie et al. 2002). The decline in P_{max} and RubisCO content in plants growing under high irradiance was shown to begin after full leaf expansion (Evans 1983; Suzuki et al. 2009) or 3–4 days after reaching the maximum values (Murchie et al. 2002). While in the barley wild type, photosynthesis tended to decline with increasing age of the fully expanded leaves, it increased with age in the also fully expanded W1 leaves similarly in LL and HL conditions. This increase in photosynthesis was accompanied by an increase in chlorophyll content from day 10 on, leveling off after day 15. Despite the different kinetics, the data on photosynthesis clearly show that WHIRLY1 deficient plants lack the typical growth irradiance dependent differences in maximum photosynthesis and carboxylation efficiencies. Rather, the missing high light acclimation seems to have caused additional problems as photosynthesis rates of HL plants tended initially to stay below those of LL plants.

To investigate RubisCO activity in vivo, photosynthesis was measured at intercellular CO_2 concentrations below 200 ppm (Long and Bernacchi 2003; Lombardozi et al. 2018). The slope of the A/C_i curve in this range, the so-called carboxylation efficiency (CE), in W1 plants was strongly reduced and did not respond to higher growth irradiance (Fig. 5). In contrast, WT leaves displayed an increased CE at HL, in parallel to higher amounts of RbcL per area. Hence, WT leaves were able to acclimate RubisCO activity to high light, whereas W1 leaves were not.

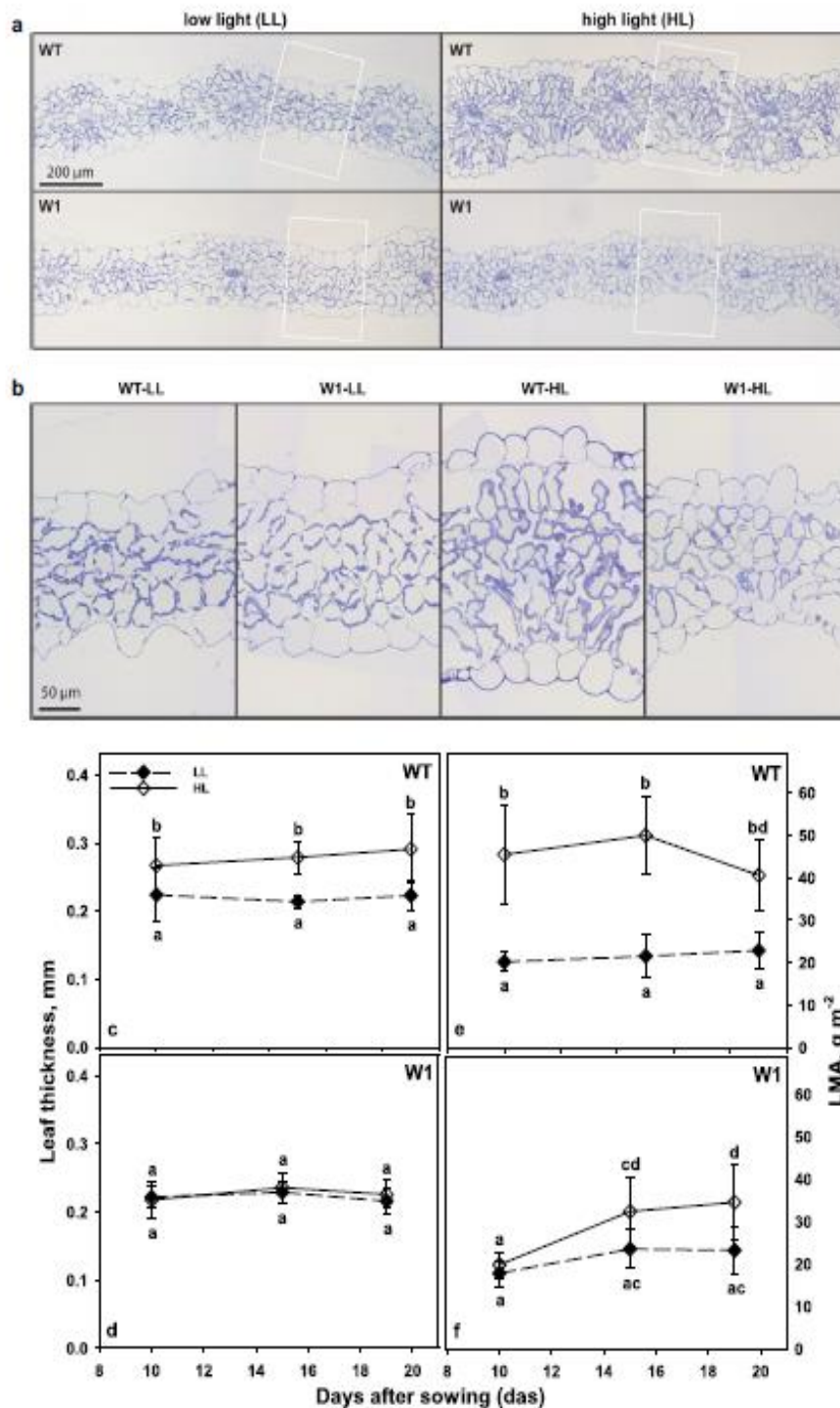


Fig. 8 Morphological analysis of WT and W1 primary foliage leaves growing under low light (LL) or high light (HL) conditions (**a, b**). Transverse, 500-nm thin sections of leaves embedded in epon were stained with Richardson's solution. Overview images taken with a $\times 10$ objective (**a**) illustrate the thickness of leaves. Areas indicated with white squares were imaged with a $\times 40$ objective (**b**) and illustrate the shape of mesophyll cells. Thickness and leaf mass per area (LMA) of primary foliage leaves of WT (**c, e**) and W1 (**d, f**) plants grown at low (filled symbols) and high irradiance (open symbols) as a function of days after sowing. Depicted values are means \pm standard deviation of 9–20 leaves in total from three independent experiments each comprising 3–7 leaves. The letters indicate statistically different values at a significance level of $P=0.05$, as determined by three-way ANOVA, followed by pairwise multiple means comparisons with the Holm–Sidak method

A comparison of CE and RbcL content might indicate how acclimation may have been achieved. In WT leaves at high light, a correlation between CE and RbcL could be observed (Fig. 7). Still considerable photosynthesis was observed in the presence of an apparently very low level of RbcL that cannot be properly quantified by colloidal Coomassie Blue staining of gels. Nevertheless, at HL, the CE of WT plants seemed to be at least partially dependent on RbcL content. While in the WT, the relationship between both parameters was altered by a senescence related decline during the observation period, in W1 leaves during the same period, the relationship between the two parameters was affected by an increase in photosynthetic activity. Also here, a good correlation between both parameters was observed, albeit at a much lower level of CE. In general, the overall range of the observed RbcL amounts were similar in both genotypes and both light conditions, indicating that carboxylation activity in vivo, as reflected by CE, was to a lesser extent governed by the amount of enzyme, but rather by an additional factor, presumably the activation state of RubisCO. These results suggest that carboxylation efficiency is a function of different parameters like age and developmental stage rather than only the amount of RubisCO in the leaf. Moreover, the results suggest that RubisCO activation is somehow controlled by the abundance of WHIRLY1.

WHIRLY1 is also required for light acclimation of leaf morphology

Besides the biochemical adjustments in chloroplast function, acclimation to light involves also changes in the anatomy of leaves (Givnish 1988; Lichtenthaler et al. 1981). Increased photosynthetic capacity in high light acclimated plants is followed by a higher carbon and nitrogen investment into RubisCO together with leaf structural changes in order to enable a faster rate of gas exchange (Seemann et al. 1987; Murchie and Horton 1997; Oguchi et al. 2003).

While wild-type leaves followed the expected trend and were thicker when grown at high light compared to low light, leaves of WHIRLY1 deficient plants did not show a light dependent change in thickness or leaf mass per area (Fig. 8). In many species, sun leaves contain more palisade layers and larger palisade cells than shade leaves (e.g., Lichtenthaler et al. 1981). Thicker leaves in high light acclimated plants of *Chenopodium album* L. were reported to be mainly caused by an elongation of palisade cells or an increase in the number of palisade cell layers (Yano and Terashima 2001, 2004). However, when leaf sections of wild-type barley and WHIRLY1 deficient plants were compared after growth at different irradiances, no difference was detected in the number of cell layers (Fig. 8a and b). Also, the thicker leaves of high light-grown rice did not differ from low light-grown rice with respect to cell number (Murchie

et al. 2005). It is likely, that dicotyledonous and monocotyledonous plants differ in the strategies to increase leaf thickness in high light. Histological analyses of images obtained from ultrathin leaf sections revealed that in the mesophyll of WT leaves from high light-acclimated plants the ratio of cytoplasm/cell volume was twice as high as in leaves of low light-grown plants (Fig. 9). In contrast, in the leaves of the WHIRLY1 deficient plants this ratio did not change in response to irradiance. Organelles in the cytoplasm presumably have a higher density than the vacuole (Poorter et al. 2009). Therefore, the higher LMA of high light-grown WT leaves may be caused mainly by the higher cytoplasm/cell volume ratio. In addition, the higher starch content of these leaves may also contribute to the high LMA. Poorter et al. (2009) reported that not leaf volume per area but rather the leaf density explains LMA in a large number of species, including grasses. Together with the reduced thickness of leaves, the low values obtained for the leaf mass per area (LMA) indicate that the W1 plants even at high irradiance have leaves morphologically resembling shade leaves.

The lack of acclimation to high irradiance of both photosynthesis and leaf morphology indicate that W1 plants are unable to properly respond to light. This suggests that WHIRLY1 might be required either for an efficient functionality of the photosensory systems such as phytochromes and/or signal transduction processes required for the appropriate responses controlled by these systems. Investigations with plants overexpressing *PHYTOCHROME B (PHY-B)* suggest that light acclimation of both the photosynthetic apparatus and leaf morphology are controlled by photoreceptors such as PHY-B (Kreslavski et al. 2018). However, in an Arabidopsis mutant lacking PHY-B, photosynthetic acclimation has been shown to respond to light (Walters et al. 1999). Therefore, besides photoreceptors, further light-measuring mechanisms might be involved in light acclimation.

Indeed, development of chloroplasts and of leaf photosynthetic structures were reported to be also controlled by light that is perceived by the chloroplasts themselves (Lepistö and Rintamäki 2012). While the impact of light on leaf thickness is an early event in leaf development occurring before leaf expansion has been stopped (Poorter et al. 2009), chloroplast differentiation and photosynthesis can be still dynamically adjusted to the local light environment in fully expanded leaves (Yano and Terashima 2001). In the WHIRLY1 deficient barley plants, light acclimation is obviously impaired at the two levels, i.e. the level of leaf morphology determined at early development and at the level of chloroplast operation in fully developed leaves. This hints at a coordinative role of WHIRLY1 in translating information about the light environment at early plant development into adjustments of chloroplast structure and the photosynthetic apparatus that match the preceding early light dependent adjustments in leaf morphology. A role of WHIRLY1 in coordinating the

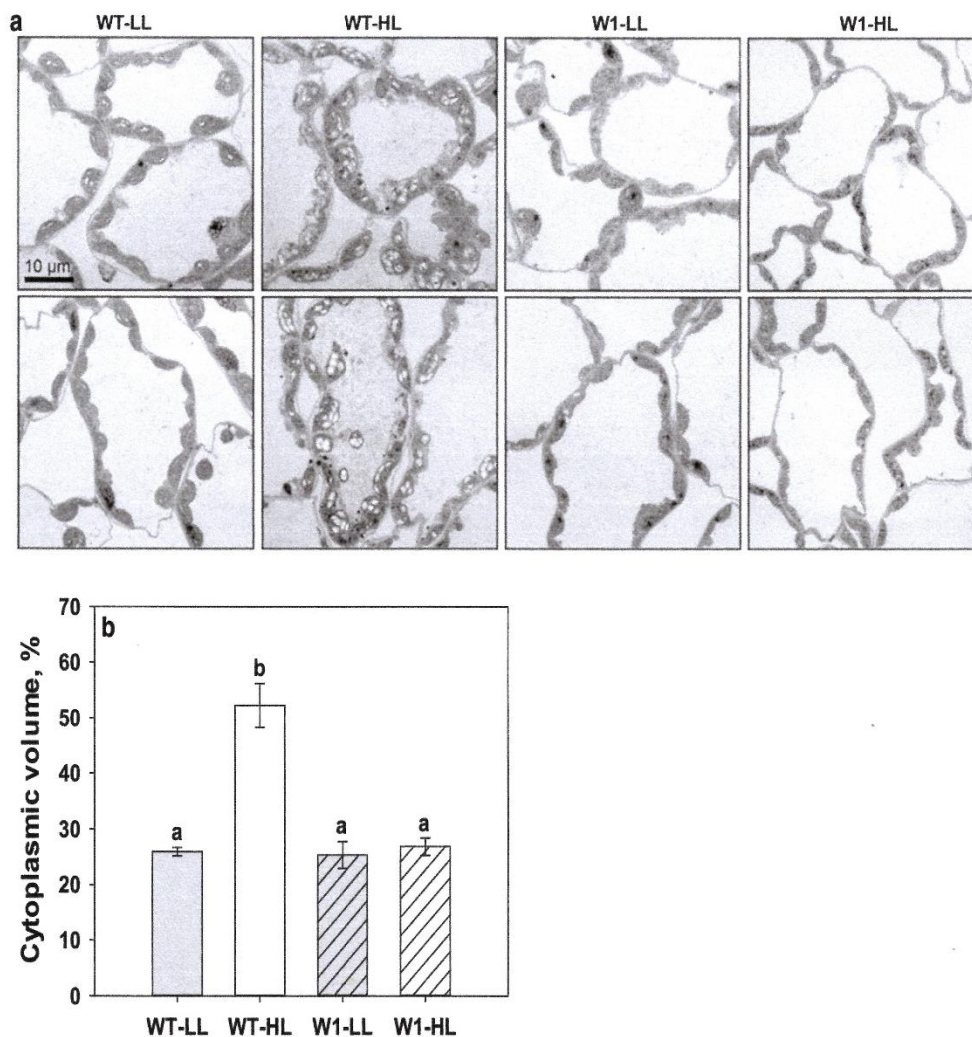


Fig. 9 Ultrastructural analysis of mesophyll in primary leaves grown under high or low light for 10 days. **a** Representative transmission electron micrographs of primary leaf mesophyll in WT and W1 plants grown under LL or HL. **b** The cytoplasm to cell volume ratio based on a stereological analysis of electron micrographs shown in **a**. Col-

umns indicate mean \pm standard error based on three leaves. For each leaf, between 15 and 23 electron micrographs were analysed. The letters indicate statistically different values at a significance level of $P=0.05$, as determined by Two-way ANOVA test, followed by pairwise multiple means comparisons with the Holm–Sidak method

light response at early leaf development is in accordance with its high abundance in undifferentiated cells at the base of primary foliage leaves (Krupinska et al. 2014). This systemic effect of WHIRLY1 on leaves and chloroplasts makes sense, as the plant cannot perform efficient photosynthesis without having the appropriate leaf morphology. How WHIRLY1 mediates coordination of the processes at the molecular level remains to be investigated.

The results of this study are in accordance with the findings of previous investigations performed with WHIRLY1 deficient barley plants (Kucharewicz et al. 2017; Swida-Barteczka et al. 2018). Whereas the impact of WHIRLY1

on senescence (Kucharewicz et al. 2017) and photosynthesis mediated ROS production at high irradiance (Swida-Barteczka et al. 2018) could be the consequence of structural changes in chloroplasts caused by the chloroplast nucleoid associated WHIRLY1, this study shows that the impact of WHIRLY1 on the responsiveness of plants to light is more comprehensive comprising the two levels of leaf morphology and chloroplast functionality. While a low level of WHIRLY1 in barley is obviously sufficient to enable light dependent chloroplast development, albeit at reduced rate, the higher abundance in the wild type is required for coordinated light acclimation at different levels.

Author contribution statement MS, WB and KK conceived and designed research. Material preparation, conduction of experiments and data analysis were performed by MS. Transmission electron microscopy and leaf cross section was done by UR. The first draft of the manuscript was written by MS. All authors commented and revised the previous versions of the manuscript. All authors read and approved the final manuscript.

Supplementary Information The online version contains supplementary material available at <https://doi.org/10.1007/s00425-022-03854-x>.

Acknowledgements We are grateful to Dr. Marta Rodriguez-Franco (University of Freiburg) for valuable suggestions on plant sample preparation for transmission electron microscopy. We would like to thank Ulrike Voigt (Institute of Botany/Central Microscopy, CAU Kiel, Germany) for her technical support in morphological and ultrastructural analyses as well as preparing seeds. Louis Scholz (Institute of Botany, CAU Kiel, Germany) was of great help in measuring leaf thickness. Further thanks to Jens Hermann (Institute of Botany, CAU Kiel, Germany) for his technical support in HPLC analysis of leaf chlorophyll contents. We also thank the two anonymous reviewers for their valuable comments helping us to improve the manuscript.

Funding Open Access funding enabled and organized by Projekt DEAL.

Data availability The data that support the findings of in this study are available in the Supplementary Information of this article. The raw datasets in this study are available from the first author or corresponding author on reasonable request.

Open Access This article is licensed under a Creative Commons Attribution 4.0 International License, which permits use, sharing, adaptation, distribution and reproduction in any medium or format, as long as you give appropriate credit to the original author(s) and the source, provide a link to the Creative Commons licence, and indicate if changes were made. The images or other third party material in this article are included in the article's Creative Commons licence, unless indicated otherwise in a credit line to the material. If material is not included in the article's Creative Commons licence and your intended use is not permitted by statutory regulation or exceeds the permitted use, you will need to obtain permission directly from the copyright holder. To view a copy of this licence, visit <http://creativecommons.org/licenses/by/4.0/>.

References

- Allen JF, de Paula WBM, Puthiyaveetil S, Nield J (2011) A structural phylogenetic map for chloroplast photosynthesis. *Trends Plant Sci* 16:645–655. <https://doi.org/10.1016/j.tplants.2011.10.004>
- Anderson JM, Chow WS, Park YI (1995) The grand design of photosynthesis: Acclimation of the photosynthetic apparatus to environmental cues. *Photosynth Res* 46:129–139. <https://doi.org/10.1007/BF00020423>
- Athanasίου K, Dyson BC, Webster RE, Johnson GN (2010) Dynamic acclimation of photosynthesis increases plant fitness in changing environments. *Plant Physiol* 152:366–373. <https://doi.org/10.1104/pp.109.149351>
- Björkman O (1981) Responses to different quantum flux densities. In: Lange OL, Nobel PS, Osmond CB, Ziegler H (eds) *Physiological plant ecology. encyclopedia of plant physiology (new series)*, vol. 12/A. Springer, Berlin. https://doi.org/10.1007/978-3-642-68090-8_4
- Boardman NK, Björkman O, Anderson JM, Goodchild DJ, Thorne SW (1975) Photosynthetic adaptation of higher plants to light intensity: relationship between chloroplast structure, composition of the photosystems and photosynthetic rates. In: Avron M (ed) *Proceedings of the 3rd international congress on photosynthesis*, vol. 3. Elsevier Amsterdam, p 1809–1823
- Bobik K, Burch-Smith TM (2015) Chloroplast signaling within, between and beyond cells. *Front Plant Sci* 6:781. <https://doi.org/10.3389/fpls.2015.00781>
- Bräutigam K, Dietzel L, Kleine T, Stroher E, Wormuth D, Dietz KJ, Radke D, Wirtz M, Hell R, Dormann P, Nunes-Nesi A, Schauer N, Fernie AR, Oliver SN, Geigenberger P, Leister D, Pfannschmidt T (2009) Dynamic plastid redox signals integrate gene expression and metabolism to induce distinct metabolic states in photosynthetic acclimation in Arabidopsis. *Plant Cell* 21:2715–2732. <https://doi.org/10.1105/tpc.108.062018>
- Chan KX, Phua SY, Crisp P, McQuinn R, Pogson BJ (2016) Learning the languages of the chloroplast: retrograde signaling and beyond. *Ann Rev Plant Biol* 67:25–53. <https://doi.org/10.1146/annurev-arplant-043015-111854>
- Cheng L, Fuchigami LH (2000) Rubisco activation state decreases with increasing nitrogen content in apple leaves. *J Exp Bot* 51:1687–1694. <https://doi.org/10.1093/jexbot/51.351.1687>
- Dietz KJ (2015) Efficient high light acclimation involves rapid processes at multiple mechanistic levels. *J Exp Bot* 66:2401–2414. <https://doi.org/10.1093/jxb/eru505>
- Dietzel L, Pfannschmidt T (2008) Photosynthetic acclimation to light gradients in plant stands comes out of shade. *Plant Signal Behav* 3:1116–1118. <https://doi.org/10.4161/psb.3.12.7038>
- Dyballa N, Metzger S (2009) Fast and sensitive colloidal coomassie G-250 staining for proteins in polyacrylamide gels. *JoVE* 30:e1431. <https://doi.org/10.3791/1431>
- Evans JR (1983) Nitrogen and photosynthesis in the flag leaf of wheat (*Triticum aestivum* L.). *Plant Physiol* 72:297–302. <https://doi.org/10.1104/pp.72.2.297>
- Evans JR (1987) The relationship between electron transport components and photosynthetic capacity in pea leaves grown at different irradiances. *Aust J Plant Physiol* 14:157. <https://doi.org/10.1071/PP9870157>
- Evans JR (1988) Acclimation by the Thylakoid membranes to growth irradiance and the partitioning of nitrogen between soluble and thylakoid proteins. *Funct Plant Biol* 15:93–106. <https://doi.org/10.1071/pp9880093>
- Foyer CH, Neukermans J, Queval G, Noctor G, Harbinson J (2012) Photosynthetic control of electron transport and the regulation of gene expression. *J Exp Bot* 63:1637–1661. <https://doi.org/10.1093/jxb/ers013>
- Foyer CH, Karpinska B, Krupinska K (2014) The functions of WHIRLY1 and REDOX-RESPONSIVE TRANSCRIPTION FACTOR 1 in cross tolerance responses in plants: a hypothesis. *Philos Trans R Soc B* 369:20130226. <https://doi.org/10.1098/rstb.2013.0226>
- Givnish T (1988) Adaptation to sun and shade: a whole-plant perspective. *Aust J Plant Physiol* 15:63–92. <https://doi.org/10.1071/PP9880063>
- Hidema J, Makino A, Mae T, Ojima K (1991) Photosynthetic characteristics of rice leaves aged under different irradiances from full expansion through senescence. *Plant Physiol* 97:1287–1293. <https://doi.org/10.1104/pp.97.4.1287>
- Hidema J, Makino A, Kurita Y, Mae T, Ojima K (1992) Changes in the levels of chlorophyll and light-harvesting chlorophyll a/b protein

- of PS II in rice leaves aged under different irradiances from full expansion through senescence. *Plant Cell Physiol* 33:1209–1214. <https://doi.org/10.1093/oxfordjournals.pcp.a078375>
- Isemer R, Krause K, Grabe N, Kitahata N, Asami T, Krupinska K (2012) Plastid located WHIRLY1 enhances the responsiveness of Arabidopsis seedlings toward abscisic acid. *Front Plant Sci* 3:283. <https://doi.org/10.3389/fpls.2012.00283>
- Kleine T, Nägele T, Neuhaus HE et al (2021) Acclimation in plants—the Green Hub consortium. *Plant J* 106:23–40. <https://doi.org/10.1111/tpj.15144>
- Kreslavski VD, Los DA, Schmitt FJ, Zharmukhamedov SK, Kuznetsov VV, Allakhverdiev SI (2018) The impact of the phytochromes on photosynthetic processes. *Biochim Biophys Acta Bioenergy* 1859:400–408. <https://doi.org/10.1016/j.bbabi.2018.03.003>
- Krupinska K, Oetke S, Desel C, Mulisch M, Schäfer A, Hollmann J, Kumlern J, Hensel G (2014) WHIRLY1 is a major organizer of chloroplast nucleoids. *Front Plant Sci* 5:432. <https://doi.org/10.3389/fpls.2014.00432>
- Krupinska K, Braun S, Saaid Nia M, Schäfer A, Hensel G, Bilger W (2019) The nucleoid-associated protein WHIRLY1 is required for the coordinate assembly of plastid and nucleus-encoded proteins during chloroplast development. *Planta* 249:1337–1347. <https://doi.org/10.1007/s00425-018-03085-z>
- Krupinska K, Blanco NE, Oetke S, Zotini M (2020) Genome communication in plants mediated by organelle-nucleus-located proteins. *Philos Trans R Soc B Biol Sci*. <https://doi.org/10.1098/rstb.2019.0397>
- Kucharewicz W, Distelfeld A, Bilger W, Muller M, Munné-Bosch S, Hensel G, Krupinska K (2017) Acceleration of leaf senescence is slowed down in transgenic barley plants deficient in the DNA/RNA-binding protein WHIRLY1. *J Exp Bot* 68:983–996. <https://doi.org/10.1093/jxb/erw501>
- Laemmli UK (1970) Cleavage of structural proteins during the assembly of the head of bacteriophage T4. *Nature* 227:680–685. <https://doi.org/10.1038/227680a0>
- Leong TY, Anderson JM (1984a) Adaptation of the thylakoid membranes of pea chloroplasts to light intensities. I. Study on the distribution of chlorophyll-protein complexes. *Photosynth Res* 5:105–115. <https://doi.org/10.1007/BF00028524>
- Leong TY, Anderson JM (1984b) Adaptation of the thylakoid membranes of pea chloroplasts to light intensities. II. Regulation of electron transport capacities, electron carriers, coupling factor (CF1) activity and rates of photosynthesis. *Photosynth Res* 5:117–128. <https://doi.org/10.1007/BF00028525>
- Lepistö A, Rintamäki E (2012) Coordination of plastid and light signaling pathways upon development of Arabidopsis leaves under various photoperiods. *Mol Plant* 5:799–816. <https://doi.org/10.1093/mp/ssr106>
- Lichtenthaler HK, Buschmann C, Döll M, Fietz HJ, Bach T, Kozel U, Meier D, Rahmsdorf U (1981) Photosynthetic activity, chloroplast ultrastructure, and leaf characteristics of high-light and low-light plants and of sun and shade leaves. *Photosynth Res* 2:115–141. <https://doi.org/10.1007/BF00028752>
- Lichtenthaler HK, Ač A, Marek MV, Kalina J, Urban O (2007) Differences in pigment composition, photosynthetic rates and chlorophyll fluorescence images of sun and shade leaves of four tree species. *Plant Physiol Biochem* 45:577–588. <https://doi.org/10.1016/j.plaphy.2007.04.006>
- Lombardozzi DL, Smith NG, Cheng SJ et al (2018) Triose phosphate limitation in photosynthesis leaf models reduces leaf photosynthesis and global terrestrial carbon storage. *Environ Res Lett* 13:074025
- Long SP, Bernacchi CJ (2003) Gas exchange measurements, what can they tell us about the underlying limitations to photosynthesis? Procedures and sources of error. *J Exp Bot* 54:2393–2401. <https://doi.org/10.1093/jxb/erg262>
- Mae T, Makino A, Ohira K (1983) Changes in the amounts of ribulose biphosphate carboxylase synthesized and degraded during the life span of rice leaf (*Oryza sativa* L.). *Plant Cell Physiol* 24:1079–1086. <https://doi.org/10.1093/oxfordjournals.pcp.a076611>
- Makino A, Mae T, Ohira K (1984) Relation between nitrogen and ribulose-1,5-bisphosphate carboxylase in rice leaves from emergence through senescence. *Plant Cell Physiol* 25:429–437. <https://doi.org/10.1093/oxfordjournals.pcp.a076730>
- Makino A, Mae T, Ohira K (1985) Photosynthesis and ribulose-1,5-bisphosphate carboxylase/oxygenase in rice leaves from emergence through senescence. Quantitative analysis by carboxylation/oxygenation and regeneration of ribulose 1,5-bisphosphate. *Planta* 166:414–420. <https://doi.org/10.1007/BF00401181>
- Munné-Bosch S (2019) Vitamin E function in stress sensing and signaling in plants. *Dev Cell* 48:290–292. <https://doi.org/10.1016/j.devcel.2019.01.023>
- Murchie EH, Horton P (1997) Acclimation of photosynthesis to irradiance and spectral quality in British plant species: chlorophyll content, photosynthetic capacity and habitat preference. *Plant Cell Environ* 20:438–448. <https://doi.org/10.1046/j.1365-3040.1997.d01-95.x>
- Murchie EH, Hubbart S, Chen Y, Peng S, Horton P (2002) Acclimation of rice photosynthesis to irradiance under field conditions. *Plant Physiol* 130:1999–2010. <https://doi.org/10.1104/pp.011098>
- Murchie EH, Hubbart S, Peng S, Horton P (2005) Acclimation of photosynthesis to high irradiance in rice: gene expression and interactions with leaf development. *J Exp Bot* 56:449–460. <https://doi.org/10.1093/jxb/eri100>
- Nelson N, Ben-Shem A (2004) The complex architecture of oxygenic photosynthesis. *Nat Rev Mol Cell Biol* 5:971–982. <https://doi.org/10.1038/nrm1525>
- Nichelmann L, Schulze M, Herppich WB, Bilger W (2016) A simple indicator for non-destructive estimation of the violaxanthin cycle pigment content in leaves. *Photosynth Res* 128:183–193. <https://doi.org/10.1007/s11120-016-0218-1>
- Oguchi R, Hikosaka K, Hirose T (2003) Does the photosynthetic light acclimation need change in leaf anatomy? *Plant Cell Environ* 26:505–512. <https://doi.org/10.1046/j.1365-3040.2003.00981.x>
- Pfannschmidt T, Terry MJ, Van Aken O, Quiros PM (2020) Retrograde signals from endosymbiotic organelles: a common control principle in eukaryotic cells. *Philos Trans R Soc B Biol Sci*. <https://doi.org/10.1098/rstb.2019.0396>
- Pogson BJ, Woo NS, Förster B, Small ID (2008) Plastid signalling to the nucleus and beyond. *Trends Plant Sci* 13:602–609. <https://doi.org/10.1016/j.tplants.2008.08.008>
- Poorter H, Niinemets Ü, Poorter L, Wright IJ, Villar R (2009) Causes and consequences of variation in leaf mass area: a meta analysis. *New Phytol* 182:565–588. <https://doi.org/10.1111/j.1469-8137.2009.02830.x>
- Poorter H, Niinemets Ü, Ntagkas N, Siebenkäs A, Mäenpää M, Matsubara S, Pons TL (2019) A meta-analysis of plant responses to light intensity for 70 traits ranging from molecules to whole plant performance. *New Phytol* 223:1073–1105. <https://doi.org/10.1111/nph.15754>
- Porra RJ, Thompson WA, Kriedemann PE (1989) Determination of accurate extinction coefficients and simultaneous equations for assaying chlorophylls *a* and *b* extracted with four different solvents: verification of the concentration of chlorophyll standards by atomic absorption spectroscopy. *Biochim Biophys Acta Bioenergy* 975:384–394. [https://doi.org/10.1016/S0005-2728\(89\)80347-0](https://doi.org/10.1016/S0005-2728(89)80347-0)
- Race HL, Herrmann RG, Martin W (1999) Why have organelles retained genomes? *Trends Genet* 15:364–370. [https://doi.org/10.1016/S0168-9525\(99\)01766-7](https://doi.org/10.1016/S0168-9525(99)01766-7)
- Schindelin J, Arganda-Carreras I, Frise E et al (2012) Fiji: an open-source platform for biological-image analysis. *Nat Methods* 9:676–682. <https://doi.org/10.1038/nmeth.2019>

- Seemann JR, Sharkey TD, Wang J, Osmond CB (1987) Environmental effects on photosynthesis, nitrogen use efficiency, and metabolite pools in leaves of sun and shade plants. *Plant Physiol* 84:796–802. <https://doi.org/10.1104/pp.84.3.796>
- Suzuki Y, Miyamoto T, Yoshizawa R, Mae T, Makino A (2009) Rubisco content and photosynthesis of leaves at different positions in transgenic rice with an overexpression of RBCS. *Plant Cell Environ* 32:417–427. <https://doi.org/10.1111/j.1365-3040.2009.01937.x>
- Suzuki Y, Kihara-Doi T, Kawazu T, Miyake C, Makino A (2010) Differences in Rubisco content and its synthesis in leaves at different positions in *Eucalyptus globulus* seedlings. *Plant Cell Environ* 33:1314–1323. <https://doi.org/10.1111/j.1365-3040.2010.02149.x>
- Swida-Barteczka A, Krieger-Liszkay A, Bilger W, Voigt U, Hensel G, Szweykowska-Kulinska Z, Krupinska K (2018) The plastid-nucleus located DNA/RNA binding protein WHIRLY1 regulates microRNA-levels during stress. *RNA Biol* 15:886–891. <https://doi.org/10.1080/15476286.2018.1481695>
- Terashima I, Hanba YT, Tazoe Y, Vyas P, Yano S (2006) Irradiance and phenotype: comparative eco-development of sun and shade leaves in relation to photosynthetic CO₂ diffusion. *J Exp Bot* 57:343–354. <https://doi.org/10.1093/jxb/erj014>
- Thiele A, Herold M, Lenk I, Quail PH, Gatz C (1999) Heterologous expression of Arabidopsis phytochrome B in transgenic potato influences photosynthetic performance and tuber development. *Plant Physiol* 120:73–81. <https://doi.org/10.1104/pp.120.1.73>
- Townsend AJ, Retkute R, Chinnathambi K, Randall JWP, Foulkes J, Carmo-Silva E, Murchie EH (2018) Suboptimal acclimation of photosynthesis to light in wheat canopies. *Plant Physiol* 176:1233–1246. <https://doi.org/10.1104/pp.17.01213>
- Vialet-Chabrand S, Matthews JS, Simkin AJ, Raines CA, Lawson T (2017) Importance of fluctuations in light on plant photosynthetic acclimation. *Plant Physiol* 173:2163–2179. <https://doi.org/10.1104/pp.16.01767>
- von Caemmerer S, Farquhar GD (1981) Some relationships between the biochemistry of photosynthesis and the gas exchange of leaves. *Planta* 153:376–387. <https://doi.org/10.1007/BF00384257>
- Walters RG, Rogers JJM, Shephard F, Horton P (1999) Acclimation of *Arabidopsis thaliana* to the light environment: the role of photoreceptors. *Planta* 209:517–527. <https://doi.org/10.1007/s004250050756>
- Yano S, Terashima I (2001) Separate localization of light signal perception for sun or shade type chloroplast and palisade tissue differentiation in *Chenopodium album*. *Plant Cell Physiol* 42:1303–1310. <https://doi.org/10.1093/pcp/pce183>
- Yano S, Terashima I (2004) Developmental process of sun and shade leaves in *Chenopodium album* L. *Plant Cell Environ* 27:781–793. <https://doi.org/10.1111/j.1365-3040.2004.01182.x>
- Zivcak M, Brestic M, Kalaji HM, Govindjee, (2014) Photosynthetic responses of sun- and shade-grown barley leaves to high light: is the lower PSII connectivity in shade leaves associated with protection against excess of light? *Photosynth Res* 119:339–354. <https://doi.org/10.1007/s11120-014-9969-8>

Publisher's Note Springer Nature remains neutral with regard to jurisdictional claims in published maps and institutional affiliations.

Chapter IV: WHIRLY1-deficient barley plants and light stress

How do barley plants with impaired photosynthetic light acclimation survive under high-light stress?

Monireh Saeid Nia¹, Louis Scholz¹, Adriana Garibay-Hernández², Hans-Peter Mock², Urska Repnik³, Jennifer Selinski¹, Karin Krupinska¹, Wolfgang Bilger¹

¹ Institute of Botany, Christian-Albrechts-University, Kiel, Germany

² Leibniz Institute for Plant Genetics and Crop Plant Research, Gatersleben, Germany

*Current address: Molekulare Biotechnologie and Systembiologie, TU Kaiserslautern, Paul-Ehrlich Straße 23, D-67663 Kaiserslautern, Germany

³ Central Microscopy, Department of Biology, Christian-Albrechts-University, Kiel, Germany

Abstract

Main Conclusion WHIRLY1-deficient barley plants are unable to acclimate to high irradiance, but nevertheless survive and grow under extended exposure to high light. We found that these plants do not display an enhanced tocopherol content nor do they have a changed ratio of reduced to oxidized glutathione. Increased non-radiative dissipation at photosystem II and enhanced contents of the carotenoid zeaxanthin and the flavonoid luteonarin appear to have contributed to protection against oxidative stress.

Abstract Plants are able to acclimate to environmental conditions to optimize their functions. With the exception of obligate shade plants, they can adjust their photosynthetic apparatus and the morphology and anatomy of their leaves to irradiance. Barley (*Hordeum vulgare* L., cv. Golden Promise) plants with reduced abundance of the protein WHIRLY1 were recently shown to be unable to acclimatise important components of the photosynthetic apparatus to high light. Nevertheless, these plants did not show symptoms of photoinhibition. High-light (HL) grown WHIRLY1 knockdown plants (W1) showed clear signs of exposure to excessive irradiance such as a low epoxidation state of the violaxanthin cycle pigments and an early light saturation of electron transport. These responses were underlined by a very large xanthophyll cycle pool size and by an increased number of plastoglobules. Whereas zeaxanthin increased with HL stress, α -tocopherol, which is another lipophilic antioxidant, showed no response to excessive light. Also the content of the hydrophilic antioxidant glutathione showed no increase in W1 plants as compared to the wild type, whereas the flavone luteonarin was induced in W1 plants. HPLC analysis of removed epidermal tissue indicated that the largest part of luteonarin was presumably located in the mesophyll. Since luteonarin is a better antioxidant than saponarin, the major flavone present in barley leaves, it is concluded that luteonarin accumulated as a response to oxidative stress. It is also concluded that zeaxanthin and luteonarin may have served as antioxidants in W1 plants, contributing to their survival in HL despite their restricted HL acclimation.

Keywords: excess excitation energy, energy partitioning, lutein, NPQ, photoinhibition, tocopherols, WHIRLY1, zeaxanthin

Introduction

Due to their sessile life style, plants are directly exposed to and in equilibrium with a large variety of environmental factors. Among them, sunlight is especially important, but this factor is also extremely variable, both on the short as well as on the long term. Plants are dependent on sunlight for photosynthesis and too little light will cause them to suffer. On the other hand, if the rate of light absorption in the photosynthetic apparatus exceeds the rate of consumption of light energy in form of reducing equivalents in the photosynthetic dark reactions and/or poisoning mechanisms, an increased amount of reactive oxygen species (ROS) may be generated (Asada 2006, Fitzpatrick et al. 2022). Among the consequences of ROS formation is a damage to the photosynthetic reaction centers, especially photosystem II (PS II), resulting in a reduction of the photochemical quantum yield of PS II, which can be quantified using the chlorophyll fluorescence parameter F_V/F_M (Demmig and Björkman 1987, Maxwell and Johnson 2000). Damage will especially occur when shade-acclimated plants are suddenly exposed to strong sunlight (Powles 1984; Anderson and Osmond 1987). However, most other plant species will acclimate to high light by enhancing the capacity of the dark reactions (Anderson et al. 1995) and/or by employing photoprotective mechanisms such as non-radiative dissipation of excessive light, increased levels of antioxidants or by adjusting the redox state (Müller et al. 2001, Jahns and Holzwarth 2012, Asada 2006, Selinski and Scheibe 2019).

Dissipation of excess light energy as heat is one important short-term mechanism (from seconds to minutes) known as non-photochemical quenching (NPQ) of chlorophyll fluorescence, which occurs in the antenna system of PS II (Demmig-Adams and Adams 1996; Holzwarth et al. 2013). Energy partitioning to non-radiative dissipation can be easily quantified in intact leaves by determining the quantum yield of non-photochemical quenching ($\Phi(\text{NPQ})$) of chlorophyll fluorescence (Kornyeyev and Hendrickson 2007, Klughammer and Schreiber 2008). NPQ has been shown to depend on the formation of zeaxanthin from violaxanthin within the xanthophyll cycle (Bilger and Björkman 1990; Niyogi et al. 1998). In addition, zeaxanthin protects the thylakoid membrane against ROS-induced lipid peroxidation (Niyogi et al. 2001; Müller et al. 2001, Havaux et al 2007, Jahns and Holzwarth 2012). A further lipophilic antioxidant protecting against $^1\text{O}_2$ is α -tocopherol (Spicher et al. 2017).

While these lipophilic antioxidants are predominantly important to detoxify $^1\text{O}_2$, H_2O_2 generated at PS I is scavenged by hydrophilic antioxidants such as ascorbate and glutathione (Foyer and Noctor 2011, Hebbelmann et al. 2012). The latter compound is a small intracellular redox-active antioxidant molecule existing in two main stable forms: the reduced thiol (GSH) or the oxidized disulfide (GSSG) form (Tausz et al. 2004). In plants growing under optimum conditions, the GSH/GSSG ratio is reported to have high values (Rahantaniaina et al. 2013; Bloem et al. 2015), with about 97% of the pool in their reduced form (Vanacker et al. 2000). Accordingly, a low GSH/GSSG ratio is often considered as a potential indicator for oxidative stress in plants, but may also be affected by other factors such as plant age (Tausz et al. 2004; Rahantaniaina et al. 2013; Bloem et al. 2015). Besides its direct role in ROS scavenging, glutathione is part of the α -tocopherol-ascorbate-glutathione triad (Szarka et al. 2012), maintaining the reduced state of tocopherol and thereby indirectly protecting cell membranes from oxidative damage (Hasanuzzaman et al. 2017). The synergistic antioxidant effect of the α -tocopherol-ascorbate-glutathione triad was also supported by the observation that the levels of these three antioxidants increased several folds in a coordinative manner under high-light conditions (Kanwischer et al. 2005).

In addition to ascorbate and glutathione, phenolic compounds such as flavonoids might also act as direct antioxidants (Havaux et al. 2007, Hernández et al. 2009; Agati et al. 2012; Nezval et al. 2017). In response to high-light stress, flavonoids bearing a catechol group, i.e. an ortho-dihydroxy group, at the flavonoid B-ring have been shown to accumulate in the vacuoles of mesophyll cells (Agati et al. 2009; Fini et al. 2011). These dihydroxy B-ring flavonoids, such as quercetin or luteolin derivatives, have a higher antioxidative activity than monohydroxy flavonoids such as kaempferol and apigenin derivatives (Rice-Evans et al. 1996; Agati et al. 2012; Alseekh et al. 2020).

When growing in high light, most plants, with the exception of obligate shade species, acclimate their photosynthetic capacities to prevent photoinhibition by reducing the excess excitation energy (Powles 1984; Gray et al. 1996). A recent study with barley plants with an RNAi-mediated knockdown of the chloroplast protein WHIRLY1 (W1) revealed that they cannot acclimate to high light both at the level of leaf morphology and at the level of the photosynthetic apparatus (Saeid

Nia et al. 2022). Therefore, these plants are expected to be prone to photoinhibition. Indeed, in the seedling stage these plants are bleached and accumulate ROS during photosynthesis as measured via electron paramagnetic spin resonance (EPR) spectroscopy on illuminated thylakoids (Swida-Bartezka et al. 2018). However, W1 plants did not show any decline in their maximum quantum yield of PS II after final chloroplast development during growth under high light (Kucharewicz et al. 2017). Hence, these plants are an excellent model system to study photoprotective mechanisms enabling plants to survive and avoid photodamage in the absence of acclimation of photosynthetic capacity. Therefore, we investigated the response of several antioxidative mechanisms in high-light exposed primary leaves of WHIRLY1-deficient plants.

Material and Methods

Plant material and growth conditions

Grains of WHIRLY1-deficient plants prepared by RNAi-mediated knockdown of *HvWHIRLY1* (W1) (Krupinska et al. 2014) together with *Hordeum vulgare* L., cv. “Golden Promise” as wildtype (WT), were sown on soil (Einheitserde ED73, Einheitswerk Werner Tantau, Uetersen, Germany). Growth conditions were as described by Saeid Nia et al. (2022). Photosynthetic photon flux densities (PPFD) incident on the leaf plane were 40-70 $\mu\text{mol m}^{-2} \text{s}^{-1}$ for low light (LL) and 350-500 $\mu\text{mol m}^{-2} \text{s}^{-1}$ for high light (HL), which corresponded to horizontal PPFDs of 150 to 1000 $\mu\text{mol m}^{-2} \text{s}^{-1}$, respectively. The incident irradiance on the adaxial and abaxial sides of the leaves was measured for every sampled individual primary leaf using a quantum sensor (Li-185 A, Li-Cor Biosciences, Lincoln, NE, USA). The area between 1.5 and 3 cm below the tip of primary leaves, containing mature chloroplasts, was used for all measurements. Primary leaves were used at different developmental stages, i.e. at 10, 15, and 19 days after sowing (das).

Chlorophyll fluorescence measurements

Chlorophyll fluorescence was measured simultaneously with photosynthetic gas exchange (data shown in Saeid Nia et al. 2022) using a portable gas exchange fluorescence system GFS-3000 (Heinz Walz GmbH, Effeltrich, Germany). The instrument was set up with a 750 $\mu\text{mol min}^{-1}$ air

flow rate, a cuvette temperature of 21°C, and 60% relative humidity. Attached primary leaves of both genotypes grown under HL and LL were measured at different days, reflecting different developmental stages. For the determination of F_v/F_M , plants were pre-darkened for at least 25 min.

The energy absorbed by PS II is partitioned into three main pathways which are expressed by their quantum yields, i.e. the quantum yield of photochemical energy conversion or $\Phi(II)$, the quantum yield of non-photochemical quenching or $\Phi(NPQ)$, and the sum of quantum yields of fluorescence and non-regulated heat dissipation of energy or $\Phi(NO)$ (Genty et al. 1996; Hendrickson et al. 2004; Klughammer and Schreiber 2008). These quantum yields were calculated as follows (Klughammer and Schreiber 2008):

$$\Phi(II) = (F_M' - F) / F_M'$$

$$\Phi(NPQ) = F / F_M' - F / F_M$$

$$\Phi(NO) = F / F_M$$

Transmission electron microscopy (TEM) for the analysis of plastoglobules (PGs)

Ultrastructural analysis of chloroplasts in 10 day-old primary leaves of WT and W1 plants grown under LL and HL was done as described before by Saeid Nia et al. (2022). Briefly, segments from the mid part of primary foliage leaves were dissected and fixed with 1% glutaraldehyde in 200 mM HEPES, pH 7.4. Samples were post-fixed with 1% OsO₄ prepared in 1.5% aqueous potassium ferricyanide, contrasted en-bloc with 2% aqueous uranyl acetate, then dehydrated with a graded ethanol series, followed by 100% acetone, next progressively infiltrated with epon resin and then heat polymerised. Ultrathin 80-nm sections were contrasted with saturated aqueous uranyl acetate and lead citrate, and inspected in a Tecnai G2 Spirit BioTWIN transmission electron microscope (FEI, now Thermo Fisher Scientific) equipped with an Eagle 4kx4k CCD camera and TIA software (both FEI).

High-performance liquid chromatography (HPLC) analysis of pigments

From the area between 1.5 and 3 cm below the tip, 1 cm long leaf segments were cut from plants in the climate chamber under the growth irradiance. After measuring the segments' widths, these samples were immediately frozen in liquid nitrogen and stored at -80°C till the time of extraction. Chlorophyll and carotenoid extraction and separation by HPLC have been described by Saeid Nia et al. (2022).

As described by Nichelmann et al. (2016), for calibrating the detector, pure extracts of carotenoids (except antheraxanthin) were prepared through thin-layer chromatography (modified after Lichtenthaler and Pfister 1978), and their concentrations were determined by spectrophotometry using the extinction coefficients provided by Davies (1976). The epoxidation state of the xanthophyll-cycle pigments (EPS) was calculated according to Thayer and Björkman (1990).

HPLC analysis of tocopherols

Leaf segments were prepared and stored at -80°C as explained above. To extract tocopherols, frozen segments were ground with 400 μL HPLC-grade n-heptane together with 5-6 glass beads in a Geno/Grinder (Type 2000; SPEX CertiPrep, Munich, Germany). Afterwards, samples were briefly centrifuged and kept at -20°C overnight. The next day, samples were mixed and supernatants were collected after centrifugation for 10 min at 13000 rpm at 4°C (Kendro Biofuge Fresco, Osterode, Germany). After a second mixing the centrifugation was repeated once more. Finally, 20 μL of supernatants were used for chromatographic analysis of tocopherols using a Shimadzu HPLC system equipped with a RF-10A XL fluorescence detector, 10-series (Shimadzu Corporation, Kyoto, Japan). Tocopherol separation was done using a Lichrospher Si 60 column (5 $\mu\text{m}/250\text{-}4\text{ mm}$, Merck, Darmstadt, Germany) and an isocratic system as described before (Sickel et al. 2012). The pump (LC-10AT VP) delivered a constant flow of 1 mL min^{-1} of the eluent (n-heptane and isopropanol (99/1, v/v)).

Analysis of leaf flavonoid content and composition by HPLC

Leaf segments from 1.5 cm below the tip of primary leaves of WT and W1 plants grown under LL or HL were sampled and frozen in liquid nitrogen as described above. Samples were kept in the freezer at -80°C until HPLC analysis. To prepare samples for HPLC, 250 µL of the cold (4°C) extraction buffer consisting of 49.5% (v/v) distilled water and 49.5% (v/v) methanol with an addition of 1% (v/v) concentrated HCl (Merck, Darmstadt, Germany) was added to each sample. The samples were homogenized for 3 min at 1700 strokes min⁻¹ in a Geno/Grinder 2000 (SPEX CertiPrep) followed by 5 min centrifugation at 16000 x g at 4°C (Biofuge Fresco, Thermo Fisher Scientific, Waltham, Massachusetts, USA). Resulting pellets were resuspended twice in 250 µL of extraction buffer and centrifuged again. All supernatants were collected and centrifuged for 10 min with 10000 x g at 4°C. 500 µL of each supernatant was purified through 0.45 µm filters (National Scientific, Rockwood, USA).

30 µL of the extracted solution were injected in a HPLC system with a diode array detector (SCL-10AT VP, SIL-10AD 145 VP, LC-10AT VP, FRC-10A, SPD-M10A VP, Shimadzu) and separated on a LiChrospher 100 RP-18 column (4 * 250 mm, 5 µm particle size, Merck, Germany). Eluent A, 0.01% phosphoric acid, and eluent B, 90% methanol with 0.1% phosphoric acid, were used in this system as mobile phases at a flow rate of 1 mL min⁻¹. The gradient started with 80% eluent A for the first 12 min followed by a linear decrease in the proportion of eluent A to 55% for 28 min. Afterwards, eluent B was increased linearly to 100% and stayed constant for 12 min. Flavonoids and hydroxycinnamic acids (HCA) were detected at 313 nm and the chromatograms were analysed using LC Solution software (Shimadzu). Representative chromatograms are presented in Fig. S1.

Identification of flavonoids by mass spectrometry

To identify the flavonoids of interest, soluble semi-polar metabolites were extracted from liquid nitrogen-frozen leaf segments in 2-mL screw cap reaction tubes (Sarstedt, Germany). After weighing the samples, ZrO₂ 58% beads (RIMAX ZS-R Ø 1.0-1.2 mm, Mühlmeier, Germany) and 400 µL of LC-MS grade methanol per 100 mg of fresh tissue were added. Sample thawing prior to methanol addition was avoided. Sample grinding and extraction was done in a Precellys

homogenizer (Bertin Instruments, France) at 8000 s^{-1} , with two cycles of 10 s each. Following centrifugation ($22,500\times g$, 4°C , 10 min), the supernatant was recovered into a clean tube and the pellet was resuspended in the same volume of methanol per 100 mg of fresh weight. After mixing, the second supernatant was recovered by centrifugation; the two supernatants were combined and stored at -20°C . Before analysis, $80\text{ }\mu\text{L}$ -aliquots from the methanolic extracts were mixed with $20\text{ }\mu\text{L}$ of 0.5% (v/v) formic acid, incubated overnight (-20°C), and centrifuged ($22,500\times g$, 4°C , 10 min) to remove precipitates.

For the identification of flavonoids, the extracts were analyzed via RP-UPLC-PDA-ESI-UHR-QTOF-MS/MS (Reversed Phase Ultra Performance Liquid Chromatography-PhotoDiode Array-Electrospray Ionization-Ultra-High-Resolution-Quadrupole Time of Flight-tandem Mass Spectrometry) as described in Garibay-Hernández et al. (2021). The analysis was carried out using an Acquity UPLC system (Waters, Germany), equipped with an Acquity PDA $e\lambda$ detector, coupled to a maXis Impact ESI-QTOF MS (Bruker Daltonik GmbH, Germany). The Compass HyStar 3.2 SR2 software (Bruker Daltonik GmbH) was used to operate and coordinate LC-PDA-MS data acquisition. Data processing, analysis, and compound identification were performed using the software packages Compass Data Analysis V4.4 and Metaboscape 5.0 (Bruker Daltonik GmbH, Germany). Compound identity was confirmed by exact mass (error $< 5\text{ ppm}$), isotopic pattern, MS/MS fragmentation, and PDA spectra (Table 1). Commercial standards were employed when available.

Localization of leaf flavonoids

To localize the main flavonoids of the leaves, the leaf abaxial epidermis was separated from the mesophyll by a careful vertical cut in the adaxial epidermis and by gently pulling the epidermis and the remainder of the leaf (leaf plus adaxial epidermis) from each other. Three to five segments of the epidermis and of the remaining part (leaf lacking the abaxial epidermis), respectively, were pooled, frozen in liquid nitrogen, and kept in a freezer at -80°C until HPLC analysis. The flavonoid content of samples was calculated per leaf segment area.

To estimate the flavonoid content in the mesophyll, the flavonoid content of the adaxial epidermis was calculated. To this end, it was assumed that the content of flavonoids in the two epidermal tissues would be proportional to their epidermal absorbance. The latter was determined by chlorophyll fluorescence analysis from both sides of the leaves using a combination of a UVA-PAM fluorometer (Gademann Instruments, Würzburg, Germany; Bilger et al. 2001) and a Mini-PAM fluorometer (Heinz Walz GmbH). After normalization of the fluorescence signals to the signal obtained with a blue plastic film (Walz), the fluorescence signal determined with the UV-A measuring beam was divided by that of the red beam. UV-A transmittance and absorbance were calculated using the fluorescence signals of epidermis-free leaves of *Vicia faba* as a reference. The flavonoid content of the adaxial epidermis was calculated from the HPLC results for the abaxial epidermis using the linear regression between the absorbances of both leaf sides. The result was subtracted from the flavonoid content of the remaining segments to calculate the flavonoid content of the mesophyll.

Gene expression analysis by quantitative RT-PCR

RNA was isolated from a pool of eight leaf segments excised from the middle part of primary leaves using the peqGOLD-TriFast reagent (Peqlab Biotechnology, Erlangen, Germany) as described (Krupinska et al. 2019). Thereafter, RNA concentration was quantified by a Nanodrop instrument 200 (Thermo Scientific). 500 ng of extracted RNA was used to synthesize cDNA using reverse a transcriptase kit (Quanti Tect®, Qiagen, Hilden, Germany) according to the protocol provided by the manufacturer. By using gene-specific primers (details about the gene accession numbers and designed primers can be found in the Supplementary Data, Tab. S1), gene expression was analysed by quantitative PCR as described by Krupinska et al. (2019) and normalized to the mRNA level of the ADP-ribosylation factor 1 as the reference gene (Rapacz et al. 2012). The expression levels of genes of interest were analysed from three independent experiments (each comprising 8 leaves) and each with three technical replicates per sample using the Rotor-Gene Q Series Software (version 2.0.2.4, Qiagen).

Quantification of transcript levels was performed relative to the expression level in LL-grown wild-type plants (as the control) by the “delta-delta C_T method” as described by Livak and Schmittgen (2001).

Determination of the glutathione content and its redox state

For each genotype grown under either LL or HL, a pool of nine primary leaves in total from three independent experiments each comprising three leaves, respectively, were ground with 5-6 glass beads in a Geno/Grinder (Type 2000; SPEX CertiPrep) to a fine powder. Liquid nitrogen was continuously used to avoid the thawing of frozen leaves or their powder. Thereafter, about 50 mg of the powder of each sample was collected in new tubes in the presence of liquid nitrogen.

Total glutathione and GSSG concentrations were determined using a glutathione colorimetric detection kit according to the manufacturer’s protocol (Invitrogen). The absorbance of samples (each with three technical replications) together with a dilution series (to perform a standard curve) of standards (provided in the kit) were measured at 405 nm by a plate reader (TECAN-infinite M200 PRO, TECAN Austria GmbH) in a kinetic assay every minute for 10 min.

To analyse the data, the average of triplicate absorbance measurements for each experimental sample, standard, and background at each time point was calculated and plotted against the incubation time. The slope from the linear part of each curve was determined. The background slope was subtracted from the slope of all standards and samples. Thereafter, the slopes of the standards were plotted against their concentration, and then the slope from the linear part of this curve was used to determine the concentration of total glutathione and GSSG, respectively, in the experimental samples. The amounts of total glutathione and of GSSG were calculated per dry weight of the sample pellets. To calculate the reduced glutathione concentration, the concentration of oxidized glutathione was subtracted from the total glutathione concentration.

Statistical analysis

Sigmaplot 13 (Systat Software GmbH, Erkrath, Germany) or GraphPad PRISM (Prism 9 for Windows, version 9.2.0 (332), GraphPad Software, San Diego, California USA) was used for

statistical analysis. Two-way ANOVA (with the factors genotype and growth irradiance or age) or three-way ANOVA (with the factors genotype, growth irradiance, and age) were used to compare among groups, and in case of significant differences, the Holm-Sidak method was used for comparison of the means.

Results

Photosynthetic electron transport rate (ETR)

Previous gas exchange measurements had revealed that HL-grown WHIRLY1-deficient transgenic plants (W1) were unable to acclimate their photosynthetic capacity to a higher irradiance in contrast to wild-type (WT) plants (Saeid Nia et al. 2022). When electron transport rates (ETR) as determined by chlorophyll fluorescence measurements were compared between WT and W1 plants, a similar difference was observed (Fig. 1). Whereas the maximal electron transport rates of W1 plants grown under HL or LL did not differ ($P = 0.093$), leaves of WT plants grown under HL showed significantly higher ETR than LL-grown WT plants (Fig. 1). Comparing WT to W1 plants, WT plants showed significantly higher maximum ETR in both LL and HL (Fig. 1).

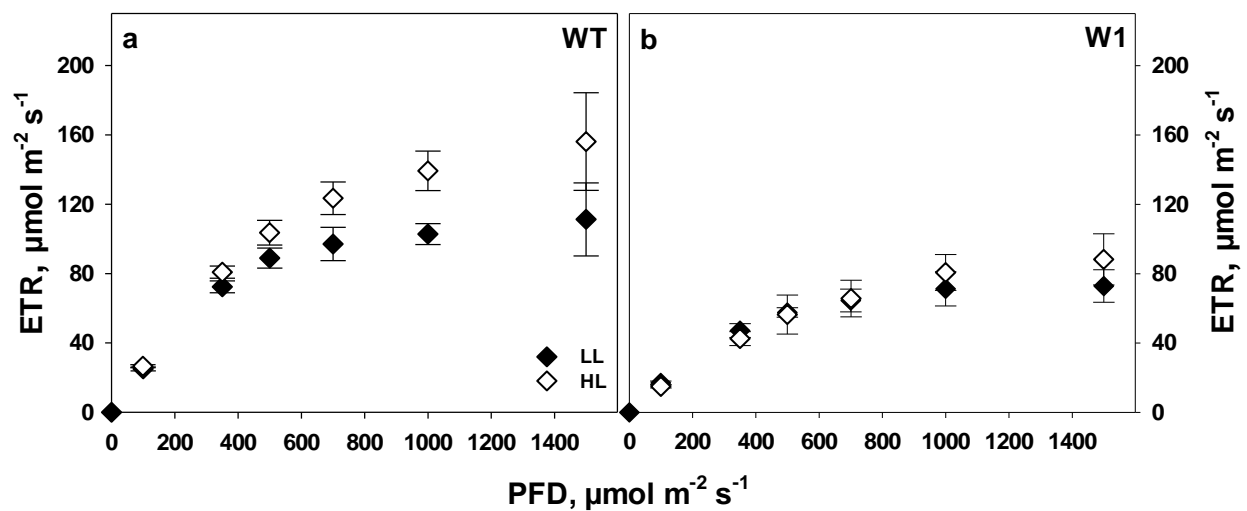


Fig. 1 Electron transport rates (ETR) in WT (a) and W1 (b) plants grown under low (LL, filled symbols) and high light (HL, open symbols) as a function of incident irradiance (PFD). Measurements were done in the presence of 1500 ppm CO₂ at 10 days after sowing (das). Depicted values are means ± standard deviation (SD) of n=9-11 leaves in total from three independent experiments each comprising 3-4 leaves

The maximal quantum yield of photosystem II

The maximal quantum yield of PS II (F_v/F_m) in leaves of LL-grown WT plants stayed stable from 10 to 19 das (Fig. 2, $P > 0.9999$). The small decrease in F_v/F_m in HL-grown WT from 10 to 15 and 19 das was not significant (Fig. 2a).

Similar to previous results (Kucharewicz et al. 2017), in leaves of 10-day old W1 plants, F_v/F_m in both LL- and HL-grown plants was significantly lower compared to the values of the WT and also compared to those of W1 plants at 15 and 19 das.

Progressing development of W1 plants from day 10 to day 15 was accompanied by a significant increase in the maximal quantum yield of PS II (Fig. 2b) reaching a value commonly observed in unstressed plants (Björkman and Demmig 1987) despite their inability to acclimate their photosynthetic capacity to high growth irradiance (Saeid Nia et al. 2022). This suggests that their lower photosynthetic capacity was compensated through other mechanisms. To investigate this, the fate of excitation energy in PS II of HL-grown WT and W1 plants, respectively, was analyzed in more detail at 10 and 15 das.

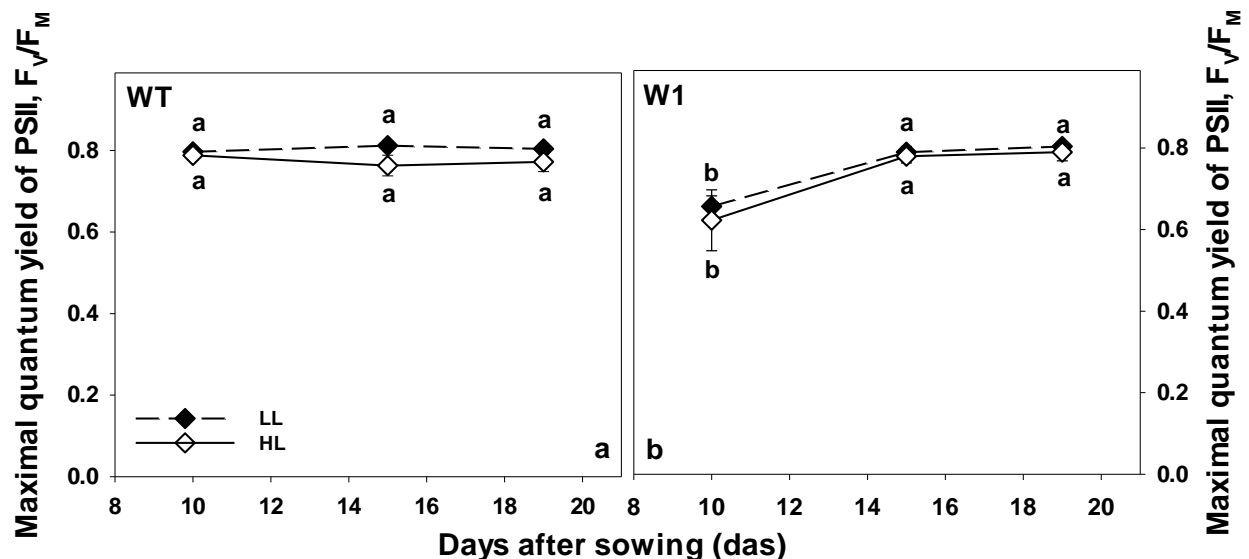


Fig. 2 Maximal quantum yield of PS II, F_v/F_m , measured in WT (a) and W1 (b) plants grown under low light (LL, filled symbols) and high light (HL, open symbols) as a function of plant age. Depicted values are means \pm standard deviation of a total of $n = 9-11$ leaves from three independent experiments, each comprising 3-4 leaves. The letters indicate statistically different values at a significance level of $P = 0.05$, as determined by two-way ANOVA with time and genotype as factors, followed by pairwise multiple means comparisons with the Holm-Sidak method

The fate of excitation energy in PS II

The analysis of the fate of absorbed energy in PS II revealed that 10 day-old W1 plants had a lower quantum yield of photosynthesis ($\Phi(II)$) (Fig. 3c) in comparison to WT plants (Fig. 3a). However, their lower $\Phi(II)$ was accompanied by a higher quantum yield of non-photochemical quenching ($\Phi(NPQ)$).

No specific changes were detected in $\Phi(II)$ and $\Phi(NPQ)$ of WT plants between 10 and 15 das (Fig. 3b). In contrast, $\Phi(II)$ increased and $\Phi(NPQ)$ decreased in W1 plants from 10 to 15 das (Fig 3d).

Since the HL-grown plants received an irradiance of about $350 \mu\text{mol m}^{-2} \text{s}^{-1}$ during growth, the fate of absorbed energy at this irradiance was analyzed further in WT and W1 plants at 10 and 15 das (boxes in Fig. 3). The two-way ANOVA analysis showed that there were no significant differences in the quantum yield of PSII or $\Phi(NPQ)$ between WT plants at 10 and 15 das.

While $\Phi(II)$ was significantly lower in WHIRLY1-deficient plants than in WT plants at 10 and 15 das, the $\Phi(NPQ)$ was significantly higher. Moreover, as development of W1 plants progressed between 10 and 15 das, a significant increase in $\Phi(II)$ was accompanied by a significant decrease in $\Phi(NPQ)$. Intriguingly, there were no significant differences between non-regulated energy dissipation ($\Phi(NO)$) of WT and W1 plants at 10 and 15 das.

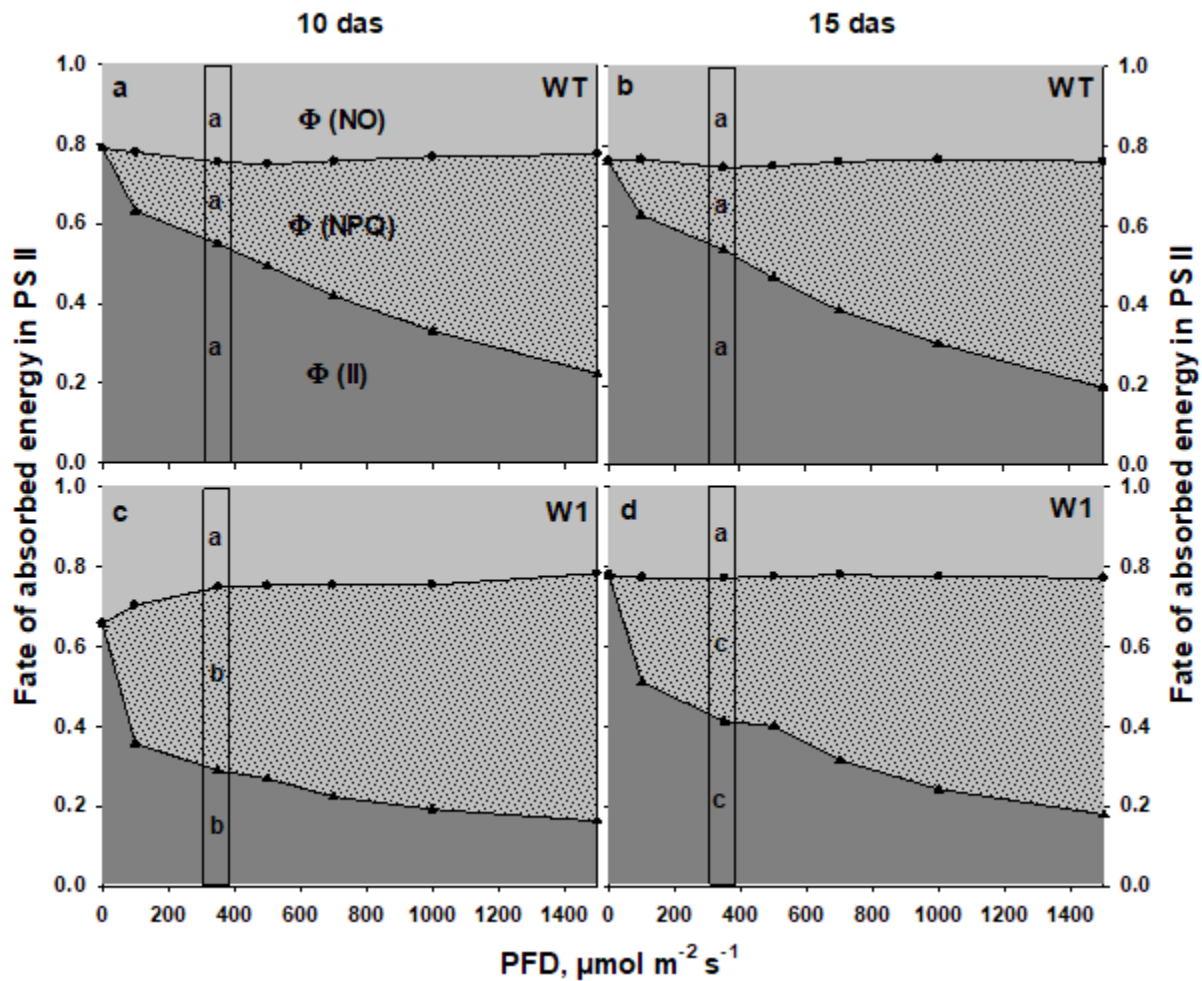


Fig. 3 The fate of excitation energy in PS II as a function of incident PFD in HL-grown WT (a, b) and W1 plants (c, d) at 10 and 15 das. Measurements were done in the presence of 1500 ppm CO_2 . Depicted values are means of a total of $n = 9-11$ leaves from three independent experiments each comprising 3-4 leaves. The boxes highlight the fate of absorbed energy in PS II at the incident light of $350 \mu\text{mol m}^{-2} \text{s}^{-1}$, which is similar to the growth irradiance of HL-grown plants. The letters indicate statistically different values at a significance level of $P = 0.05$, as determined by two-way ANOVA with das and genotype as factors, followed by pairwise multiple means comparisons with the Holm-Sidak method

Ultrastructural analyses revealed an accumulation of plastoglobules in high-light grown W1 leaves

Oxidative stress in chloroplasts is accompanied by an accumulation of plastoglobules (Austin et al., 2006). To compare the abundance and size of these lipid particles, the chloroplast ultrastructure of WT and W1 plants grown under HL or LL for 10 das was analyzed (Fig. 5). In WT and W1 plants grown under LL, the abundance of plastoglobules, their size (maximum diameter ~ 80 nm) and their localization along stroma thylakoids were similar. In HL-grown W1 plants,

plastoglobules were larger (maximum diameter ~130 nm) and more abundant. A particularly prominent feature of increased abundance were row-like clusters of plastoglobules that were lined up along adjacent stroma thylakoid membranes. In accordance with the data obtained by characterization of photosynthesis (Fig. 1-3), these observations suggest that W1 plants exposed to excessive light suffered from oxidative stress (Bréhélin et al. 2007; Rottet et al. 2016).

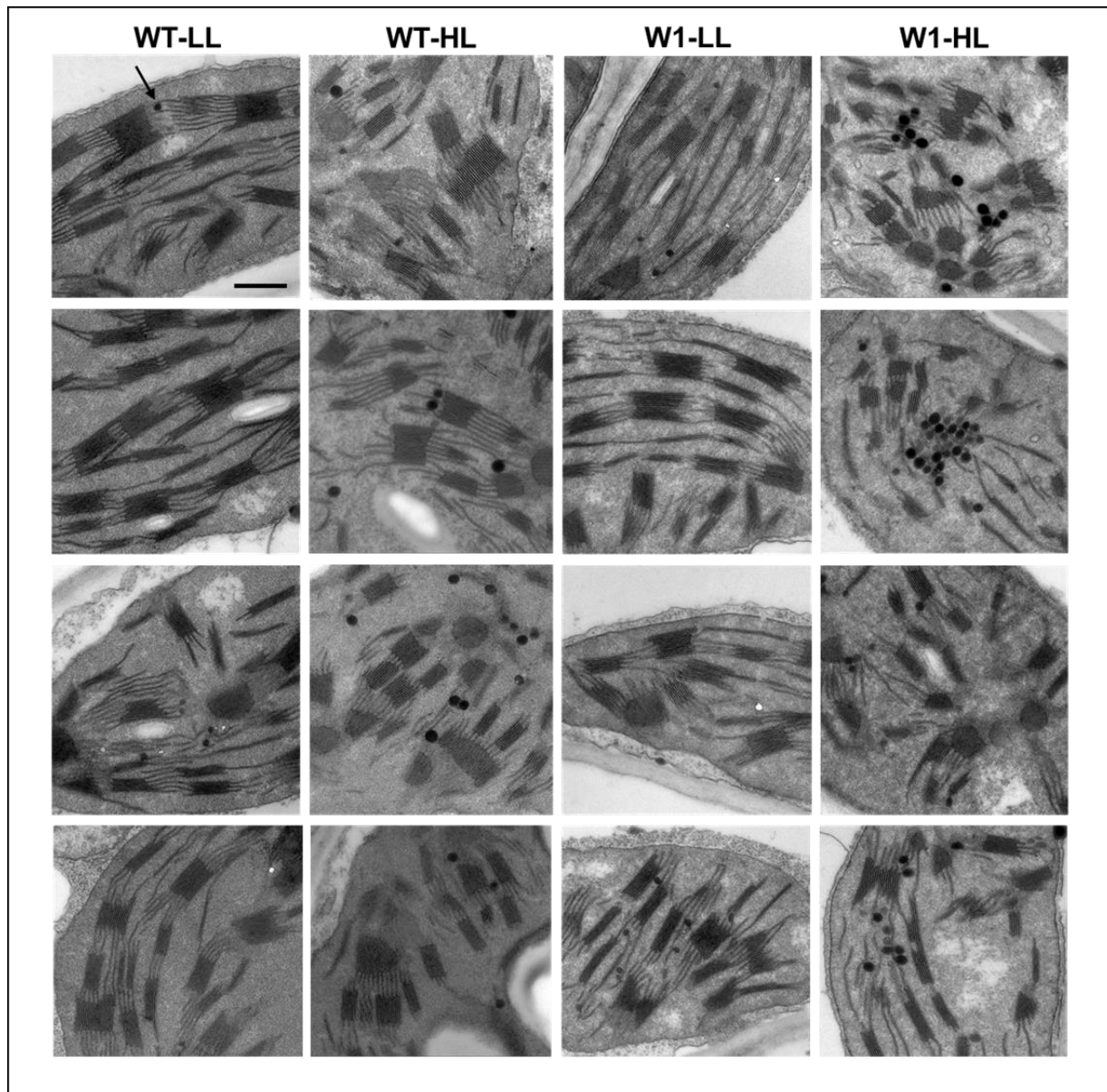


Fig. 4 Ultrastructural analysis of chloroplasts in primary foliage leaves of WT and W1 plants grown under high light (HL) or low light (LL) for 10 days. Plastoglobules (arrow) appear as electron-dense granules associated with stroma thylakoid membranes. Under HL, plastoglobules increased in size and abundance. Four images per condition are shown to illustrate the diversity of plastoglobule phenotype observed on thin sections. Scale bar, 500 nm

Pigments of the photosynthetic apparatus

In view of the well-known formation of zeaxanthin in response to excessive excitation energy and its role in the mediation of NPQ (Demmig-Adams and Adams 1996; Jahns and Holzwarth 2012), the carotenoid content of WT and W1 leaves 10 and 15 das was analyzed. For comparison, the chlorophyll content of plants was also analyzed since it represents the progress of development of W1 plants from day 10 to day 15.

As shown previously by Kucharewicz et al. (2017) and Saeid Nia et al. (2022), the chlorophyll content of WT plants, especially HL-grown ones, decreased from day 10 to day 15 (Fig. 5a), whereas it increased in the case of W1 plants (Fig. 5b). This indicates that the development of chloroplasts in W1 plants is delayed, in accordance with our previous observations (Krupinska et al. 2019).

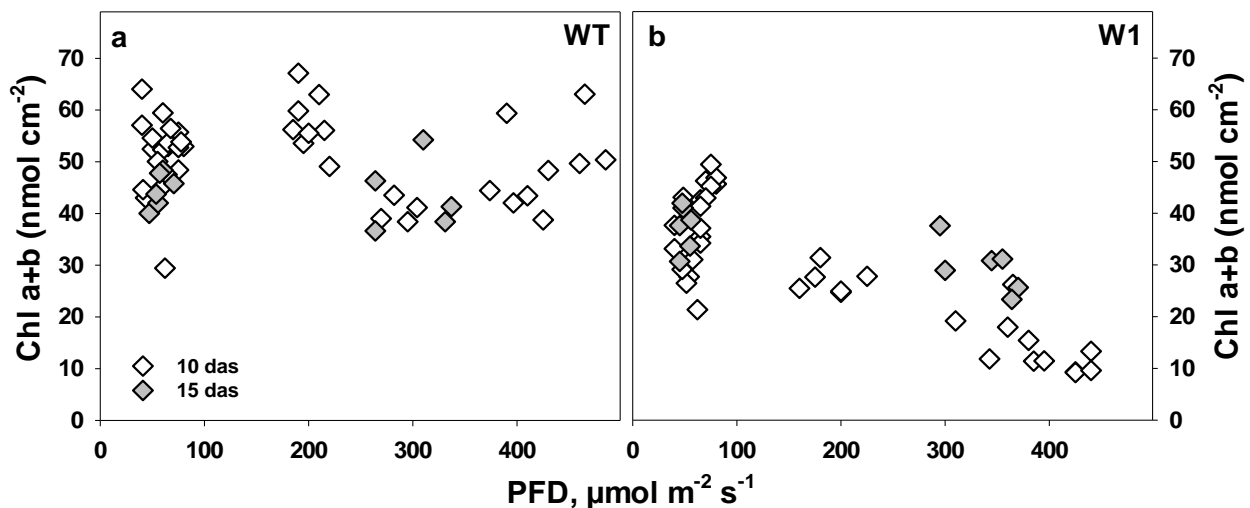


Fig. 5 Chlorophyll content as a function of growth PFD incident on each investigated leaf of WT (a) and W1 (b) plants. Open and filled symbols denote determinations in single leaves of plants at 10 and 15 das, respectively

Under excessive light, zeaxanthin is formed in chloroplasts causing a low epoxidation state (EPS) of the xanthophyll cycle pigments which is an *in vivo* indicator of excessive PFD (Demmig-Adams et al. 1990; Ort 2001). In line with the photosynthesis measurements taken *ex situ* (Saeid Nia et al. 2022, Fig. 1), EPS determined *in situ* under growth conditions significantly declined in W1 plants to values close to zero with increasing growth irradiance (Fig. 6a). In both WT and W1

plants, the xanthophyll cycle pool (V+A+Z) size increased significantly with increasing light. However, in leaves of W1 plants, the VAZ pool was considerably larger than in the WT ($p < 0.0001$) (Fig. 6b). Also lutein increased strongly with increasing PFD in the W1 plants (Fig. S3). WHIRLY1-deficient plants had a significantly lower epoxidation state of the cycle and larger VAZ pool size in comparison to WT plants even under LL conditions (Figs. 6a and b).

As chloroplast development in the W1 plants progressed, indicated by the higher chlorophyll content at 15 das in comparison to 10 das (Fig. 5b), EPS increased ($p < 0.0001$) (Fig. 6a), and the xanthophyll cycle pigment pool size decreased ($p < 0.0001$) (Fig. 6b). Nevertheless, at 15 das, HL-grown W1 plants still showed a significantly larger VAZ pool size (Fig. 6b) and significantly lower EPS compared to the WT (Fig. 6a). These data are in accordance with the results obtained with barley WT and W1 plants grown in continuous light (Swida-Barteczka et al. 2018).

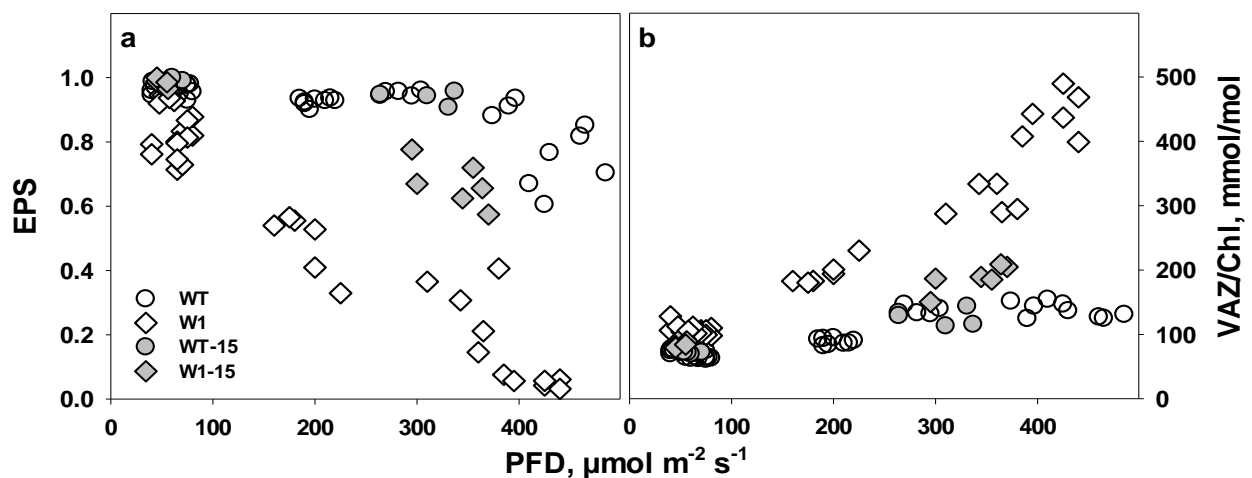


Fig. 6 The epoxidation state (EPS) (a) and the pool size of the violaxanthin cycle (VAZ) per chlorophyll (b) in single WT and W1 leaves as a function of the growth irradiance (PFD) incident on these leaves. Circles and diamonds denote WT and W1 plants, respectively. Open and filled symbols denote 10- and 15-day old plants, respectively

It has been proposed that the VAZ pool size increases as a function of excessive PFD (Bilger et al. 1995). To investigate this relationship, the VAZ pool size was plotted as a function of EPS. The data for both genotypes, WT and W1 collected at 10 das, followed a single common function (Fig. 7). With further development in the W1 plants, the decline in VAZ/Chl was coordinated with the increase in EPS, causing the LL data points from 15 das to fall on the same relationship as data

from 10 das. Only samples from HL showed a slightly enhanced VAZ pool size at 15 das in both genotypes, WT and W1, in comparison to 10 das.

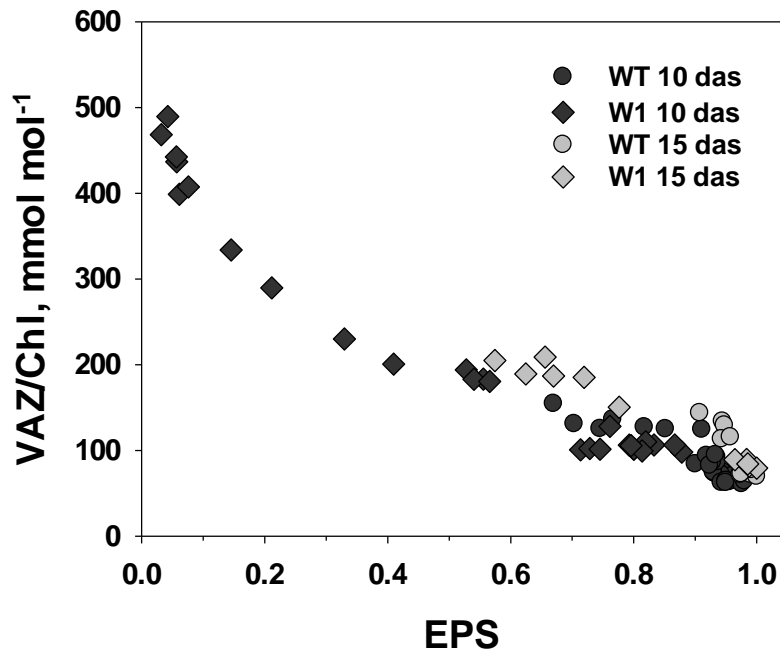


Fig. 7 VAZ / Chl in single leaves of WT and W1 plants grown under different irradiance as a function of the violaxanthin cycle epoxidation state (EPS).

Expression of genes required for zeaxanthin formation and its epoxidation

Relative expression levels of genes encoding β -carotene hydroxylase-1 (*HvbcHYD*) and zeaxanthin epoxidase (*HvZEP*) were measured.

HvbcHYD is the key enzyme of zeaxanthin biosynthesis (Sun et al. 1996; Davison et al. 2002). As expected, expression of *HvbcHYD* was increased in WT plants in HL, however, the increase was not strong enough to be significant. In comparison, the relative expression level of *HvbcHYD* in HL-grown W1 plants was significantly higher than in LL-grown W1 plants as well as in HL-grown WT plants (Fig. 8a).

HL-grown WT plants also showed significantly higher *HvZEP* expression in comparison to those grown in LL, while no significant difference in the expression of *HvZEP* was detectable between transgenic plants grown in LL or HL (Fig. 8b).

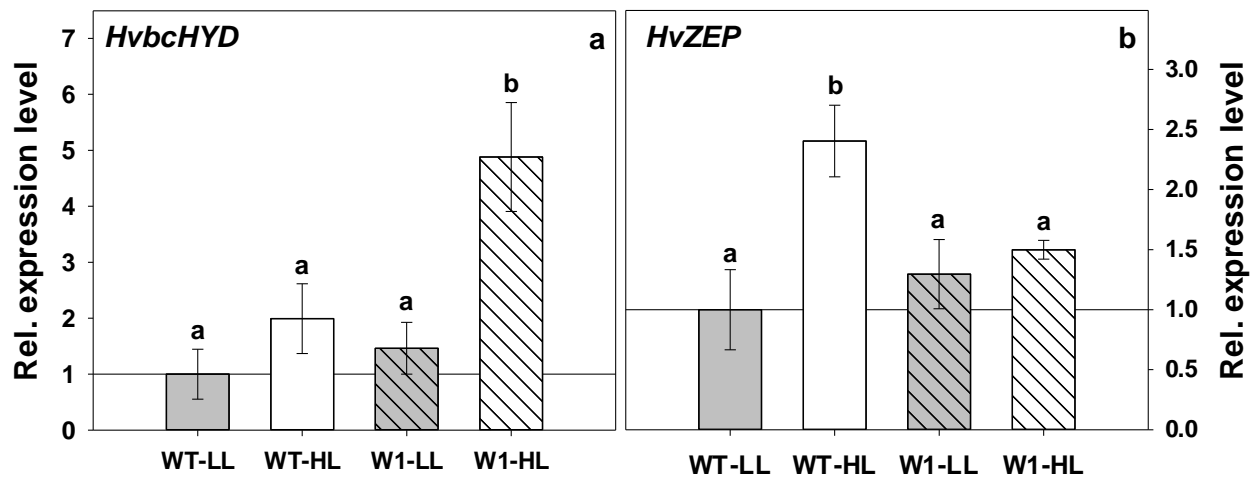


Fig. 8 Relative expression level of β -carotene hydroxylase-1, HvbCHYD, (a) and zeaxanthin epoxidase, HvZEP, (b) in WT and W1 grown under low (LL, grey bars) and high light (HL, grey bars) at 10 das. Columns are means \pm standard deviation from three independent experiments. Quantification of transcript levels was performed relative to the expression level in LL-grown WT plants as the control (WT-LL is set at 1.0). The letters indicate statistically different values at a significance level of $P = 0.05$, as determined by two-way ANOVA, followed by pairwise multiple means comparisons by the Holm-Sidak method

Tocopherol content of leaves

Tocopherols are important lipophilic antioxidants, which might protect the thylakoid membrane during growth in HL (Munné-Bosch and Alegre 2002; Li et al. 2012). Unexpectedly, the α -tocopherol content did not differ between WT and W1 plants when grown for 10 or 15 das in either LL or HL (Fig. 9 a and b, see also Tab. S2). In contrast, at a later stage of development, i.e. after 19 das, the α -tocopherol content increased in WT leaves, whereas it stayed constant in W1 leaves (Fig. 9).

In addition to the predominant α -tocopherol, also minor contents of β -tocopherol and γ -tocopherol as well as the total tocopherol content of WT and W1 plants grown under LL and HL at different developmental stages were analyzed (Tab. S2). The tendency of the data matches that obtained for α -tocopherol (see Tab. S2).

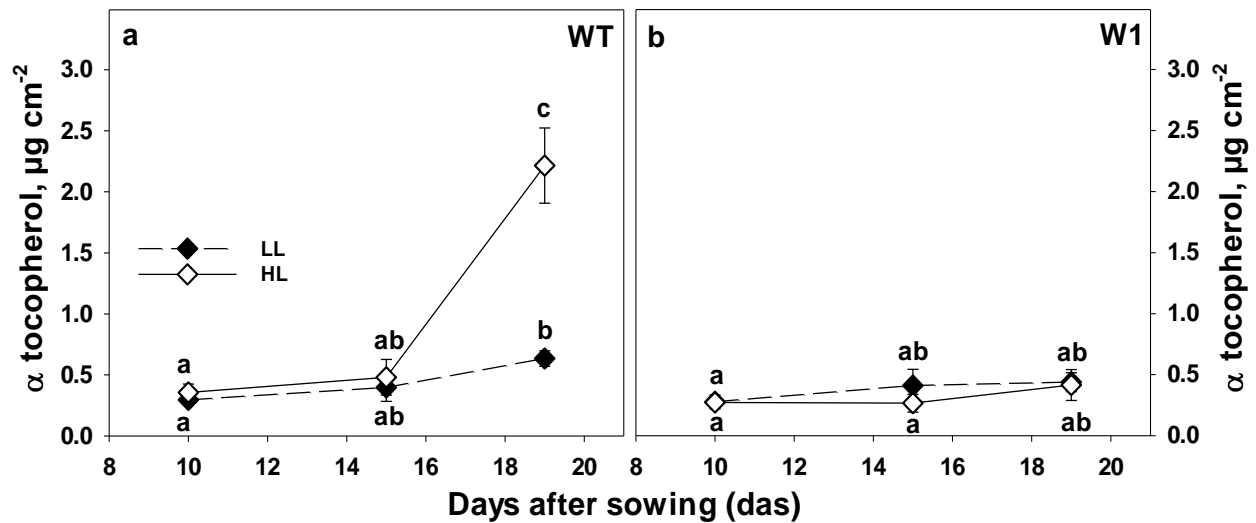


Fig. 9 α -tocopherol content of leaves in WT (a) and W1 (b) plants grown under low light (LL, filled symbols) and high light (HL, open symbols) as a function of days after sowing (das). Depicted values are means \pm standard deviation of $n = 6$ samples. The letters indicate statistically different values at a significance level of $P = 0.05$, as determined by three-way ANOVA with genotype, irradiance, and das as factors, followed by pairwise multiple means comparisons by the Holm-Sidak method (see Tab. S2)

HPLC analysis of flavonoid content

Among the more hydrophilic antioxidants assumed to support photoprotection in plants are the flavonoids (Agati et al. 2013). Accordingly, HPLC analysis showed a significant increase in the total content of flavonoids as a response to HL in both genotypes. However, there was no significant difference between WT and W1 plants, neither under LL (analyzed with two-way ANOVA) nor under HL (Fig. 10a).

Nevertheless, the relative expression level of the gene encoding one of the key enzymes in flavonoid biosynthesis, chalcone synthase (*CHS*) (Agati et al. 2012), was significantly enhanced in WT plants ($P = 0.001$) during growth in HL (Fig. 10b). The tendential increase of the expression of *CHS* in W1 plants in response to HL was not significant ($P = 0.137$).

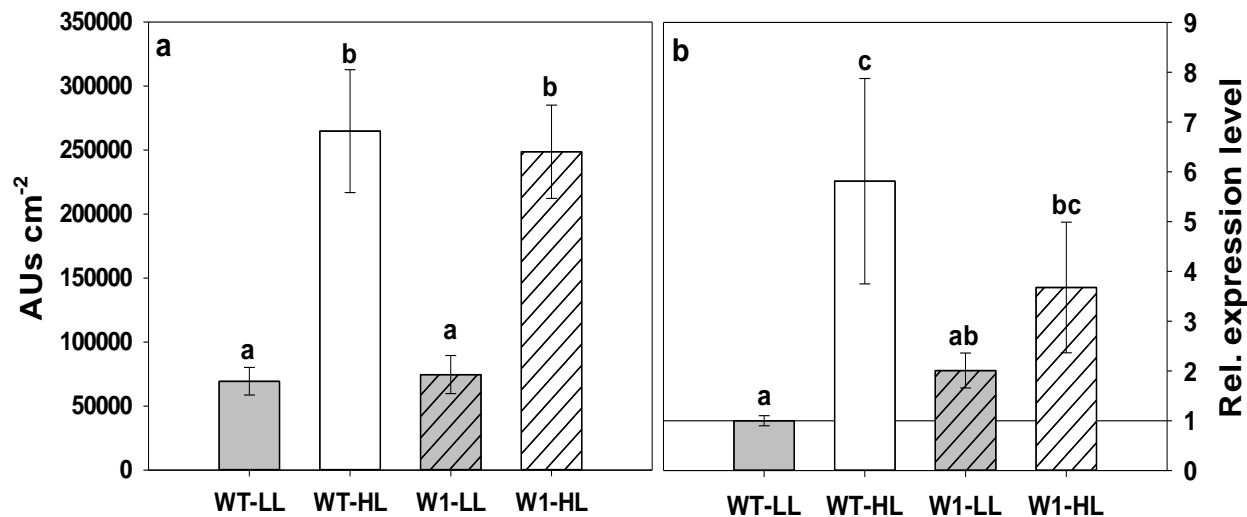


Fig. 10 (a) The total amount of flavonoids in leaves of WT and W1 plants grown under low (LL, grey bars) and high light (HL, white bars) at 10 das expressed as the sum of all peaks detected at 313 nm in the chromatograms. The data show means \pm standard deviation of $n = 20$ -23 leaves in total from three independent experiments each comprising 6-8 leaves. (b) The relative expression level of the gene encoding chalcone synthase (*CHS*) in WT and W1 plants grown under LL and HL at 10 das. Quantification of transcript levels was performed relative to the expression level in LL-grown WT plants as the control and therefore WT-LL is set at 1.0. The data show the means \pm standard deviation of three independent experiments. The letters indicate statistically different values at a significance level of $P = 0.05$, as determined by two-way ANOVA with genotype and irradiance as factors, followed by pairwise multiple means comparisons by the Holm-Sidak method

Flavonoid composition of leaves

Whereas the total flavonoid content did not differ between WT and W1 leaves, the flavonoid composition differed considerably between WT and W1 plants in HL conditions (Fig. 11). The two prominent peaks in HPLC chromatograms of the HL grown W1 plants (see representative chromatograms in Fig. S1) were identified based on their UV and MS spectra (Table 1). The highest peak in both genotypes under either HL or LL was confirmed as saponarin (apigenin-6-*C*-glucosyl-7-*O*-glucoside). In line with the total amount of flavonoids, HL-grown plants showed a significantly higher content of saponarin than LL-grown plants. Moreover, the amount of saponarin was 10% higher in HL-grown WT plants than in W1 plants (Fig. 11a). The compound with the second highest abundance in HL grown W1 samples was confirmed to be lutonarin (luteolin-6-*C*-glucosyl-7-*O*-glucoside). Similar to saponarin, this flavonoid showed an increased abundance in HL-grown plants from both genotypes. Interestingly, W1 plants grown at HL displayed an eightfold higher amount of lutonarin in comparison to the HL-grown WT (Fig. 11b).

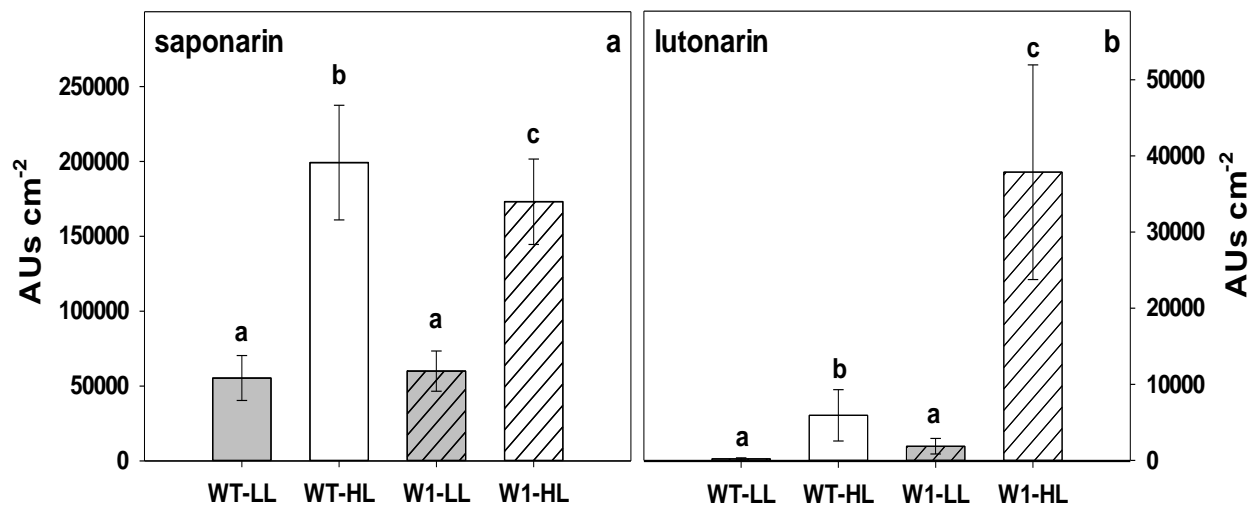


Fig. 11 Leaf content of saponarin (a) and lutonarin (b) expressed as HPLC peak area in WT and W1 grown under low (LL, grey bars) and high light (HL, white bars) at 10 das. The data show the means \pm standard deviation of $n = 28-31$ leaves in total from four independent experiments each comprising 7-8 leaves. The letters indicate statistically different values at a significance level of $P = 0.05$, as determined by two-way ANOVA with genotype and irradiance as factors, followed by pairwise multiple means comparisons by the Holm-Sidak method

Localization of saponarin and lutonarin

To localize the main flavonoids within the leaves, their abaxial epidermis was gently removed from an area of about 1 cm^2 . With respect to saponarin, the leaf area-related flavonoid content of isolated epidermal peels showed similar trends for the various light conditions and genotypes as the contents of total leaves (Fig.12, left panels). However, the lutonarin content was strongly reduced in the epidermal peels (Fig. 12, right panels). Since it was not possible to remove the adaxial epidermis at the same time from the remaining piece of mesophyll, the content of this epidermis was extrapolated using measurements of epidermal UV-A transmittance with PAM fluorometry. These measurements revealed that epidermal UV-A transmittance in the adaxial side was very close to that of the abaxial side (Fig. S2). Assuming that not only the total flavonoid content, but also the flavonoid composition of both epidermal tissues are similar, the major amount of lutonarin should be located in the mesophyll. Roughly 50% of the saponarin content of WT leaves was expected to be located in the mesophyll, whereas only a minor part of saponarin was estimated for the mesophyll of W1 plants. It is possible that the formation of lutonarin in these leaves occurred to some extent at the expense of saponarin accumulation.

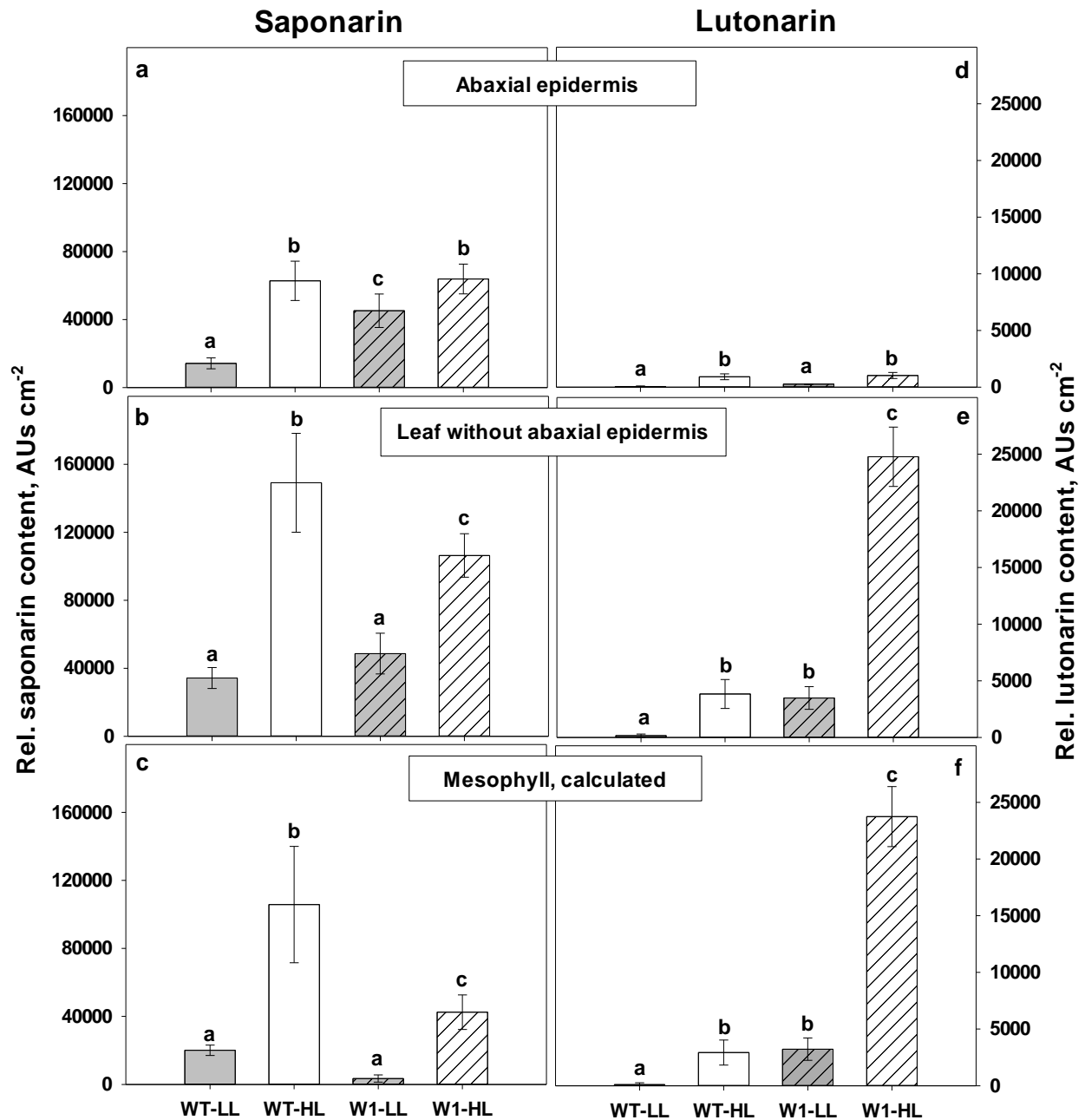


Fig. 12 Relative contents of saponarin (a-c) and lutonarin (d-f) in the abaxial epidermis, in the segments with removed epidermis ('leaf without abaxial epidermis') and in the mesophyll, respectively, in WT and W1 grown under low (LL, grey bars) and high light (HL, white bars) at 10 das. The data show means \pm standard deviation of $n = 3$ samples from three independent experiments. Each sample was a pool of 3-5 leaves. The letters indicate statistically different values at a significance level of $P = 0.05$, as determined by two-way ANOVA with genotype and irradiance as factors, followed by pairwise multiple means comparisons by the Holm-Sidak method

The ratio of reduced (GSH) to oxidized (GSSG) glutathione

Glutathione, being a hydrophilic antioxidant found in all cell compartments (Zechmann 2014; Gasperl et al. 2022) may have been involved in ROS protection at HL (Hebbelmann et al. 2012; Heyneke et al. 2013; Dorion et al. 2021). Unlike to LL-grown WT plants, in HL-grown WT the ratio of reduced to oxidized glutathione decreased with increasing age (Fig. 13a).

In contrast, in W1 plants grown either at LL or HL, the ratio of GSH/GSSG did not show any decrease with age, but stayed at a similar level as the ratio of 10 day-old WT plants. Rather, the GSH/GSSG ratio of HL-grown W1 showed even slightly higher values than that of LL-grown ones (Fig. 13b).

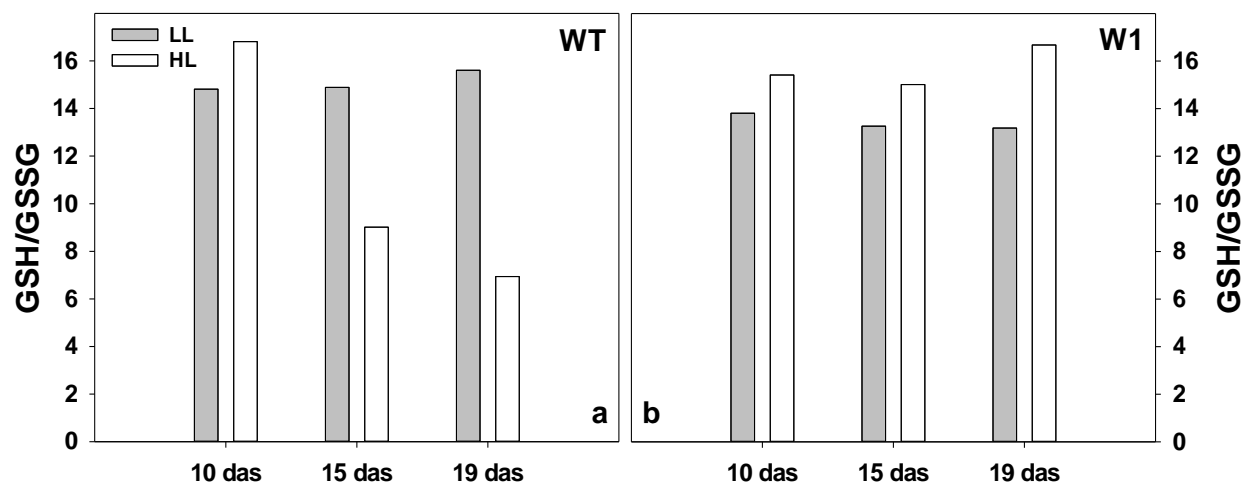


Fig. 13 Ratio of reduced (GSH) and oxidized (GSSG) glutathione in WT (a) and W1 (b) plants grown under low (LL, grey bars) and high light (HL, white bars) on different days after sowing. The data show determinations on pools of 9 primary leaves each, from three independent experiments each comprising three leaves

Discussion

As reported in previous studies, WHIRLY1-deficient barley plants (W1) have reduced photosynthetic activity and show retarded chloroplast development and senescence (Kucharewicz et al. 2017, Krupinska et al. 2019). Recently, these plants were also shown to be inhibited in photosynthetic acclimation to high irradiance (Saeid Nia et al. 2022). In accordance with the previous results, in this study, the W1 plants showed a reduced electron transport rate

(ETR) in comparison to WT plants (Fig. 1). Also, under their growth conditions, they showed typical signs of being exposed to excessive irradiance as indicated by the low epoxidation state (EPS) of the xanthophyll cycle (Fig. 6). A low EPS is indicative of the formation of zeaxanthin as result of a high transthylakoidal proton gradient, activating the enzyme violaxanthin de-epoxidase (Yamamoto 1979; Bilger et al. 1989). It is well-known that EPS follows the photochemical quantum yield of PS II under varying illumination (e.g., Bilger and Lesch 1995). Hence, there is no doubt that W1 plants suffered from stress caused by high PFD, especially those grown under HL. It should be noted that the irradiance was always measured parallel to the surface of the barley leaves which were mostly oriented vertically. Horizontal irradiance measured above the plants was $1000 \mu\text{mol m}^{-2} \text{s}^{-1}$, which is comparatively high for a growth chamber experiment. It was expected that the W1 plants, which are impaired in light acclimation, should develop symptoms of photoinhibition when grown under HL conditions, e.g., a reduction in F_V/F_M (Aro et al. 1993; Demmig-Adams and Adams 2006; Takahashi and Badger 2011) and eventually loss of chlorophyll (Havaux et al. 2005).

Unexpectedly, the chlorophyll content of W1 plants did increase between 10 and 15 das both under LL and HL conditions indicating that the delayed chloroplast development in W1 plants (Krupinska et al. 2019) was not affected by the light conditions the plants were exposed to. In parallel, F_V/F_M starting at a reduced level of about 0.65 at 10 das increased to the WT level at 15 das. Considering that W1 plants cannot enhance photosynthetic capacity at high light (Saeid Nia et al. 2022) as further corroborated by the ETR measurements shown in Fig. 1, they required alternative strategies to cope with excessive light stress. To elucidate these strategies, the fate of the absorbed light was determined. As described above, energy absorbed in PS II is partitioned into three main pathways, $\Phi(\text{II})$, $\Phi(\text{NPQ})$ and $\Phi(\text{NO})$. In leaves of W1 plants the quantum yield of photochemical energy conversion, $\Phi(\text{II})$, was reduced. Even at irradiances higher than those encountered during growth in the climate chamber, the W1 plants were able to compensate for the reduced $\Phi(\text{II})$ by increased quantum efficiency for non-radiative dissipation, $\Phi(\text{NPQ})$ (Fig. 3). Only at the youngest developmental stage and at lower irradiance, the remaining fraction of the energy corresponding to the energy that is passively dissipated by either fluorescence or heat, $\Phi(\text{NO})$, was increased in W1 leaves, indicating a stressful situation (Klughammer and Schreiber

2008). However, at 15 das, when chloroplasts were further developed, as indicated by an increased leaf chlorophyll content (Fig. 5), this symptom had disappeared.

To investigate whether oxidative stress affected the ultrastructure of W1 chloroplasts, electron microscopy images were analysed at 10 das. By this approach, it became obvious that chloroplasts of W1 plants grown at HL contained larger and a higher amount of plastoglobules than those of the WT (Fig. 4). Plastoglobules are plastid lipoprotein particles surrounded by a lipid monolayer and thereby being contiguous with the outer leaflet of thylakoid membranes, which enables an exchange of lipophilic compounds (van Wijk and Kessler 2017). Their multiple functions include the metabolism of prenyl lipids such as tocopherols and the remobilization of thylakoid lipids during stress and senescence. Since long time it is known that chloroplasts of sun plants have more and larger plastoglobules than chloroplasts of shade plants and that light promotes the accumulation of tocopherols and also zeaxanthin in the plastoglobules (reviewed by Lichtenthaler 2013). An increase in the number and/or size of plastoglobules hence is indicative of oxidative stress as a result of excessive light (Bréhélin et al. 2007; Rottet et al. 2016).

To investigate whether W1 plants possess antioxidative mechanisms in addition to non-radiative dissipation in order to cope with the stressful situation of excessive light, four different types of antioxidative metabolites were measured. Two of them are lipophilic, i.e. zeaxanthin and α -tocopherol, and two are mainly hydrophilic, i.e. glutathione and flavonoid glycosides. Based on chlorophyll content, the xanthophyll cycle pool in W1 leaves was very large at higher irradiances, exceeding by far the number of possible xanthophyll binding sites in the light-harvesting complexes (Caffarri et al. 2014) (Fig. 6b). Furthermore, the majority of the xanthophyll cycle pigments were in the de-epoxidized form zeaxanthin (Fig. 6a). A part of the zeaxanthin pool may have been involved in the mechanism of NPQ, which was strongly enhanced in W1 plants (Fig. 3). In addition to its function in promoting NPQ, zeaxanthin is known to prevent the oxidation of membrane lipids (Havaux and Niyogi 1999; Havaux et al. 2007). Presumably, the larger fraction of zeaxanthin in HL-grown W1 plants was not bound to an LHC, but freely located in plastoglobules and in chloroplast membranes. In a chl *b*-deficient *Arabidopsis* mutant, free zeaxanthin was shown to be the only carotenoid conferring protection against high light damage (Havaux et al. 2007). Havaux et al. (2007) suggested that quenching of $^1\text{O}_2$ or scavenging of free

radicals by zeaxanthin molecules either located close to the lipid interfaces of LHCII or freely located in the lipid matrix provides photoprotection. Zeaxanthin's physicochemical interactions with lipids and its orientation in the membrane lipid bilayer (McNulty et al. 2007; Havaux et al. 2007), the extended number of double bonds (Mathews-Roth et al. 1974; Havaux et al. 2007) and its polarity (Wisniewska et al. 2006; Havaux et al. 2007) are considered as important factors determining the specific role of zeaxanthin in protection of thylakoid membrane lipids.

Further analyses of carotenoids revealed that the increase in growth irradiance and excessive excitation energy as indicated by the large VAZ pool and its low epoxidation state (Fig. 6) was accompanied by a strong enhancement of the lutein content of leaves (Fig. S3). In light-harvesting complexes (LHCs), lutein is known as the main quencher of $^3\text{Chl}^*$ (Mozzo et al. 2008; Jahns and Holzwarth 2012; Nezval et al. 2017). Moreover, lutein is involved in the prevention of the formation of $^1\text{Chl}^*$ through its contribution to NPQ (Johnson et al. 2009; Jahns and Holzwarth 2012). However, similar to the xanthophyll cycle pigments, the amount of lutein did by far exceed the number of binding sites in the LHC. Therefore, free lutein may have fulfilled an antioxidative role (Havaux et al. 2007; Demmig-Adams et al. 2020). Havaux et al. (2007) reported that lutein associated with high amounts of zeaxanthin was even more effective in the photoprotection of plants than zeaxanthin itself. In egg yolk liposomal membranes, lutein proved to be an antioxidant as efficient as zeaxanthin (Sujak et al. 1999). Therefore, it is likely that in addition to the free zeaxanthin pool, the elevated amount of lutein was important for the photoprotection of HL-grown W1 plants.

The high zeaxanthin content of W1 leaves at HL correlated positively with the enhanced total pool size of VAZ (Fig. 7). It has been previously hypothesized that the well-known increase of the VAZ pool size (Thayer and Björkman 1990, Demmig-Adams et al. 2012) is not regulated by PFD directly, but rather in response to excessive PFD (Bilger et al. 1995; García-Plazaola et al. 2002). As shown in Fig. 7, the VAZ pool size was a close function of EPS, as already observed earlier (Bilger et al. 1995). Furthermore, when EPS increased during further development of the W1 plants, presumably as a response to improved $\Phi(\text{II})$ (Fig. 3d), also the VAZ pool size was reduced, keeping the data points close to the previously observed relationship (Fig. 6). This indicates that the VAZ pool size could be regulated by an as yet unknown mechanism that responds to excessive PFD.

One factor controlling the VAZ pool size is the expression of the gene encoding β -carotene hydroxylase (*HYD*, named also as *CHY* (Kawabata and Takeda 2014)). Both the VAZ pool size and the expression of *HYD/CHY1,2* genes in Arabidopsis were shown to increase under HL conditions (Kawabata and Takeda 2014). Using inhibitors of photosynthesis (DCMU, DBMIB), the authors revealed furthermore that the expression of the *CHY* genes, as well as the VAZ pool size, is controlled by the redox state of plastoquinone (even at LL) (Kawabata and Takeda 2014). Overexpression of the *HYD/CHYB* gene in Arabidopsis was shown to enhance tolerance to HL (Davison et al. 2002). The expression of *HYD* was strongly enhanced in the W1 line, especially at high PFD. At the same time, the gene encoding ZEP which catalyses epoxidation of zeaxanthin to violaxanthin (Jahns and Holzwarth 2012), was strongly induced at HL in the WT, but not in the W1 line (Fig. 8b). This pattern of gene expression is in accordance with the increased VAZ pool and the low epoxidation state of the xanthophyll cycle pigments.

In contrast to the zeaxanthin content, the content of tocopherols did neither change in the WT nor in W1 plants in response to HL (Fig. 9). This finding was unexpected considering that α -tocopherol has been described as a potent lipophilic antioxidant (Falk and Munné-Bosch 2010; Lushchak and Semchuk 2012), whose level increased together with the level of any ROS species (Kruk et al. 2016) or with increasing irradiance as shown in several studies with Arabidopsis (Lushchak and Semchuk 2012; Collakova and DellaPenna 2003a and b). In contrast to these reports, it has been also observed that the tocopherol content did either not increase with high irradiance (Szymańska et al. 2017) or even declined, e.g. in maize (Leipner et al. 2000; Munné-Bosch and Alegre 2002) and in the cyanobacterial strain *Synechocystis* sp. PCC6803 (Maeda et al. 2005). An increase in tocopherols is regulated at the level of the rate-limiting step of tocopherol biosynthesis which is the transfer of phytyl diphosphate to homogentisate (HGT) catalyzed by the homogentisate phytyltransferase (HPT) enzyme (Collakova and DellaPenna 2003a; Lushchak and Semchuk 2012). Overexpression of *HPT* was shown to increase the tocopherol content of Arabidopsis plants (Collakova and DellaPenna 2003b) and its silencing in tobacco leads to an up to 98% reduction of α -tocopherol which was compensated by γ -tocopherol. Simultaneous silencing of the γ -tocopherol methyltransferase gene (γ TMT) decreased the total tocopherol level

and increased the sensitivity of the plants to various stress conditions imposing oxidative stress dramatically (Abbasi et al. 2007).

In contrast to W1 plants, in older WT plants (19 das) that showed already signs of senescence as declining chlorophyll concentration and RubisCO content (Saeid Nia et al. 2022), the level of α -tocopherol increased dramatically (Fig. 8). Indeed, an increased tocopherol content is a characteristic feature of senescence (Falk and Munné -Bosch 2010; Lichtenthaler 2013; Lichtenthaler 1966), which was shown to be delayed in W1 plants (Kucharewicz et al. 2017).

It is known that an interplay between tocopherols and carotenoids is crucial for the prevention of photooxidative stress in *Arabidopsis* (Kumar et al. 2020). Both lipophilic antioxidants preserve PS II from photoinactivation and protect membrane lipids from photooxidation. *Arabidopsis* mutants impaired in the biosynthesis of tocopherols (*vte1*, *vte2*) or zeaxanthin (*npq1*, *npq4*), respectively, showed no signs of stress when grown in high irradiance. When, however, zeaxanthin formation was inhibited in the *vte1* mutant, PS II was photoinhibited, accompanied by oxidation of lipids and pigments (Havaux et al. 2005). In the barley plants, tocopherols presumably were not required, because in our work the HL treatment led to a strong accumulation of zeaxanthin (Fig. 5). This result is in accordance with the idea that zeaxanthin can compensate for the lack of α -tocopherol.

Nevertheless, it was unexpected that the W1 plants accumulate zeaxanthin instead of tocopherols. In a previous study it was shown that thylakoids from W1 plants generate more ROS (H_2O_2 and/or superoxide, but not singlet oxygen) than thylakoids from WT plants when illuminated (Swida-Barteczka et al. 2018). Very recently it has been demonstrated that H_2O_2 inactivates the enzyme epoxidising zeaxanthin to violaxanthin, i.e. ZEP (Holzmann et al. 2022). In four different dicot species it has been demonstrated that D1 and ZEP during photooxidative stress are degraded coordinately (Bethmann et al. 2019). This degradation might be preceded by the inactivation of ZEP by H_2O_2 (Holzmann et al. 2022). Presumably, both, the HL-induced down-regulation of *ZEP* expression (Fig. 8b) and presumably also activity coordinately ensured the retention of a high amount of zeaxanthin under excessive light (Bethmann et al. 2019), which

might have been sufficient to prevent accumulation of singlet oxygen enabling the W1 plants to survive this stress.

In addition to zeaxanthin and tocopherols, two hydrophilic antioxidants were compared between wild-type and W1 plants grown at LL and HL, respectively. Glutathione is the major determinant of the overall cellular redox state (Foyer and Noctor 2005, Mullineaux and Rausch, 2005). Any imbalance in the redox situation caused by oxidative stress should shift the ratio between reduced and oxidized glutathione to the side of the oxidized compound (Tausz and Grill 2000; Rahantaniaina et al. 2013; Bloem et al. 2015). In the HL-grown WT leaves, GSH/GSSG declined after 10 das. HL-accelerated premature senescence (Lushchak and Semchuk 2012) in HL-grown WT plants (Kucharewicz et al. 2017; Saeid Nia et al. 2022), as also supported by the increase in α -tocopherol, may explain the reduction in the level of the reduced form of glutathione in WT leaves. In contrast, from 10 to 19 das, the GSH/GSSG ratio remained high in the W1 line and was even higher in the HL-grown leaves than in the LL leaves (Fig. 13). Hence, apparently the W1 leaves were able to control oxidative stress to a level that the overall redox state in the cells was not affected. Considering that glutathione acts synergistically together with α -tocopherol and ascorbate under HL conditions (Kanwischer et al. 2005), the stable GSH/GSSG ratio is in accordance with the unaltered levels of tocopherols in the W1 plants.

Whereas the redox state of the glutathione pool was not specifically altered in the W1 leaves, the composition of the flavonoids changed. In HL-grown leaves, luteonarin increased significantly, and in the W1 leaves to an even higher extent than in WT leaves (Fig. 12). In these leaves, it seemed that the level of luteonarin increased at the expense of the related flavone-glucoside saponarin. While saponarin is a monohydroxyflavone, luteonarin is a dihydroxyflavone. Due to the catechol (ortho-dihydroxylated) group in the latter, these compounds are known to be better antioxidants than the corresponding monohydroxy-compounds (Rice-Evans et al. 1996; Burda and Oleszek 2001; Nezval et al. 2017). Based on this property, the strong increase in the proportion of di- to mono-hydroxy B-ring flavonoids induced by UV radiation (Markham et al. 1998; Tattini et al. 2005; Agati et al. 2009; Agati and Tattini 2010) or, in the absence of UV, by excessive light (Agati et al. 2009; Fini et al. 2011) may be explained as a response enhancing tolerance of oxidative stress.

Often, flavonoids are located in the epidermis. In this case when H₂O₂ or other oxidative agents would have to diffuse from the origin of oxidative stress, i.e., the photosynthetically active cells, to the epidermis, a function as antioxidant is difficult to imagine. Agati et al. (2002) have shown that in *Phillyrea latifolia* the di-hydroxy-flavonol quercetin is specifically formed in the mesophyll, where it can act as an antioxidant. Moreover, under excessive light stress, quercetin and luteolin glycosides were detected in chloroplasts of *P. latifolia* leaves in association with the chloroplast envelope and were shown to scavenge ¹O₂ (Agati et al. 2007), potentially in a complementary action with other singlet oxygen scavengers like carotenoids (Agati et al. 2012).

To investigate the location of luteonarin in the barley leaves, the abaxial epidermis was removed from the leaves. The HPLC analyses revealed that luteonarin was indeed largely absent from the abaxial epidermis (Fig. 12d). Although the luteonarin detected in the remaining part of the leaf could be at least partially located in the adaxial epidermis, which could not be removed simultaneously with the abaxial epidermis from the leaves, it seems tempting to speculate that a significant fraction was present in the mesophyll that contains the chloroplasts (Fig. 12f). It was also shown by Agati and Tattini (2010) that the concentration of the ortho-dihydroxylated flavonoids, quercetin 3-O-glycosides and luteolin 7-O-glycosides, increased by about 95 % in leaves of *Ligustrum vulgare*, where the increase was mainly observed in the mesophyll cells. The finding of the presence of these flavonoids in vacuoles of mesophyll cells and in the chloroplasts close to the ROS generation site in plants was considered as beneficial for the prevention of oxidative damage (Agati and Tattini 2010; Agati et al. 2012; Nezval et al. 2017). By growing under full sunlight and in the absence of UV radiation, these leaves had even a higher concentration of the mentioned flavonoids which accumulated strongly in the palisade parenchyma cells (Agati and Tattini 2010). On the other hand, Kaspar et al. (2010) showed that saponarin as the main phenolic compound of barley primary leaves accumulated mainly in the epidermal cells. Recently, it was reported based on the observation of fluorescence induced by Naturstoff reagent A that the epidermal pavement cells of the elite barley cultivar Barke were devoid of flavonoids (Hunt et al. 2021). This observation cannot be supported by our findings in the cultivar Golden Promise, which may be due to either cultivar-specific variations or to the use of different analytical methods.

To conclude, we demonstrated that the irradiance to which W1 leaves were exposed during growth was excessive for photosynthesis, since the EPS in W1 leaves growing in HL was very low and the light saturated ETR was reduced in both, LL and HL W1 leaves in comparison to WT. The formation of the flavonoid luteonarin and the strong increase of the VAZ pool size, together with the higher abundance of plastoglobules indirectly indicate that these plants suffered from oxidative stress. However, direct evidence for oxidative stress in the form of an oxidized glutathione pool could not be found, nor was PS II inhibited in leaves at 15 das. Enhanced NPQ may have reduced the light stress, and the carotenoids zeaxanthin and lutein as well as the flavonoid luteonarin likely acted as antioxidants preventing oxidative damage. Since in our study no changes in the amount of α -tocopherol or in the ratio of GSH/GSSG were found in leaves at 10 and 15 das in our study, the α -tocopherol-ascorbate-glutathione triad did not appear to play an important role in protection of the plants. Hence, although the deficiency of WHIRLY1 compromises barley plants in acclimation to HL (Saeid Nia et al. 2022), photoprotective reactions are still sufficient to prevent serious damage in these plants.

Author Contribution Statement

MSN, WB, and KK conceived and designed the research. Material preparation, conduction of experiments (except from transmission electron microscopy which was done by UR, analysis of flavonoid content and composition which was done by LS, saponarin/luteonarin identification which was done by AGH) were performed by MSN. The glutathione measurements were done with the advice of JS. Graphs and statistical analysis were performed by MSN. The first draft of the manuscript was written by MSN. All authors commented and revised the first version of the manuscript. All authors read and approved the final manuscript.

Acknowledgments

We greatly thank Jens Hermann (Institute of Botany, CAU Kiel, Germany) for his professional support in the HPLC analysis of photosynthetic pigments and flavonoids. We are grateful to Anke Schäfer (Institute of Botany, CAU Kiel, Germany) for designing the primers, and for her technical assistance during gene expression analysis. We would like to thank Ulrike Voigt (Institute of Botany, CAU Kiel, Germany) for preparing seeds and for technical assistance in the Central

Microscopy. Elena Brückner is acknowledged for her help in mass spectrometry and analysis of flavonoid composition. We would like to acknowledge Mahshid Dashti for her great help during the localization of saponarin and lutonarin. Further thanks to Dr. Christoph Plieth (Center for Biochemistry and Molecular Biology, CAU Kiel, Germany) for providing a plate reader needed in the process of GSH/GSSG ratio measurement and for his great technical and scientific assistance.

Data availability

The data that support the findings of this study are available in the Supplementary Information of this article. The raw datasets in this study are available from the first author or corresponding author on reasonable request.

References

- Abbasi A, Hajirezaei M, Hofius D, Sonnewald U, Voll LM (2007) Specific roles of α - and γ -tocopherol in abiotic stress responses of transgenic tobacco (*Nicotiana tabacum* L.). *Plant Physiol* 143:720–1738. <https://doi.org/10.1104/pp.106.094771>
- Agati G, Azzarello E, Pollastri S, Tattini M (2012) Flavonoids as antioxidants in plants: Location and functional significance. *Plant Sci* 196:67–76. <https://doi.org/10.1016/j.plantsci.2012.07.014>
- Agati G, Brunetti C, Di Ferdinando M, Ferrini F, Pollastri S, Tattini M (2013) Functional roles of flavonoids in photoprotection: New evidence, lessons from the past. *Plant Physiol Biochem* 72:35–45. <https://doi.org/10.1016/j.plaphy.2013.03.014>
- Agati G, Galardi C, Gravano E, Romani A, Tattini M (2002) Flavonoid distribution in tissues of *Phillyrea latifolia* L. leaves as estimated by microspectrofluorometry and multispectral fluorescence microimaging. *Photochem Photobiol* 76:350–360. [https://doi.org/10.1562/0031-8655\(2002\)076<0350:fditop>2.0.co;2](https://doi.org/10.1562/0031-8655(2002)076<0350:fditop>2.0.co;2)
- Agati G, Matteini P, Goti A, Tattini M (2007) Chloroplast-located flavonoids can scavenge singlet oxygen. *New Phytol* 174:7–89. <https://doi.org/10.1111/j.1469-8137.2007.01986.x>
- Agati G, Stefano G, Biricolti S, Tattini M (2009) Mesophyll distribution of “antioxidant” flavonoid glycosides in *Ligustrum vulgare* leaves under contrasting sunlight irradiance. *Ann Bot* 104:853–861. <https://doi.org/10.1093/aob/mcp177>

- Agati G, Tattini M (2010) Multiple functional roles of flavonoids in photoprotection. *New Phytol* 186:786–793. <https://doi.org/10.1111/j.1469-8137.2010.03269.x>
- Alseekh S, Perez de Souza L, Benina M, Fernie AR (2020) The style and substance of plant flavonoid decoration; towards defining both structure and function. *Phytochemistry* 174:112347. <https://doi.org/10.1016/j.phytochem.2020.112347>
- Anderson JM, Chow WS, Park YI (1995) The grand design of photosynthesis: Acclimation of the photosynthetic apparatus to environmental cues. *Photosynth Res* 46:129–139. <https://doi.org/10.1007/BF00020423>
- Anderson JM, Osmond CB (1987) Shade-sun responses: Compromises between acclimation and photoinhibition. In: Kyle DJ, Osmond CB, Arntzen CJ (ed) *Photoinhibition*. Elsevier Amsterdam, pp 1-38.
- Aro EM, Virgin I, Andersson B (1993) Photoinhibition of Photosystem II. Inactivation, protein damage and turnover, *Biochim Biophys Acta Bioenerg* 1143:113-134. [https://doi.org/10.1016/0005-2728\(93\)90134-2](https://doi.org/10.1016/0005-2728(93)90134-2)
- Asada K (2006) Production and scavenging of reactive oxygen species in chloroplasts and their functions. *Plant Physiol* 141:391–396. <https://doi.org/10.1104/pp.106.082040>
- Bethmann S, Melzer M, Schwarz N, Jahns P (2019) The zeaxanthin epoxidase is degraded along with the D1 protein during photoinhibition of photosystem II. *Plant Direct* 3:1-13. <https://doi.org/10.1002/pld3.185>
- Bilger W, Björkman O (1990) Role of the xanthophyll cycle in photoprotection elucidated by measurements of light-induced absorbance changes, fluorescence and photosynthesis in leaves of *Hedera canariensis*. *Photosynth Res* 25:173–185. <https://doi.org/10.1007/BF00033159>
- Bilger W, Björkman O, Thayer SS (1989) Light-induced spectral absorbance changes in relation to photosynthesis and the epoxidation state of xanthophyll cycle components in cotton leaves. *Plant Physiol* 91:542–551. <https://doi.org/10.1104/pp.91.2.542>
- Bilger W, Fisahn J, Brummet W, Kossmann J, Willmitzer L (1995) Violaxanthin cycle pigment contents in potato and tobacco plants with genetically reduced photosynthetic capacity. *Plant Physiol* 108:1479–1486.

- Bilger W, Johnsen T, Schreiber U (2001) UV-excited chlorophyll fluorescence as a tool for the assessment of UV-protection by the epidermis of plants. *J Exp Bot* 52:2007–2014. <https://doi.org/10.1093/jexbot/52.363.2007>
- Bilger W, Lesch M (1995) The epoxidation state of the violaxanthin cycle is linearly correlated with photosystem II quantum yield under natural conditions. In: Mathis P (ed) *Photosynthesis: from light to biosphere. Proceedings of the 10th International Photosynthesis Congress*. Kluwer Academic Publishers, Dordrecht, pp 107–110.
- Björkman O, Demmig B (1987) Photon yield of O₂ evolution and chlorophyll fluorescence characteristics at 77 K among vascular plants of diverse origins. *Planta* 170:489–504. <https://doi.org/10.1007/BF00402983>
- Bloem E, Haneklaus S, Schnug E (2015) Suitability of the ratio between reduced and oxidized glutathione as an indicator of plant stress. In: De Kok L, Hawkesford M, Rennenberg H, Saito K, Schnug E (eds) *Molecular physiology and ecophysiology of sulfur. Proceedings of the international plant sulfur Workshop*. Springer, Cham. https://doi.org/10.1007/978-3-319-20137-5_12
- Bréhélin C, Kessler F, van Wijk KJ (2007) Plastoglobules: versatile lipoprotein particles in plastids. *Trends Plant Sci* 12:260–266. <https://doi.org/10.1016/j.tplants.2007.04.003>
- Burda S, Oleszek W (2001) Antioxidant and antiradical activities of flavonoids. *J Agric Food Chem* 49:2774–2779. <https://doi.org/10.1021/jf001413m>
- Caffarri S, Tibiletti T, Jennings RC, Santabarbara S (2014) A comparison between plant photosystem I and photosystem II architecture and functioning. *Curr Protein Pept Sci* 15:296–331. <https://doi.org/10.2174/1389203715666140327102218>
- Collakova E, DellaPenna D (2003a) Homogentisate phytyltransferase activity is limiting for tocopherol biosynthesis in *Arabidopsis thaliana*. *Plant Physiol* 131:632–642. <https://doi.org/10.1104/pp.015222>
- Collakova E, DellaPenna D (2003b) The role of homogentisate phytyltransferase and other tocopherol pathway enzymes in the regulation of tocopherol synthesis during abiotic stress. *Plant Physiol* 133:930–940. <https://doi.org/10.1104/pp.103.026138>
- Davies BH, (1976) Carotenoids. In: Goodwin TW (ed) *Chemistry and Biochemistry of Plant Pigments*. Academic Press, London, pp 38–165

- Davison PA, Hunter CN, Horton, P (2002) Overexpression of β -carotene hydroxylase enhances stress tolerance in *Arabidopsis*. *Nature* 418:203–206.
<https://doi.org/10.1038/nature00861>
- Demmig-Adams B, Adams WW (1996) The role of xanthophyll cycle carotenoids in the protection of photosynthesis. *Trends Plant Sci* 1:21–26. [https://doi.org/10.1016/S1360-1385\(96\)80019-7](https://doi.org/10.1016/S1360-1385(96)80019-7)
- Demmig-Adams B, Adams WW (2006) Photoprotection in an ecological context: the remarkable complexity of thermal energy dissipation. *New Phytol* 172:11–21.
<https://doi.org/10.1111/j.1469-8137.2006.01835.x>
- Demmig-Adams B, Adam, WW, Heber U, Neimanis S, Winter K, Krüger A, Czygan FC, Bilger W, Björkman O (1990) Inhibition of zeaxanthin formation and of rapid changes in radiationless energy dissipation by dithiothreitol in spinach leaves and chloroplasts. *Plant Physiol* 92:293–301. <https://doi.org/10.1104/pp.92.2.293>
- Demmig-Adams B, Cohu CM, Muller O, Adams WW (2012) Modulation of photosynthetic energy conversion efficiency in nature: from seconds to seasons. *Photosynth Res* 113:75–88.
<https://doi.org/10.1007/s11120-012-9761-6>
- Demmig-Adams B, López-Pozo M, Stewart JJ, Adams WW (2020) Zeaxanthin and lutein: photoprotectors, anti-inflammatories, and brain food. *Molecules* 25:3607.
<https://doi.org/10.3390/molecules25163607>
- Demmig B, Björkman O (1987) Comparison of the effect of excessive light on chlorophyll fluorescence (77K) and photon yield of O₂ evolution in leaves of higher plants. *Planta* 171, 171–184. <https://doi.org/10.1007/BF00391092>
- Demmig B, Winter K, Krüger A, Czygan FC (1987) Photoinhibition and zeaxanthin formation in intact leaves : A possible role of the xanthophyll cycle in the dissipation of excess light energy. *Plant physiol* 84:218–224. <https://doi.org/10.1104/pp.84.2.218>
- Falk J, Munné-Bosch, S (2010) Tocochromanol functions in plants: antioxidation and beyond. *J Exp Bot* 61:1549–1566. <https://doi.org/10.1093/jxb/erq030>
- Fini A, Brunetti C, Di Ferdinando M, Ferrini F, Tattini M (2011) Stress-induced flavonoid biosynthesis and the antioxidant machinery of plants. *Plant Signal Behav* 6:709–711.
<https://doi.org/10.4161/psb.6.5.15069>

- Fitzpatrick D, Aro EM, Tiwari A (2022) True oxygen reduction capacity during photosynthetic electron transfer in thylakoids and intact leaves. *Plant Physiol* 189:112–128.
<https://doi.org/10.1093/plphys/kiac058>
- Foyer CH, Noctor G (2005) Redox homeostasis and antioxidant signaling: a metabolic interface between stress perception and physiological responses. *Plant Cell* 17:1866–1875.
<https://doi.org/10.1105/tpc.105.033589>
- Foyer CH, Noctor G (2011) Ascorbate and glutathione: the heart of the redox hub. *Plant Physiol* 155:2–18. <https://doi.org/10.1104/pp.110.167569>
- Gasperl A, Zellnig G, Kocsy G, Müller M (2022) Organelle-specific localization of glutathione in plants grown under different light intensities and spectra. *Histochem Cell Biol* 158:213–227. <https://doi.org/10.1007/s00418-022-02103-2>
- García-Plazaola JI, Hernández A, Artetxe U, Becerril JM (2002) Regulation of the xanthophyll cycle pool size in duckweed (*Lemna minor*) plants. *Physiol Plant* 116:121–126.
<https://doi.org/10.1034/j.1399-3054.2002.1160115.x>
- Garibay-Hernández A, Kessler N, Józefowicz AM, Türksoy GM, Lohwasser U, Mock HP (2021) Untargeted metabotyping to study phenylpropanoid diversity in crop plants. *Physiol Plant* 173, 680–697. <https://doi.org/10.1111/ppl.13458>
- Genty B, Harbinson J, Cailly AL and Rizza F (1996) Fate of excitation at PS II in leaves: the non-photochemical side. Presented at the third BBSRC Robert Hill symposium on photosynthesis, March 31-April 3, University of Sheffield, Department of Molecular Biology and Biotechnology, Western Bank, Sheffield, UK, Abstract no. P28
- Gray G, Savitch, L, Ivanov A, Huner N (1996) Photosystem II excitation pressure and development of resistance to photoinhibition (II. Adjustment of photosynthetic capacity in winter wheat and winter rye). *Plant Physiol* 110:61–71.
<https://doi.org/10.1104/pp.110.1.61>
- Gruszecki WI, Strzałka K (2005) Carotenoids as modulators of lipid membrane physical properties. *Biochim Biophys Acta* 1740:108–115.
<https://doi.org/10.1016/j.bbadis.2004.11.015>

- Hasanuzzaman M, Nahar K, Anee TI, Fujita M (2017) Glutathione in plants: biosynthesis and physiological role in environmental stress tolerance. *Physiol Mol Biol Plants* 23:249–268. <https://doi.org/10.1007/s12298-017-0422-2>
- Havaux M, Dall'Osto L, Bassi R (2007) Zeaxanthin has enhanced antioxidant capacity with respect to all other xanthophylls in *Arabidopsis* leaves and functions independent of binding to PSII antennae. *Plant Physiol* 145:1506–1520. <https://doi.org/10.1104/pp.107.108480>
- Havaux M, Eymery F, Porfirova S, Rey P, Dörmann P (2005) Vitamin E protects against photoinhibition and photooxidative stress in *Arabidopsis thaliana*. *Plant Cell* 17:3451–3469. <https://doi.org/10.1105/tpc.105.037036>
- Havaux M, Niyogi KK (1999) The violaxanthin cycle protects plants from photooxidative damage by more than one mechanism. *PNAS* 96:8762–8767. <https://doi.org/10.1073/pnas.96.15.8762>
- Hebbelmann I, Selinski J, Wehmeyer C, Goss T, Voss I, Mulo P, Kangasjärvi S, Aro EM, Oelze ML, Dietz KJ, Nunes-Nesi A, Do PT, Fernie AR, Talla SK, Raghavendra AS, Linke V, Scheibe R (2012) Multiple strategies to prevent oxidative stress in *Arabidopsis* plants lacking the malate valve enzyme NADP-malate dehydrogenase. *J Exp Bot* 63:1445–1459. <https://doi.org/10.1093/jxb/err386>
- Hendrickson L, Furbank RT, Chow WS (2004) A Simple alternative approach to assessing the fate of absorbed light energy using chlorophyll fluorescence. *Photosynth Res* 82:73–81. <https://doi.org/10.1023/B:PRES.0000040446.87305.f4>
- Hernández I, Alegre L, Van Breusegem F, Munné-Bosch S (2009) How relevant are flavonoids as antioxidants in plants? *Trends in Plant Sci* 14:125–132. <https://doi.org/10.1016/j.tplants.2008.12.003>
- Holzmann D, Bethmann S, Jahns P (2022) Zeaxanthin epoxidase activity is downregulated by hydrogen peroxide. *Plant Cell Physiol* 63:1091–1100. <https://doi.org/10.1093/pcp/pcac081>
- Holzwarth, AR, Lenk D, Jahns P (2013) On the analysis of non-photochemical chlorophyll fluorescence quenching curves: I. Theoretical considerations. *Biochim Biophys Acta-Bioenerg* 1827:786–792. <https://doi.org/10.1016/j.bbabi.2013.02.011>

- Hunt L, Klem K, Lhotáková Z, Vosolsobě S, Oravec M, Urban O, Špunda V, Albrechtová J (2021) Light and CO₂ modulate the accumulation and localization of phenolic compounds in barley leaves. *Antioxidants (Basel)* 10:385. <https://doi.org/10.3390/antiox10030385>
- Jahns P, Holzwarth AR (2012) The role of the xanthophyll cycle and of lutein in photoprotection of photosystem II. *Biochim. Biophys. Acta* 1817:182–193. <https://doi.org/10.1016/j.bbabi.2011.04.012>
- Kanwischer M, Porfirova S, Bergmüller E, Dörmann P (2005) Alterations in tocopherol cyclase activity in transgenic and mutant plants of *Arabidopsis* affect tocopherol content, tocopherol composition, and oxidative stress. *Plant Physiol* 137:713–723. <https://doi.org/10.1104/pp.104.054908>
- Kaspar S, Matros A, Mock HP (2010) Proteome and flavonoid analysis reveals distinct responses of epidermal tissue and whole leaves upon UV-B radiation of barley (*Hordeum vulgare L.*) seedlings. *J Proteome Res* 9:2402–2411. <https://doi.org/10.1021/pr901113z>
- Kawabata Y, Takeda S (2014) Regulation of xanthophyll cycle pool size in response to high light irradiance in *Arabidopsis*. *Plant Biotech* 31:229240 <https://doi.org/10.5511/plantbiotechnology.14.0609a>
- Klughammer C, Schreiber U (2008) Complementary PS II quantum yields calculated from simple fluorescence parameters measured by PAM fluorometry and the saturation pulse method. *PAM Application Notes* 1:27-35
- Kornyeyev D, Hendrickson L (2007) Energy partitioning in photosystem II complexes subjected to photoinhibitory treatment. *Funct Plant Biol* 34:214–220. <https://doi.org/10.1071/FP06327>
- Kruk J, Szymańska R, Nowicka B, Dłużewska J (2016) Function of isoprenoid quinones and chromanols during oxidative stress in plants. *N Biotechnol* 33:636–643. <https://doi.org/10.1016/j.nbt.2016.02.010>
- Krupinska K, Braun S, Saeid Nia M, Schäfer A, Hensel G, Bilger W (2019) The nucleoid-associated protein WHIRLY1 is required for the coordinate assembly of plastid and nucleus-encoded proteins during chloroplast development. *Planta* 249:1337–1347. <https://doi.org/10.1007/s00425-018-03085-z>

- Krupinska K, Oetke S, Desel C, Mulisch M, Schäfer A, Hollmann J, Kumlehn J, Hensel G (2014) WHIRLY1 is a major organizer of chloroplast nucleoids. *Front Plant Sci* 5, 432. <https://doi.org/10.3389/fpls.2014.00432>
- Kucharewicz W, Distelfeld A, Bilger W, Müller M, Munné-Bosch S, Hensel G, Krupinska K (2017) Acceleration of leaf senescence is slowed down in transgenic barley plants deficient in the DNA/RNA-binding protein WHIRLY1. *J Exp Bot* 68:983–996. <https://doi.org/10.1093/jxb/erw501>
- Kumar A, Prasad A, Sedlarova M, Ksas B, Havaux M, Pospisil P (2020) Interplay between antioxidants in response to photooxidative stress in Arabidopsis. *Free Radical Biology and Medicine* 160:894–907. doi:10.1016/j.freeradbiomed.2020.08.027
- Leipner J, Stamp P, Fracheboud Y (2000) Artificially increased ascorbate content affects zeaxanthin formation but not thermal energy dissipation or degradation of antioxidants during cold-induced photooxidative stress in maize leaves. *Planta* 210:964–969. <https://doi.org/10.1007/s004250050704>
- Lichtenthaler HK (1966) Plastoglobuli und Plastidenstruktur (Kurzfassung). *Berichte der Deutschen Botanischen Gesellschaft* 79:82–88. <https://doi.org/10.1111/j.1438-8677.1966.tb04061.x>
- Lichtenthaler HK (2013) Plastoglobuli, thylakoids, chloroplast structure and development of plastids. In: Biswal B, Krupinska K, Biswal UC (ed) *Plastid development in leaves during growth and senescence. Advances in Photosynthesis and Respiration*. Springer Netherlands Dordrecht, pp 337–361. https://doi.org/10.1007/978-94-007-5724-0_15
- Lichtenthaler HK, Pfister K (1978) *Praktikum der Photosynthese*, Quelle & Meyer Verlag, Heidelberg
- Livak KJ, Schmittgen TD (2001) Analysis of relative gene expression data using real-time quantitative PCR and the $2^{-\Delta\Delta C_T}$ method. *Methods* 25:402–408. <https://doi.org/10.1006/meth.2001.1262>
- Lushchak VI, Semchuk NM (2012) Tocopherol biosynthesis: chemistry, regulation and effects of environmental factors. *Acta Physiol Plant* 34:1607–1628. <https://doi.org/10.1007/s11738-012-0988-9>

- Mathews-Roth MM, Wilson T, Fujimori E, Krinsky NI (1974) Carotenoid chromophore length and protection against photosensitization. *Photochem Photobiol* 19:217–222.
<https://doi.org/10.1111/j.1751-1097.1974.tb06501.x>
- Markham KR, Ryan KG, Bloor SJ, Mitchell KA (1998) An increase in the luteolin : apigenin ratio in *Marchantia polymorpha* on UV-B enhancement. *Phytochem* 48:791–794.
[https://doi.org/10.1016/S0031-9422\(97\)00875-3](https://doi.org/10.1016/S0031-9422(97)00875-3)
- Maxwell K, Johnson GN (2000) Chlorophyll fluorescence - a practical guide. *J Exp Bot* 51:659–668. <https://doi.org/10.1093/jexbot/51.345.659>
- McNulty HP, Byun J, Lockwood SF, Jacob RF, Mason RP (2007) Differential effects of carotenoids on lipid peroxidation due to membrane interactions: X-ray diffraction analysis. *Biochim Biophys Acta* 1768:167–174. <https://doi.org/10.1016/j.bbamem.2006.09.010>
- Mozzo M, Passarini F, Bassi R, van Amerongen H, Croce R (2008) Photoprotection in higher plants: the putative quenching site is conserved in all outer light-harvesting complexes of Photosystem II. *Biochim Biophys Acta* 1777:1263–1267.
<https://doi.org/10.1016/j.bbabbio.2008.04.036>
- Müller P, Li XP, Niyogi KK (2001) Non-photochemical quenching. A response to excess light energy. *Plant Physiol* 125:1558–1566. <https://doi.org/10.1104/pp.125.4.1558>
- Maeda H, Sakuragi Y, Bryant DA, DellaPenna D (2005) Tocopherols protect *Synechocystis* sp. strain PCC 6803 from lipid peroxidation. *Plant Physiol* 138:1422–1435.
<https://doi.org/10.1104/pp.105.061135>
- Mullineaux PM, Rausch T (2005) Glutathione, photosynthesis and the redox regulation of stress-responsive gene expression. *Photosynth Res* 86:459–474.
<https://doi.org/10.1007/s11120-005-8811-8>
- Nezval J, Štroch M, Materová Z, Špunda V, Kalina J (2017) Phenolic compounds and carotenoids during acclimation of spring barley and its mutant *Chlorina f2* from high to low irradiance. *Biologia Plant* 61:73–84. <https://doi.org/10.1007/s10535-016-0689-0>
- Nichelmann L, Schulze M, Herppich WB, Bilger W (2016) A simple indicator for non-destructive estimation of the violaxanthin cycle pigment content in leaves. *Photosyn Res* 128:183–193. <https://doi.org/10.1007/s11120-016-0218-1>

- Niyogi KK, Grossman AR, Björkman O (1998) Arabidopsis mutants define a central role for the xanthophyll cycle in the regulation of photosynthetic energy conversion. *Plant Cell* 10:1121–1134. <https://doi.org/10.1105/tpc.10.7.1121>
- Niyogi KK, Shih C, Soon Chow W, Pogson BJ, Dellapenna D, Björkman O (2001) Photoprotection in a zeaxanthin- and lutein-deficient double mutant of Arabidopsis. *Photosyn Res* 67:139–145. <https://doi.org/10.1023/A:1010661102365>
- Powles SB (1984) Photoinhibition of photosynthesis induced by visible light. *Annu Rev Plant Physiol* 35:15–44. <https://doi.org/10.1146/annurev.pp.35.060184.000311>
- Rahantaniaina MS, Tuzet A, Mhamdi A, Noctor G (2013) Missing links in understanding redox signaling via thiol/disulfide modulation: how is glutathione oxidized in plants? *Front Plant Sci* 4:477. <https://doi.org/10.3389/fpls.2013.00477>
- Rice-Evans CA, Miller NJ, Paganga G (1996) Structure-antioxidant activity relationships of flavonoids and phenolic acids. *Free Radical Biol Med* 20:933–956. [https://doi.org/10.1016/0891-5849\(95\)02227-9](https://doi.org/10.1016/0891-5849(95)02227-9)
- Rottet S, Besagni C, Kessler F (2015) The role of plastoglobules in thylakoid lipid remodeling during plant development. *Biochim Biophys Acta* 1847:889–899. <https://doi.org/10.1016/j.bbabi.2015.02.002>
- Saeid Nia M, Repnik U, Krupinska K, Bilger W (2022) The plastid-nucleus localized DNA-binding protein WHIRLY1 is required for acclimation of barley leaves to high light. *Planta* 255,84. <https://doi.org/10.1007/s00425-022-03854-x>
- Selinski J, Scheibe R (2019) Malate valves: old shuttles with new perspectives. *Plant Biol* 21:21–30. <https://doi.org/10.1111/plb.12869>
- Sickel H, Bilger W, Ohlson M (2012) High levels of α -tocopherol in Norwegian alpine grazing plants. *J Agric Food Chem* 60:7573–7580. <https://doi.org/10.1021/jf301756j>
- Spicher L, Almeida J, Gutbrod K, Pipitone R, Dörmann P, Glauser G, Rossi M, Kessler F (2017) Essential role for phytol kinase and tocopherol in tolerance to combined light and temperature stress in tomato. *J Exp Bot* 68:5845–5856. <https://doi.org/10.1093/jxb/erx356>
- Sujak A, Gabrielska J, Grudziński W, Borc R, Mazurek P, Gruszecki WI (1999) Lutein and zeaxanthin as protectors of lipid membranes against oxidative damage: the structural

- aspects. Arch Biochem Biophys 371:301–307. <https://doi.org/10.1006/abbi.1999.1437>
- Sun Z, Gantt E, Cunningham FX (1996) Cloning and functional analysis of the β -carotene hydroxylase of *Arabidopsis thaliana*. J Biol Chem 271:24349–24352. <https://doi.org/10.1074/jbc.271.40.24349>
- Swida-Barteczka A, Krieger-Liszkay A, Bilger W, Voigt U, Hensel G, Szweykowska-Kulinska Z, Krupinska K (2018) The plastid-nucleus located DNA/RNA binding protein WHIRLY1 regulates microRNA-levels during stress in barley (*Hordeum vulgare* L.). RNA Biology 15:886–891. doi:10.1080/15476286.2018.1481695
- Szarka A, Tomasskovics B, Bánhegyi G (2012) The ascorbate-glutathione- α -tocopherol triad in abiotic stress response. Int J Mol Sci 13:4458–4483. <https://doi.org/10.3390/ijms13044458>
- Szymańska R, Ślesak I, Orzechowska A, Kruk J (2017) Physiological and biochemical responses to high light and temperature stress in plants. Env Exp Bot 139:165–177. <https://doi.org/10.1016/j.envexpbot.2017.05.002>
- Takahashi S, Badger MR (2011) Photoprotection in plants: a new light on photosystem II damage. Trends Plant Sci 16:53–60. <https://doi.org/10.1016/j.tplants.2010.10.001>
- Tattini M, Guidi L, Morassi-Bonzi L, Pinelli P, Remorini D, Degl’Innocenti E, Giordano C, Massai R, Agati G (2005) On the role of flavonoids in the integrated mechanisms of response of *Ligustrum vulgare* and *Phillyrea latifolia* to high solar radiation. New Phytol 167:457–470. <https://doi.org/10.1111/j.1469-8137.2005.01442.x>
- Tausz M, Grill D (2000) The role of glutathione in stress adaptation of plants. Phyton 40:111–118.
- Tausz M, Šircelj H, Grill D (2004) The glutathione system as a stress marker in plant ecophysiology: is a stress-response concept valid? J Exp Bot 55:1955–1962. <https://doi.org/10.1093/jxb/erh194>
- Thayer SS, Björkman O (1990) Leaf xanthophyll content and composition in sun and shade determined by HPLC. Photosynth Res 23:331–343. <https://doi.org/10.1007/BF00034864>
- Vanacker H, Carver TLW, Foyer CH (2000) Early H₂O₂ accumulation in mesophyll cells leads to induction of glutathione during the hyper-sensitive response in the barley-powdery mildew interaction. Plant Physiol 123:1289–1300

van Wijk KJ, Kessler F (2017) Plastoglobuli: Plastid microcompartments with integrated functions in metabolism, plastid developmental transitions, and environmental adaptation. *Ann Rev Plant Biol* 68:253–289. <https://www.ncbi.nlm.nih.gov/pubmed/28125283>.

Wisniewska A, Widomska J, Subczynski WK (2006) Carotenoid-membrane interactions in liposomes: effect of dipolar, monopolar, and nonpolar carotenoids. *Acta Biochim Pol* 53:475–484.

Yamamoto HY (1979) Biochemistry of the violaxanthin cycle in higher plants. *Pure Appl Chem* 51:639–648. <https://doi.org/10.1351/pac197951030639>

Zechmann B (2014) Compartment-specific importance of glutathione during abiotic and biotic stress. *Front Plant Sci* 5:566. <https://doi.org/10.3389/fpls.2014.00566>

Table. 1 Flavonoid identification by mass spectrometry. The flavonoids of interest were identified by RP-UPLC-PDA-ESI-HR-QTOF-MS/MS. Compound annotations were confirmed by exact mass, isotopic pattern, MS/MS fragmentation, and PDA spectra. The percentage of relative intensities of the MS fragment ions are indicated in parenthesis. The PDA- and MS-spectra were compared to the available literature (Brauch et al. 2018; Garibay-Hernández et al. 2021; Piasecka et al. 2015). The identification of saponarin was also confirmed with a commercial standard (1238S, Extrasynthèse, France). Abbreviations: Api, Apigenin; Hex: hexosyl moiety (neutral loss 162.05); Lut, Lutonarin; m/z , mass to charge ratio; s, shoulder.

Annotation	λ max (nm)	Molecular formula	Monoisotopic mass	Precursor ion	Calculated (m/z)	Measured (m/z)	Δ ppm	Fragment ions	Measured (m/z)
Lutonarin (<i>Isoorientin 7-O-glucoside</i> ; <i>Luteolin 6-C-glucosyl-7-O-glucoside</i>)	268 (s), 348	C ₂₇ H ₃₀ O ₁₆	610.1534	[M+H] ⁺	611.1606	611.1636	4.8	[Lut+H+Hex] ⁺ [Lut+H+C ₂ H ₂ O] ⁺ [Lut+H+C] ⁺ [Lut+H] ⁺	449.1093 (29.2) 329.0657 (98) 299.0551 (100) 287.0547 (4.1)
Saponarin (<i>Isovitexin 7-O-glucoside</i> ; <i>Apigenin 6-C-glucosyl-7-O-glucoside</i>)	269, 336	C ₂₇ H ₃₀ O ₁₅	594.1585	[M+H] ⁺	595.1657	595.1681	4.0	[Api+H+Hex] ⁺ [Api+H+C ₂ H ₂ O] ⁺ [Api+H+C] ⁺ [Api+H] ⁺	433.1139 (58.6) 313.0711 (100) 283.0607 (82.6) 271.059 (4.4)

Supplementary data

Tab. S1 A list of genes, their accession numbers and primers, which were used to analyze their relative expression in low and high light

Acc. No.	gene	5' - 3' forward primer	5' - 3' reverse primer	bp
AK366573	<i>HvbcHYD</i>	gggatggcatacatgttcgt	ccatgtggtgtatcttgtgagc	118
AK362500	<i>HvZEP</i>	atgaatgactgccacgttgt	catctgctccaaccaagaga	106
AK357384	<i>HvCHS</i>	gggctcatctccaagaacat	cgctatccaaaagacggagt	90

Tab. S2 Tocopherol and chlorophyll (chl) content of leaves in WT and W1 plants grown under LL and HL at different days after sowing. Data for chl content was presented before by Saeid Nia et al. (2022). Values are means \pm standard deviation of n = 6 samples (for tocopherol content analysis) and in case of chl content, n = 23–37 leaves in total from three independent experiments each comprising 7–13 leaves (Saeid Nia et al. 2022). The letters indicate statistically different values at a significance level of P = 0.05, as determined by three-way ANOVA, followed by pairwise multiple means comparisons by the Holm-Sidak method

Samples name	das	α -tocopherol ($\mu\text{g cm}^{-2}$)	β -tocopherol ($\mu\text{g cm}^{-2}$)	γ -tocopherol ($\mu\text{g cm}^{-2}$)	Total-tocopherol ($\mu\text{g cm}^{-2}$)	Chl <i>a+b</i> (nmol cm^{-2})
WT-LL	10	0.30 \pm 0.04 ^a	0.002 \pm 0.0006 ^a	0.008 \pm 0.001 ^a	0.30 \pm 0.04 ^a	41.24 \pm 5.17 ^a
	15	0.40 \pm 0.11 ^{ab}	0.002 \pm 0.0008 ^a	0.007 \pm 0.002 ^a	0.40 \pm 0.12 ^a	45.40 \pm 3.54 ^a
	19	0.63 \pm 0.64 ^b	0.144 \pm 0.01 ^b	0.008 \pm 0.002 ^a	0.79 \pm 0.07 ^b	44.96 \pm 4.72 ^a
WT-HL	10	0.35 \pm 0.07 ^a	0.007 \pm 0.003 ^a	0.01 \pm 0.002 ^a	0.40 \pm 0.071 ^{ab}	44.63 \pm 5.30 ^a
	15	0.48 \pm 0.15 ^{ab}	0.003 \pm 0.001 ^a	0.009 \pm 0.005 ^a	0.5 \pm 0.15 ^{ab}	42.58 \pm 7.88 ^a
	19	2.21 \pm 0.31 ^c	0.275 \pm 0.073 ^c	0.12 \pm 0.05 ^b	2.61 \pm 0.39 ^d	32.88 \pm 9.18 ^b
W1-LL	10	0.28 \pm 0.06 ^a	0.002 \pm 0.001 ^a	0.01 \pm 0.004 ^a	0.29 \pm 0.06 ^a	28.69 \pm 3.85 ^c
	15	0.41 \pm 0.13 ^{ab}	0.004 \pm 0.002 ^a	0.008 \pm 0.004 ^a	0.42 \pm 0.14 ^{ab}	36.46 \pm 5.48 ^d
	19	0.44 \pm 0.08 ^{ab}	0.16 \pm 0.02 ^b	0.011 \pm 0.005 ^a	0.61 \pm 0.1 ^{ab}	39.19 \pm 3.97 ^d
W1-HL	10	0.28 \pm 0.03 ^a	0.007 \pm 0.009 ^a	0.01 \pm 0.004 ^a	0.29 \pm 0.04 ^a	16.66 \pm 2.89 ^b
	15	0.27 \pm 0.07 ^a	0.004 \pm 0.003 ^a	0.01 \pm 0.006 ^a	0.28 \pm 0.074 ^a	30.91 \pm 5.95 ^e
	19	0.41 \pm 0.13 ^{ab}	0.212 \pm 0.073 ^{bc}	0.012 \pm 0.004 ^a	0.64 \pm 0.20 ^{ab}	30.72 \pm 9.73 ^{eb}

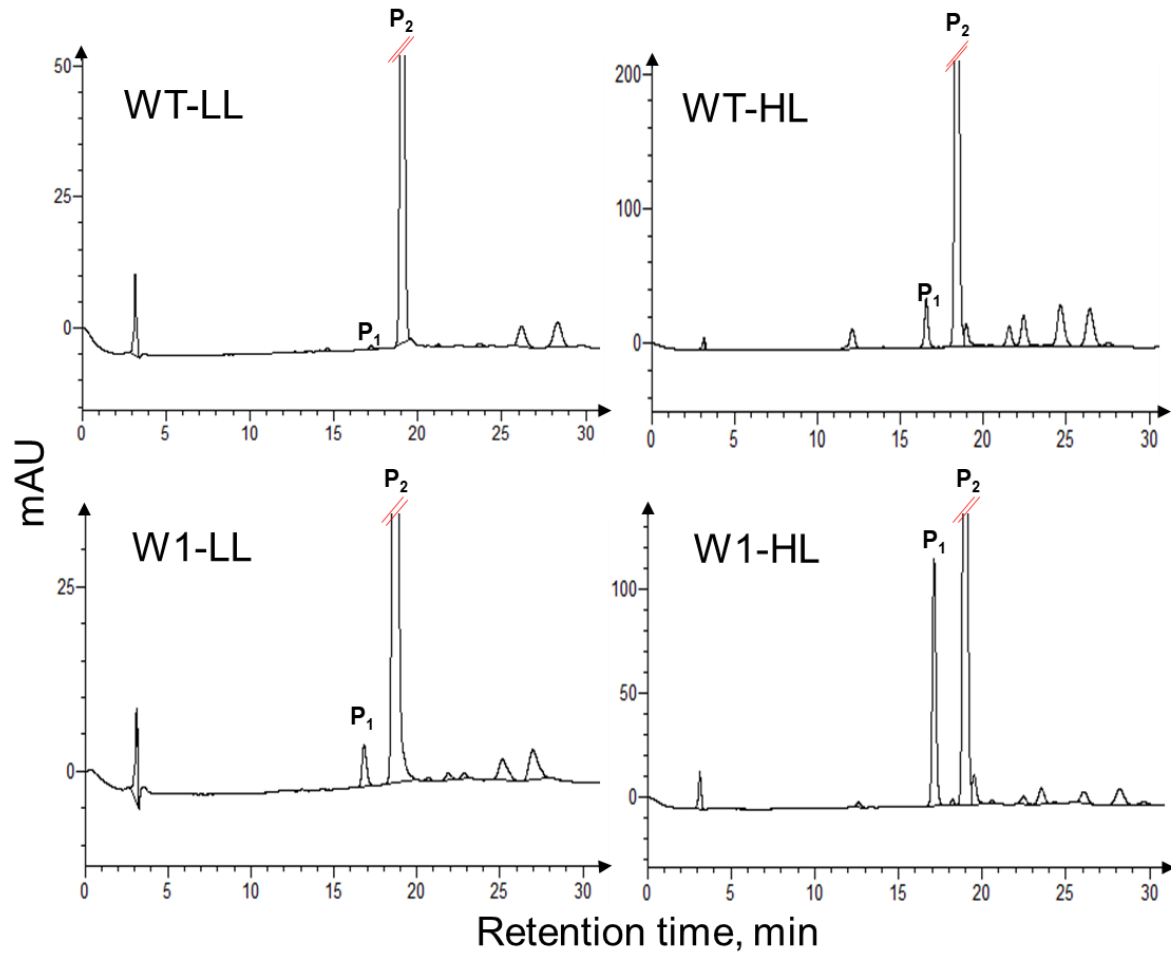


Fig. S1 Representative HPLC chromatograms for W1 and WT grown under low and high light detected at 313 nm. Peak 1 (P₁), lutanarin; peak 2 (P₂), saponarin. Please note, that the scale of the y-axis differs between the different chromatograms.

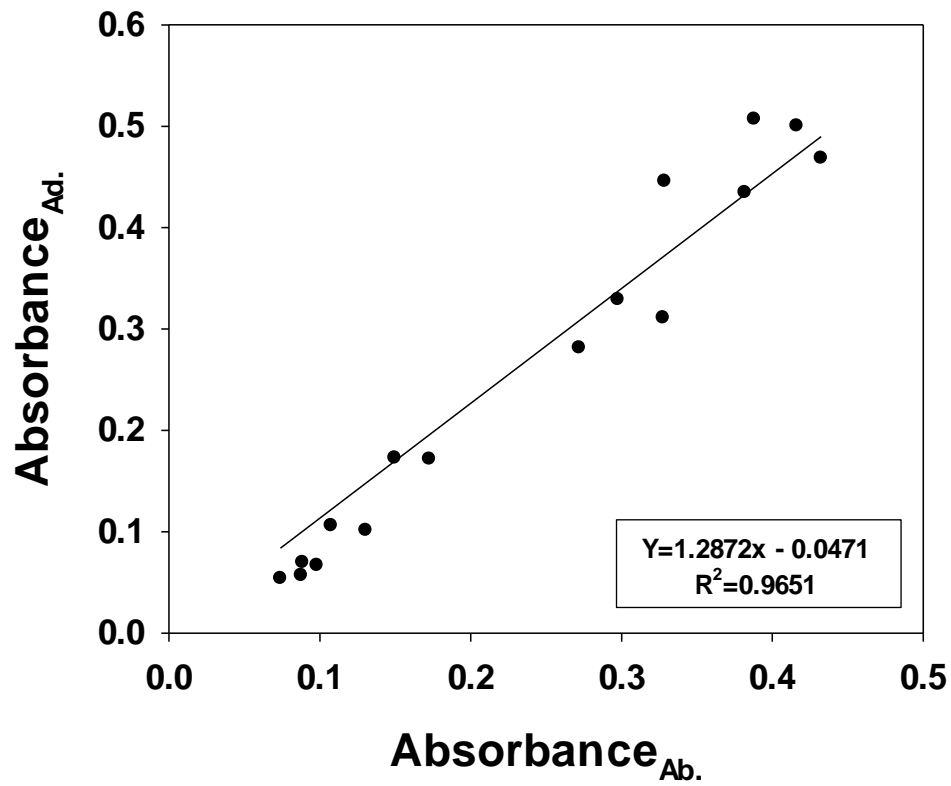


Fig. S2 The UV-A absorbance measured in the adaxial epidermis as a function of UV-A absorbance in the abaxial epidermis in WT plants grown under low and high light at day 10 after sowing

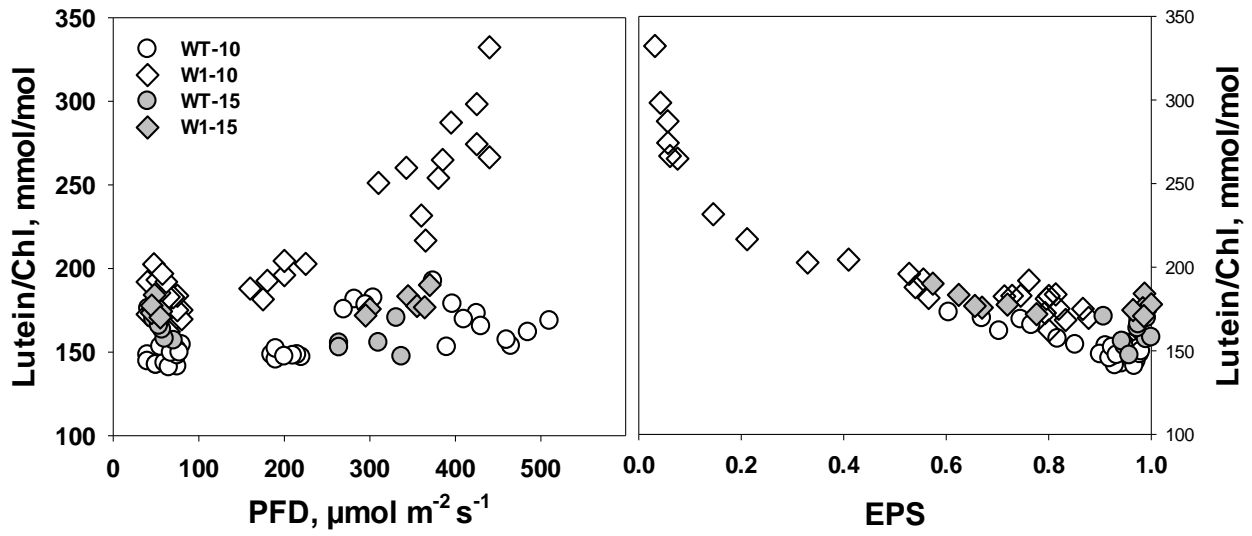


Fig. S3 Leaf lutein content per chlorophyll *a+b* as a function of incident irradiance (PFD) (a) and as a function of EPS (b) in WT and W1. Circles and diamonds denote WT and W1 plants, respectively. Open and filled symbols denote 10 and 15 day old plants, respectively

Chapter V: The balance between growth and resistance in WHIRLY1-overexpressing barley plants

The balance between growth and resistance is shifted to the latter by over-accumulation of chloroplast-nucleus located WHIRLY1 in barley

Monireh Saeid Nia¹, Susann Frank¹, Anke Schäfer¹, Christine Desel¹, Maria Mulisch¹, Ulrike Voigt¹, Daniela Nowara^{2#}, Yudelsy Antonia Tandron Moya², Wolfgang Bilger¹, Nicolaus von Wiren², Götz Hensel^{2§}, Karin Krupinska¹

¹*Institute of Botany, Christian-Albrechts-University (CAU), Kiel, Germany*

²*Leibniz Institute of Plant Genetics and Crop Plant Research (IPK), Seeland, OT Gatersleben, Germany*

[§]*current address: Centre for Plant Genome Engineering (CPGE), Institute of Plant Biochemistry, Heinrich-Heine-University, Düsseldorf, Germany*

[#]*current address: Institute of Plant Pathology, University of Bonn, Germany*

Summary

WHIRLY1 is a chloroplast-nucleus located DNA/RNA-binding protein with functions in development and stress tolerance. By overexpression of *HvWHIRLY1* in barley, lines with a 10- and two lines with a 50-fold accumulation of the protein were obtained. In these lines, the relative abundance of the nuclear form exceeded that of the chloroplast form indicating that over-accumulating WHIRLY1 exceeded the amount that chloroplasts can sequester. Growth of the plants was shown to be compromised in a WHIRLY1 abundance-dependent manner. Over-accumulation of WHIRLY1 in chloroplasts had neither an evident impact on nucleoid morphology nor on the composition of the photosynthetic apparatus. Nevertheless, oeW1 plants were found to be compromised in the efficiency of photosynthesis. The reduction in growth and photosynthesis was shown to be accompanied by a decrease in the levels of cytokinins and an increase in the level of jasmonic acid. Gene expression analyses revealed that already in non-stress conditions the oeW1 plants had enhanced levels of pathogen response (PR) gene expression indicating activation of constitutive defense. During growth in continuous light of high irradiance, *PR1* expression further increased in addition to an increase in the expression of *PR10* and of the gene encoding phenylalanine lyase (*PAL*), the key enzyme of salicylic acid biosynthesis in barley. The activation of defense gene expression in oeW1 plants coincided with an enhanced resistance towards powdery mildew, which in barley is independent of salicylic acid. Taken together, the results show that over-accumulation of WHIRLY1 in barley to levels of 10 or more, amplified the tradeoff between growth and stress resistance.

Introduction

WHIRLY proteins are multifunctional DNA/RNA binding proteins localized to the DNA-containing organelles and the nucleus of higher plants (Krupinska *et al.*, 2022). Investigations with mutants and knockdown plants have shown that WHIRLIES affect developmental processes and stress tolerance (Krupinska *et al.*, 2022).

Initially, the WHIRLY1 protein has been identified as a transcriptional activator of the pathogen response gene *PR10a* in potato (Desveaux *et al.*, 2000). Its binding to the promoters of PR genes that are enriched in elicitor response elements (ERE) was shown to depend on salicylic acid (SA) (Desveaux *et al.*, 2004). In recent years it has been shown that the role of SA is not limited to pathogen defense but that SA has an essential role in the regulation of redox homeostasis and thereby affects plants' responses towards abiotic and biotic stress (Mateo *et al.*, 2006, Karpinski *et al.*, 2013). Accordingly, the abundance of WHIRLY1 as a critical protein in SA signaling was shown to impact the plants' tolerance to diverse abiotic stress situations as well as pathogen defense. In *whirly1 (why1)* Tilling mutants of Arabidopsis, in which the binding of WHIRLY1 to the promoter of *PR1* was reduced, resistance to *Peronospora parasitica* was relieved, too (Desveaux *et al.*, 2004). Very recently, it has been reported that overexpression of *WHIRLY1* from *Vitis vinifera* under the control of a strong pathogen response promoter enhances resistance towards *Phytophthora capsica* (Lai *et al.*, 2022).

Besides its positive effect on defense, WHIRLY proteins were also found to promote tolerance towards abiotic stress. In tomato plants, overexpression of *WHIRLY1* was shown to enhance thermotolerance by upregulating the expression of the *HSP21.5A* gene which has an ERE in its promoter and encodes an endoplasmic reticulum-localized heat shock protein (Zhuang *et al.*, 2020a). Another study by the same research group showed that the plants overexpressing *SIWHIRLY1* had an enhanced chilling tolerance (Zhuang *et al.*, 2019). Vice versa, tomato plants with an RNAi-mediated knockdown of *SIWHIRLY1* showed reduced resistance to chilling (Zhuang *et al.*, 2019) and heat (Zhuang *et al.*, 2020a). In maize and barley, it has been demonstrated that a reduction of WHIRLY1 negatively affects chloroplast development (Prikryl *et al.*, 2008, Krupinska *et al.*, 2019). Furthermore, barley plants deficient in WHIRLY1 were shown to be compromised in light acclimation (Saeid Nia *et al.*, 2022).

Intriguingly, WHIRLY1 in barley was shown to locate in both, chloroplasts and nucleus of the same cell (Grabowski *et al.*, 2008). In transplastomic tobacco plants synthesizing a tagged WHIRLY1 protein, this tagged protein was found in the nucleus indicating a translocation of WHIRLY1 from chloroplasts to the nucleus. In these plants, the expression of PR genes was enhanced (Isemer *et al.*, 2012b). It has been hypothesized that storage of a transferable resistance protein such as WHIRLY1 in plastids might allow the plants to react immediately to pathogen attack avoiding the time and costs of gene expression (Krause and Krupinska, 2009). The translocation was suggested to occur in response to stress-associated redox changes in the photosynthetic apparatus (Foyer *et al.*, 2014). WHIRLY1 is a positive regulator of both plant development and stress tolerance. Hence, WHIRLY1 promotes two traits that usually are inversely correlated. Indeed, enhanced stress tolerance coincides with lower growth and productivity (Herms and Mattson, 1992). This tradeoff is thought to be caused by resource restrictions demanding a prioritization of either growth or defense in response to environmental factors (Huot *et al.*, 2014). The tradeoff is seemingly inevitable because the energy required for resistance is no longer available for biomass accumulation and production of seeds (Karasov *et al.*, 2017). Thousands of genes are typically activated to fight a pathogen or cope with another stressful situation. Among others, the tradeoff between growth and defense is regulated by crosstalk between defense and growth hormones (Huot *et al.*, 2014). Regulation of the level of free auxin is a significant determinant of adaptive growth in response to biotic and abiotic stress (Park *et al.*, 2007). Recently, it has been demonstrated that MAP kinases activated during the immune response are involved in the downregulation of the expression of photosynthesis-associated genes, thereby exerting a negative impact on growth (Su *et al.*, 2018).

Several studies with different dicot species have clearly shown a positive impact of over-accumulating WHIRLY1 on stress tolerance, however, without reporting effects on development and growth in these plants. Regarding the multifunctionality of WHIRLIES (Krupinska *et al.*, 2022a) it is expected that other physiological parameters are altered besides stress tolerance. This study aimed to investigate the impact of a much higher abundance of multifunctional WHIRLY1 on plant growth and stress tolerance.

Results

Overexpression of HvWHIRLY1 altered the abundance of HvWHIRLY1 in chloroplasts and the nucleus

By transforming barley with *HvWHIRLY1* under the control of the constitutive *UBIQUITIN 1* promoter of maize (Figure 1a), three homozygous lines were selected and used for characterization. Immunoblot analysis with the HvWHIRLY1 specific antibody (Grabowski *et al.*, 2008) revealed that in primary foliage leaves of line oeW1-14, the level of HvWHIRLY1 was enhanced by a factor of about 50 (Figure 1b) as it was also in line oeW1-2 (Figure S1a). For comparison, in line oeW1-15 the level of WHIRLY1 was enhanced by a factor of 10 (Figure 1b).

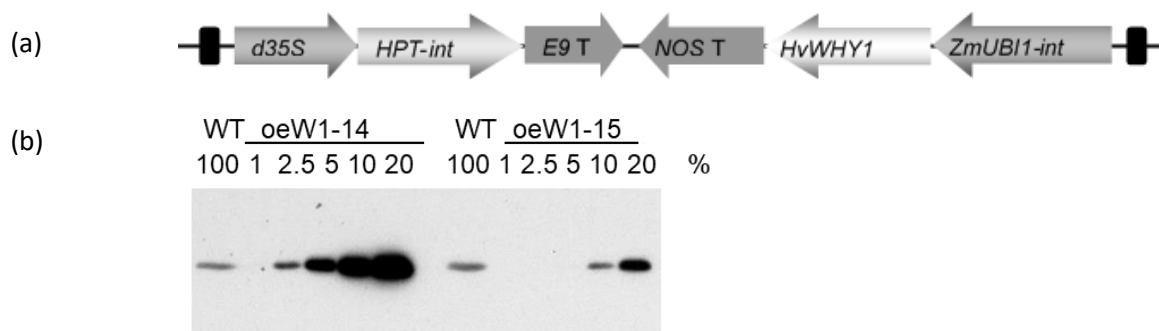


Figure 1. Overexpression of *HvWHIRLY1* in barley. (a) Schematic drawing of the T-DNA used for overexpression of *HvWHIRLY1* under control of the *Ubiquitin 1* promoter of maize. (b) Accumulation of the WHIRLY1 protein in total protein extracts derived from primary foliage leaves of the two transgenic lines, oeWHIRLY1-14 and oeWHIRLY1-15. For comparison, different amounts of leaf protein were used and indicated as a percentage of protein from wild-type plants (WT). d35S – doubled enhanced *CaMV 35S* promoter, HPT-int – *Hygromycin phosphotransferase* gene with *StLS1* intron, E9 T - Terminator of *Rbcs-E9* gene, ZmUBI1-int – maize *UBIQUITIN 1* promoter with the first intron, HvWHY1 – barley *WHIRLY1*, NOS T – *Agrobacterium tumefaciens Nopaline synthase* gene termination signal.

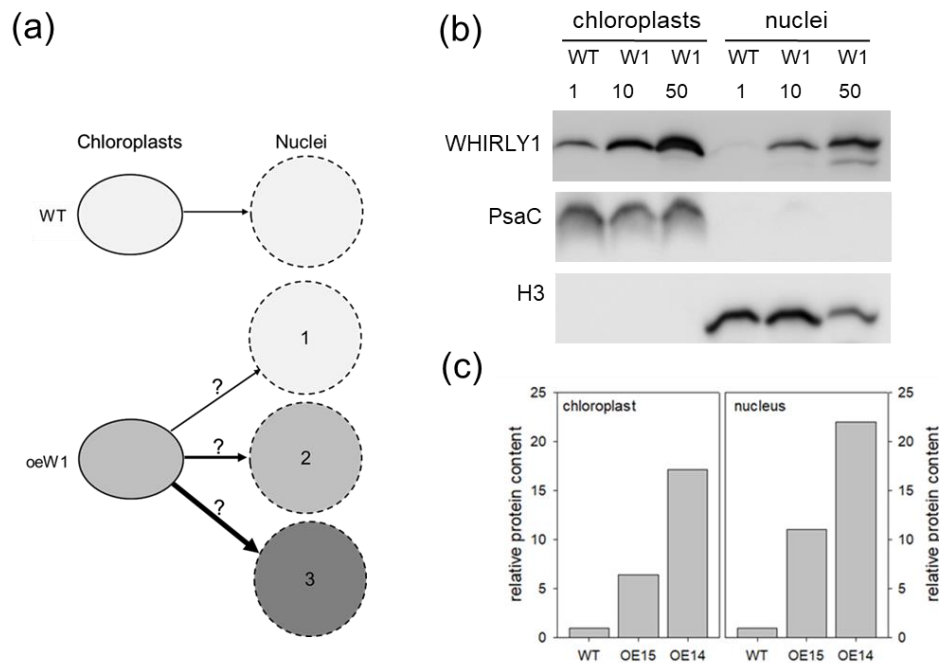


Figure 2. Relative WHIRLY1 levels in extracts from chloroplasts and nuclei, respectively.

(a) Putative consequences of WHIRLY1 overexpression (oeW1) for the distribution of the WHIRLY1 protein between chloroplasts and the nucleus. Different levels of WHIRLY1 are illustrated by light, medium, or dark grey symbols that represent chloroplasts or nuclei. The distribution in chloroplasts and nuclei of the wild type (WT) is normalized (light grey area). Either the transfer of WHIRLY1 to the nucleus will be not altered in comparison to the wild type (1), or the transfer will be enhanced resulting in a similar relative over-accumulation of WHIRLY1 in chloroplasts and the nucleus (2) or the transfer will be relatively higher as expected resulting in a higher relative abundance of WHIRLY1 in the nucleus compared to chloroplasts (3).

(b) Subcellular fractions were prepared from primary foliage leaves of WT, oeW1-15 (10-fold accumulation of WHIRLY1), and oeW1-14 (50-fold accumulation of WHIRLY1) plants.

Immunoblot analysis was performed with extracts from chloroplasts (CP) and nuclei (N). Each lane was loaded with 6 μg of protein. To show the purity of fractions, antibodies directed towards PsaC and histone 3 (H3) have been used.

(c) Relative abundances of the WHIRLY1 protein were calculated from the signal intensities measured by the ChemiDoc MP Imaging Systems after different times of exposure using the Image Lab 6.1 software. The relative intensities of the WHIRLY1 signals detected in chloroplast and nuclei samples, respectively, are based on the signal intensities of WT samples.

WHIRLY1 is dually located in chloroplasts and nucleus. To investigate whether the over-accumulation of the protein occurred in both compartments and whether the relative distribution between chloroplasts and nucleus is altered by the overexpression of *WHIRLY1* leaves (Fig. 2a) WHIRLY1 abundance was immunologically investigated in chloroplast and nuclei fractions prepared from primary foliage leaves of the oeW1-15 and the oeW1-14 lines. Theoretically, excess WHIRLY1 could accumulate only in chloroplasts or could also accumulate in nuclei, whereby the ratio between chloroplast and nuclear WHIRLY1 could be similar to in WT plants or could be shifted towards the nuclear form (Figure 2a). Immunoblots with the specific antibody for HvWHIRLY1 showed that the abundance of HvWHIRLY1 was enhanced in both chloroplasts and nuclei (Figure 2b, Figure S1b). Thereby the relative increase in quantity

was higher in nuclei than in chloroplasts (Fig. 2c). Considering that the proteins in chloroplasts and nucleus have the same molecular weight, the higher abundance in the nucleus likely results from an enhanced flux of protein from chloroplasts to the nucleus. This result suggests that the capacity to sequester HvWHIRLY1 in chloroplasts is saturated, and relatively more WHIRLY1 is transferred to the nucleus (Figure 2).

Growth of barley oeW1 plants

To investigate whether WHIRLY1 overaccumulation has consequences for growth, the lengths of primary foliage leaves were measured every day until they were fully expanded (Figure 2a). An apparent growth reduction correlated with an abundance of WHIRLY1. Growth curves showed that the seedlings of oeW1-10 were longer than those of the oeW1-50 line (Figure 2a). The growth kinetics did not differ between WT and oeW1 seedlings. The maximal expansion of the primary foliage leaves was terminated at the same time after sowing, i.e. at 9 days (Fig. 2a).

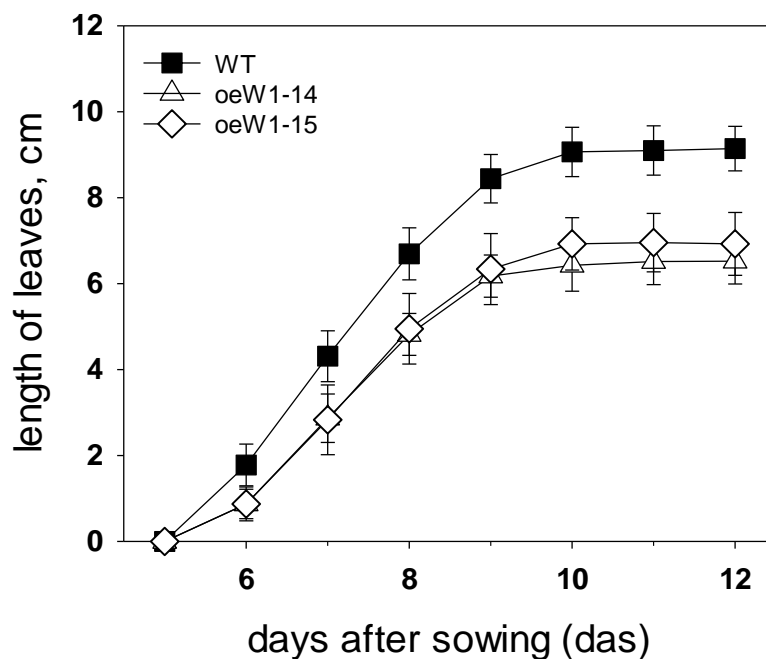


Figure 3. The lengths of entire primary foliage leaves of WT, oeW15, and oeW14 were determined by measuring the lengths from the kernel, where the leaf sheath starts, to the leaf tip at 5-12 days after sowing. Symbols represent means \pm SD of $n = 13-20$ leaves.

Characterization of the photosynthetic apparatus

To investigate whether changes in the photosynthetic apparatus are responsible for the reduced growth of the *oeW1* seedlings, the functionalities of the two photosystems were examined during the development of barley seedlings in a daily light/dark regime. Chlorophyll fluorescence measurements revealed that the maximal quantum yield of photosystem II, F_V/F_M , which is a measure of photosystem II efficiency, in WT seedlings was already relatively high at 7 das (0.7) and increased to nearly 0.8 at 10 das. In comparison, F_V/F_M of the *oeW1-50* leaves stayed rather low, reaching a maximal value of about 0.5 at 10 das (Figure 4a).

For comparison, in *oeW1-10* seedlings, F_V/F_M had a value of 0.6 at 7 das and a value of 0.7 at 9 and 10 das (Fig. 4a). In contrast to F_V/F_M , which barely changed in wild-type leaves during the growth period investigated, the capacity of photosystem I measured by the maximal absorbance change of P_{700} (P_M) increased from 0.3 at 7 das until 0.7 at 10 das (Figure 4a). The values stayed significantly lower in both *oeW1* lines, whereby *oeW1-14* seedlings had lower values than *oeW1-15* seedlings (Fig. 4a).

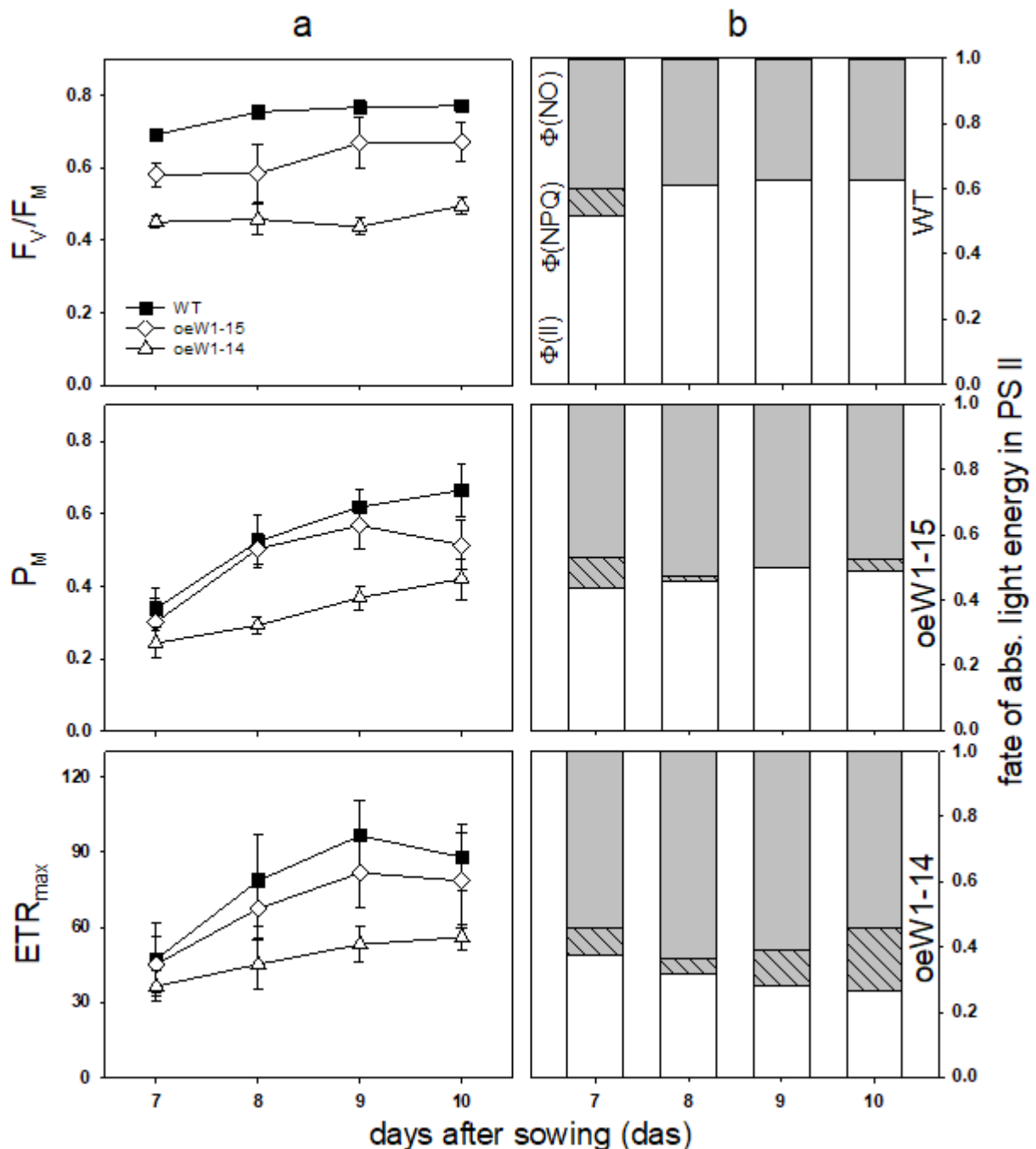


Figure 4. Characterizing the photosynthetic apparatus in primary foliage leaves of WT, oeW1-14, and oeW1-15 seedlings grown under a daily light-dark cycle (L/D). (a) The optimal quantum yield of photosystem II, F_v/F_M , the maximum P700 signal (P_M), and the maximal electron transport rate (ETR_{max}) were measured at room temperature at different days after sowing (7-10 das). Depicted values are mean \pm SD of $n=6$ leaves. (b) Fate of the light energy absorbed at PS II was determined at an irradiance of $60 \mu\text{mol m}^{-2} \text{s}^{-1}$. The quantum yield of photochemistry ($\Phi(II)$), of regulated non-photochemical quenching ($\Phi(NPQ)$) and non-regulated non-photochemical quenching ($\Phi(NO)$) were calculated according to the formulas given in Materials and Methods. Columns are means \pm SD of $n=6$ leaves.

In addition to the efficiency of photosystem II, the maximum electron transport rate of photosystem II (ETR_{max}) was reduced in the primary foliage leaves of oeW1 seedlings measured on different days after sowing (7-10 das). The results showed that oeW1-14 leaves

had only about 50% of the electron transport capacity of WT leaves, while oeW1-15 leaves had about 80% of the WT level (Figure 4a). Whereas the transport rate in WT and oeW1-15 leaves was maximal already at 9 das, it still increased in oeW1-14 leaves from 9 das until 10 das. An analysis of the partitioning of absorbed energy in photosystem II revealed that the quantum yield of photosystem II ($\Phi(\text{II})$) was lower in oeW1 plants at all stages of development compared to WT plants. The remaining fraction was dissipated mainly as heat or fluorescence ($\Phi(\text{NO})$). Only a small fraction was used for non radiative dissipation in the oeW1 leaves (Figure 4b).

To investigate putative differences in the composition of the photosynthetic apparatus, the concentrations of pigments and the relative abundances of photosynthesis-associated proteins were analyzed. Pigment analyses by HPLC showed that the chlorophyll content per leaf area of primary foliage leaves from seedlings of the oeW1-50 leaves was lower than the chlorophyll contents of line oeW1-15 and the wild-type, which were similar (Figure 5). The ratio of chlorophyll a/b was reduced in both oeW1 lines (Figure 5) and was independent of the leaves developmental stage.

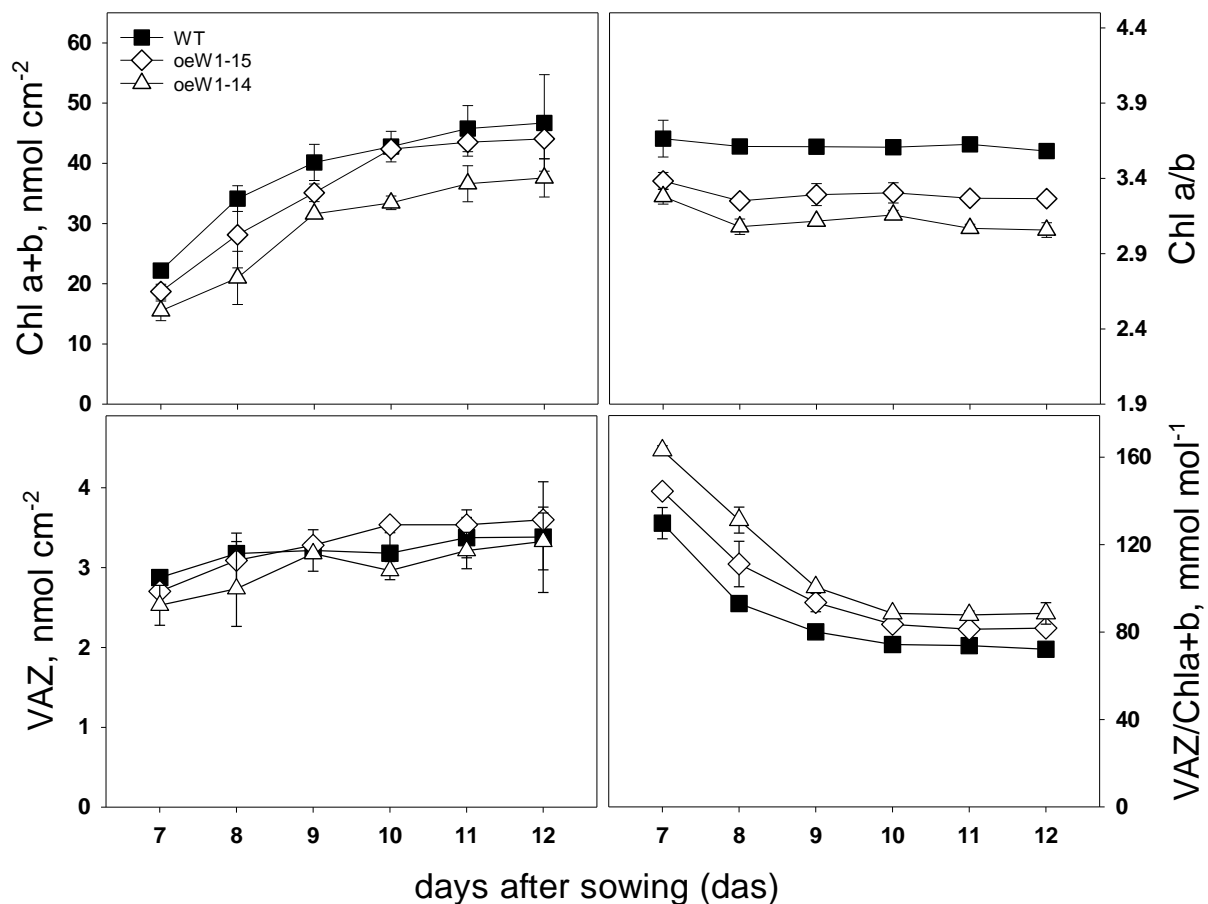


Figure 5. Pigment content of primary foliage leaves of barley wild type, oeW1-14 and oeW1-15 lines. Leaves were collected in the growth period from day 7 until day 12 after sowing. Depicted values are means \pm SD of n=3 leaves.

The content of xanthophyll cycle pigments was similar in all genotypes. However, the xanthophyll pool/chlorophyll ratio was higher in the leaves of the oeW1 lines, in particular in the oeW1-50 leaves.

Protein extracts from primary foliage leaves of WT and oeW1 seedlings were immunologically analyzed for the levels of central photosystem I (PsaA), photosystem II (D1/PsbA) proteins, and two light-harvesting proteins, i.e. LHCA1 and LHCB1, respectively. As already reported, the abundance of WHIRLY1 in the WT declined with the increasing age of the leaves (Kucharewicz *et al.*, 2017, Krupinska *et al.*, 2019). The levels of all tested proteins were similar in the WT and the oeW1 lines. (Figure 6). The staining also indicates that the two subunits of RubisCO had the same abundance as in the WT and that the levels are stable during development from 7 das until 12 das.

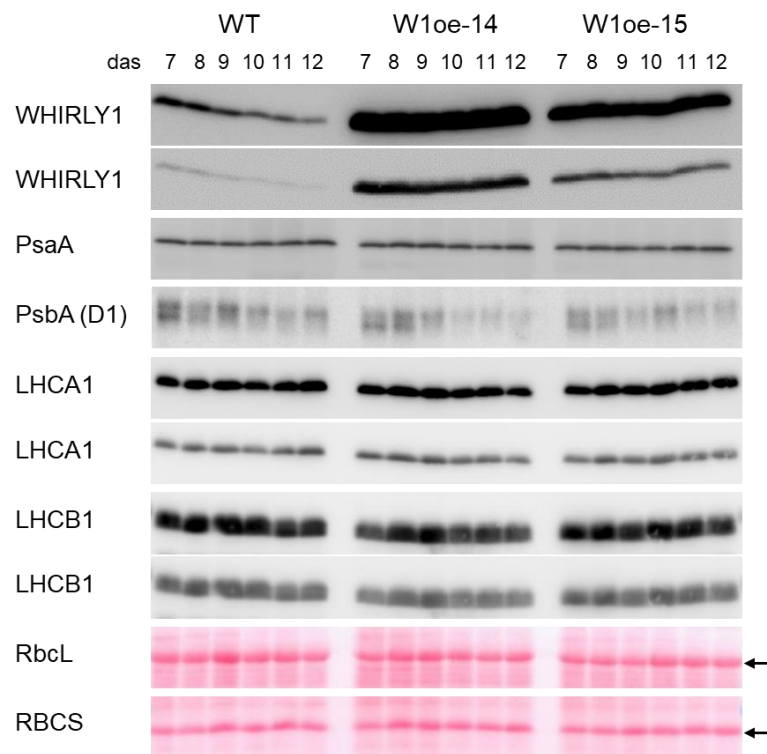


Figure 6. Relative amounts of proteins of the photosynthetic apparatus in primary foliage leaves of the WT, the oeW1-14 line, and the oeW1-15 line. Protein extracts were prepared from the leaves at different times after sowing (7-12 das). Immunological analyses were performed with specific antibodies directed towards WHIRLY1 and selected proteins of the photosynthetic apparatus: PsaA, PsbA (D1), LHCA1, and LHCB1. In the case of WHIRLY1 and LHCB1, two different exposures are shown, respectively. At the bottom, Ponceau stained gel parts showing the large and the small subunits of RubisCO (indicated by arrows) are presented.

In order to investigate gene expression in chloroplasts from oeW1 leaves in comparison to WT leaves, mRNA levels of genes encoding central components of the photosynthetic apparatus were analyzed by RT-PCR (Figure S2). While mRNA levels of all genes declined during the development of WT leaves, the mRNAs stayed at relatively high levels during the development of the oeW1 leaves. While in RNAi-W1 plants, plastid gene expression was mainly due to the activity of the nuclear-encoded RNA polymerase (NEP) (Krupinska *et al.*, 2019), in the oeW1 lines transcripts of both NEP (*rpoB*, *clpP*) and PEP (*psbE*) were present at higher levels than in WT plants. This result indicates that overexpression of *WHIRLY1* did not hamper transcription in chloroplasts.

Chloroplast ultrastructure and nucleoid morphology

When primary foliage leaves of barley were fully expanded (10 das), ultrathin sections from WT and oeW1-14 seedlings grown in a daily light/dark cycle were fixed for ultrastructural analyses by transmission electron microscopy. While mitochondria and peroxisomes looked

rather similar in WT and oeW1 samples (Figure 7a), chloroplasts showed noticeable morphological differences (Figure 7b). Chloroplasts of oeW1 plants apparently contained more plastoglobules (Figure 7). Plastoglobules are lipoprotein particles surrounded by a lipid monolayer, which is contiguous with the outer leaflet of thylakoid membranes. They contain mainly isoprenoid-derived lipophilic compounds and function in remodeling the lipid phase of thylakoids (van Wijk and Kessler, 2017). An increase in the number and/or size of plastoglobules was reported to indicate excess light in the photosynthetic apparatus (Brehelin *et al.*, 2007, Rottet *et al.*, 2016) and was observed during various stressful situations (Lichtenthaler, 2013, van Wijk and Kessler, 2017). Thylakoids in the chloroplasts of oeW1 leaves showed a tendency to swell. Following the lower photosynthetic activity of oeW1 leaves (Figure 3), chloroplasts of the oeW1 plants did not contain starch grains which were frequently observed in the wild-type chloroplasts.

Considering that WHIRLY1 is a major nucleoid-associated protein (Pfalz *et al.*, 2006, Krupinska *et al.*, 2022b), special attention was committed to the structure of nucleoids in mature chloroplasts of the primary foliage leaves of WT and oeW1 seedlings. Ultrastructural analyses did, however, not reveal apparent differences between nucleoids in WT and oeW1 sections (Fig. 6c-d). In addition, nucleoids of mature chloroplasts were also visualized by light microscopy after staining sections with SYBR Green (Figure 7e). By this procedure, neither differences in size nor the distribution of nucleoids were observed between the two genotypes.

Previous studies revealed a profound impact of WHIRLY1 on the packaging of plastid DNA (Krupinska *et al.*, 2014) and bacterial nucleoids (Oetke *et al.*, 2022). Considering that WHIRLY1 also plays a significant role in chloroplast development (Prikryl *et al.*, 2008, Krupinska *et al.*, 2019, Krupinska *et al.*, 2022), it might be possible that putative differences in nucleoid morphology depend on the developmental stage of plastids. Using the developmental gradient of the leaves of small-grained cereals (Boffey *et al.*, 1980), putative development-related changes in nucleoid morphology were investigated by staining sections prepared from the base and the middle part of the leaves of WT, oeW1-2 having a 50-fold over-accumulation as in oeW1-14 plants, and oeW1-15 seedlings with a 10-fold over-accumulation of WHIRLY1, respectively. Although WHIRLY1 abundances in chloroplasts are dramatically different between WT and an oeW1-50 line, no apparent differences in nucleoid morphology were

observed. In all genotypes, nucleoids in undifferentiated plastids at the base are arranged like pearls on a string. In contrast, nucleoids in mature chloroplasts are dispersed inside the chloroplasts (Figure S3) due to their attachment to thylakoid membranes (Powikrowska *et al.*, 2014).

Hormone levels and defense-related gene expression

To elucidate whether the reduced growth of the *oeW1* plants was related to changes in the levels of growth hormones, cytokinins, and auxins were determined at 7 and 10 das in primary foliage leaves of plants grown at a light intensity of $100 \mu\text{mol m}^{-2} \text{s}^{-1}$. These measurements revealed that independent of the developmental stage, the levels of the cytokinin N⁶-isopentenyl adenosine (iPR) were reduced by about 30% or 60% in the primary foliage leaves of *oeW1-15* or *oeW1-14* plants, respectively (Figure 8). For comparison, indole-3-acetic acid (IAA) levels were similar among the lines. At 10 das a reduction in the level of IAA by about 20% was measured in the leaves of the *oeW1-14* line (Figure 8)

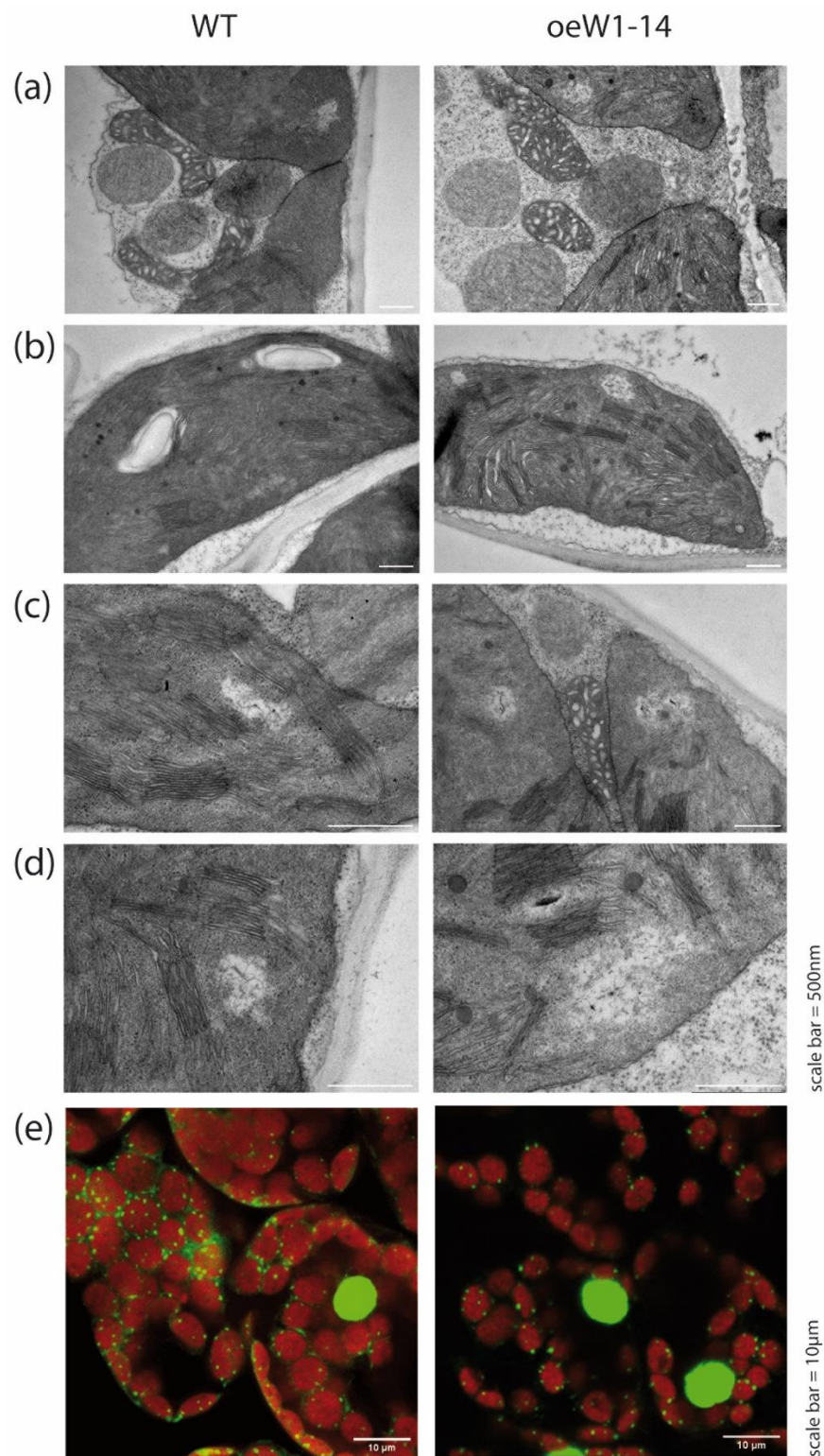


Figure 7. Microscopic analyses of chloroplasts and nucleoids from WT and oeW1-14 seedlings by transmission electron microscopy (a-d) and confocal fluorescence microscopy (e) where the green fluorescence was emitted by DNA stained with SYBR Green. Samples were excited by an argon laser at 488 nm (5% power). Emission was detected between 510-570 nm (HV750) and 690-760 nm (HV480).

For comparison, the levels of hormones involved in defense were determined. While free salicylic acid was too low to be determined, its precursor and storage compound were detectable. It has been shown that in barley during pathogen defense, SA is not produced via the isochorismate (ICS) pathway (Vlot *et al.*, 2009, Rekhter *et al.*, 2019), but rather by the phenylpropanoid pathway controlled by phenylalanine lyase (PAL) (Qin *et al.*, 2019) whereby dihydroxybenzoic acids precede the formation of SA. The levels of 3,4-dihydroxy benzoic acid were about twofold higher in young leaves of the oeW1-14 leaves compared to the other lines, but this difference disappeared when leaves were collected at 10 das (Figure S6). Levels of SA glucosides which is a storage form of SA (Vlot *et al.*, 2009), showed a tendency to be higher in the leaves from oeW1-14 plants, in particular in young leaves (7 das) (Figure S6). The determination of jasmonic acid (JA) revealed that at 8 das overexpression of *HvWHIRLY1* significantly increased its level by a factor of 3 or 5 in oeW1-15 or oeW1-14 lines, respectively. Thereby the basis level measured in the WT leaves was slightly enhanced at 10 das, compared to 8 das (Figure 8). Taken together, the results revealed that over-accumulation of WHIRLY1 induced reciprocal changes in the levels of iPR and JA which might cause a shift from growth to defense.

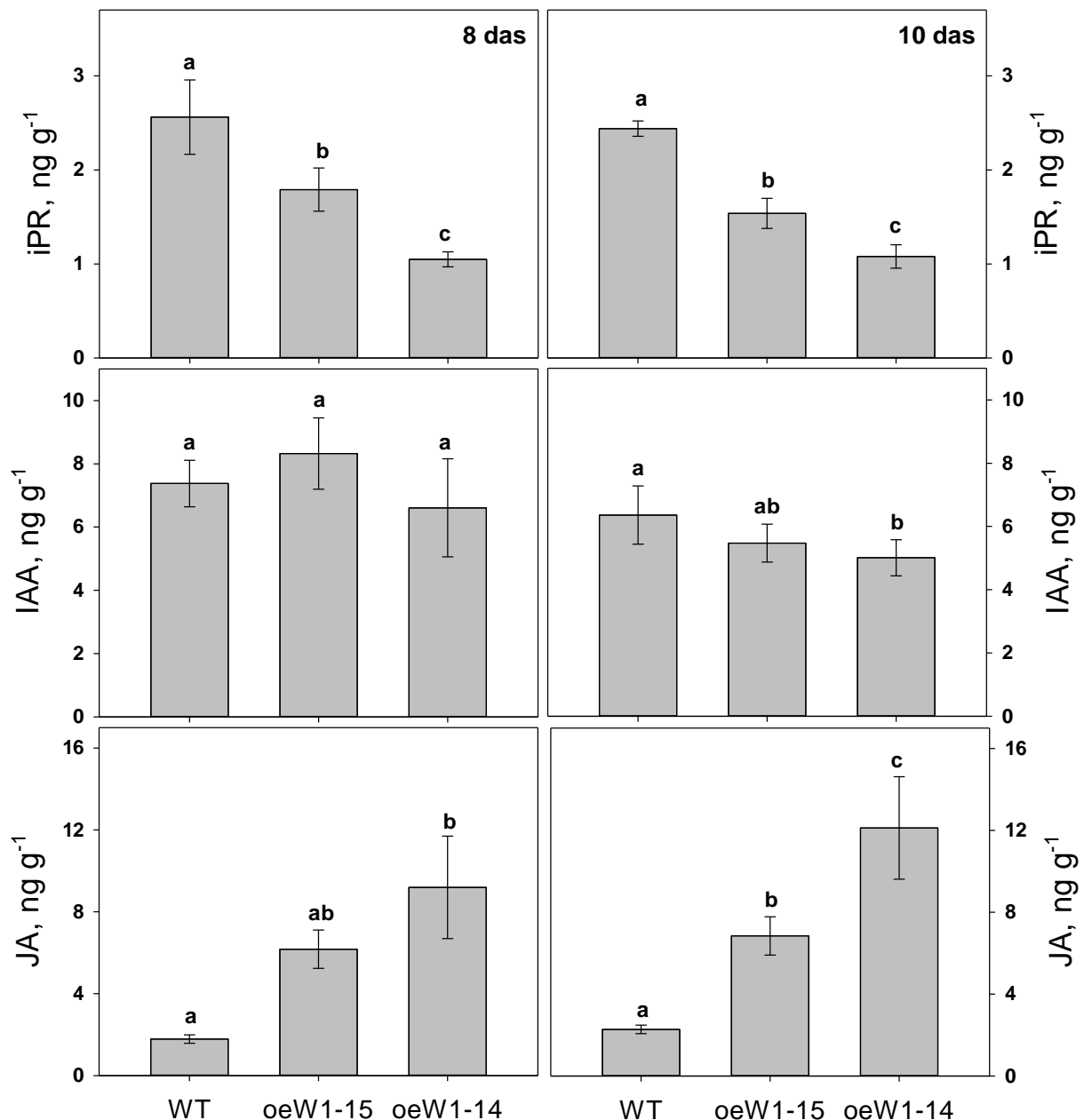


Figure 8. Hormone levels in primary foliage leaves of the WT in comparison to the oeW1-15 and oeW1-14 lines: N⁶-isophentenyladenosine (iPR), indole acetic acid (IAA) and jasmonic acid (JA). Leaves were collected at 8 das and at 10 das, respectively. Columns are means \pm SD of n=5 leaves.

To investigate whether according changes in gene expression accompanied the transition from development to defense, mRNA levels of key enzymes in the biosynthesis of defense hormones were determined besides the levels of *WHIRLY1* mRNA and *PR1* mRNA by quantitative real-time PCR. The result showed that *HvWHIRLY1* had an up to 20-fold higher mRNA level in primary foliage leaves of oeW1-14 seedlings compared to the WT. *PR1* is known as a marker of SAR (Linthorst, 1991). While in *Arabidopsis* and other dicots, it was reported to be a target gene of salicylic acid (Van Loon and Van Strien, 1999, Golshani *et al.*, 2015), *PR1* in

rice was shown to accumulate in response to JA (Rakwal and Komatsu, 2000, Jwa *et al.*, 2006). In this study, barley *PR1* expression was upregulated in WT and *oeW1* seedlings when the leaves became fully expanded. While in the WT, *PR1* expression was upregulated by a factor of 6 at 10 das and by a factor of 11 at 12 das, in *oeW1* seedlings, expression of the gene was highly upregulated by a factor of 120 at 10 das (Figure 9). Upregulation of *PR1* in the *oeW1* seedlings was neither accompanied by upregulation of the gene encoding PAL nor ICS, which are the key enzymes of the two pathways of salicylic acid biosynthesis (Vlot *et al.*, 2009) (Figure 9).

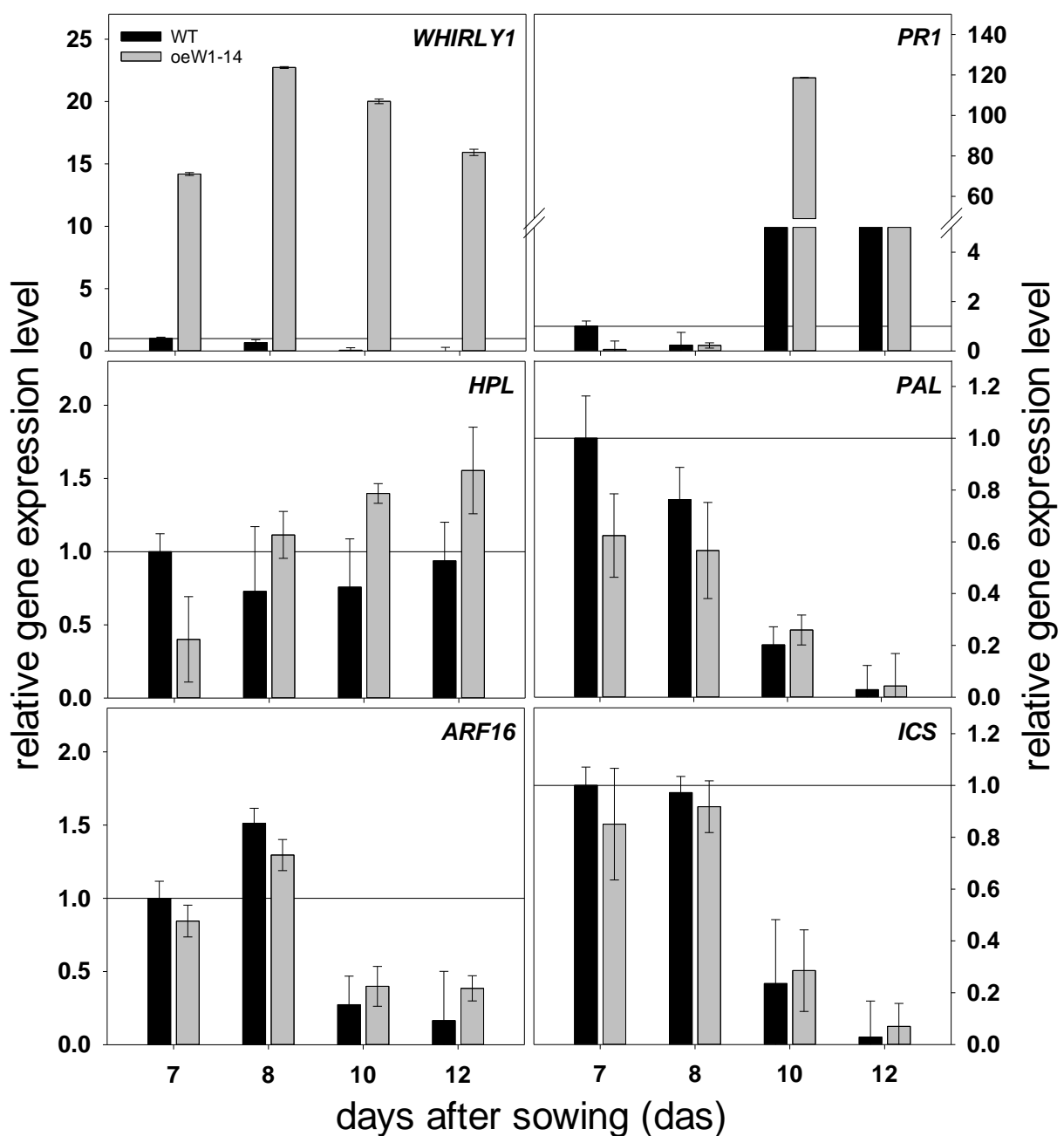


Figure 9. Expression of *HvWHIRLY1* and selected stress-associated genes measured by qRT-PCR using *GCN5* (see Material and Methods) as standard. RNA was extracted from primary foliage leaves of WT and oeW1-14 seedlings grown for different times (7, 8, 10 and 12 das) in a daily light/dark cycle. Columns are means \pm SD of n=3 samples (each sample comprised 10 pooled leaves).

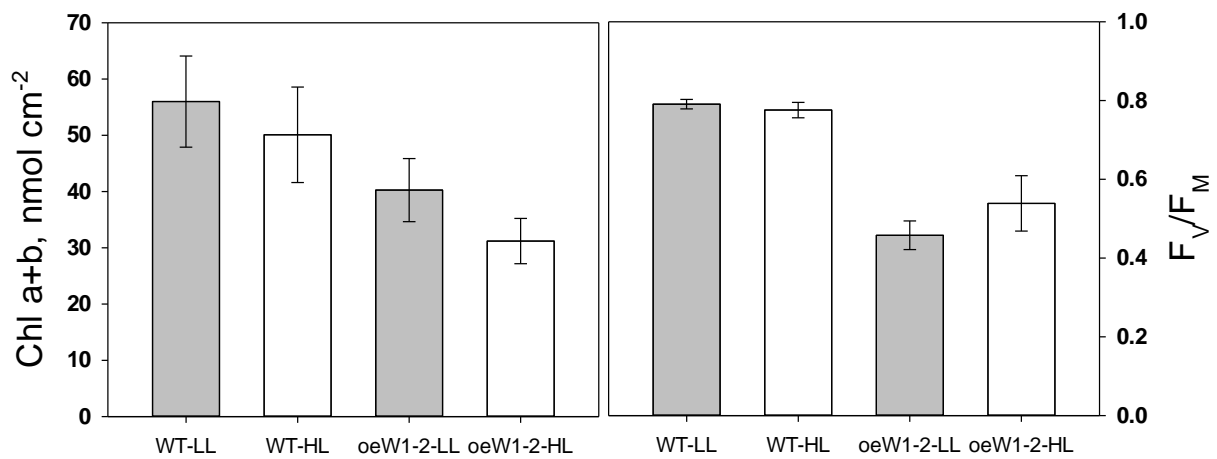
Expression of the general stress associated *HPL* gene encoding hydroperoxide lyase, a chloroplast protein of the oxylipin pathway shown to protect against photoinhibition (Savchenko *et al.*, 2017), was only upregulated by about 50% in fully expanded primary foliage leaves of the oeW1 seedlings. This gene was chosen because it is known to be a stress indicator gene regulated by retrograde signaling during stress in Arabidopsis (Xiao *et al.*, 2012, Xiao *et al.*, 2013). Its expression barely changed in WT seedlings during normal growth (Figure 9). In contrast to *PR1*, the expression of *THIO1*, another barley defense gene (Leybourne *et al.*, 2022), was downregulated during growth in both WT and oeW1 seedlings (Figure S4).

Response of oeW1 plants to high light

In Arabidopsis, defense signaling is also activated in response to high light (Mateo *et al.*, 2006, Karpinski *et al.*, 2013). To induce high light stress, oeW1-14 and WT seedlings were grown in continuous light of $350 \mu\text{mol m}^{-2} \text{s}^{-1}$ (HL) and were compared to seedlings grown at only $100 \mu\text{mol m}^{-2} \text{s}^{-1}$ (LL) as described previously (Swida-Barteczka *et al.*, 2018). Growth at high light leads to a decrease in the chlorophyll content of both WT and oeW1 plants. The reduction in chlorophyll content of oeW1 plants was significantly more pronounced than the WT (Figure 10a) but was not as prominent as in the case of the *WHIRLY1* knockdown plants prepared by RNAi (Swida-Barteczka *et al.*, 2018). In WT seedlings, F_v/F_m was not affected by higher irradiance during growth, while it even slightly increased in the case of oeW1-14 seedlings (Figure 10a).

When WT seedlings were grown at HL, *PR1*, and *PR10* expression levels were elevated compared to the levels determined in LL-grown plants. This result follows the idea that SA is involved in response to HL. Overexpression of *WHIRLY1* led to a dramatic increase in the expression of both PR genes (Figure 10b). Moreover, over-accumulation of HvWHIRLY1 led to enhanced expression of *PAL*, which was more pronounced at HL than at LL (4-fold in comparison to LL) (Figure 10b). Expression of *PAL* but not of *ICS* was also enhanced in the WT at HL. In comparison, *ICS* expression was enhanced in oeW1 plants only at LL, but not at HL. The high expression of *ICS* at LL could be related to an increased demand for phylloquinone (Qin *et al.*, 2019).

In addition, the expression of genes encoding two key enzymes of the two branches of the oxylipin biosynthesis in chloroplasts (Savchenko *et al.*, 2017) was determined, i.e. HPL leading to the biosynthesis of aldehydes and allene oxide synthase (AOS), a key enzyme of JA biosynthesis (Delker *et al.*, 2006). In the WT, *HPL* was upregulated by 4-fold, while AOS was upregulated by a factor of 5.5 (Figure 10b). In the *oeW1* seedlings, expression of *HPL* was already enhanced at LL and was only upregulated by 40% in HL. Indeed, the expression levels at HL were identical between WT and *oeW1* plants. The expression of *AOS* is upregulated likewise in HL in both the WT and the *oeW1* plants.

a

b

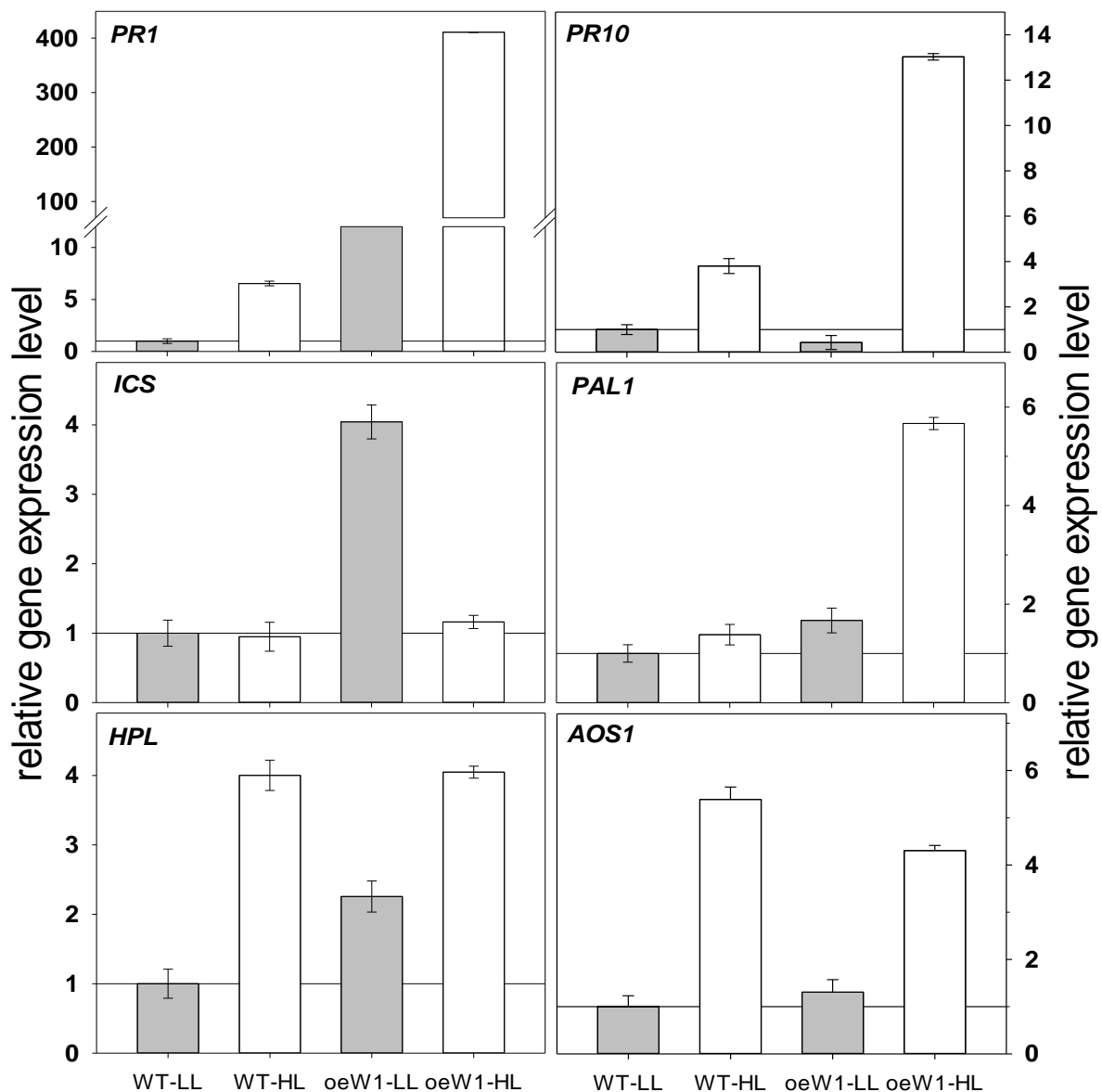


Figure 10. Characterization of primary foliage leaves of WT and oeW1-2 seedlings during growth in continuous light of different irradiance (low light=LL in grey and high light =HL in open columns). (a) Chlorophyll content and F_v/F_m , (b) expression of defense-related genes putatively associated with HL stress and SA: *PR1*, *PR10*, *ICS*, *PAL*, *HPL*, *PAL1*, *AOS1*.

Response of oeW1 plants to powdery mildew

To investigate the impact of WHIRLY1 accumulation on pathogen resistance, leaves were inoculated with spores of the powdery mildew fungus *Blumeria graminis*, an important barley pathogen. The susceptibility to powdery mildew was compared among WT, oeW1-14, oeW1-2 (two lines over-accumulating WHIRLY1 by a factor of 50), and two barley plants with an RNAi-mediated knockdown of *HvWHIRLY1*, W1-1 and W1-7 (with 10% and 1% of the protein

in WT, respectively), which had been used in several investigations before (Krupinska *et al.*, 2014b, Krupinska *et al.*, 2019). Both oeW1-14, oeW1-2 were less susceptible to powdery mildew than the WT, as determined by estimating the percentage of the leaf surface infected by the fungus (Figure 11). Inversely, the leaves of the *WHIRLY* knockdown plants (W1-1 and W1-7) were less susceptible to inoculation with powdery mildew spores. The results show that a high abundance of *WHIRLY* positively affects the resistance towards powdery mildew.

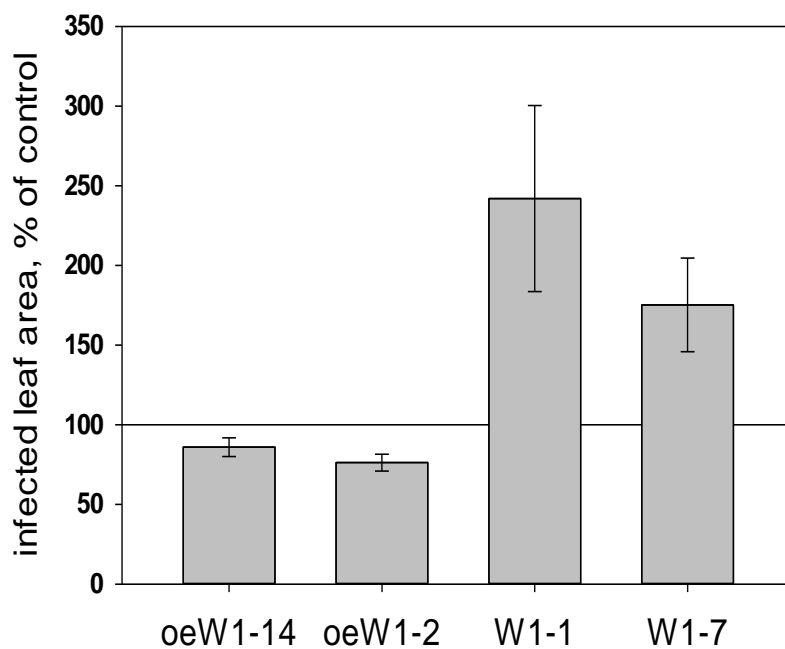


Figure 11. Infection of barley leaves by powdery mildew (*Blumeria graminis*). WT leaves were compared with leaves of two oeW1 lines over-accumulating *WHIRLY1* by a factor of 50 (oeW1-14, oeW1-2), and with the *knockdown* plants having residual amounts of about 10% (W1-1) or 1% (W1-7) of *WHIRLY1* protein (Krupinska *et al.*, 2014b). Susceptibility was determined by the percentage of leaf area infected by the fungus. The susceptibility of the WT has been defined as 100% represented by horizontal lines.

Discussion

Overexpression of *WHIRLY1* in barley resulted in an up to 50-fold higher abundance of the *WHIRLY1* protein, an improved tolerance towards powdery mildew, and diminished growth, indicating a typical tradeoff between growth and defense (Herms and Mattson, 1992, Huot *et al.*, 2014). Although the tradeoff has often been explained by the competition of energy requirements of defense responses in relation to those for growth and reproduction, this apparently plausible explanation has also been questioned. Instead, the dilemma between development and defense was shown to stem from antagonistic crosstalks between growth

and defense-related hormones (Karasov *et al.*, 2017), which can be uncoupled in mutants (Campos *et al.*, 2016).

Impact of WHIRLY1 overexpression on growth and photosynthesis

For *oeAtWHIRLY1* plants, no obvious phenotype has been reported (Isemer *et al.*, 2012a). A more detailed characterization has been performed with tomato lines overexpressing *SIWHIRLY1* (Zhuang *et al.*, 2019). In these plants, the mRNA level increased dramatically by factors of about a thousand. In contrast, the protein level was only enhanced by an estimated factor of approximately five (estimated from Figure 2 in Zhuang *et al.* 2019). No significant difference was observed in the phenotypes between tomato *oeSIWHIRLY1* lines and the wild type at standard growth conditions. However, under chilling conditions, the *oeSIWHIRLY1* lines grew better than the wild-type (WT) coinciding with a reduced level of ROS, as shown by fluorescence after staining with H₂DCFDA (Zhuang *et al.*, 2019). At the ultrastructural level, the *oeSIWHIRLY1* plants were shown to retain intact grana thylakoids and to accumulate less starch at chilling conditions. However, in contrast to the barley lines overexpressing *HvWHIRLY1* (*oeW1*), the abundance of starch grains did apparently not differ between WT and *oeSIWHIRLY1* plants (Zhuang *et al.*, 2019). Also in contrast to the barley *oeW1* lines, the *oeSIWHIRLY1* plants showed no difference in F_v/F_m at 25°C and even higher F_v/F_m values under chilling conditions (Zhuang *et al.*, 2020b). Also, in contrast to the barley *oeW1* plants, RubisCO content was higher in the *oeSIWHIRLY1* plants than in the WT, both at 25°C and 4°C (Zhuang *et al.*, 2020b). Under heat stress, the *oeSIWHIRLY1* plants showed less wilting than WT tomato plants coinciding with increased sugar content and a reduced level of ROS (Zhuang *et al.*, 2020a).

In contrast to the barley *oeW1* plants, the two *WHIRLY1* overexpressing dicot species investigated didn't show a pronounced decrease in growth under standard conditions. Compared to the barley lines used in this study, over-accumulation of the protein in tomato is relatively low and could be a reason for the discrepancies between barley and tomato. Alternatively, the growth-related difference between *WHIRLY1* over-accumulation in barley on the one hand, and tomato or Arabidopsis, on the other hand, could be due to differences in the impact of *WHIRLY1* proteins on chloroplast nucleoid architecture. Only in monocots *WHIRLY1* proteins were shown to have a specific PRAPP motif required for the compaction of

nucleoids (Oetke *et al.*, 2022). However, despite the over-accumulation of WHIRLY1, nucleoids did not show differences in their compactness and organization between WT and oeW1 plants as investigated by DNA staining (Figure 7, S3). This result is in line with the almost normal levels of plastid-encoded mRNAs (Figure S2) and the unvaried protein composition of the photosynthetic apparatus (Figure 6). Regarding these results, it is rather unlikely that alterations in the nucleoid compactness and the composition of the photosynthetic apparatus are responsible for the reduced growth of barley plants over-accumulating WHIRLY1.

On the other hand, the efficiencies of both photosystems, the maximal electron transport rate (ETR_{MAX}), and the quantum yield of photosystem II ($\Phi(II)$) were reduced in plants over-accumulating WHIRLY1. Inversely, the loss of absorbed energy by heat and fluorescence was enhanced in oeW1 plants indicating a malfunctioning of the photosynthetic apparatus. Potentially, changes in the hormone equilibrium could underlie the lower functionality of the photosynthetic apparatus (Muller and Munne-Bosch, 2021, Cackett *et al.*, 2022). In this regard, the barley oeW1 plants might be comparable with mutants showing constitutive defense signaling. Arabidopsis mutants with *constitutive expression of pathogenesis-related proteins (cpr)* showed a dwarf phenotype (Zhang *et al.*, 2003, Heidel *et al.*, 2004). To investigate whether the impaired growth is a consequence of deteriorated photosynthesis or energy-consuming defense mechanisms, Mateo *et al.*, (2006) investigated the photosynthetic properties of *cpr* mutants in comparison to the WT. Similar to the Arabidopsis *cpr* mutants, barley seedlings overexpressing WHIRLY1 have a reduced F_v/F_m , a higher ratio of VAZ pool pigments to chlorophylls, and reduced starch content as a consequence of the reduced capacity of the photosynthetic apparatus (Figure 5, 7).

Overexpression of WHIRLY1 caused changes in the equilibrium of hormones

Over-accumulation of WHIRLY1 indeed caused a shift in the hormone equilibrium. While the level of the cytokinin isopentenyl riboside (iPR) was reduced, the level of jasmonic acid (JA) is enhanced in oeW1 plants. Cytokinins are well-known for their positive impact on cell division and expansion during leaf development and growth (Brzobohaty *et al.*, 1994, Wu *et al.*, 2021). Moreover, cytokinins were shown to promote chlorophyll biosynthesis, assembly, and functioning of the photosynthetic complexes (Yaronskaya *et al.*, 2006) and to play a role in responses to stress (Albrecht and Argueso, 2017, Cortleven *et al.*, 2019). Cytokinins were

found to regulate more than 100 genes involved in photosynthesis, including the genes of RubisCO and LHCs (Brenner and Schumling, 2012) and those encoding sigma factors required for plastid gene transcription by PEP (Danilova *et al.*, 2017). Applying cytokinins to wheat leaves increased endogenous cytokinin content and photosynthesis parameters $\Phi(\text{PSII})$, F_v/F_m , and ETR, whereas inhibition of cytokinin biosynthesis had opposite effects (Yang *et al.*, 2018). The published data suggest that a decreased cytokinin level led to an inactivation of photosystem II reaction centers (Muller and Munne-Bosch, 2021). Hence, the reduced efficiencies of the photosystems, together with the decreased ETR and quantum yield of photosystem II in the oeW1 leaves, are potentially caused by the decrease in the level of iPR. Under HL, cytokinins were reported to promote D1 repair (Cortleven *et al.*, 2019). Whereas in the barley plants grown at continuous light of low irradiance, cytokinin levels were low in all genotypes, at high irradiance, the level increased in the WT but not in the oeW1 plants (Figure 8).

Nevertheless, F_v/F_m was higher in the oeW1-14 plants in HL compared to LL. This might indicate that oeW1 plants, compared to WT plants, have a better capacity to respond to HL. A similar finding has been reported for the response of tomato plants overexpressing *WHIRLY1* towards chilling (Zhuang *et al.*, 2020b).

In comparison to the cytokinin level, the level of the major auxin IAA was less affected in the barley oeW1 plants. This coincided with similar expression levels of selected genes responding to auxin, i.e. *PIN1* and *TIR1* (Figure S 4). Expression of genes related to auxine biosynthesis such as the YUCCA genes was neither detectable in the WT nor in the oeW1 plants. The level of JA was enhanced in oeW1 plants under standard growth conditions (Figure 8) and during growth in continuous light of low irradiance (Figure S6). It is known that a rise in JA has a negative impact on photosynthesis (Attaran *et al.*, 2014, Muller and Munne-Bosch, 2021) and growth (Staswick *et al.*, 1992). Recently it has been shown that the treatment of barley leaves with JA affects photosynthesis at the level of the oxygen-evolving complex (Kurowska *et al.*, 2020). During growth in continuous light of high irradiance, the level of JA increased in the wild type. As a consequence, the differences among the genotypes measured at low light irradiance disappeared (Figure S6).

In leaves collected under standard growth conditions, the higher expression of defense-related genes such as *PR1* and *HPL*, the latter of which has been proposed as general stress

indicator genes (Savchenko *et al.*, 2017), indicates that over-accumulation of WHIRLY1 activates defense signaling. Unexpectedly, the level of salicylic acids (SA) stayed below the method's lowest quantification limit, i.e. 0.1 μM . If the over-accumulation of WHIRLY1 would have induced its synthesis, SA would have increased above a level of 1 μM . The SA-related compounds also did not show changes associated with WHIRLY1 quantities. It may be supposed that SA signaling is not affected by the overexpression of WHIRLY1 in barley. While in barley, only a limited number of pathogens induced an increase in the level of SA, all tested pathogens induced the expression of PR genes, including PR1 (Vallelian-Bindschedler *et al.*, 1998). Obviously, SA in barley is not always required for defense-related gene expression. In the barley plants grown at continuous high light, also PR10 expression was enhanced. This gene might be expressed in response to the simultaneous presence of JA and light as reported for rice (Rakwal *et al.*, 2001, Zheng *et al.*, 2021). A minor contribution of SA to the defense response cannot be excluded considering that expression of PAL encoding the key enzyme of salicylic acid biosynthesis is activated in HL both in the WT and much more in the oeW1-50 plants (Figure 10b).

In Arabidopsis, WHIRLY1 was shown to be involved in salicylic acid (SA) signaling independent of NPR1 in the cytosol (Desveaux *et al.*, 2004, Vlot *et al.*, 2009, An and Mou, 2011, Carella *et al.*, 2015). NPR1 is known to translocate from the cytosol to the nucleus upon binding of salicylic acid and thioredoxin-mediated reduction (Mou *et al.*, 2003). It has been proposed that WHIRLY1 is translocated from chloroplasts to the nucleus in a similar fashion upon stress-associated redox changes in the photosynthetic apparatus (Foyer *et al.*, 2014), whereby the mechanism of translocation remains unknown (Krupinska *et al.*, 2022). In the oeW1 plants described in this study, the level of nucleus-located WHIRLY1 is highly upregulated even in the absence of stress. Consequently, in the barley oeW1 plants, defense signaling is constitutively activated, as evident by the expression of PR1 in fully expanded leaves of seedlings grown under standard growth conditions (Figure 9) and during continuous illumination of low irradiance (Figure 10b). It is obvious that the WHIRLY1-activated defense signaling is mediated by JA rather than by SA. This result is in accordance with reports on JA-dependent defense activation involving PR1 in rice (Yang *et al.*, 2013).

By the growth of the oeW1 plants at high irradiance, a dramatic increase in expression of PR1 (450-fold instead of 70-fold in the wild type) and PAL (6-fold instead of only 50% in the WT)

was observed (Figure 10b). This indicates that the oeW1 plants are capable of further enhancing defense responses. Considering that the abundance of WHIRLY1 is already high in non-stress conditions, it is unlikely that the higher expression of defense genes is caused by a further increase in WHIRLY1-dependent transcription of these genes. Rather WHIRLY1 abundance may intensify the binding of activating factors to the promoter of *PR1* under certain conditions. Recently, it has been demonstrated that NPR1-mediated *PR1* gene expression requires the formation of an activating complex consisting of histone acetyltransferase (HAC), NPR1, and a TGA transcription factor (Jin *et al.*, 2018). Potentially, WHIRLY1 might regulate the accessibility of promoters for defense-associated transcription factors (Krupinska *et al.*, 2014a, Krupinska *et al.*, 2022a).

Surprisingly, in barley plants overexpressing *WHIRLY1*, the gene encoding isochorismate synthase (ICS) is activated at control conditions. This high expression could be related to a demand for phylloquinone which is essential for electron transfer in photosystem I. A barley *ics* mutant was reported to be deficient in phylloquinone, whereas it was not altered in the basal level of salicylic acid (Qin *et al.*, 2019). Salicylic acid biosynthesis may proceed by two possible pathways, the ICS and PAL pathways, which both start from chorismate in chloroplasts (Lefevere *et al.*, 2020). In Arabidopsis, only 10% of SA is produced by the PAL pathway, while 90% is produced by the ICS pathway (Garcion *et al.*, 2008). By contrast in barley, *ICS* expression during HL exposure is lower than at LL (Figure 10b), while *PAL* expression is enhanced by a factor of 6. This is in accordance with the idea that in barley during stress the PAL pathway of SA biosynthesis is more critical than the ICS pathway. Since, in contrast to *PR1*, the expression levels of *PAL* (Figure 10) and of the defense gene *THIO1* (Figure S4) were not elevated by overexpression of *WHIRLY1* under normal growth conditions, it is unlikely that these genes are directly regulated by *WHIRLY1*. In contrast, *PR1* and *HPL* were activated in the oeW1 plants both under normal growth conditions and at HL and, therefore might be directly activated by *WHIRLY1*.

The role of chloroplast-nucleus located WHIRLY1 in the growth-defense tradeoff

The reduced growth of oeW1 plants and the enhanced resistance towards powdery mildew indicate that overexpression of *WHIRLY1* shifts the balance between growth and resistance to the latter. In recent years hormone crosstalk has emerged as a major player in regulating the

growth-defense tradeoff (Huot *et al.*, 2014). Although the antagonistic crosstalk between SA and the growth hormone auxin mostly has been reported to determine the tradeoff between growth and defense (Huot *et al.*, 2014), overexpression of *WHIRLY1* in barley had more impact on the levels of cytokinins and JA than on those of auxin and SA, suggesting that in this species the tradeoff is regulated by cytokinin and JA. However, most studies on hormonal interactions during growth and defense have been performed with *Arabidopsis*. It is likely, that hormonal interactions in monocot plants are different, as has been reported for rice (De Vleeschauwer *et al.*, 2013). It has been postulated that during immune responses in rice, NPR1-dependent SA-signaling is activated by JA binding to the COI1 receptor without a change in the level of SA (Yang *et al.*, 2013). This model is in accordance with earlier reports on barley infection by powdery mildew, in which sensitivity to powdery mildew was found to be not accompanied by accumulation of SA (Vallelian-Bindschedler *et al.*, 1998, Hüchelhoven *et al.*, 1999).

The high accumulation of *WHIRLY1* in chloroplasts of the barley *oeW1* plants had neither consequences for nucleoid organization nor plastid gene expression. Hence the reduced growth was likely not caused by changes in the plastid gene expression machinery but rather by the enhanced level of nucleus-located *WHIRLY1*, inducing changes in gene expression that eventually lead to a rewiring of hormonal homeostasis. The identical molecular weights of chloroplast-located *WHIRLY1* and nucleus-located *WHIRLY1* clearly indicate that both pools of *WHIRLY1* had been processed to the mature form inside chloroplasts. Hence *WHIRLY1* over-accumulating in the nucleus was transferred from chloroplasts to the nucleus as demonstrated before with transplastomic tobacco plants synthesizing *WHIRLY1* inside chloroplasts (Isemer *et al.*, 2012b). In another previous study, it had been shown that *Arabidopsis* plants accumulating *WHIRLY1* outside the chloroplasts behave like a *WHIRLY1*-deficient mutant (Isemer *et al.*, 2012a). Hence, the nuclear activities of *WHIRLY1* require its preceding presence in chloroplasts. Whether *WHIRLY1* undergoes a modification inside chloroplasts and how its transfer to the nucleus is mediated remains to be determined. Taken together, the findings of this study suggest that the *WHIRLY1*-mediated adjustment of hormonal homeostasis is controlled by chloroplasts which are crucial sensors of environmental information (Pfalz *et al.*, 2012, Zhang *et al.*, 2020).

According to the elevated *PR1* expression in the absence of stress, barley *oeW1* plants showed a constitutive defense response. To avoid a negative impact on growth, the expression of

resistance genes might be restricted to the time of stress perception and the subsequent defense response (Karasov *et al.*, 2017). Sequestering of WHIRLY1 in chloroplasts is a means to avoid its nuclear activity under non-stress conditions and to allow a fast response to stress only under conditions that induce the transfer of WHIRLY1 from chloroplasts to the nucleus (Krause and Krupinska, 2009). However, the 10 to 50 times higher level of WHIRLY1 in the oeW1 plants obviously exceeded the capacity for WHIRLY1 sequestration by chloroplasts. It remains to be tested whether a moderate increase in WHIRLY1 accumulation in the chloroplast is possible without transfer to the nucleus in non-stress conditions, thereby avoiding the constitutive expression of *PR1* in the nucleus.

Experimental procedures

Plant material and growth conditions

Transgenic barley plants overexpressing *HvWHIRLY* under the control of the maize *UBIQUITIN 1* promoter were generated by the transformation of barley immature embryos by *Agrobacterium tumefaciens* as described (Hensel *et al.*, 2008). The pENTR/TOPO Gateway vector (Invitrogen, Karlsruhe, Germany) was used for the transfer to the pIPKb007 binary vector using Gateway™ LR as described (Himmelbach *et al.*, 2007). Plantlets resistant to hygromycin were transferred into soil and cultivated in a greenhouse. Additionally, PCR analyses with primers (Krupinska *et al.* 2014, Supplementary Table 1) for the hygromycin resistance cassette were performed to verify the transgene integration. As control plants, the barley cultivar “Golden Promise” and for powdery mildew assays, the *HvWHIRLY1* knockdown plants (RNAiW1-7) (Krupinska *et al.*, 2014b) were used.

Barley grains were sown on soil (Einheitserde ED73, Tantau, Ütersen, Germany) and transferred for three days in a dark and cold chamber (6°C) to synchronize germination. Thereafter, the grains were transferred to a climate chamber where the seedlings were grown either in a standard daily light/dark cycle (16:8) as described (Krupinska *et al.*, 2019) or in continuous light of different irradiances (100 or 350 $\mu\text{mol photons m}^{-2} \text{s}^{-1}$) as also described previously (Swida-Barteczka *et al.*, 2018). Primary foliage leaves collected after 10 days after sowing were used for all measurements described.

Quantum yields of the photosystems and electron transport rate

The maximum quantum yield of photosystem II, F_V/F_M , and the maximum P700 (P_M) signal were measured in parallel by Dual-PAM-100 (Walz GmbH, Effeltrich, Germany). The leaves were kept for about 10-15 minutes under low light ($20\text{-}40 \mu\text{mol m}^{-2} \text{s}^{-1}$) before starting the measurement. The measurement was done at 13 different light levels, starting from zero and gradually increasing during six minutes to $1600 \mu\text{mol m}^{-2} \text{s}^{-1}$. In between of these light levels, there was a step with $60 \mu\text{mol m}^{-2} \text{s}^{-1}$ which is similar to the growth light in the climate chamber. The quantum yields of photosystem II as well as of non-radiative and radiative dissipation were calculated as follows (Klughammer and Schreiber, 2008):

$$\Phi(\text{II}) = (F_{M'} - F) / F_{M'}$$

$$\Phi(\text{NPQ}) = F / F_{M'} - F / F_M$$

$$\Phi(\text{NO}) = F / F_M$$

Determination of pigments by high-performance liquid chromatography

For the analysis of pigments, one cm long leaf segments excised from the area between 1.5 and 3 cm below the leaf tip were immediately frozen in liquid nitrogen and kept at -80°C . Pigments were extracted and HPLC analysis was performed as described (Saeid-Nia *et al.*, 2022). To calibrate the detector (Nichelmann *et al.*, 2016), pure carotenoid extracts (except antheraxanthin) were prepared through thin-layer chromatography (modified after Lichtenthaler and Pfister 1978). Afterwards, the concentrations of the pure pigment solutions were determined by spectrophotometry using the extinction coefficients provided by Davies (1976).

Immunoblot analyses

Total proteins were extracted from ground leaf material and subjected to SDS-PAGE, as reported (Krupinska *et al.*, 2014, 2019). Proteins were transferred onto the nitrocellulose membrane by semi-dry electroblotting. Antibodies against PsaA (AS06172), PsbA/D1 (AS01016), LHCA1 (AS01005), and LHCB1 (AS01004) were purchased from Agrisera. The antibody directed towards HvWHIRLY1 was prepared against a synthetic peptide and can be purchased from Agrisera (AS163953). Immunoreactive complexes were visualized using a peroxidase-coupled secondary antiserum with chemiluminescence detection kits (ECL Select,

Amersham, USA; Lumigen, Southfield, MI, USA). The ChemiDoc MP Imaging Systems and the Image Lab 6.1 software (Bio-Rad Laboratories, Munich, Germany) were used for the quantification of signal intensities.

Determination of hormones

Leaf samples of ca. 30 mg (fresh weight) were weighed into 2 ml safe lock tubes (Eppendorf AG, Germany) and kept at -80°C until analysis. Empty tubes were used as blanks. Before extraction, two 3 mm ceria-stabilized zirconium oxide beads were placed into each tube. The samples were extracted and purified as described by Šimura *et al.* (2018) with minor modifications (Simura *et al.*, 2018). The absolute quantification of all targeted phytohormones, excluding salicylates, was performed as described (Eggert and von Wiren, 2017).

The analysis of salicylates was performed using UHPLC-HESI-HRMS (Vanquish UPLC) coupled to QExactive Plus Mass Spectrometer (San Jose, CA, USA). The MS was equipped with a HESI source operating in negative ion mode. Salicylates baseline separation was achieved on a reversed-phase Acquity UPLC® HSS T3 column (10 Å, 2.1 × 100mm, 1.8µm, Waters) using a gradient elution of A (Water, 0.1% FA) and B (ACN, 0.1% FA) as follows: 0–5min, 5% B; 5–10min, 5% to 80% B. Additional five minutes were added for column washing and equilibration (total run time, 15min). The column temperature was set at 45°C and the flow rate at 0.5 ml·min⁻¹. The injection volume was 5µl. Source values were set as follows: Spray voltage 2.5kV; capillary temperature 255°C; S-lens RF level 40; Aux gas heater temp 320°C; Sheath gas flow rate 47; Aux gas flow rate 11. For spectra acquisition, a Full MS/dd-MS² experiment was performed. Resolution in Full Scan was set as 70000. For MS/MS experiments, resolution 17,500 and NCE 40V were used. The identification of compounds found in extracts was based on a comparison of their retention times, MS² spectrum and exact mass with standards.

RNA isolation and real-time PCR analysis

Total RNA was isolated from primary foliage leaves of seedlings using the peqGOLD-TriFast reagent (Peqlab Biotechnology, Erlangen, Germany) according to the manufacturer's protocol. cDNA biosynthesis and real-time PCR were performed as described previously (Krupinska *et al.*, 2019). Data were normalized to the level of the ADP-ribosylation factor 1 mRNA (Rapacz

et al., 2012) or to mRNA of the barley histone acetyltransferase (HORVU.MOREX.r2.1HG0027750), which has the alternative name GENERAL CONTROL NONREPRESSIBLE 5 (GCN5).

Transmission electron microscopy

Leaf segments from primary foliage leaves (2×2mm) at a position of 2 cm below the leaf tip were fixed and processed as described (Krupinska *et al.*, 2014b).

Staining and localization of nucleoids

Leaf cross-sections were produced from the primary foliage leaf of 7d plants by hand or by a hand microtome. Sections were fixed by 4% (w/v) paraformaldehyde in phosphate-buffered saline (PBS) overnight at 4°C. After washing with PBS containing 0.12 % (w/v) Glycin, the sections were stained with SYBR®Green (1:5000, S7563 Invitrogen™) for 45 min in darkness at room temperature. After washing with 1x PBS for 15 min, the sections were transferred onto a slide, capped with PBS/glycerol (v/v: 1:1), and a coverslip. Imaging was done at Leica SP5 confocal microscope system with an HCX PL APO CS 63.0 x 1.2 W objective. Excitation was done by an argon laser line 488 (5% power). Emission was detected between 510-570 nm (HV750) and 690-760 nm (HV480). A minimum of five images out of different regions of the specimen were taken from each sample. Image analysis, coloring, and composition were done by ImageJ 1.53q.

Infection with powdery mildew

Five plants were grown in 12 cm pots in compost soil. In an inoculation device, transgenic lines with two pots each were arranged, with three pots containing wild type. While rotating in the inoculation tower, the fourteen-day-old seedlings were inoculated with *Blumeria graminis* spores (isolate CH4.8) until a spore density of approx. 10 spores per mm² have been reached. The disease scored 7 d after inoculation, as described (Schweizer *et al.*, 1995).

Author Contribution Statement

KK conceived and designed the overall research. The transgenic barley lines were prepared by GH. Selection and growth of the plant material were performed by UV. The experiments on photosynthesis were designed by MSN and WB. Conduction of experiments and data analysis were performed by MSN, SF, AS, CD, and DN. Thereof, the hormone analyses were performed by YATM and NvW. Transmission electron microscopy and leaf cross-section were done by MM. The final manuscript was written by KK, WB, and NvW. MSN prepared the first draft of the part on photosynthesis and nearly all the figures. All authors read and approved the final manuscript.

Acknowledgments

We thank Sabine Sommerfeld (IPK Gatersleben) and Susanne Braun (Institute of Botany, CAU, Kiel) for their excellent technical assistance. We are grateful to the German Research Foundation for financial support (KR1350-19-1).

References

- Albrecht, T. and Argueso, C.T.** (2017) Should I fight or should I grow now? The role of cytokinins in plant growth and immunity and in the growth-defence trade-off. *Annals of Botany*, **119**, 725-735.
- An, C.F. and Mou, Z.L.** (2011) Salicylic acid and its function in plant immunity. *Journal of Integrative Plant Biology*, **53**, 412-428.
- Attaran, E., Major, I.T., Cruz, J.A., Rosa, B.A., Koo, A.J.K., Chen, J., Kramer, D.M., He, S.Y. and Howe, G.A.** (2014) Temporal dynamics of growth and photosynthesis suppression in response to jasmonate signaling. *Plant Physiology*, **165**, 1302-1314.
- Brenner, W.G. and Schmulling, T.** (2012) Transcript profiling of cytokinin action in Arabidopsis roots and shoots discovers largely similar but also organ-specific responses. *Bmc Plant Biology*, **12**.
- Brzobohaty, B., Moore, I. and Palme, K.** (1994) Cytokinin metabolism - implications for regulation of plant growth and development *Plant Molecular Biology*, **26**, 1483-1497.
- Cackett, L., Luginbuehl, L.H., Schreier, T.B., Lopez-Juez, E. and Hibberd, J.M.** (2022) Chloroplast development in green plant tissues: the interplay between light, hormone, and transcriptional regulation. *New Phytologist*, **233**, 2000-2016.
- Campos, M.L., Yoshida, Y., Major, I.T., Ferreira, D.D., Weraduwage, S.M., Froehlich, J.E., Johnson, B.F., Kramer, D.M., Jander, G., Sharkey, T.D. and Howe, G.A.** (2016) Rewiring of jasmonate and phytochrome B signalling uncouples plant growth-defense tradeoffs. *Nature Communications*, **7**.
- Carella, P., Wilson, D.C. and Cameron, R.K.** (2015) Some things get better with age: differences in salicylic acid accumulation and defense signaling in young and mature Arabidopsis. *Frontiers in Plant Science*, **5**.

- Cortleven, A., Leuendorf, J.E., Frank, M., Pezzetta, D., Bolt, S. and Schmulling, T.** (2019) Cytokinin action in response to abiotic and biotic stresses in plants. *Plant Cell and Environment*, **42**, 998-1018.
- Danilova, M.N., Kudryakova, N.V., Doroshenko, A.S., Zabrodin, D.A., Rakhmankulova, Z.F., Oelmuller, R. and Kusnetsov, V.V.** (2017) Opposite roles of the Arabidopsis cytokinin receptors AHK2 and AHK3 in the expression of plastid genes and genes for the plastid transcriptional machinery during senescence. *Plant Molecular Biology*, **93**, 533-546.
- De Vleeschauwer, D., Gheysen, G. and Hofte, M.** (2013) Hormone defense networking in rice: tales from a different world. *Trends in Plant Science*, **18**, 555-565.
- Delker, C., Stenzel, I., Hause, B., Miersch, O., Feussner, I. and Wasternack, C.** (2006) Jasmonate biosynthesis in *Arabidopsis thaliana* - Enzymes, products, regulation. *Plant Biology*, **8**, 297-306.
- Desveaux, D., Despres, C., Joyeux, A., Subramaniam, R. and Brisson, N.** (2000) PBF-2 is a novel single-stranded DNA binding factor implicated in PR-10a gene activation in potato. *Plant Cell*, **12**, 1477-1489.
- Desveaux, D., Subramanian, R., Després, C., Mess, J.-N., Lévesque, C., Fobert, P., Dangl, J. and Brisson, N.** (2004) A "Whirly" transcription factor is required for salicylic acid-dependent disease resistance in Arabidopsis. *Developmental Cell*, **6**, 229-240.
- Eggert, K. and von Wiren, N.** (2017) Response of the plant hormone network to boron deficiency. *New Phytologist*, **216**, 868-881.
- Foyer, C.H., Karpinska, B. and Krupinska, K.** (2014) The functions of WHIRLY1 and REDOX-RESPONSIVE TRANSCRIPTION FACTOR 1 in cross tolerance responses in plants: a hypothesis. *Philosophical Transactions of the Royal Society B-Biological Sciences*, **369**.
- Garcion, C., Lohmann, A., Lamodièrè, E., Catinot, J., Buchala, A., Doermann, P. and Metraux, J.P.** (2008) Characterization and biological function of the ISOCHORISMATE SYNTHASE2 gene of Arabidopsis. *Plant Physiology*, **147**, 1279-1287.
- Golshani, F., Fakheri, B.A., Behshad, E. and Vashvaei, R.M.** (2015) PRs proteins and their mechanism in plants. *Biological Forum*, **7**, 477-495.
- Grabowski, E., Miao, Y., Mulisch, M. and Krupinska, K.** (2008) Single-stranded DNA binding protein Whirly1 in barley leaves is located in plastids and the nucleus of the same cell. *Plant Physiology*, **147**, 1800-1804.
- Heidel, A.J., Clarke, J.D., Antonovics, J. and Dong, X.N.** (2004) Fitness costs of mutations affecting the systemic acquired resistance pathway in *Arabidopsis thaliana*. *Genetics*, **168**, 2197-2206.
- Hensel, G., Valkov, V., Middlefell-Williams, J. and Kumlehn, J.** (2008) Efficient generation of transgenic barley: the way forward to modulate plant-microbe interactions. *Journal of Plant Physiology* **165**, 71-82.
- Hermis, D.A. and Mattson, W.J.** (1992) THE DILEMMA OF PLANTS - TO GROW OR DEFEND. *Quarterly Review of Biology*, **67**, 283-335.
- Himmelbach, A., Zierold, U., Hensel, G., Riechen, R., Douchkov, D., Schweizer, P. and Kumlehn, J.** (2007) A set of modular binary vectors for transformation of cereals. *Plant Physiology*, **145**, 1192-1200.
- Hückelhoven, R., Fodor, J., Preis, C. and Kogel, K.H.** (1999) Hypersensitive cell death and papilla formation in barley attacked by the powdery mildew fungus are associated with hydrogen peroxide but not with salicylic acid accumulation. *Plant Physiology*, **119**, 1251-1260.
- Huot, B., Yao, J., Montgomery, B.L. and He, S.Y.** (2014) Growth-Defense Tradeoffs in Plants: A Balancing Act to Optimize Fitness. *Molecular Plant*, **7**, 1267-1287.

- Isemer, R., Krause, K., Grabe, N., Kitahata, N., Asami, T. and Krupinska, K. (2012a) Plastid located WHIRLY1 enhances the responsiveness of Arabidopsis seedlings toward abscisic acid. *Frontiers in Plant Science*, **3**.
- Isemer, R., Mulisch, M., Schäfer, A., Kirchner, S., Koop, H.U. and Krupinska, K. (2012b) Recombinant Whirly1 translocates from transplastomic chloroplasts to the nucleus. *Febs Letters*, **586**, 85-88.
- Jin, H., Choi, S.M., Kang, M.J., Yun, S.H., Kwon, D.J., Noh, Y.S. and Noh, B. (2018) Salicylic acid-induced transcriptional reprogramming by the HAC-NPR1-TGA histone acetyltransferase complex in Arabidopsis. *Nucleic Acids Research*, **46**, 11712-11725.
- Jwa, N.S., Agrawal, G.K., Tamogami, S., Yonekura, M., Han, O., Iwahashi, H. and Rakwal, R. (2006) Role of defense/stress-related marker genes, proteins and secondary metabolites in defining rice self-defense mechanisms. *Plant Physiology and Biochemistry*, **44**, 261-273.
- Karasov, T.L., Chae, E., Herman, J.J. and Bergelson, J. (2017) Mechanisms to mitigate the trade-off between growth and defense. *Plant Cell*, **29**, 666-680.
- Karpinski, S., Szechynska-Hebda, M., Wituszynska, W. and Burdiak, P. (2013) Light acclimation, retrograde signalling, cell death and immune defences in plants. *Plant Cell and Environment*, **36**, 736-744.
- Klughammer, C. and Schreiber, U. (2008) Complementary PS II quantum yields calculated from simple fluorescence parameters measured by PAM fluorometry and the saturation pulse method. *PAM Application Notes*, **1**, 27-35.
- Krause, K. and Krupinska, K. (2009) Nuclear regulators with a second home in organelles. *Trends Plant Sci*, **14**, 194-199.
- Krupinska, K., Braun, S., Nia, M.S., Schäfer, A., Hensel, G. and Bilger, W. (2019) The nucleoid-associated protein WHIRLY1 is required for the coordinate assembly of plastid and nucleus-encoded proteins during chloroplast development. *Planta*, **249**, 1337-1347.
- Krupinska, K., Dahnhardt, D., Fischer-Kilbienski, I., Kucharewicz, W., Scharrenberg, C., Trosch, M. and Buck, F. (2014a) Identification of WHIRLY1 as a factor binding to the promoter of the stress- and senescence-associated gene *HvS40*. *Journal of Plant Growth Regulation*, **33**, 91-105.
- Krupinska, K., Desel, C., Frank, S. and Hensel, G. (2022a) WHIRLIES are multifunctional DNA-binding proteins with impact on plant development and stress resistance. *Frontiers in Plant Science*, **13**.
- Krupinska, K., Desel, C., Frank, S. and Hensel, G. (2022b) WHIRLIES are multifunctional DNA binding proteins with impact on plant development and stress resistance. *Frontiers in Plant Sciences*.
- Krupinska, K., Oetke, S., Desel, C., Mulisch, M., Schäfer, A., Hollmann, J., Kumlehn, J. and Hensel, G. (2014b) WHIRLY1 is a major organizer of chloroplast nucleoids. *Frontiers in Plant Science*, **5**.
- Kucharewicz, W., Distelfeld, A., Bilger, W., Muller, M., Munne-Bosch, S., Hensel, G. and Krupinska, K. (2017) Acceleration of leaf senescence is slowed down in transgenic barley plants deficient in the DNA/RNA-binding protein WHIRLY1. *Journal of Experimental Botany*, **68**, 983-996.
- Kurowska, M.M., Daszkowska-Golec, A., Gajecka, M., Koscielniak, P., Bierza, W. and Szarejko, I. (2020) Methyl jasmonate affects photosynthesis efficiency, expression of HvTIP genes and nitrogen homeostasis in barley. *International Journal of Molecular Sciences*, **21**.

- Lai, C.C., Que, Q.X., Pan, R., Wang, Q., Gao, H.Y., Guan, X.F., Che, J.M. and Lai, G.T.** (2022) The single-stranded DNA-binding gene Whirly (Why1) with a strong pathogen-induced promoter from *Vitis pseudoreticulata* enhances resistance to *Phytophthora capsici*. *International Journal of Molecular Sciences*, **23**.
- Lefevere, H., Bauters, L. and Gheysen, G.** (2020) Salicylic acid biosynthesis in plants. *Frontiers in Plant Science*, **11**.
- Leybourne, D.J., Valentine, T.A., Binnie, K., Taylor, A., Karley, A.J. and Bos, J.I.B.** (2022) Drought stress increases the expression of barley defence genes with negative consequences for infesting cereal aphids. *Journal of Experimental Botany*, **73**, 2238-2250.
- Lichtenthaler, H.** (2013) Plastoglobuli, thylakoids, chloroplast structure and development of plastids. In *Plastid Development in Leaves during Growth and Senescence* (Biswal, B., Krupinska, K. and Biswal, U. eds). Dordrecht, Heidelberg, New York, London: Springer, pp. 337-361.
- Linthorst, H.J.M.** (1991) Pathogenesis-related proteins of plants. *Critical Reviews in Plant Sciences*, **10**, 123-150.
- Mateo, A., Funck, D., Mühlenbock, P., Kular, B., Mullineaux, P.M. and Karpinski, S.** (2006) Controlled levels of salicylic acid are required for optimal photosynthesis and redox homeostasis. *Journal Experimental Botany*, **57**, 1795-1807.
- Mou, Z., Fan, W.H. and Dong, X.N.** (2003) Inducers of plant systemic acquired resistance regulate NPR1 function through redox changes. *Cell*, **113**, 935-944.
- Muller, M. and Munne-Bosch, S.** (2021) Hormonal impact on photosynthesis and photoprotection in plants. *Plant Physiology*, **185**, 1500-1522.
- Nichelmann, L., Schulze, M., Herppich, W.B. and Bilger, W.** (2016) A simple indicator for non-destructive estimation of the violaxanthin cycle pigment content in leaves. *Photosynthesis Research*, **128**, 183-193.
- Oetke, S., Scheidig, A. and Krupinska, K.** (2022) WHIRLY1 of barley and maize share a PRAPP motif conferring nucleoid compaction. *Plant Cell Physiology*, **63**, 234-247.
- Park, J.E., Park, J.Y., Kim, Y.S., Staswick, P.E., Jeon, J., Yun, J., Kim, S.Y., Kim, J., Lee, Y.H. and Park, C.M.** (2007) GH3-mediated auxin homeostasis links growth regulation with stress adaptation response in Arabidopsis. *Journal of Biological Chemistry*, **282**, 10036-10046.
- Pfalz, J., Liebers, M., Hirth, M., Grubler, B., Holtzegel, U., Schroter, Y., Dietzel, L. and Pfannschmidt, T.** (2012) Environmental control of plant nuclear gene expression by chloroplast redox signals. *Frontiers in Plant Science*, **3**.
- Pfalz, J., Liere, K., Kandlbinder, A., Dietz, K.-J. and Oelmüller, R.** (2006) pTAC2, -6, and -12 are components of the transcriptionally active plastid chromosome that are required for plastid gene expression. *Plant Cell*, **18**, 176-197.
- Powikrowska, M., Oetke, S., Jensen, P.E. and Krupinska, K.** (2014) Dynamic composition, shaping and organization of plastid nucleoids. *Frontiers in Plant Science*, **5**.
- Prikryl, J., Watkins, K.P., Friso, G., van Wijk, K.J. and Barkan, A.** (2008) A member of the Whirly family is a multifunctional RNA- and DNA-binding protein that is essential for chloroplast biogenesis. *Nucleic Acids Research*, **36**, 5152-5165.
- Qin, Y., Torp, A.M., Glauser, G., Pedersen, C., Rasmussen, S.K. and Thordal-Christensen, H.** (2019) Barley isochorismate synthase mutant is phylloquinone-deficient, but has normal basal salicylic acid level. *Plant Signaling & Behavior*, **14**.

- Rakwal, R., Agrawal, G.K. and Yonekura, M.** (2001) Light-dependent induction of *OsPR10* in rice (*Oryza sativa* L.) seedlings by the global stress signaling molecule jasmonic acid and protein phosphatase 2A inhibitors. *Plant Science*, **161**, 469-479.
- Rakwal, R. and Komatsu, S.** (2000) Role of jasmonate in the rice (*Oryza sativa* L.) self-defense mechanism using proteome analysis. *Electrophoresis*, **21**, 2492-2500.
- Rapacz, M., Stepień, A. and Skorupa, K.** (2012) Internal standards for quantitative RT-PCR studies of gene expression under drought treatment in barley (*Hordeum vulgare* L.): the effects of developmental stage and leaf age. *Acta Physiologiae Plantarum*, **34**, 1723-1733.
- Rekhter, D., Ludke, D., Ding, Y.L., Feussner, K., Zienkiewicz, K., Lipka, V., Wiermer, M., Zhang, Y.L. and Feussner, I.** (2019) Isochorismate-derived biosynthesis of the plant stress hormone salicylic acid. *Science*, **365**, 498-502.
- Saeid Nia, M., Repnik, U., Krupinska, K. and Bilger, W.** (2022) The plastid-nucleus localized DNA-binding protein WHIRLY1 is required for acclimation of barley leaves to high light. *Planta*, **255**.
- Savchenko, T., Yanykin, D., Khorobrykh, A., Terentyev, V., Klimov, V. and Dehesh, K.** (2017) The hydroperoxide lyase branch of the oxylipin pathway protects against photoinhibition of photosynthesis. *Planta*, **245**, 1179-1192.
- Schweizer, P., Vallelianbindschedler, L. and Mosinger, E.** (1995) Heat-induced resistance in barley to the powdery mildew fungus *Erysiphe graminis* f. sp. *hordei*. *Physiological and Molecular Plant Pathology*, **47**, 51-66.
- Simura, J., Antoniadi, I., Siroka, J., Tarkowska, D., Strnad, M., Ljung, K. and Novak, O.** (2018) Plant hormonomics: multiple phytohormone profiling by targeted metabolomics. *Plant Physiology*, **177**, 476-489.
- Staswick, P.E., Su, W.P. and Howell, S.H.** (1992) Methyl jasmonate inhibition of root growth and induction of a leaf protein are decreased in an *Arabidopsis thaliana* mutant. *Proceedings of the National Academy of Sciences of the United States of America*, **89**, 6837-6840.
- Su, J.B., Yang, L.Y., Zhu, Q.K., Wu, H.J., He, Y., Liu, Y.D., Xu, J., Jiang, D.A. and Zhang, S.Q.** (2018) Active photosynthetic inhibition mediated by MPK3/MPK6 is critical to effector-triggered immunity. *Plos Biology*, **16**.
- Swida-Barteczka, A., Krieger-Liszkay, A., Bilger, W., Voigt, U., Hensel, G., Szweykowska-Kulinska, Z. and Krupinska, K.** (2018) The plastid-nucleus located DNA/RNA binding protein WHIRLY1 regulates microRNA-levels during stress in barley (*Hordeum vulgare* L.). *RNA Biology*.
- Vallelian-Bindschedler, L., Metraux, J.P. and Schweizer, P.** (1998) Salicylic acid accumulation in barley is pathogen specific but not required for defense-gene activation. *Molecular Plant-Microbe Interactions*, **11**, 702-705.
- Van Loon, L.C. and Van Strien, E.A.** (1999) The families of pathogenesis-related proteins, their activities, and comparative analysis of PR-1 type proteins. *Physiological and Molecular Plant Pathology*, **55**, 85-97.
- van Wijk, K.J. and Kessler, F.** (2017) Plastoglobuli: plastid microcompartments with integrated functions in metabolism, plastid developmental transitions, and environmental adaptation. In *Annual Review of Plant Biology*, Vol 68 (Merchant, S.S. ed, pp. 253-289).
- Vlot, A.C., Dempsey, D.A. and Klessig, D.F.** (2009) Salicylic acid, a multifaceted hormone to combat disease. *Annual Review of Phytopathology*, **47**, 177-206.

- Wu, W.Q., Du, K., Kang, X.Y. and Wei, H.R.** (2021) The diverse roles of cytokinins in regulating leaf development. *Horticulture Research*, **8**.
- Xiao, Y.M., Savchenko, T., Baidoo, E.E.K., Chehab, W.E., Hayden, D.M., Tolstikov, V., Corwin, J.A., Kliebenstein, D.J., Keasling, J.D. and Dehesh, K.** (2012) Retrograde Signaling by the Plastidial Metabolite MEcPP Regulates Expression of Nuclear Stress-Response Genes. *Cell*, **149**, 1525-1535.
- Xiao, Y.M., Wang, J.Z. and Dehesh, K.** (2013) Review of stress specific organelles-to-nucleus metabolic signal molecules in plants. *Plant Science*, **212**, 102-107.
- Yang, D.L., Yang, Y.N. and He, Z.H.** (2013) Roles of plant hormones and their interplay in rice immunity. *Molecular Plant*, **6**, 675-685.
- Yang, D.Q., Luo, Y.L., Dong, W.H., Yin, Y.P., Li, Y. and Wang, Z.L.** (2018) Response of photosystem II performance and antioxidant enzyme activities in stay-green wheat to cytokinin. *Photosynthetica*, **56**, 567-577.
- Yaronskaya, E., Vershilovskaya, I., Poers, Y., Alawady, A.E., Averina, N. and Grimm, B.** (2006) Cytokinin effects on tetrapyrrole biosynthesis and photosynthetic activity in barley seedlings. *Planta*, **224**, 700-709.
- Zhang, Y., Zhang, A.H., Li, X.M. and Lu, C.M.** (2020) The Role of Chloroplast Gene Expression in Plant Responses to Environmental Stress. *International Journal of Molecular Sciences*, **21**.
- Zhang, Y.L., Goritschnig, S., Dong, X.N. and Li, X.** (2003) A gain-of-function mutation in a plant disease resistance gene leads to constitutive activation of downstream signal transduction pathways in suppressor of npr1-1, constitutive 1. *Plant Cell*, **15**, 2636-2646.
- Zheng, E.S., Wang, X.M., Xu, R.M., Yu, F.B., Zheng, C., Yang, Y., Chen, Y., Chen, J.P., Yan, C.Q. and Zhou, J.** (2021) Regulation of *OsPR10a* promoter activity by phytohormone and pathogen stimulation in rice. *Rice Science*, **28**, 442-456.
- Zhuang, K.Y., Gao, Y.Y., Liu, Z.B., Diao, P.F., Sui, N., Meng, Q.W., Meng, C. and Kong, F.Y.** (2020a) WHIRLY1 regulates HSP21.5A expression to promote thermotolerance in tomato. *Plant and Cell Physiology*, **61**, 169-177.
- Zhuang, K.Y., Kong, F.Y., Zhang, S., Meng, C., Yang, M.M., Liu, Z.B., Wang, Y., Ma, N.N. and Meng, Q.W.** (2019) Whirly1 enhances tolerance to chilling stress in tomato via protection of photosystem II and regulation of starch degradation. *New Phytologist*, **221**, 1998-2012.
- Zhuang, K.Y., Wang, J.Y., Jiao, B.Z., Chen, C., Zhang, J.J., Ma, N.N. and Meng, Q.W.** (2020b) WHIRLY1 maintains leaf photosynthetic capacity in tomato by regulating the expression of RbcS1 under chilling stress. *Journal of Experimental Botany*, **71**, 3653-3663.

Chapter VI: Discussion

WHIRLY1 protein, the main architectural protein of nucleoids, compacts the nucleoids

WHIRLY1 has been detected as a major DNA-binding protein of nucleoids. It has been also found in the transcriptionally active chromosomes (TAC) which overlaps in protein composition with nucleoids (Melonek et al. 2016) and has been also named PTAC1 (Pfalz et al., 2006; Melonek et al., 2010). WHIRLY1 protein provides nucleoid compactness which is mediated through its proline-rich motif, PRAAP (Krupinska et al., 2014; Oetke et al., 2022).

In Chapter II it was shown that the reduced compactness of nucleoids in WHIRLY1-deficient plants (W1) coincides with a significantly higher level of UV-B-induced cyclobutane pyrimidine dimers (CPDs) in their plastid DNA (ptDNA) in comparison to the wild type (WT). Since less compactness increases the volume of the nucleoids, the higher UV-B-induced CPDs formation in nucleoids of W1 is in accordance with the target theory (Ballarini, 2010) which says that the probability that a given target is hit by radiation is proportional to the volume of the target. These results indicate that chloroplast-located WHIRLY1 in barley protected ptDNA against UV-B-induced CPDs formation, the most important lesions induced by UV-B (Mitchell and Narin, 1989; Takahashi et al., 2011), potentially through its structural impact on the compactness of nucleoids (Chapter II).

In contrast to the nucleoids in the chloroplasts, UV-B-induced CPD formation in nuclei did not differ between WT and W1 plants (Chapter II). The WHIRLY1 protein is not involved in nucleus architecture or genomic DNA compactness (Krupinska et al., 2022). Therefore, these expectable results provided a further piece of evidence that the WHIRLY1 protein may maintain plastid genome stability by physical protection through nucleoid packaging.

Light acclimation is impaired in WHIRLY1-deficient barley plants (W1) at the levels of photosynthesis and leaf morphology

In contrast to the WT, W1 plants did not show an increase in their photosynthetic capacity when growing under high light (HL) in comparison to plants grown under low light (LL). W1 plants compared to WT plants were shown to have delayed chloroplast development (Krupinska et al., 2019). To exclude that differences in development are responsible for the difference in photosynthesis, measurements were performed with seedlings of different ages. Neither at 10 days after sowing (das) nor at 19 das (Saeid Nia et al., 2022), when leaves had more developed chloroplasts (Krupinska et al., 2019; Saeid Nia et al., 2022), photosynthetic capacity increased in W1 plants at HL. Therefore, the putative impact of retarded chloroplast development in the high light-acclimation of W1 plants cannot be taken into consideration.

In Chapter III it has been demonstrated that the W1 leaves stayed longer green than WT leaves (Saeid Nia et al., 2022), although the levels of senescence-associated hormones increased with the increasing age of the leaves (Kucharewicz et al., 2017). Results from this study showed an age-dependent (Mae et al., 1983; Makino et al., 1984; Suzuki et al., 2010) and HL-accelerated (Makino et al., 1985; Hidema et al., 1991; 1992; Murchie et al., 2002) decline in photosynthetic capacity, carboxylation efficiency, Rubisco content as well as chlorophyll content in HL-grown WT plants (Saeid Nia et al., 2022). In contrast, HL-grown W1 plants showed an increasing tendency in their photosynthetic capacity and RubisCO content which were accompanied by an increase in their chlorophyll content from 10 to 19 das. In other words, HL had almost no impact on the senescence of W1 leaves (Saeid Nia et al., 2022). These results, in accordance with the previous study from Kucharewicz et al. (2017) suggest a relative stay green phenotype for the WHIRLY1-deficient barley plants.

The leaf morphology of WT plants also showed typical signs of HL acclimation. The leaves got thicker caused by an increased volume of cell layers close to the abaxial and adaxial epidermis.

Moreover, leaves in HL-grown WT plants showed higher leaf mass per area (LMA) than LL-grown WT, probably due to their higher cytoplasm/cell volume ratio and higher starch content. However, leaf thickness and LMA did not differ in the leaves of LL- and HL-grown W1 plants, suggesting that HL-grown W1 plants do morphologically resemble shade leaves (Chapter III: Saeid Nia et al., 2022). These results revealed that the WHIRLY1 protein affects the plant's responsiveness to light both at the level of photosynthesis and leaf morphology.

According to the hypothesis by Foyer et al. (2014) and results from this study, the dually located WHIRLY1 protein with its initial location in chloroplast and its close contact with both thylakoid membrane and nucleoids is potentially an ideal candidate to be involved in retrograde signaling and therefore in the acclimation. However, since the absence of proper nucleoid architecture affects the right position and probably also the function of many proteins other than WHIRLY1, indeed, nucleoid compaction could explain impaired light acclimation also alone.

Despite missing light acclimation and appropriate nucleoid compactness, W1 plants survived excessive excitation energy

The compromised HL-acclimation in W1 plants while they were grown under high irradiance, made them a perfect model to investigate light stress responses in the absence of light acclimation. It is expected that plants with impaired light acclimation growing under excessive light, show reduced F_V/F_M (Aro et al., 1993; Demmig-Adams and Adams, 2006; Takahashi and Badger, 2011) together with a loss of chlorophyll (Havaux et al., 2005). 10-day old W1 plants were shown to have lower F_V/F_M than WT plants (Chapter IV) either as a sign of photoinhibition (Powles, 1984; Aro et al. 1993) or potentially caused by their delayed chloroplast development (Björkman and Demmig, 1987, Xu et al., 2019). Intriguingly and in contrast to 10 day-old W1 plants, 15 day-old ones, however, showed an increase in their F_V/F_M to values of 0.8, similar to the WT, as well as rising chlorophyll contents in both LL- and HL-grown plants (Chapter IV). These values for F_V/F_M are like those reported for healthy plants under no-stress conditions (Bjorkman and Demmig, 1987). Therefore, W1 plants must have used alternative strategies to survive under excessive light stress.

Results from energy partitioning in W1 plants showed that the lower quantum yield of photosynthesis ($\Phi(II)$) was compensated by a higher quantum yield of regulated non-

photochemical quenching ($\Phi(\text{NPQ})$) in a way that both WT and W1 plants had a similar remaining fraction of energy dissipated by either fluorescence or non-regulated non-photochemical quenching ($\Phi(\text{NO})$). The only higher values for $\Phi(\text{NO})$ were detected in the young immature 10-day old W1 plants, and disappeared during further or advanced chloroplast development in mature 15 day-old plants.

Advanced chloroplast development in W1 plants was accompanied by an increase in the photosynthetic efficiency, $\Phi(\text{II})$, and a complementary reduction in the $\Phi(\text{NPQ})$. The latter was in accordance with the reduced size of their xanthophyll cycle pool size with a higher epoxidation state (EPS) at 15 das (Chapter IV). Since the EPS is an *in vivo* index for the extent of the excessive energy (Demmig-Adams et al., 1990; Ort, 2001) and follows the $\Phi(\text{II})$ (Bilger and Lesch, 1995), enhanced $\Phi(\text{II})$ together with higher EPS, suggest that at this stage, the W1 plants had to cope with less excessive excitation energy.

In the extra larger xanthophyll cycle pool of HL-grown W1 plants, the majority of xanthophyll pigments were in the de-epoxidized form, zeaxanthin (Chapter IV). Since the size of this pool is exceeding the possible number of xanthophyll binding sites in the light-harvesting complexes (LHCs) (Caffarri et al., 2001), the majority of zeaxanthin molecules from this pool must have been freely located either in the plastoglobuli or in the chloroplast membrane. Hence, elevated amounts of zeaxanthin in the HL-grown W1 plants, in addition to their role in enhanced NPQ, are suggested to be involved in the photoprotection of PS II and lipid-protection of chloroplast membrane through their function as an antioxidant by quenching and scavenging of free radicals (Havaux and Niyogi, 1999; Havaux et al., 2007).

In addition to zeaxanthin, a larger portion of the elevated amount of lutein content of HL-grown W1 plants likely has been also used as an antioxidant (Havaux et al., 2007; Demmig-Adams et al., 2020) and may have played an important role in the protection of W1 plants against oxidative stress, too.

In this study, the flavonoid content of WT and W1 plants was also studied. Although the total contents of flavonoids of WT and W1 plants did not differ, W1 plants had a significantly higher amount of the dihydroxyflavone luteonarin, apparently at the expense of a lower level of the related flavone saponarin, a monohydroxyflavone (Chapter IV).

Dihydroxyflavones are known as better antioxidants than their related monohydroxyflavones (Rice-Evans et al., 1996; Burda and Oleszek, 2001; Nezval et al., 2017). They are usually found in the chloroplasts containing mesophyll cells, rather than in the epidermis which contains only undifferentiated plastids (Agati and Tattini, 2010). The location in the mesophyll is the perfect position for an antioxidant which is playing a role in the protection of chloroplasts against oxidative damage (Agati et al., 2002; 2007). Hence, the higher luteonarin content of HL-grown W1 plants, which was speculated to be mostly located in the mesophylls of W1 plants (Chapter IV) is considered to play an important complementary role together with carotenoids (Agati et al., 2012) in the protection of W1 plants against oxidative stress.

WHIRLY1-deficient barley plants with impaired high light acclimation and nucleoid packaging survived under high irradiance as healthy plants through different photoprotective mechanisms, such as enhanced NPQ, elevated amounts of antioxidants including the carotenoids zeaxanthin and lutein as well as the dihydroxyflavone luteonarin.

Barley plants overexpressing WHIRLY1 protein (oeW1) with similar nucleoid compactness as the wild type are impaired in photosynthesis

Plants overexpressing *HvWHIRLY1 protein*, i.e. oeW1 plants, have 10 or 50 times more (oeW1-15 and oeW1-14 or oeW1-2, respectively) WHIRLY1 protein than WT plants. Therefore, oeW1 plants were initially expected to show higher photosynthetic capacity and better function under HL conditions than WT plants as well as W1 plants. Moreover, since these plants did not show any changes in the packaging of their nucleoids (Part V), they provided a unique chance to investigate the function of the WHIRLY1 protein in the absence of alterations in nucleoid compactness.

Our results showed that a higher amount of W1 protein accumulates in both chloroplasts and the nucleus. It is known that the WHIRLY1 protein in potato and *Arabidopsis thaliana* plays a role in salicylic acid-dependent gene expression during pathogen attack (Deveaux et al., 2000, 2004). Hence, as expected, the expression of PR genes was generally increased in the oeW1 plants in comparison to WT plants with a much higher increase under HL than in LL (Chapter V). These results suggested that also in barley the WHIRLY1 protein plays a role in SA signaling. Unexpectedly, however, hormone analyses revealed that instead of SA, the level of the defense hormone jasmonic acid (JA) was enhanced in the leaves of the oeW1 plants.

The increased capacity of stress resistance or defense in the oeW1 plants was shown to be accompanied by growth reduction. Our results showed that oeW1 seedlings are significantly smaller than WT. Moreover, the reduction in growth tendentially depends on the amount of WHIRLY1; primary leaves of the oeW1-15 plants (10 fold) are larger in comparison to the W1-14 plants (50 fold; Chapter V). The reduction of growth was found to be accompanied by a decline in the level of cytokinins. Cytokinins not only promote growth (Brzobohaty et al., 1994, Wu et al., 2021) but also have positive impacts on chloroplast development and photosynthesis (Yaronskaya et al., 2006).

Despite similar RubisCO content, photosystem composition and thylakoid architecture in WT and oeW1 plants, photosynthesis was compromised in oeW1 in comparison to WT plants. Considering the interrelationship of photosynthesis and growth (Sweet and Wareing, 1966; Körner, 2015), it is equally possible that either compromised photosynthesis impaired the plant growth or lowered growth reduced photosynthesis by the corresponding lower sink strength. Similar to the growth, the efficiencies of the two photosystems and ETR showed significant decreases, which depended on the amount of WHIRLY1. The more WHIRLY1 accumulated in the plants, the worse the photosystems performed and the worse the plants grew.

The significantly reduced levels of cytokinins in oeW1 plants in comparison to WT plants (Chapter V), could be considered as one of the putative factors for the reduced growth and photosynthesis (McIntyre et al., 2021). Moreover, considering the significant increase in the stress-associated hormone jasmonic acid while cytokinin content decreased in OeW1 plants in comparison to WT plants (Chapter V), WHIRLY1 overaccumulation obviously caused a shift in the balance between growth and biotic stress resistance to the latter. Indeed, the oeW1 plants showed a higher expression of defense genes and were more resistant to powdery mildew than the WT.

Opposite to the W1 plants, oeW1 plants showed normal compaction of nucleoids and have more WHIRLY1 protein. Unexpectedly, photosynthesis was also compromised in these plants in comparison to WT (Chapter V). Besides, similar to W1 plants, HL acclimation of leaf morphology is also missing in oeW1 plants (Figure 6.1). Consequently, results from our studies on the WHIRLY1-deficient and WHIRLY1 overexpressing plants generally suggest that for the

optimal function of photosynthesis and HL acclimation of barley plants, an appropriate amount of WHIRLY1, rather than a higher amount of protein, plays a crucial role.

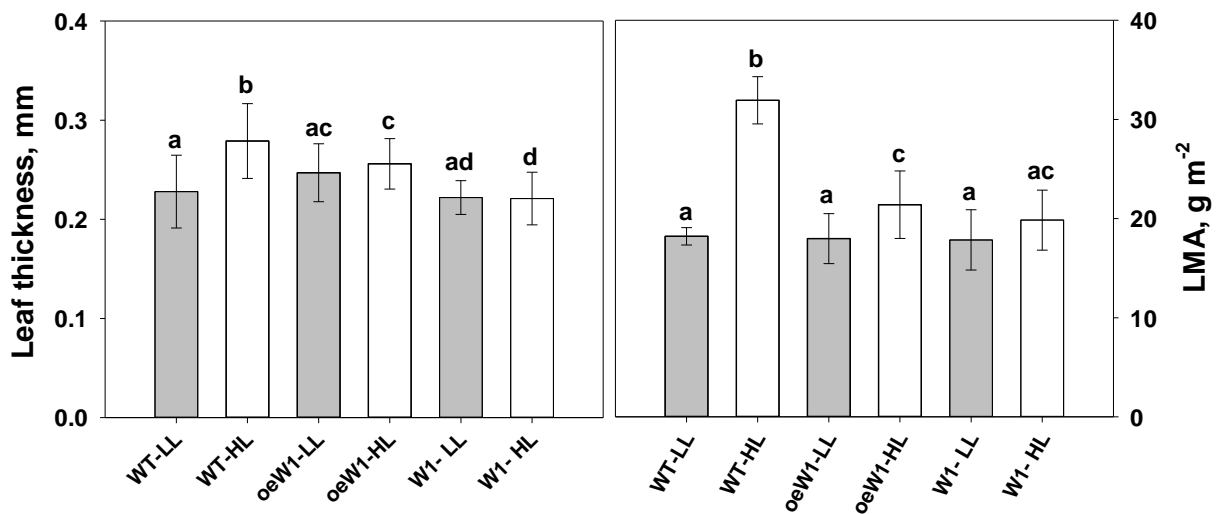


Figure 6.1 Leaf thickness and leaf mass per area (LMA) of 10 day-old primary foliage leaves of WT oeW1-2 (50 times more WHIRLY1 protein), and W1 plant grown at low (filled symbols) and high irradiance (open symbols). Columns are means \pm standard deviation of 9-23 leaves in total from three independent experiments each comprising 3-8 leaves. The letters indicate statistically different values at a significance level of $P=0.05$, as determined by two-way ANOVA, followed by pairwise multiple means comparisons with the Holm-Sidak method.

Conclusions

WHIRLY1-deficient barley plants (W1) showed a heterogeneous population of nucleoids. The latter means that although the majority of nucleoids were found to have reduced compaction, the minute amount of remaining WHIRLY1 protein in W1 plants was able to compact a minor part of the nucleoids population (Krupinska et al., 2014; see also Chapter II). Loose nucleoid compaction in W1 plants affected chloroplast development which was reflected in low chlorophyll contents as well as low values for the optimal quantum yield of photosystem II, F_v/F_m in 10-day old ones. However, the minor population of compact nucleoids in W1 plants was eventually able to provide delayed chloroplast development followed by an increase in chlorophyll content and high values of F_v/F_m similar to that of WT, at in older plants. However, high light (HL) acclimation was shown to be impaired at all different developmental stages in W1 plants

High light acclimation was shown to be impaired in either oeW1 plants overexpressing WHIRLY1 protein with similar nucleoid architecture (as WT) or W1 plants with minutes amounts of WHIRLY1 protein and loosely packed nucleoids. Hence, these results, on one hand,

suggest that the nucleoid compactness might not be the reason for the impaired HL acclimation of W1 plants and could be taken out of consideration. On the other hand, they strongly propose that, for the optimal HL acclimation of photosynthesis and leaf morphology, an ‘appropriate’ amount of WHIRLY1 protein (i.e. in WT), rather than a higher amount, play a crucial role (Figure 6.2).

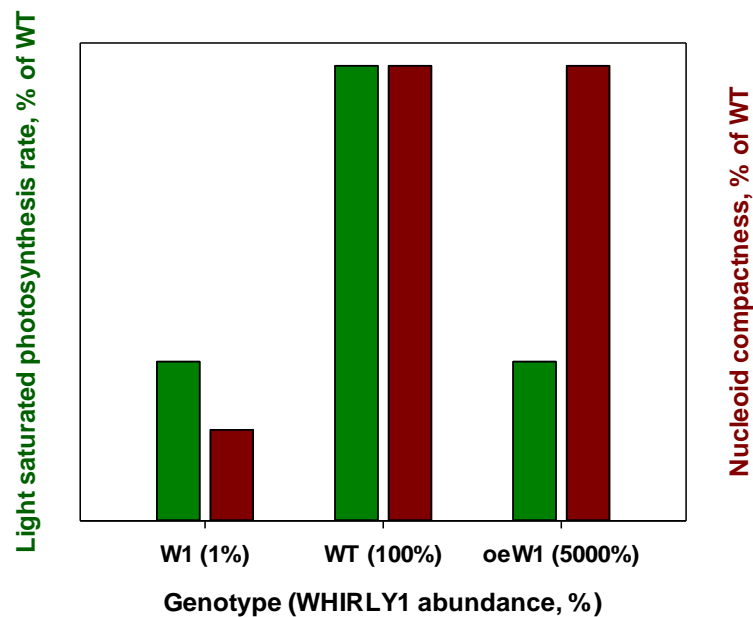


Figure 6.2 Scheme pointing out WHIRLY1-abundance-dependent changes in light acclimation and nucleoid compaction.

As mentioned above, for HL acclimation of photosynthesis as well as leaf morphology, neither low nor high concentration of the WHIRLY1 protein, but the optimal concentration of the protein is required. Moreover, our results showed that down- or upregulation of the WHIRLY1 protein has pleiotropic effects at different levels in barley plants. The needed optimal concentration together with the diverse effects of WHIRLY1 protein (Good et al., 2011; Witzel et al., 2012; Casar and Crespo, 2016), especially in the light sensing and retrograde signaling suggest that WHIRLY1 can be considered as a scaffold protein which possibly also provides a platform for other proteins involved in these processes. Hence, any concentration beyond or beneath the optimal level attenuates its functions or efficiency (Witzel et al., 2012), especially its involvement in retrograde signalling and light acclimation.

Chapter VII: Summary

WHIRLY1 is a chloroplast-nucleus located DNA-binding protein with multiple functions. Its association to nucleoids, which are in close contact with thylakoid membranes, makes this protein an ideal candidate to be involved in responses to environmental changes, which are signalled to the nucleus by retrograde signalling. The latter consequently leads to orchestrating gene expression in the plastid and nucleus in response to environmental changes.

In this study, light acclimation was compared at the levels of photosynthesis and leaf anatomy between transgenic barley plants with an RNAi-mediated knockdown of *HvWHIRLY1* (W1) and wild-type plants (WT) growing at low and high light (LL and HL, respectively). Whereas WT plants showed the typical light acclimation responses, e.g. higher photosynthetic capacity and thicker leaves, W1 did not respond to high irradiance at any developmental stage. The results revealed a systemic role of WHIRLY1 in light acclimation by coordinating responses at both levels of photosynthesis and leaf morphology.

Intriguingly, W1 plants did not show symptoms of photoinhibition after chloroplast development. Therefore, their survival under light energy exceeding their photosynthetic capacity with compromised HL acclimation must have been owed to different photoprotective strategies. Among many possible strategies and mechanisms, this study revealed some. An

extremely large xanthophyll cycle pool, mostly present in de-epoxidized form, zeaxanthin, was in accordance with enhanced NPQ which compensated their low photosynthetic efficiency by dissipating excess energy. Beyond its role in NPQ, enhanced zeaxanthin content together with a high lutein content was assumed to function as an antioxidant. Moreover, the absence of α -tocopherol response to HL suggested that an elevated amount of zeaxanthin was probably sufficient to protect membrane lipids against photooxidative damage. Besides, the dihydroxyflavone lutonarin was highly induced in W1 plants and presumably was mostly located in the mesophyll. Due to its antioxidant properties, lutonarin was proposed to be involved in the photoprotection of W1 plants under HL conditions in addition to the carotenoids zeaxanthin and lutein.

For comparison, lines overexpressing *HvWHIRLY1* (oeW1 plants) with 10- and 50-fold accumulation of the WHIRLY1 protein were also investigated and compared to WT plants. WHIRLY1 over-accumulation in chloroplasts affected neither nucleoid morphology nor the photosynthetic apparatus composition. Unexpectedly, besides plant growth, photosynthetic efficiency and light acclimation were also shown to be compromised in a WHIRLY1 abundance-dependent manner. The elevated levels of *PR1* and *HPL* expression in oeW1 plants already in non-stress conditions coincided with an enhanced resistance towards powdery mildew, proposed activation of constitutive defense in oeW1 plants.

Additionally, the results of this study also revealed that the WHIRLY1 protein as a multi-functional protein was also involved in chloroplast development as well as maintaining plastid genome stability toward UV-B exposure putatively through nucleoid packaging. Taken together, the results on photosynthesis and light acclimation in W1 and OeW1 plants suggest that multi-functional WHIRLY1 might be a scaffold protein whose 'optimal abundance' rather than 'high or low abundance' is required for the light acclimation of barley plants.

Zusammenfassung

WHIRLY1 ist ein in den Chloroplasten lokalisiertes DNA-bindendes Protein mit vielfältigen Funktionen. Seine Assoziation mit Nukleoiden, die in nahem Kontakt mit Thylakoidmembranen stehen, macht dieses Protein zu einem idealen Kandidaten für eine Rolle bei Reaktionen auf Umweltveränderungen, die dem Zellkern durch retrograde Signale signalisiert werden. Die letztere führt folglich zur Orchestrierung der Genexpression in den Plastiden und im Zellkern als Reaktion auf Umweltveränderungen.

In dieser Studie wurde die Lichtakklimatisierung auf den Ebenen der Blattanatomie und der Photosynthese zwischen transgenen Gerstenpflanzen mit einem RNAi-vermittelten Knockdown von HvWHIRLY1 (W1) und Wildtyp-Pflanzen (WT) verglichen, die bei niedrigem und hohem Licht (LL bzw. HL) wachsen. Während WT-Pflanzen die typischen Lichtakklimatisierungsreaktionen zeigten, z. B. eine höhere photosynthetische Kapazität und dickere Blätter, reagierte W1 in keinem untersuchten Entwicklungsstadium auf eine hohe Lichtintensität. Die Ergebnisse zeigten, dass WHIRLY1 eine systemische Rolle bei der Lichtakklimatisierung spielt, indem es die Reaktionen auf beiden Ebenen der Photosynthese und der Blattmorphologie koordiniert.

Merkwürdigerweise zeigten die W1-Pflanzen nach der Entwicklung der Chloroplasten keine Symptome einer Photoinhibition. Da sie eine gestörte HL-Akklimatisierung aufweisen, muss ihr Überleben bei einer Lichtenergie, die ihre photosynthetische Kapazität übersteigt, auf andere photoprotektive Strategien zurückzuführen sein. Unter den vielen möglichen Strategien und Mechanismen hat diese Studie einige aufgedeckt. Ein extrem großer Xanthophyll-Zyklus-Pool, der hauptsächlich in der de-epoxidierten Form Zeaxanthin vorliegt, steht im Einklang mit einer erhöhten NPQ, die ihre geringe photosynthetische Effizienz durch die Dissipation von zusätzlicher Energie kompensiert. Neben seiner Rolle im NPQ sollte der erhöhte Zeaxanthin-Gehalt zusammen mit einem hohen Lutein-Gehalt als antioxidativ wirken. Außerdem deutet das Fehlen einer Reaktion von Tocopherol auf HL darauf hin, dass die erhöhte Menge an Zeaxanthin wahrscheinlich ausreicht, um Membranlipide vor photooxidativen Schäden zu schützen. Im Übrigen wurde das Dihydroxyflavon Lutonarin in W1-Pflanzen stark induziert und befand sich vermutlich hauptsächlich im Mesophyll. Aufgrund seiner antioxidativen Eigenschaften wurde vorgeschlagen, dass Lutonarin zusätzlich zu den

Carotinoiden Zeaxanthin und Lutein an der Photoprotektion von W1-Pflanzen unter HL-Bedingungen beteiligt ist.

Zum Vergleich wurden auch HvWHIRLY1-überexprimierende Linien (oeW1-Pflanzen) mit 10- und 50-facher Akkumulation des WHIRLY1-Proteins untersucht und mit WT-Pflanzen verglichen. Die Überakkumulation von WHIRLY1 in den Chloroplasten hatte keinen Einfluss auf die Morphologie der Nukleole oder die Komposition des photosynthetischen Apparats. Unerwarteterweise zeigte sich, dass neben dem Pflanzenwachstum auch die photosynthetische Effizienz und die Lichtakklimatisierung in Abhängigkeit von der WHIRLY1-Häufigkeit gestört sind. Die erhöhte Expression von *PR1* und *HPL* in oeW1-Pflanzen, die bereits unter Nicht-Stress-Bedingungen eine erhöhte Resistenz gegen Mehltau zeigen, deutet auf eine Aktivierung der konstitutiven Abwehr in oeW1-Pflanzen hin.

Die Resultate dieser Studie zeigten aber auch, dass das WHIRLY1-Protein als multifunktionales Protein auch an der Chloroplastenentwicklung beteiligt ist und die Stabilität des Plastidengenoms gegenüber UV-B Strahlung aufrechterhält, vermutlich durch Nukleoidverpackung. Zusammengenommen deuten die Ergebnisse zur Photosynthese und Lichtakklimatisierung in W1- und OeW1-Pflanzen darauf hin, dass das multifunktionale WHIRLY1-Protein ein Scaffoldprotein sein könnte, dessen "optimale Abundanz" und nicht "hohe oder niedrige Abundanz" für die Lichtakklimatisierung von Gerstenpflanzen erforderlich ist.

References

In the following bibliography, only the references which were cited in **Chapters I** and **VI** can be found. The references cited in other Chapters can be found at the end of each Chapter.

- Agati G, Azzarello E, Pollastri S, Tattini M (2012) Flavonoids as antioxidants in plants: Location and functional significance. *Plant Sci* 196:67–76.
<https://doi.org/10.1016/j.plantsci.2012.07.014>
- Agati G, Galardi C, Gravano E, Romani A, Tattini M (2002) Flavonoid distribution in tissues of *Phillyrea latifolia* L. leaves as estimated by microspectrofluorometry and multispectral fluorescence microimaging. *Photochem Photobiol* 76:350–360.
[https://doi.org/10.1562/0031-8655\(2002\)0760350FDITOP2.0.CO2](https://doi.org/10.1562/0031-8655(2002)0760350FDITOP2.0.CO2)
- Agati G, Matteini P, Goti A, Tattini M (2007) Chloroplast-located flavonoids can scavenge singlet oxygen. *New Phytol* 174:7–89. <https://doi.org/10.1111/j.1469-8137.2007.01986.x>
- Agati G, Tattini M (2010) Multiple functional roles of flavonoids in photoprotection. *New Phytol* 186:786–793. <https://doi.org/10.1111/j.1469-8137.2010.03269.x>
- Andrews D, Bradshaw D, Dinshaw R, Scholes GD (2015) Resonance energy transfer. In: *Photonics: scientific foundations, technology and applications*. pp. 101–127.
<https://doi.org/10.1002/9781119011804.ch3>
- Aro EM, Virgin I, Andersson B (1993) Photoinhibition of photosystem II. Inactivation, protein damage and turnover, *Biochim Biophys Acta Bioenerg* 1143:113–134.
[https://doi.org/10.1016/0005-2728\(93\)90134-2](https://doi.org/10.1016/0005-2728(93)90134-2)
- Asada K (2000) The water–water cycle as alternative photon and electron sinks. *Phil Trans R Soc Lond B* 355:1419–1431. <http://doi.org/10.1098/rstb.2000.0703>
- Asada K (2006) Production and scavenging of reactive oxygen species in chloroplasts and their functions. *Plant Physiol* 141:391–6. <https://doi.org/10.1104/pp.106.082040>
- Baker NR (2008) Chlorophyll fluorescence: a probe of photosynthesis in vivo. *Ann Rev Plant Biol* 59:89–113. <https://doi.org/10.1146/annurev.arplant.59.032607.092759>
- Ballarini F (2010) From DNA radiation damage to cell death: theoretical approaches. *J Nucleic Acids*. 2010:350608. <https://doi.org/10.4061/2010/350608>

- Bilger W, Lesch M (1995) The epoxidation state of the violaxanthin cycle is linearly correlated with photosystem II quantum yield under natural conditions. In: Mathis P (ed) Photosynthesis: from light to biosphere. Proceedings of the 10th International Photosynthesis Congress. Kluwer Academic Publishers, Dordrecht, pp 107-110.
- Björkman O, Demmig B (1987) Photon yield of O₂ evolution and chlorophyll fluorescence characteristics at 77 K among vascular plants of diverse origins. *Planta* 170:489-504. <https://doi.org/10.1007/BF00402983>
- Bobik K, Burch-Smith TM (2015) Chloroplast signaling within, between and beyond cells. *Front Plant Sci* 6:781. <https://doi.org/10.3389/fpls.2015.00781>
- Bradbury M, Baker NR (1981) Analysis of the slow phases of the in vivo chlorophyll fluorescence induction curve. Changes in the redox state of photosystem II electron acceptors and fluorescence emission from photosystems I and II. *Biochim Biophys Acta* 635:542–551. [https://doi.org/10.1016/0005-2728\(81\)90113-4](https://doi.org/10.1016/0005-2728(81)90113-4)
- Brzobohaty B, Moore I, Palme K (1994) Cytokinin metabolism - implications for regulation of plant growth and development. *Plant Mol Biol* 26:1483-1497. <https://doi.org/10.1007/BF00016486>
- Burda S, Oleszek W (2001) Antioxidant and antiradical activities of flavonoids. *J Agric Food Chem* 49:2774–2779. <https://doi.org/10.1021/jf001413m>
- Butler WL (1978) Energy distribution in the photochemical apparatus of photosynthesis. *Annu Rev Plant Physiol* 29:345–378. <https://doi.org/10.1146/annurev.pp.29.060178.002021>
- Caffarri S, Croce R, Breton J, Bassi R (2001) The major antenna complex of photosystem II has a xanthophyll binding site not involved in light harvesting. *J Biol Chem* 276: 35924–35933. <https://doi.org/10.1074/jbc.M105199200>
- Cappadocia L, Parent JS, Zampini É, Lepage É, Sygusch J, Brisson N (2012) A conserved lysine residue of plant Whirly proteins is necessary for higher order protein assembly and protection against DNA damage. *Nucleic Acids Res* 40:258–269. <https://doi.org/10.1093/nar/gkr740>
- Cappadocia L, Sygusch J, Brisson N (2008) Purification, crystallization and preliminary X-ray diffraction analysis of the Whirly domain of StWhy2 in complex with single-stranded DNA. *Acta Crystallogr Sect F Struct Biol Cryst Commun* 64:1056–1059. <https://doi.org/10.1107/S1744309108032399>

- Casar B, Crespo P (2016) ERK Signals: Scaffolding Scaffolds? *Front Cell Dev Biol* 4, 49.
<https://doi.org/10.3389/fcell.2016.00049>
- Chan KX, Phua SY, Crisp P, McQuinn R, Pogson BJ (2016) Learning the languages of the chloroplast: retrograde signaling and beyond. *Annu Rev Plant Biol* 67:25-53 DOI:
<https://doi.org/10.1146/annurev-arplant-043015-111854>
- Curien G, Flori S, Villanova V, Magneschi L, Giustini C, Forti G, Matringe M, Petroutsos D, Kuntz M, Finazzi G (2016) The water to water cycles in microalgae. *Plant Cell Physiol* 57:1354–1363. <https://doi.org/10.1093/pcp/pcw048>
- Desveaux D, Allard J, Brisson N, Sygusch J (2002) A new family of plant transcription factors displays a novel ssDNA-binding surface. *Nat Struct Biol* 9:512–517.
<https://doi.org/10.1038/nsb814>
- Desveaux D, Després C, Joyeux A, Subramaniam R, Brisson N (2000) PBF-2 is a novel single-stranded DNA binding factor implicated in PR-10a gene activation in potato. *Plant Cell* 12:1477–1489. <https://doi.org/10.1105/tpc.12.8.1477>
- Desveaux D, Maréchal A, Brisson N (2005) Whirly transcription factors: defense gene regulation and beyond. *Trends in Plant Sci* 10:95–102.
<https://doi.org/10.1016/j.tplants.2004.12.008>
- Desveaux D, Subramaniam R, Després C, Mess JN, Lévesque C, Fobert P, Dangl J, Brisson N (2004) A "Whirly" transcription factor is required for salicylic acid-dependent disease resistance in Arabidopsis. *Dev Cell* 6:229-240. [https://doi.org/10.1016/S1534-5807\(04\)00028-0](https://doi.org/10.1016/S1534-5807(04)00028-0)
- Demmig-Adams B, Adams WW (2006) Photoprotection in an ecological context: the remarkable complexity of thermal energy dissipation. *New Phytol* 172:11–21.
<https://doi.org/10.1111/j.1469-8137.2006.01835.x>
- Demmig-Adams B, Adam, WW, Heber U, Neimanis S, Winter K, Krüger A, Czygan FC, Bilger W, Björkman O (1990) Inhibition of zeaxanthin formation and of rapid changes in radiationless energy dissipation by dithiothreitol in spinach leaves and chloroplasts. *Plant Physiol* 92:293–301. <https://doi.org/10.1104/pp.92.2.293>
- Demmig-Adams B, López-Pozo M, Stewart JJ, Adams WW (2020) Zeaxanthin and lutein: photoprotectors, anti-inflammatories, and brain food. *Molecules* 25:3607.
<https://doi.org/10.3390/molecules25163607>

- Dietz KJ (2015) Efficient high light acclimation involves rapid processes at multiple mechanistic levels. *J Exp Bot* 66:2401–2414. <https://doi.org/10.1093/jxb/eru505>
- Duysens LNM (1951) Transfer of light energy within the pigment systems present in photosynthesizing cells. *Nature* 168:548
- Duysens LNM (1989) The discovery of the two photosynthetic systems: a personal account. *Photosynth Res* 21:61–79. <https://doi.org/10.1007/BF00033361>
- Exposito-Rodriguez M, Laissue PP, Yvon-Durocher G, Smirnoff N, Mullineaux PM (2017) Photosynthesis-dependent H₂O₂ transfer from chloroplasts to nuclei provides a high-light signalling mechanism. *Nat Commun* 29:49. <https://doi.org/10.1038/s41467-017-00074-w>
- Fey V, Wagner R, Braütigam K, Wirtz M, Hell R, Dietzmann A, Leister D, Oelmüller R, Pfannschmidt T (2005) Retrograde plastid redox signals in the expression of nuclear genes for chloroplast proteins of *Arabidopsis thaliana*. *J Biol Chem* 280:5318–5328. <https://doi.org/10.1074/jbc.M406358200>
- Foyer CH, Harbinson J (1994) Oxygen metabolism and the regulation of photosynthetic electron transport. In: Foyer CH, Mullineaux PM (ed) *Causes of Photooxidative stress and amelioration of defense systems in plants*. CRC Press. Boca Roton. USA. pp. 1-42.
- Foyer CH, Karpinska B, Krupinska K (2014) The functions of WHIRLY1 and REDOX-RESPONSIVE TRANSCRIPTION FACTOR 1 in cross tolerance responses in plants: a hypothesis. *Phil Trans R Soc B* 369:20130226. <https://doi.org/10.1098/rstb.2013.0226>
- Foyer CH, Neukermans J, Queval G, Noctor G, Harbinson J (2012) Photosynthetic control of electron transport and the regulation of gene expression. *J Exp Bot* 63:1637–1661 <https://doi.org/10.1093/jxb/ers013>
- Gaffron H and Wohl K (1936) Zurtheorie der Assimilation. *Naturwissenschaften* 24:81-90 <https://doi.org/10.1007/BF01473561>
- Genty B, Briantais JM, Baker NR (1989) The relationship between the quantum yield of photosynthetic electron transport and quenching of chlorophyll fluorescence. *Biochim Biophys Acta Gen Subj* 990:87-92. [https://doi.org/10.1016/S0304-4165\(89\)80016-9](https://doi.org/10.1016/S0304-4165(89)80016-9).
- Genty B, Harbinson J, Cailly AL and Rizza F (1996) Fate of excitation at PS II in leaves: the non-photochemical side. Presented at the third BBSRC Robert Hill symposium on

- photosynthesis, March 31-April 3, University of Sheffield, Department of Molecular Biology and Biotechnology, Western Bank, Sheffield, UK, Abstract no. P28
- Givnish T (1988) Adaptation to sun and shade: a whole-plant perspective. *Aust J Plant Physiol* 15:63-92. <https://doi.org/10.1071/PP9880063>
- Good MC, Zalatan JG, Lim WA (2011) Scaffold proteins: hubs for controlling the flow of cellular information. *Science* 332:680–686. <https://doi.org/10.1126/science.1198701>
- Grabowski E, Miao Y, Mulisch M, Krupinska K (2008) Single-stranded DNA-binding protein Whirly1 in barley leaves is located in plastids and the nucleus of the same cell. *Plant Physiol* 147:1800–1804. <https://doi.org/10.1104/pp.108.122796>
- Green BR (2011) Chloroplast genomes of photosynthetic eukaryotes: Chloroplast genomes of photosynthetic eukaryotes. *Plant J* 66:34–44. <https://doi.org/10.1111/j.1365-313X.2011.04541.x>
- Havaux M, Eymery F, Porfirova S, Rey P, Dörmann P (2005) Vitamin E protects against photoinhibition and photooxidative stress in *Arabidopsis thaliana*. *Plant Cell* 17:3451-3469. <https://doi.org/10.1105/tpc.105.037036>
- Havaux M, Niyogi KK (1999) The violaxanthin cycle protects plants from photooxidative damage by more than one mechanism. *PNAS* 96:8762-8767. <https://doi.org/10.1073/pnas.96.15.8762>
- Hendrickson L, Furbank RT, Chow WS (2004) A Simple alternative approach to assessing the fate of absorbed light energy using chlorophyll fluorescence. *Photosynth Res* 82:73-81. <https://doi.org/10.1023/B:PRES.0000040446.87305.f4>
- Hidema J, Makino A, Mae T, Ojima K (1991) Photosynthetic characteristics of rice leaves aged under different irradiances from full expansion through senescence. *Plant Physiol* 97:1287–1293. <https://doi.org/10.1104/pp.97.4.1287>
- Hidema J, Makino A, Kurita Y, Mae T, Ojima K (1992) Changes in the levels of chlorophyll and light-harvesting chlorophyll a/b protein of PS II in rice leaves aged under different irradiances from full Expansion through senescence. *Plant Cell Physiol* 33:1209–1214. <https://doi.org/10.1093/oxfordjournals.pcp.a078375>
- Isemer R, Krause K, Grabe N, Kitahata N, Asami T, Krupinska K (2012). Plastid located WHIRLY1 enhances the responsiveness of *Arabidopsis* seedlings toward abscisic acid. *Front Plant Sci* 3:283. <https://doi.org/10.3389/fpls.2012.00283>
- Körner C (2015) Paradigm shift in plant growth control. *Curr Opin Plant Biol* 25:107-114.

- <https://doi.org/10.1016/j.pbi.2015.05.003>.
- Krupinska K, Braun S, Saeid Nia M, Schäfer A, Hensel G, Bilger W (2019) The nucleoid-associated protein WHIRLY1 is required for the coordinate assembly of plastid and nucleus-encoded proteins during chloroplast development. *Planta* 249:1337–1347. <https://doi.org/10.1007/s00425-018-03085-z>
- Klughammer C, Schreiber U (2008) Complementary PS II quantum yields calculated from simple fluorescence parameters measured by PAM fluorometry and the saturation pulse method. *PAM Application Notes* 1:27-35
- Knox RS (1996) Electronic excitation transfer in the photosynthetic unit: Reflections on work of William Arnold. *Photosynth Res* 48:35–39. <https://doi.org/10.1007/BF00040993>
- Krause K, Herrmann U, Fuß J, Miao Y, Krupinska K (2009) Whirly proteins as communicators between plant organelles and the nucleus? *Endocytosis Cell Res.* 19:51–62
- Krause K, Kilbiński I, Mulisch M, Rödiger A, Schäfer A, Krupinska K (2005) DNA-binding proteins of the Whirly family in *Arabidopsis thaliana* are targeted to the organelles. *FEBS Letters* 579:3707–3712. <https://doi.org/10.1016/j.febslet.2005.05.059>
- Krause K, Krupinska K (2009) Nuclear regulators with a second home in organelles. *Trends Plant Sci* 14:194–199. <https://doi.org/10.1016/j.tplants.2009.01.005>
- Krupinska K, Blanco NE, Oetke S, Zottini M (2020) Genome communication in plants mediated by organelle-nucleus-located proteins. *Phil Trans Roy Soc B-Biol Sci* 375 <https://doi.org/10.1098/rstb.2019.0397>
- Krupinska K, Braun S, Saeid Nia M, Schäfer A, Hensel G, Bilger W (2019) The nucleoid-associated protein WHIRLY1 is required for the coordinate assembly of plastid and nucleus-encoded proteins during chloroplast development. *Planta* 249:1337–1347. <https://doi.org/10.1007/s00425-018-03085-z>
- Krupinska K, Desel C, Frank S, Hensel G (2022) WHIRLIES are multifunctional DNA-binding proteins with impact on plant development and stress resistance. *Front Plant Sci* 13:880423. <https://doi.org/10.3389/fpls.2022.880423>
- Krupinska K, Oetke S, Desel C, Mulisch M, Schäfer A, Hollmann J, Kumlehn J, Hensel G (2014) WHIRLY1 is a major organizer of chloroplast nucleoids. *Front Plant Sci* 5, 432. <https://doi.org/10.3389/fpls.2014.00432>
- Kucharewicz W, Distelfeld A, Bilger W, Müller M, Munné-Bosch S, Hensel G, Krupinska K (2017) Acceleration of leaf senescence is slowed down in transgenic barley plants

- deficient in the DNA/RNA-binding protein WHIRLY1. *J Exp Bot* 68:983–996.
<https://doi.org/10.1093/jxb/erw501>
- Laloi C, Przybyla D, Apel K (2006) A genetic approach towards elucidating the biological activity of different reactive oxygen species in *Arabidopsis thaliana*. *J Exp Bot* 57:1719–1724. <https://doi.org/10.1093/jxb/erj183>
- Lichtenthaler HK, Babani F, Langsdorf G (2007) Chlorophyll fluorescence imaging of photosynthetic activity in sun and shade leaves of trees. *Photosynth Res* 93:235–44.
doi: 10.1007/s11120-007-9174-0. Epub 2007 May 8.
- Mae T, Makino A, Ohira K (1983) Changes in the amounts of ribulose biphosphate carboxylase synthesized and degraded during the life span of rice leaf (*Oryza sativa* L.). *Plant Cell Physiol* 24:1079–1086.
<https://doi.org/10.1093/oxfordjournals.pcp.a076611>
- Majeran W, Friso G, Asakura Y, Qu X, Huang M, Ponnala L et al. (2012) Nucleoid-enriched proteomes in developing plastids and chloroplasts from maize leaves; a new conceptual framework for nucleoid function. *Plant Physiol.* 158:156–189.
<https://doi.org/10.1104/pp.111.188474>
- Makino A, Mae T, Ohira K (1984) Relation between nitrogen and Ribulose-1,5-bisphosphate carboxylase in rice leaves from emergence through senescence. *Plant Cell Physiol* 25:429–437. <https://doi.org/10.1093/oxfordjournals.pcp.a076730>
- Makino A, Mae T, Ohira K (1985) Photosynthesis and ribulose-1,5-bisphosphate carboxylase/oxygenase in rice leaves from emergence through senescence. Quantitative analysis by carboxylation/oxygenation and regeneration of ribulose 1,5-bisphosphate. *Planta* 166:414–420. <https://doi.org/10.1007/BF00401181>
- Maxwell K, Johnson GN (2000) Chlorophyll fluorescence—a practical guide. *J Exp Bot* 51:659–668. <https://doi.org/10.1093/jexbot/51.345.659>
- McIntyre KE, Bush DR, Argueso CT (2021) Cytokinin regulation of source-sink relationships in plant-pathogen interactions. *Front Plant Sci* 12:677585
<https://doi.org/10.3389/fpls.2021.677585>
- Melonek J, Mulisch M, Schmitz-Linneweber C, Grabowski E, Hensel G, Krupinska K (2010) Whirly1 in chloroplasts associates with intron containing RNAs and rarely co-localizes with nucleoids. *Planta* 232:471–481

- Melonek J, Oetke S, Krupinska K (2016) Multifunctionality of plastid nucleoids as revealed by proteome analyses. *Biochim Biophys Acta Proteins Proteom* 1864:1016-1038.
<https://doi.org/10.1016/j.bbapap.2016.03.009>
- Miao Y, Jiang J, Ren Y, Zhao Z (2013) The single-stranded DNA-binding protein WHIRLY1 represses *WRKY53* expression and delays leaf senescence in a developmental stage-dependent manner in *Arabidopsis*. *Plant Physiol* 163:746–756.
<https://doi.org/10.1104/pp.113.223412>
- Mitchell DL, Nairn RA (1989) The biology of the (6-4) photoproduct. *Photochem Photobiol* 49:805–819. <https://doi.org/10.1111/j.1751-1097.1989.tb05578.x>
- Murchie EH, Hubbart S, Chen Y, Peng S, Horton P (2002) Acclimation of rice photosynthesis to irradiance under field conditions. *Plant Physiol* 130:1999–2010.
<https://doi.org/10.1104/pp.011098>
- Murchie EH, Lawson T (2013) Chlorophyll fluorescence analysis: a guide to good practice and understanding some new applications. *J Exp Bot* 64:3983–3998.
<https://doi.org/10.1093/jxb/ert208>
- Nezval J, Štroch M, Materová Z, Špunda V, Kalina J (2017) Phenolic compounds and carotenoids during acclimation of spring barley and its mutant *Chlorina f2* from high to low irradiance. *Biologia Plant* 61:73–84. <https://doi.org/10.1007/s10535-016-0689-0>
- Oetke S, Scheidig A, Krupinska K (2022) WHIRLY1 of barley and maize share a PRAPP motif conferring nucleoid compaction. *Plant Cell Physiol* 63:234-247.
<https://doi.org/10.1093/pcp/pcab164>
- Ort DR (2001) When there is too much light. *Plant Physiol* 125:29–32.
<https://doi.org/10.1104/pp.125.1.29>
- Ort DR, Baker NR (2002) A photoprotective role for O₂ as an alternative electron sink in photosynthesis? *Curr Opin Plant Biol* 5: 193-198. [https://doi.org/10.1016/S1369-5266\(02\)00259-5](https://doi.org/10.1016/S1369-5266(02)00259-5).
- Pérez-Llorca M, Munné-Bosch S (2021) Aging, stress, and senescence in plants: what can biological diversity teach us? *GeroScience* 43:167–180.
<https://doi.org/10.1007/s11357-021-00336-y>
- Pfalz J, Liere K, Kandlbinder A, Dietz KJ, Oelmüller R. (2006) pTAC2, -6, and -12 are components of the transcriptionally active plastid chromosome that are required for

- plastid gene expression. *Plant Cell* 18: 176–197.
<https://doi.org/10.1105/tpc.105.036392>
- Powles SB (1984) Photoinhibition of photosynthesis induced by visible light. *Annu Rev Plant Physiol* 35:15–44. <https://doi.org/10.1146/annurev.pp.35.060184.000311>
- Prikryl J, Watkins KP, Friso G, Van Wijk KJ, Barkan A (2008) A member of the Whirly family is a multifunctional RNA- and DNA-binding protein that is essential for chloroplast biogenesis. *Nucleic Acids Res* 36:5152–5165.
<https://doi.org/10.1093/nar/gkn492>
- Quick WP, Horton P, Walker DA (1984) Studies on the induction of chlorophyll fluorescence in barley protoplasts. I. Factors affecting the observation of oscillations in the yield of chlorophyll fluorescence and the rate of oxygen evolution. *Proc R Soc Lond B*. 220:361–370. <https://doi.org/10.1098/rspb.1984.0006>
- Rice-Evans CA, Miller NJ, Paganga G (1996) Structure-antioxidant activity relationships of flavonoids and phenolic acids. *Free Radical Biol Med* 20:933–956.
[https://doi.org/10.1016/0891-5849\(95\)02227-9](https://doi.org/10.1016/0891-5849(95)02227-9)
- Rosenqvist E, van Kooten O (2003) Chlorophyll fluorescence: A general description and nomenclature. In: DeEll JR, Toivonen PMA (ed) *Practical applications of chlorophyll fluorescence in plant biology*. Springer US, Boston, MA. pp. 31–77.
https://doi.org/10.1007/978-1-4615-0415-3_2
- Saeid Nia M, Repnik U, Krupinska K, Bilger W (2022) The plastid-nucleus localized DNA-binding protein WHIRLY1 is required for acclimation of barley leaves to high light. *Planta* 255,84. <https://doi.org/10.1007/s00425-022-03854-x>
- Schreiber U (1986) Detection of rapid induction kinetics with a new type of high-frequency modulated chlorophyll fluorescence. *Photosynth. Res* 9:261–272.
<https://doi.org/10.1007/BF00029749>
- Schreiber U, Bilger W (1987) Rapid assessment of stress effects on plant leaves by chlorophyll fluorescence measurements. In: Tenhunen JD, Catarino FM, Lange OL, Oechel WC (eds) *Plant Response to Stress*. NATO ASI Series, vol 15. Springer, Berlin, Heidelberg. pp 27–53. https://doi.org/10.1007/978-3-642-70868-8_2
- Sewelam N, Jaspert N, Van Der Kelen K, Tognetti VB, Schmitz J, Frerigmann H, Stahl E, Zeier J, Van Breusegem F, Maurino VG (2014) Spatial H₂O₂ signaling specificity: H₂O₂ from

- chloroplasts and peroxisomes modulates the plant transcriptome differentially. *Mol Plant* 7:1191–1210. <https://doi.org/10.1093/mp/ssu070>
- Ströher E, Dietz KJ (2008) The dynamic thiol-disulphide redox proteome of the *Arabidopsis thaliana* chloroplast as revealed by differential electrophoretic mobility. *Physiol Plant* 133:566–583. <https://doi.org/10.1111/j.1399-3054.2008.01103.x>
- Suzuki Y, Kihara-Doi T, Kawazu T, Miyake C, Makino A (2010) Differences in Rubisco content and its synthesis in leaves at different positions in *Eucalyptus globulus* seedlings. *Plant Cell Environ* 33:1314–1323. <https://doi.org/10.1111/j.1365-3040.2010.02149.x>
- Sweet GB, Wareing PF (1966) Role of plant growth in regulating photosynthesis. *Nature* 210:77-9
- Takahashi S, Badger MR (2011) Photoprotection in plants: a new light on photosystem II damage. *Trends Plant Sci* 16:53–60. <https://doi.org/10.1016/j.tplants.2010.10.001>
- Takahashi M, Teranishi M, Ishida H, Kawasaki J, Takeuchi A, Yamaya T, Watanabe M, Makino A, Hidema J (2011) Cyclobutane pyrimidine dimer (CPD) photolyase repairs ultraviolet-B-induced CPDs in rice chloroplast and mitochondrial DNA. *Plant J* 66:433–442. <https://doi.org/10.1111/j.1365-313X.2011.04500.x>
- Wu WQ, Du K, Kang XY, Wei HR (2021) The diverse roles of cytokinins in regulating leaf development. *Hortic Res* 8:1-13 <https://doi.org/10.1038/s41438-021-00558-3>
- Witzel F, Maddison L, Blüthgen N (2012) How scaffolds shape MAPK signaling: what we know and opportunities for systems approaches. *Front Physiol* 3, 475. <https://doi.org/10.3389/fphys.2012.00475>
- Xu D, Marino G, Klingl A, Enderle B, Monte E, Kurth J, Hiltbrunner A, Leister D, Kleine T (2019) Extrachloroplastic PP7L functions in chloroplast development and abiotic stress tolerance. *Plant Physiol* 180:323–341. <https://doi.org/10.1104/pp.19.00070>
- Yaronskaya E, Vershilovskaya I, Poers Y, Alawady AE, Averina N, Grimm B (2006) Cytokinin effects on tetrapyrrole biosynthesis and photosynthetic activity in barley seedlings. *Planta*, 224,700-709. <https://doi.org/10.1007/s00425-006-0249-5>
- Zhuang K, Kong F, Zhang S, Meng C, Yang M, Liu Z, Wang Y, Ma N, Meng Q (2019) Whirly1 enhances tolerance to chilling stress in tomato via protection of photosystem II and regulation of starch degradation. *New Phytol* 221:1998-2012. <https://doi.org/10.1111/nph.15532>. Epub 2018 Nov 15

Zhuang K, Wang J, Jiao B, Chen C, Zhang J, Ma N, Meng Q (2020) WHIRLY1 maintains leaf photosynthetic capacity in tomato by regulating the expression of *RbcS1* under chilling stress. *J Exp Bot* 71:3653-3663. <https://doi.org/10.1093/jxb/eraa145>

Acknowledgments

I would like to express my deepest gratitude and appreciation to:

My 'Doktorvater'; Prof. Dr. Wolfgang. Bilger, for his trust and for giving me the opportunity to start my journey in his lab, which became the turning point of my life, for encouraging me to pursue my ideas, work independently, and grow up, for always being available and consistently supportive, for the barriers he pushed them away, for his innovative attitude, his precise and critical point of view in science and for giving me another nice horizon point of view not only in science but also in my life.

My co-supervisor; Prof. Dr. Karin Krupinska, for her trust in me and providing a unique opportunity to work on an interdisciplinary topic for my thesis, for her generous consistent scientific support and invaluable advice, for all her bright ideas and for all the difficulties that she eased and pushed away.

Prof. Dr. Jennifer Selinski, for her valuable time and great support in the determination of the glutathione content and its redox state, for the fruitful scientific discussion and her guidance.

Jens Hermann and Susanne Wolf, not only because of their generous technical support and for all I learned from them in the laboratory, but especially because of their golden hearts and being there for me to care and share, to help, to have an ear to hear.

Ulrike Voigt, Susanne Braun, and Anke Schäfer, for being always supportive and kindly helpful and for all I have learned from their generous share of invaluable experience.

My former and current colleagues; Luca, Andrea, Weronika, Paul, Frauke, Lars, and specially Susann, Giannina, and Andrea for all the nice time we shared and for the support and helps I got from them.


My friends; Fahimeh and Jana, for all the tears and laughs, for all your caring and sharing, for the hugs, and for what we learned and experienced every day together.

My Mother, my father, my brother, and my sister who live far away but are always close, for their unconditional love.

My love Hossein and our son; Mahur, for giving me strength, confidence, courage, and love, for being always patient, and for being my reason to go on. I could have never undertaken this journey without them.

Erklärung

Hiermit erkläre ich, dass die vorliegende Arbeit-abgesehen von der Beratung durch meine Betreuer selbstständig verfasst und keine anderen als die angegebenen Hilfsmittel genutzt habe und unter Einhaltung der Regeln guter wissenschaftlicher Praxis der Deutschen Forschungsgemeinschaft angefertigt wurde. Die Arbeit wurde bis jetzt weder ganz noch teilweise an anderen Stellen im Rahmen eines Prüfungsverfahrens an der Christian-Albrechts-Universität zu Kiel oder an einer anderen Hochschule vorgelegt. Die Teile dieser Arbeit, die in einer Journal veröffentlicht oder eingereicht wurden, wurden in Kapitel 1 erwähnt. Ferner erkläre ich, dass ich noch keine früheren Promotionsversuche unternommen habe.

A handwritten signature in black ink that reads "Monireh Saeid Nia". The signature is written in a cursive style with a large initial 'M'.

Kiel, den 30.05.2023

Monireh Saeid Nia